

Sheffield Hallam University

The catalytic transformation of polymer waste using modified clay catalysts.

TAYLOR, Scott.

Available from the Sheffield Hallam University Research Archive (SHURA) at:

<http://shura.shu.ac.uk/20428/>

A Sheffield Hallam University thesis

This thesis is protected by copyright which belongs to the author.

The content must not be changed in any way or sold commercially in any format or medium without the formal permission of the author.

When referring to this work, full bibliographic details including the author, title, awarding institution and date of the thesis must be given.

Please visit <http://shura.shu.ac.uk/20428/> and <http://shura.shu.ac.uk/information.html> for further details about copyright and re-use permissions.

CITY CAMPUS, HOWARD STREET
SHEFFIELD S1 1WB

101 698 960 1



REFERENCE

ProQuest Number: 10701074

All rights reserved

INFORMATION TO ALL USERS

The quality of this reproduction is dependent upon the quality of the copy submitted.

In the unlikely event that the author did not send a complete manuscript and there are missing pages, these will be noted. Also, if material had to be removed, a note will indicate the deletion.



ProQuest 10701074

Published by ProQuest LLC (2017). Copyright of the Dissertation is held by the Author.

All rights reserved.

This work is protected against unauthorized copying under Title 17, United States Code
Microform Edition © ProQuest LLC.

ProQuest LLC.
789 East Eisenhower Parkway
P.O. Box 1346
Ann Arbor, MI 48106 – 1346

**THE CATALYTIC TRANSFORMATION
OF POLYMER WASTE USING
MODIFIED CLAY CATALYSTS**

SCOTT TAYLOR

**A thesis submitted in partial fulfilment of the
requirements of**

Sheffield Hallam University

for the degree of Doctor of Philosophy

September 2002

Collaborating organisation: University of Sheffield

DECLARATION

The work described in this thesis was carried out by the author in the Materials Research Institute at Sheffield Hallam University, between September 1998 and September 2001. The author declares that this work has not been submitted for any other degree, and is entirely original except where acknowledged by reference.

Author:

Scott Taylor

Supervisor:

Prof. Christopher Breen



ACKNOWLEDGEMENTS

To say thank you is one thing, to mean it is another. Likewise, gratitude is something that few people desire and yet those very same people deserve in abundance. It is therefore with true sincerity that the following acknowledgements are offered to each and every individual who has aided in the evolution of the work leading to the presentation of this thesis.

Thanks are extended to Professor Christopher Breen for maintaining a belief in my ability and dedication to "Pushing back the frontiers of science." It would be unfair to say that stumbling over those frontiers became an occupational hazard, but I do have several bruises which remain unaccounted for.

The fine art of synergy mastering is something which takes years to perfect, needless to say, despite the stalwart dedication of a select few, veritable attainment of this goal has remained elusive. Ex-deputy synergy master, currently acting senior synergy master (I think I got that right), Dr. Forsyth, has remained an enthused co-conspirator in keeping "The Synergiser" active – I think I'm grateful for that?

One of the first quotes I heard when I joined the MRI was that research students should endeavour to remain "At the cutting edge of science," I couldn't agree more. However, it transpires that some of my 'acquaintances' have severely defective hearing, consequently believing that MRI students should remain, quite literally, – At The Cutting Edge, whole afternoons in some cases. The specific caffeine capacity of Bennet and D'Mello has proven to be quite high, leading to certain SHU catering outlets becoming secondary offices.

Thanks also to those who have shared in communal humor and despair throughout the years, to Andy C, Paul H, Sharon L, Alex M, Mirkka L, John M and Deebea Z. Professionally, thanks must be given to Mike Dyson (Mr. Mass Spec), to Bob Burton and Margaret West (Mr. And Mrs. XRF) and to the MRI administrative staff.

Extensive gratitude is also reserved for those family and friends who have provided support in a range of guises, to Nicola, Dean, The Loudens and The Sheldons, Last, but certainly not least to my Mum and my Dad, words could never express how sincerely grateful I am to you both. You are two of the most inspirational, genuine and special people that I know. Forever Thankful.

"In loving memory of Tara, a guardian and companion to the end."

"To Cairo, you're a star, a true and faithful friend"

ABSTRACT

A variety of modified minerals have been screened to determine their effectiveness as agents for the catalytic transformation of the thermally generated off gases arising from the pyrolysis of the polyolefinic plastic High Density Polyethylene (HDPE). This polymer has been shown to degrade through a series of known mechanisms to yield a hydrocarbon product mixture consisting of an homologous series of saturated and unsaturated hydrocarbons which include alk-1-enes, n-alkanes, alk-x-enes and α - ω -dienes.

Modification treatments have been wide ranging having included activation of the parent mineral by means of pillaring, ion exchange and acid activation. The activated products have been characterised by XRD, XRF, TGA and vibrational spectroscopy. Moreover, evolved gas analysis has been employed to perform catalytic screening runs on these modified minerals. In particular, attention has been paid to the activity of these materials in respect of the formation of potentially fuel applicable hydrocarbons, namely those exhibiting high octane ratings, including aromatics and branched aliphatics from the feedstock species present in the HDPE pyrolysate gas mixture.

Pillared clays (PILC's) have proven ineffective in this role as a consequence of their poor reproducibility and lack of selectivity towards the formation of single ring aromatics.

Likewise, ion exchange has been found to influence strongly the catalytic behaviour of previously acid activated clays, with autotransformed samples offering dehydrocyclisation (DHC) activity at levels significantly greater than seen with some ion exchanged samples, particularly protons.

Acid activated metakaolinites have demonstrated poor selectivity in terms of aromatic formation, although total DHC activity is good. Metakaolin also gave rise to appreciable activity in respect of the formation of the single ring aromatics selected for monitoring in this work. Isomerisation activity was prevalent over these materials, but coking levels were high.

Acid activated smectites represent the most suitable candidates to fulfil the role of single step fuel generation from the transformation of the gas stream resulting from HDPE pyrolysis. It has been found that careful control over the chemical and physical properties of acid activated clays can be achieved through consideration of the severity of the activation parameters chosen to induce modification. In addition, the nature of the activated product is strongly dependant on the nature of the base clay. In particular, acid activated beidellites have been shown to exhibit high levels of surface acidity as determined through the thermal desorption of cyclohexylamine. These materials consequently give rise to respectable activity and selectivity in terms of the formation of highly octane rated methyl substituted single ring aromatics, principally trimethylbenzene.

In contrast, acid activated montmorillonites have been seen to offer lower levels of total surface acidity and have been shown to be active in promoting skeletal isomerisation reactions to yield branched aliphatics, again, highly octane rated.

This activity variation has been attributed to the formation of highly Brønsted acidic silanol containing Surface Localised Acid Pools (SLAP's) on the exposed surfaces of the former as a consequence of the isomorphous substitution patterns observed in the tetrahedral sheets of beidellites.

CONTENTS

Declaration	i
Acknowledgements	ii
Abstract	iii

PREFACE **1**

CHAPTER ONE **4**

Introduction to Polymers	5
1.1. The Polymer Industry	7
1.1.1. Classification of Polymers	8
1.1.2. Terminology	9
1.1.3. Nomenclature	9
1.2. Handling of Spent Polymers	11
1.2.1. Traditional Waste Disposal Methodologies	12
1.2.1.1. Landfilling	13
1.2.1.2. Direct Incineration	13
1.2.2. Energy Recovery from Waste Plastics	14
1.2.2.1. Processed Engineered Fuels (PEF's)	14
1.2.3. Advanced Recycling Technologies	15
1.2.3.1. Chemical Recycling	15
1.2.3.2. Feedstock Recycling	16
1.2.4. Catalytic Transformation	17
1.2.4.1. Zeolites	21
1.2.4.2. Zeolites as Solid Acid Catalysts	22

CHAPTER TWO **24**

Introduction to Clay Minerals	25
2.1. Clay Minerals	25
2.1.1. The Structure of Clay Minerals	26
2.1.1.1. The Tetrahedral Sheet	28
2.1.1.2. The Octahedral Sheet	30
2.1.2. The Phyllosilicates	31
2.1.2.1. Dimorphic Clay Minerals	31
2.1.2.2. Trimorphic Clay Minerals	31
2.2. Smectites	33
2.3. Properties of Smectites	33

2.3.1.	Isomorphous Substitution	33
2.3.2.	Cation Exchange Capacity (C.E.C.)	35
2.3.2.1.	Determination of the C.E.C.	36
2.3.3.	Hydration and Swelling Capacity of Clays	37
2.4.	Kaolinites	39
2.5.	Thermal Behaviour of Clay Minerals	41
2.5.1.	Low Temperature Reactions	42
2.5.1.1.	Cation Migration	43
2.5.1.2.	Structural Reorganisation	44
2.5.2.	Intermediate Temperature Reactions	44
2.5.2.1.	Proton Delocalisation	47
2.5.3.	Dehydroxylation Products	48
2.5.3.1.	Kaolinite	48
2.5.3.2.	Smectites	49
2.6.	Acidity of Clay Minerals	50
2.7.	Ion Exchange Activation	54
2.7.1.	The Process of Ion Exchange Activation	54
2.7.2.	The Effects of Ion Exchange Activation	54
2.7.3.	Applications of Ion Exchanged Clays	55
2.8.	Acid Activation	56
2.8.1.	The Mechanism of Acid Activation	59
2.8.1.1.	Nature of the Starting Material	61
2.8.1.2.	Nature of the Treatment Acid	65
2.8.1.3.	Effect of Activation Temperature	67
2.8.1.4.	Duration of Activation	68
2.8.2.	The Effects of Acid Activation	68
2.8.2.1.	The Effects of Ion Exchange	69
2.8.2.2.	Increase in Acidity	69
2.8.2.3.	Surface Area Enhancements	73
2.8.2.4.	Alteration of Structural Chemistry	74
2.8.3.	Major Uses of Acid Activated Clays	75
2.8.3.1.	Carbonless Copying Paper	75
2.8.3.2.	Clarification of Edible Food Oils	77
2.8.3.3.	Alkene Removal (BTX Hydrocarbons)	78
2.8.3.4.	Production of Speciality Chemicals	80

2.9.	Activation by Pillaring	84
2.9.1.	Preparation of Pillared Clays	85
2.9.1.1.	Intercalation of the Pillaring Species	87
2.9.1.2.	Calcination of the P.P.C.	88
2.9.1.3.	Nature of the Starting Material	88
2.9.1.4.	Nature of the Pillaring Species	90
2.9.1.5.	Concentration of the Pillaring Agent	91
2.9.1.6.	Conditioning of the P.P.C.	91
2.9.2.	Effects of the Pillaring of Smectites	92
2.9.2.1.	Increasing Thermal Stability	92
2.9.2.2.	Increasing Acidity	92
2.9.2.3.	Increasing Surface Area	94
2.9.2.4.	Installing Defined Porosity	94
2.9.3.	Application of Pillared Clays	94
CHAPTER THREE		96
Introduction to Analytical Theory		97
3.1.	Synergic Chemical Analysis	97
3.1.1.	Thermogravimetric Analysis (TGA)	100
3.1.2.	Infra Red Analysis (IR)	101
3.1.3.	Organic Trap Module (OTM)	102
3.1.4.	Gas Chromatography (GC)	102
3.1.5.	Mass Spectrometry (MS)	103
3.2.	X-Ray Fluorescence Spectrometry (XRF)	105
3.3.	X-Ray Diffraction (XRD)	108
3.4.	Gas Chromatography – Mass Spectrometry (GC-MS)	109
3.5.	Inductively Coupled Plasma – Mass Spectrometry (ICP-MS)	109
3.6.	Fourier Transform Infra Red Spectroscopy (FTIR)	110
3.7.	Diffuse Reflectance (IR) (FT) Spectroscopy (DRIFTS)	112
CHAPTER FOUR		114
Experimental		115
4.1.	Clay Minerals Employed	115
4.1.1.	Pillared Saponite	115
4.1.2.	Acid Activated Stebno (ST)	116
4.1.3.	Acid Activated Jelsovy Potok (JP)	116
4.1.4.	Acid Activated SWy-2	117
4.1.5.	Commercially Available Acid Activated Clays	117
4.1.6.	Kaolin Amorphous Derivatives	119

4.2.	Sample Preparation	120
4.2.1.	Preparation of Acid Activated SWy-2	120
4.2.2.	Preparation of Acid Activated KAD's	120
4.2.3.	Ion Exchange Activation	121
4.3.	Materials Characterisation	121
4.3.1.	Synergic Chemical Analysis	122
4.3.2.	X-Ray Fluorescence Spectrometry	126
4.3.3.	X-Ray Diffraction Analysis	126
4.3.4.	Gas Chromatography – Mass Spectrometry	126
4.3.5.	Inductively Coupled Plasma – Mass Spectrometry	126
4.3.6.	Fourier Transform Infra Red Spectroscopy	126
4.3.7.	Diffuse Reflectance (IR) (FT) Spectroscopy	127
4.3.8.	Thermogravimetric Analysis	127
4.3.9.	Determination of Catalyst Coke Values	127
CHAPTER FIVE		128
Polymer Pyrolysis in Recycling		129
5.1.	Characterisation of High Density Polyethylene (HDPE)	130
5.1.1.	Thermogravimetric Analysis	131
5.1.2.	Evolved Gas Analysis	132
5.2.	Thermal Decomposition of Polyolefins	133
5.3.	Mechanistic Aspects of Polymer Cracking	135
5.4.	Constructional Arrangement of Results	138
5.5.	Interpretation of Normalised TIC's	139
CHAPTER SIX		141
Introduction (Results & Discussion – Al/Cr Pillared Spanish Clays)		142
6.1.	Materials Characterisation	143
6.1.1.	Thermogravimetric Analysis	143
6.1.2.	Elemental Analysis	144
6.1.3.	X-Ray Diffraction Analysis	145
6.1.4.	FTIR Analysis	146
6.2.	Catalytic Activity	146
6.2.1.	HDPE Catalytic Transformation Activity	152
6.2.2.	Determination of Coke	173
6.3.	Summary of Catalytic Behaviour	174
CHAPTER SEVEN		175
Introduction (Results & Discussion – Acid Activated Metakaolins)		176
7.1.	Materials Characterisation	177

7.1.1.	Thermogravimetric Analysis	178
7.1.2.	Elemental Analysis	181
7.1.3.	X-Ray Diffraction Analysis	182
7.1.4.	FTIR Analysis (DRIFTS)	185
7.2.	Catalytic Activity	189
7.2.1.	HDPE Catalytic Transformation Activity	190
7.2.2.	Determination of Coke	196
7.3.	Summary of Catalytic Behaviour	197
CHAPTER EIGHT		199
Introduction (Characterisation Results – Acid Activated Stebno)		200
8.1.	Materials Characterisation	201
8.1.1.	Thermogravimetric Analysis	201
8.1.2.	Elemental Analysis	204
8.1.3.	X-Ray Diffraction Analysis	205
8.2.	Catalytic Activity	206
8.2.1.	HDPE Catalytic Transformation Activity	206
8.2.2.	Determination of Coke	217
CHAPTER NINE		219
Introduction (Characterisation Results – Acid Activated SWy-2)		220
9.1.	Materials Characterisation	220
9.1.1.	Thermogravimetric Analysis	220
9.1.2.	Elemental Analysis	221
9.1.3.	X-Ray Diffraction Analysis	223
9.1.4.	FTIR Analysis (DRIFTS)	226
9.2.	Catalytic Activity	229
9.2.1.	HDPE Catalytic Transformation Activity	229
9.2.2.	Determination of Coke	236
9.3	Summary of Catalytic Behaviour	238
CHAPTER TEN		240
Introduction (Characterisation Results – Commercial Acid Activated Clays)		241
10.1.	Materials Characterisation	241
10.1.1.	Thermogravimetric Analysis	242
10.1.2.	Elemental Analysis	243
10.1.3.	X-Ray Diffraction Analysis	245
10.1.4.	FTIR Analysis (DRIFTS)	248

10.2. Catalytic Activity	251
10.2.1. HDPE Catalytic Transformation Activity	251
10.2.2. Determination of Coke	260
10.3. Summary of Catalytic Behaviour	260
CHAPTER ELEVEN	262
Introduction (Further Investigations – Fulacolor Derivatives)	263
CHAPTER TWELVE	284
Acid Activated Clays – Catalytic Activity Discussion Forum	285
12.1. Surface Localised Acid Pools (SLAPs)	285
12.2. Effect of Acidity on Aromatic Production	288
12.3. Influence of Tetrahedral Al on Products	289
12.4. Product Selectivity – Mechanistic Factors	290
12.5. Product Selectivity – Pore Size Effects	293
12.6. Product Selectivity – Proximity of Acid Sites	293
12.7. Catalyst Requirements	299
12.8. Comparison of AAC Activity with Zeolites	301
12.9. Concluding Remarks	305
CHAPTER THIRTEEN	306
Conclusions and Further Work	307
13.1. Modified Mineral Summaries	308
13.1.1. Spanish Pillared Saponites (R)	309
13.1.2. Acid Activated Metakaolins (AAMK)	310
13.1.3. Acid Activated Stebno (ST)	311
13.1.4. Acid Activated SWy-2 (SWy-2-X-A)	312
13.1.5. Commercial Acid Activated Clays	313
13.2. Activity Summary	316
13.3. Concluding Remarks	319
CHAPTER FOURTEEN	322
14.1. Conferences Attended	323
14.2. Postgraduate Studies	324
14.3. Published Materials	324
CHAPTER FIFTEEN	326
Appendix	

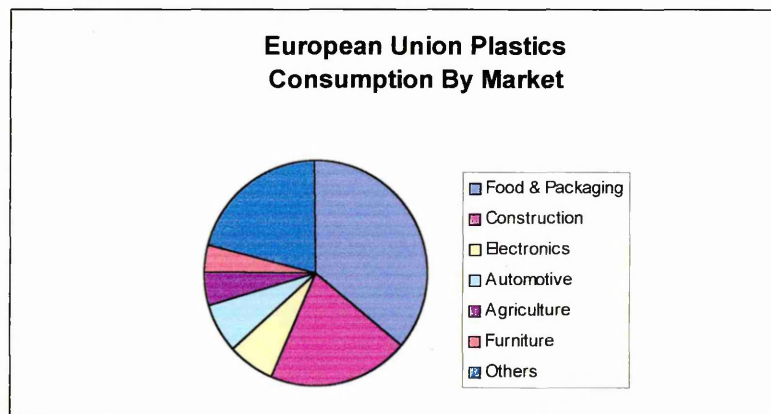
PREFACE

Current environmental concerns over the fate of waste polymeric materials entering post consumer waste streams have highlighted the need for the development of new technologies to better deal with the problems associated with the disposal of these versatile, yet durable materials.

Over recent years polymers, and in particular plastics have been the material of choice for an ever expanding number of applications. This is due in part to the ability of chemists to engineer highly desirable properties into these versatile materials. Combined with the relative economy of manufacturing and processing, plastics are now common place in the industrialised world.

Primarily as a consequence of their aesthetic and barrier attributes, plastics are routinely used in the food packaging industry. Such applications are typically single use, with the resultant waste considered disposable on grounds of economy. Figure 1 below shows that currently, 36% of plastics consumed within the European Union are used in food and packaging applications.¹

Figure 1 – European Union Plastics Consumption By Market



¹ "Plastics – Meeting Today's Building and Construction Needs," APME Technical Publication, 1997.

disposal methodologies applied to spent polymers. In particular, landfilling and direct incineration have come under particular scrutiny due to their resultant loss of the chemical and energy content of the waste plastics. Direct incineration has also received considerable negative press in respect of the emission of potentially environmentally hazardous products, such as carcinogenic dioxins which result from the burning of plastic.

The majority of commercially manufactured plastics are polymerised via processes that involve a degree of catalytic control in order to determine the precise nature of the polymer product. It is therefore logical, that as catalysts become more prolific in the chemical industry, that catalytically active materials will one day form an integral component of both the manufacturing and recycling aspects of the polymer industry.

Recent attempts to incorporate catalytically active materials into existing polymer recycling technologies have seen the application of Zeolites in this role. Zeolites are three dimensional aluminosilicate frameworks which exhibit several features which lead to their efficient operation as hydrocarbon reforming catalysts, including high surface area, high thermal stability and high levels of acidity. While initial results involving the use of Zeolites as post pyrolysis polymer transformation catalysts have been promising, in that potentially fuel applicable hydrocarbon mixtures have been

obtained, the relatively high cost of synthetically manufactured Zeolites has proven to be a significant deterrent to the commercial development of this technology.

In contrast, modified clay minerals, which possess many of the advantageous catalytic properties of their synthetically manufactured Zeolitic counterparts, have received little attention with regards to their potential application in this role. Raw clays have been shown to exhibit minimal levels of catalytic activity in this respect, whereas modified minerals, and in particular acid activated and pillared clays, represent a cheap and widely available alternative for use as hydrocarbon reforming catalysts in such novel plastic recycling technologies. The relative economy of modified clays over their synthetically manufactured counterparts also allows for their disposal after a single application, with the consequence of eliminating costly catalyst regeneration processes.

The efficiency of acid activated clays as hydrocarbon reforming catalysts was realised more than 50 years ago, when Eugene Houdry found that acid activated smectites gave fuel range hydrocarbons in high yield when used in the treatment of crude oils.

The primary aim of the work presented in this thesis relates to the determination of the relative efficiency and selectivity of a variety of modified minerals with respect to the reformation of the thermally generated off gases produced during high density polyethylene decomposition. Activity and selectivity comparisons will be drawn with commercially available materials including silica alumina's and zeolites.

CHAPTER ONE

Introduction to Polymers and Plastics

1. INTRODUCTION TO POLYMERS

The term '*polymer*' is a generality which is applied to an ever increasing range of materials, all of which share a common feature, they are all large molecules which are made up of simple repeating units.

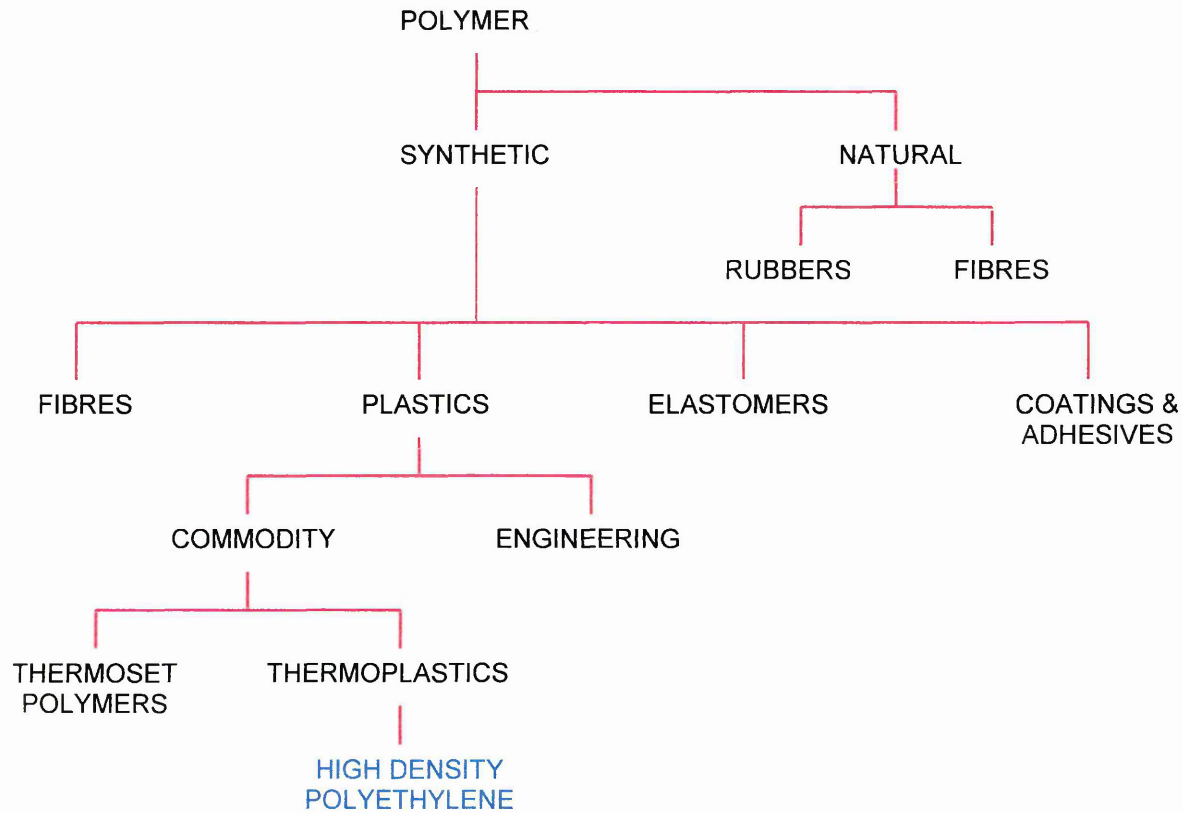
The number of different types of these structural building blocks occurring in any given polymer, in addition to the chemical composition and loci of appearance in the overall polymer chain of these groups, collectively combine to determine the resultant chemical, physical and mechanical properties of the processed polymeric material. Moreover, polymer properties can be enhanced through the addition of additive materials at the processing stage. Furthermore, catalysts can be employed to exert control over the polymerisation process and examples of this will be given later.

In recent years, a massive industry has grown around the design and development of polymeric materials to fulfil a wide range of industrial and commercial applications. Indeed, it could be stated that following on from the importance of the stone and iron ages to the development of society as we know it, we currently live in the age of the polymer.

As the field of polymer chemistry has grown, it has become necessary to develop a classification system so as to assign materials to a general class. Such classifications are made on the basis of the physical properties of the resultant polymer materials following processing of the raw polymer resins. The flow diagram shown in figure 2 below illustrates this classification system. Of the subdivisions shown, the plastics, and in particular the thermoplastics are by far the most widely employed of polymeric materials. Recent figures¹ show that the European Union currently consumes 30 million tonnes of plastics per year, of which 12% (3.6 million tonnes) are the

polyolefinic thermoplastics High Density Polyethylene (HDPE) and Low Density Polyethylene (LDPE). This in turn equates to a waste plastic total approaching 17 million tonnes per year throughout the European Union.²

Figure 2 – Polymer Classification Flow Chart



It should be noted that of the 17 million tonnes per year of waste plastics generated within Europe, only 6.5% (1.1 million tonnes) is subject to recycling. In addition, when the lifecycle variability of plastic products is taken into consideration, it can be seen that low lifetime products such as packaging are frequently manufactured from plastics such as HDPE, whereas products with longer lifecycles are usually made from thermoset plastics such as Polyvinylchloride (PVC) and Polystyrene (PS).

² "Plastics Recycling in the Construction Industry," Halliwell, S.M, BRE Information Paper PD 66/97.

1.1. THE POLYMER INDUSTRY

The growth in the global use of polymers has been explosive. During the 1980's, global consumption of plastic polymer resins overtook that of both iron and steel. This growth is due in part to the ability of chemists to engineer highly desirable attributes into polymer systems. By selecting a suitable starting material and catalyst to incorporate into the polymerisation process, materials can be generated which are highly suited to particular applications.

Examination of the polyethylenes is perhaps the best illustration of this point. The polyethylenes represent a sizeable range of materials with a diverse range of properties and applications, ranging from insulation in the electronics industry, through light weight flexible carrier bags, to rigid high performance pipes for the transport of fluidised media.³ The ability to engineer such a diverse range of physical and mechanical properties into a single family of polymeric materials is due, in part, to the utilisation of catalysts which exert control over the degree of branching of the feedstock monomer which occurs during the polymerisation process.

An example of this control can be seen with HDPE which itself is a completely linear high molecular weight material, exhibiting a high degree of impact strength. In comparison, Low Density Polyethylene (LDPE) contains significant numbers of both short and long chain branches along the length of the carbon backbone. In addition, Linear Low Density Polyethylene (LLDPE), which has a molecular weight comparable to that of HDPE, has a relatively small number of short chain branches attached to the main chain. In terms of physical properties, the low density analogues of the family are much more flexible, a feature which dictates their ultimate use.

³ V. Gibson & D. Wass, *Chemistry in Britain* **35**, 7 (1999) 20.

1.1.1. CLASSIFICATION OF POLYMERS

In the case of all polymers, the individual structural units that compose the material are known as monomers. It should be noted that it is not uncommon for a single polymer to contain monomeric units of more than one type, these materials being referred to as copolymers. In contrast, the term homopolymer describes a polymeric material which is composed of a single type of monomeric unit.

In the case of copolymers, these materials can be further divided into categories which describe the arrangements of their monomers with respect to each other. Table 1 below illustrates the nature of this sub classification.

Table 1 – Sub Classification of Co-Polymers

1 = Copolymer Number 1

2 = Copolymer Number 2

NAME	STRUCTURAL DESCRIPTION
Random Copolymer	1-1-2-1-2-2-1-2-1-1-1-2-1-2-1
Alternating Copolymer	1-2-1-2-1-2-1-2-1-2-1-2-1
Block Copolymer	1-1-1-1-2-2-2-2-1-1-1-1-2-2-2
Graft Copolymer	1-1-1-1-1-1-1-1-1-1-1-1-1-1-1-1 2-2-2-2-2-2-2-2-2-2-2-2-2-2-2-2

Although polymers are generally considered to be macromolecular structures, careful control over the polymerisation process, can lead to the formation of short chain polymers which due to the Greek word oligo, meaning few, are collectively known as oligomers.

1.1.2. TERMINOLOGY

Typically, polymer names are based on the monomer from which the material is made. Families of polymers can be grouped and named according to the presence of a particular functional group within their structures. For instance, the polyesters are so called due to the existence of the ester linkage (C-O-CO) within their respective monomeric units.

Although such systematic names are in widespread use, many polymer chemists still refer to polymers using their more traditional names which are based on the presence of particular functional groups. For instance, alkene derived polymers are often referred to as vinyl polymers, or as polyolefins.

1.1.3. NOMENCLATURE

Prior to the introduction of catalytically controlled polymerisation processes in the early 1950's, unsaturated hydrocarbon polymerisation was achieved through the use of high temperature and high pressure induced free radical reactions. Such processes gave rise to highly branched polymers such as LDPE for the ethene (ethylene) monomer. The introduction, in 1953 of Karl Ziegler's transition metal catalysts for ethene polymerisation permitted a higher degree of control to be achieved over the branching arrangements during the polymerisation process, thus allowing property refinement in the finished product.

More recently, the introduction of catalysts based on metallocene complexes of group 4 metals,^{4,5} have seen further enhancements in branching control and thus the capability to engineer polyethylene polymers for specific applications.

⁴ H.H. Brintzinger *et al*, *Angew. Chem. Int. Ed. Engl.* **34** (1995) 1143.

⁵ M. Bochmann, *J. Chem. Soc. Dalton Trans.* (1996) 255.

The polymer industry typically employs one of two methods to facilitate polymer production. Depending upon the cost of the appropriate starting materials and or the viability of one process over another, in terms of chemical engineering aspects, it is often the case that manufacturers can select the type of polymerisation process to employ. Figure 3 below illustrates two competing processes for the production of HDPE.

Process One

In this case, the monomer employed is ethene ($\text{H}_2\text{C}=\text{CH}_2$), and the resultant polymer consists of repeating units of CH_2CH_2 . In this instance, the atomic makeup of the product is identical to that of the starting material, and therefore it can be seen that the polymerisation proceeds via monomeric addition to form an addition polymer.

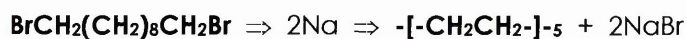
Process Two

In this instance, the monomer used to produce HDPE is α - ω -dibromide ($\text{BrCH}_2(\text{CH}_2)_8\text{CH}_2\text{Br}$). However, in this instance, there is a discrepancy between the atomic makeup of the monomer and that of the final product. This is due to the formation of a secondary reaction product which is eliminated after polymer formation. Such polymers are referred as condensation polymers, a term used due to the fact that the secondary reaction product is very often water.

Figure 3 – Competing Polymerisation Processes for the Formation of HDPE



(Addition Polymer / Chain Reaction Polymer)



(Condensation Polymer / Step Reaction Polymer)

1.2. HANDLING OF SPENT POLYMERS

Recycling of post consumer products is frequently viewed as the only viable option for the management of society's waste streams. Indeed, technologies for the effective disposal and reuse of waste paper materials are now well established.

However, in the case of polymers, the very properties which make these materials both commercially and industrially attractive, inhibit their efficient recycling. Plastics are durable, versatile and relatively resistant to chemical attack. They have significant variation in structural and chemical composition, and are manufactured in a variety of contrasting shapes and colours. In addition, virgin polymers are often cheaper and of significantly higher quality than their recycled counterparts.

To facilitate the recycling process, 1988 saw the introduction of a Voluntary Plastic Container Coding System, as adopted by the Society of the Plastics Industry (SPI). Under the system, consumer end products manufactured from plastics are stamped with an identification symbol such as that indicated for HDPE in figure 4, below.

Figure 4 - SPI Identification Symbol For HDPE



Table 2, illustrates the main classes of the identification system applied to plastic materials.

Table 2 :- Plastic Recycling Codes As Adopted By The SPI

NUMBER	ABBREVIATION	PLASTIC
1	PETE	Poly(ethylene terephthalate)
2	HDPE	High-density polyethylene
3	V or PVC	Poly (vinyl chloride)
4	LDPE	Low-density polyethylene
5	PP	Polypropylene
6	PS	Polystyrene
7	OTHER	Mixed Plastics

The reason that only six main categories exist is accounted for on the basis that the six identified plastics account for >90% of the total plastic incorporated into consumer end products.

Polymers are typically formed from hydrocarbon feedstock's, and as such are rich in energy. In recent years, the potential exploitation of this energy has been examined, with the resultant introduction of processes for the recovery of chemical energy from waste polymers.

1.2.1. TRADITIONAL WASTE DISPOSAL METHODOLOGIES

In these modern times of environmental awareness, the waste disposal and treatment strategies of the past have come under increasing scrutiny. Two of the oldest methods in particular have received considerable attention, these being landfilling and direct incineration. Traditionally, these waste treatment methods were viewed as a rapid and economically viable option for the removal of waste materials from the overall waste stream.

1.2.1.1. LANDFILLING

The committal of spent plastics to landfill sites has been carried out for many years. Research has shown that landfill sites are typically responsible for the generation of significant quantities of methane, a known contributor to greenhouse gases. The durability of plastics prevents their rapid degradation, but over time these materials will degenerate, and so provide carbon and hydrogen precursors for the subsequent generation of potential greenhouse gases. More importantly, the placement of waste plastic in landfill sites means that the valuable chemical and potential energy contents of these materials are lost.

1.2.1.2. DIRECT INCINERATION

Direct incineration of waste plastic has been widely practised. While the method reduces the volume of waste by upto 90%, it also presents many of the same problems encountered with landfilling. Uncontrolled combustion of plastics has the potential to generate considerable air pollution, including high levels of dioxins which can ultimately enter the human food chain.⁶ In addition, the burning of waste plastic results in the loss of both the chemical and energy content of the material.

Such problems have been counteracted by the introduction of waste-to-energy technologies in which the energy content of the polymer is reclaimed for further use.⁷ This was initially achieved through the use of controlled incineration, in which the resultant energy was harnessed and used to generate renewable energy in the form of steam, hot water and electricity. However, such waste-to-energy plants have been slow to achieve universal acceptance due to the constraints on the use of the resultant energy produced.

⁶ C. Schaschke, *Biological Sciences Review*, September 2000, **19**.

⁷ C. Molgaard, *Resources, Conservation and Recycling*, **15** (1995) 51-63.

Typically, such energy is employed on site. In addition, many have voiced concern over the emissions from such plants, particularly the loss of dioxans and furans typically formed through the breakdown of polyesters, which may ultimately enter the human food chain. Another negative aspect associated with such plants has been the relatively low cost of landfill which has reduced the growth and investment in incineration technology.

However, times are changing. With the introduction by the United Kingdom (UK) government of landfill regulations in 1996, and the subsequent initialisation in 1998 of a landfill tax, alternatives to direct disposal of plastics have become increasingly attractive.

1.2.2. ENERGY RECOVERY FROM WASTE PLASTICS

The recovery of energy from plastics is rapidly amassing importance as the disposal of waste and conservation of current resources takes on a greater degree of importance. As indicated previously, due to their derivation from petroleum feedstock's, plastics possess a very high energy content, which in terms of British thermal units (Btu) is comparative to that of coal, and superior to that of paper and wood. It should be noted that in the overall field of spent polymer treatments, the energy recovery option should be viewed as complimentary to mechanical recycling and depolymerisation, and not as a replacement for these vital components of the recycling family.

1.2.2.1. PROCESSED ENGINEERED FUEL (PEF's)

The term Processed Engineered Fuel (PEF) is that applied to a processed material composed of a mixture of waste plastics and paper. Generally supplied in the form of processed pellets, PEF is typically a low ash, high energy value product. Due mainly to the incorporation of the plastic content of this material, PEF's have heating

values in the range 7000 to 16000 Btu per pound whereas coal typically generates 9000 to 12000 Btu per pound.

One of the major advantages of PEF is the ability to use the material as fuel in existing energy supply facilities without the need for extensive modification. In addition, due to the burning characteristics of the composite, it is perceived that the material has environmental advantages over coal, in that the emission levels of both sulfur dioxide and carbon dioxide are significantly reduced relative to the fossil fuel.

1.2.3. ADVANCED RECYCLING TECHNOLOGIES

In contrast to the direct disposal and energy recovery options outlined above, focus is increasingly falling on the options of chemical and feedstock recycling of waste polymers. Collectively these technologies have become known as Advanced Recycling Technologies (ART).

Although ART is increasingly seen as the way forward in the field of polymer recycling, it remains complimentary to mechanical recycling, which is useful for the recovery of clean plastic for direct reuse in new plastic products. Mechanical recycling however is not always practical due to the inclusion of additives and colouring agents in a significant proportion of consumer polymer waste.

1.2.3.1. CHEMICAL RECYCLING

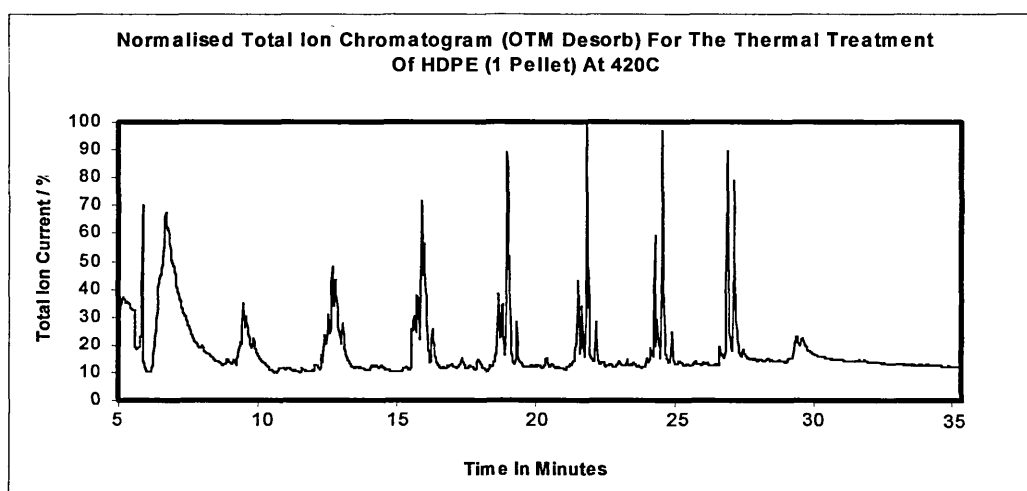
The term chemical recycling is used to describe technologies, which involve the use of chemicals to induce depolymerisation of condensation and addition polymers back to their original monomers. Typically, condensation polymers such as PETE are treated in this fashion, and the resultant monomers are blended with virgin polymer resins and formulated into new products.

1.2.3.2. FEEDSTOCK RECYCLING

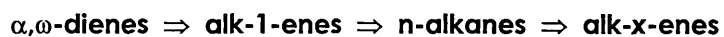
This term is applied to processes that involve the thermal depolymerisation of linear and substituted polyolefins such as HDPE, into smaller hydrocarbon intermediates. Depending upon the conditions used to execute the process, the resultant hydrocarbon mixture often has a chemical makeup which would allow for its application as a low grade fuel.

The following chart is a Total Ion Chromatogram recorded for the post pyrolysis molecular trap desorption of the products obtained for the pyrolysis of HDPE at 420°C in an atmosphere of Nitrogen. (Figure 5).

Figure 5 - Total Ion Chromatogram For The Pyrolysis Of HDPE At 420°C



The work, reported by Breen et al⁸, identified the characteristic quartets (figure 5) attributed to an homologous series of saturated and unsaturated hydrocarbons. Mass spectrometric analysis based on individual molecular fragmentation patterns allowed for the identification of the quartet components, in order of increasing retention time, as follows;



⁸ C. Breen & P. M. Last, *Journal of Materials Chemistry*, **9** (1999) 813 – 818.

The product mixture from such a treatment of HDPE can therefore be seen to yield a range of hydrocarbons, a significant proportion of which are unsaturated. Such a hydrocarbon mixture has limited application as a fuel due to the lower combustion temperatures required by hydrocarbons containing single or multiple double bonds, when compared directly to saturated materials.

The author noted that the levels of branched materials seen in the product mixture were low, particularly in the case of the higher carbon number analogues. In addition the level of aromatics seen was extremely low, although such observations are in agreement with others.^{9,10,11}

1.2.4. CATALYTIC TRANSFORMATION

As interest in the field of polymer recycling has grown, so too has an interest in the incorporation of catalysts into existing ART programmes. Numerous research groups have used catalytically active materials to alter the chemical makeup of intermediate mixtures obtained through established feedstock recycling technologies.

Zhibo et al¹² have shown that the catalytic transformation of the gases evolved during the pyrolysis of plastic waste, can lead to the production of product mixtures containing levels of aromatic and branched hydrocarbons which are significantly elevated above those found in uncatalysed product mixtures. The importance of the aromatic and branched species lies in the octane rating of fuels intended for use in combustion engines. Typically, the higher the octane rating, the smoother the process of fuel burning within the engine.

⁹ W. McCaffery, M. Kamal & D. Cooper, *Polymer Degradation and Stability*, **47** (1995) 133.

¹⁰ A. Uddin, K. Koizumi, K. Murata & Y. Sakata, *Polymer Degradation and Stability*, **56** (1997) 37 – 44.

¹¹ H. Kastner & W. Kaminsky, *Hydrocarbon Processing*, May (1995) 109 – 112.

¹² Z. Zhibo et al, *Catalysis Today*, **29** (1996) 303 – 308.

The following definition relates to the process by which fuel octane ratings are calculated;

'Motor or aviation gasolines are designated for knock rating by the arbitrary scale of octane number. Iso – octane (2,2,4-trimethylpentane) is given a value of 100 and n-heptane a value of 0. The octane number of the gasoline is the percentage of iso-octane in a blend with n-heptane which has the same anti-knock performance as the gasoline under standard test conditions.'

Knocking refers to a phenomenon which occurs in combustion engines when air fuel mixtures are detonated, and hence explode, prior to combustion. Knocking occurs due to the existence of low octane rated material in the petrol mixture. Table 3 below, shows the Research Octane Number (RON) determined for a series paraffinic, olefinic and aromatic hydrocarbons.¹³

Table 3 – Octane Numbers and Boiling Points for Some Hydrocarbons

COMPOUND	OCTANE NUMBER	B.Pt (°C)
Paraffins		
n - Butane	113	0
n - Hexane	19	69
n - Heptane	0	98
Isooctane	100	-
2,2,3 - Trimethylbutane	113	-
Naphthenes		
Cyclopentane	141	49
Olefins		
3 - methyl - 2 - pentene	97	68
Aromatics		
Benzene	99	80
Toluene	124	111
m - Xylene	145	139
1,3,5 - Trimethylbenzene	171	148

¹³ A. G. Buekens & H. Huang, *Resources, Conservation and Recycling*, **23** (1998) 163 – 181.

As can be seen from the data in table 3 above, materials which have high octane ratings are aromatics as well as branched aliphatics. As such, it is these types of species which are preferential for inclusion in commercial fuel mixtures, as they enhance the overall octane rating and hence the efficient combustibility of the fuel mixture.

Several interested parties have employed a range of materials as solid acid catalysts to effect the catalytic transformation of the relatively low octane hydrocarbons evolved during the thermal decomposition of waste polyolefinic polymers such as HDPE.

Nakamura and Fujimoto¹⁴ have shown that the use of an iron supported coal-derived active carbon catalyst shows excellent activity towards the liquefaction of polypropylene (PP) at low reaction temperatures. While the material demonstrated high levels of cracking activity, generation of aromatics over the surface was particularly low.

Likewise, Blazsó¹⁵ found that copper and iron chlorides could be employed to depress the occurrence of radical transfer reactions during the decomposition of polyolefins. The transition metal chlorides were also found to enhance aromatic yield, although temperatures of around 1000°C were required to promote this type of aromatisation activity via hydrogen elimination.

A much more common theme throughout such research work has been the utilisation of solid acid catalysts, and in particular acidic silica alumina's (SA) in addition to members of the zeolite family.

¹⁴ I. Nakamura & K. Fujimoto, *Catalysis Today*, **27** (1996) 175 – 179.

¹⁵ M. Blazsó, *Journal of Analytical and Applied Pyrolysis*, **51** (1999) 73 – 88.

In 1983, Uemichi and co-workers¹⁶ found that passage of post pyrolysis gases from the thermal decomposition of HDPE over acidic synthetic SA's gave rise to enhanced aromatic yields relative to the non catalysed process. Likewise, Ohkita *et al*¹⁷ were also able to illustrate the effectiveness of acidic SA's in promoting such aromatisation reactions to yield potentially fuel applicable liquid hydrocarbons.

By far the most widely employed of the synthetic acidic solids used to effect these preferential hydrocarbon reforming reactions have been the zeolites and in particular H⁺ZSM-5. It has been found that in addition to enhancing aromatic yields, zeolites can also offer the economic benefits of lower pyrolysis temperatures,¹⁰ an increase in the rate of polymer decomposition¹⁸ in addition to an increase in product selectivity, and hence individual component yield.¹⁶

Typically, one of two experimental set ups is used to execute these investigations.

1. Physical mixing of the polymer and catalyst.^{9,10,18,19,20,21,22,23}
2. Physically separating the polymer and catalyst.^{24,25,26,27}

¹⁶ Y. Uemichi, A. Ayame, Y. Kashiwaya & H. Kanoh, *Journal of Chromatography*, **259** (1983) 69 – 77.

¹⁷ H. Ohkita *et al*, *Industrial Engineering and Chemistry Research*, **32** (1993) 3112 – 3116.

¹⁸ W. Ding, J. Liang & L. L. Anderson, *Fuel Processing Technology*, **51** (1997) 47 – 62.

¹⁹ K. Liu & H. Meuzelaar, *Fuel Processing Technology*, **49** (1996) 1.

²⁰ Y. Uemichi, Y. Kashiwaya, M. Tsukidate, A. Ayame & H. Kanoh, *Bulletin of the Chemical Society of Japan*, **56** (1983) 2768.

²¹ R. Mordí, R. Fields & J. Dwyer, *Journal of Analytical and Applied Pyrolysis*, **29** (1994) 45.

²² G. Audisio, A. Silvani, P. Beltrame & P. Carniti, *Journal of Analytical and Applied Pyrolysis*, **7** (1984) 83.

²³ X. Xiao, W. Zmierczak & J. Shabtai, *Div. Fuel Chem.*, **40** (1995) 4.

²⁴ P. L. Beltrame, P. Carniti, G. Audisio & F. Bertini, *Polymer Degradation and Stability*, **26** (1989) 209.

²⁵ T. Yoshida, A. Ayame & H. Kanoh, *Bulletin of the Japanese Petroleum Institute*, **17** (1975) 218.

²⁶ C. Vasile, P. Onu, V. Barboiu, M. Sabliovschi, G. Moroi, D. Ganju & M. Florea, *Acta Polymerica*, **29** (1998) 306.

²⁷ C. Vasile, P. Onu, V. Barboiu, M. Sabliovschi, G. Moroi, *Acta Polymerica*, **36** (1985) 543.

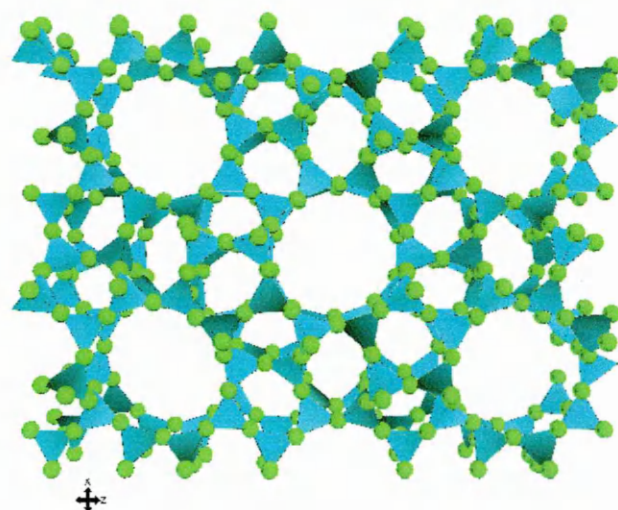
1.2.4.1. ZEOLITES

Zeolites are three dimensional, microporous, crystalline solids with well defined pore structures. Their regular framework is typically composed of aluminium, silicon and oxygen. The silicon and aluminium atoms are tetrahedrally co-ordinated and the tetrahedra link through shared oxygen atoms. The arrangement of atoms allows for the construction of a regular, well defined pore network which can host cations, water and other molecules.

Although Zeolites occur naturally, the majority of those used in commercial applications are synthetically produced. One of the most renowned zeolites is ZSM-5. Developed by the global oil consortium Mobil in 1965,²⁸ the material first found employment as a hydrocarbon cracking catalyst for crude oil feedstocks in 1983. Figure 6 shows a diagrammatic representation of the structure of the Zeolite ZSM-5;

Figure 6 – Structure of the Zeolite ZSM-5

Molecular Formula = $\text{Na}_n[\text{Al}_n\text{Si}_{96-n}\text{O}_{192}] \sim 16\text{H}_2\text{O}$



²⁸ T. F. Degnan, G. K. Chitnis & P. H. Schipper, *Microporous and Mesoporous Materials*, **35-36** (2000) 245 – 252.

It has been found that in order to effect efficient catalytic transformation of the gases evolved during the pyrolysis of polymer waste, the catalytic material must exhibit a significant degree of acidity. The role of the structural acidic sites is to promote the formation of carbonium ions on the surface of the catalyst.²⁹ This in turn allows the hydrocarbon intermediates to undergo further reactions to effect final product formation. Catalytic cracking reactions are promoted over both Brønsted and Lewis acid centres. Brønsted catalysed processes include the addition of a proton across the double bond of an olefin to generate a reactive carbocation which can subsequently crack or undergo charge or skeletal isomerisation. In the case of Lewis catalysed reactions, hydride ion abstraction from linear alkanes also induces carbocation formation, and likewise a range of secondary reactions involving the carbocation become possible. The following list gives some of the secondary transformation reactions which may occur during the passage of the pyrolysis gas through the catalyst bed;

- a. Dehydrocyclisation
- b. Hydrogenation
- c. Catalytic alkylation

1.2.4.2. ZEOLITES AS SOLID ACID CATALYSTS

The structure of many Zeolites is negatively charged due to the presence of tetrahedrally co-ordinated aluminium atoms within the molecular framework. This negative charge is balanced through the introduction of charge compensating cations. The replacement of these cations by protons allows for a convenient method of introducing strong acid sites into the material. The direct treatment of Zeolites with mineral acids results in the partial degradation of the structural framework. Therefore, compensating sodium ions are removed by washing the

²⁹ A. Korma & B. W. Wojciechowski, *Catal. Rev. Soc. Eng.*, **27** (1985) 29.

material with ammonia, which results in one for one exchange of ammonium for sodium ions. The material is then heated to approximately 500°C. The calcination process causes decomposition of the ammonium ion, with the resultant loss of ammonia and the residence of protons in place of the original sodium cations.

While there is no doubt that Zeolites have proved an invaluable test bed for the process of post pyrolysis catalytic transformation of polymer waste, the relatively high cost of producing these materials synthetically has and will continue to limit their application on a commercial scale.

Examinations of the potential candidates to provide a competitor to Zeolites shows that clay minerals appear to present an excellent alternative. It is perhaps not by coincidence that these materials found employment in the petroleum industry during the 1960's, when they were used as cracking catalysts. Following the development of Zeolites, with their increased control over the cracking parameters, clay minerals were rapidly made redundant.

CHAPTER TWO

Clays and Clay Minerals

2. INTRODUCTION TO CLAY MINERALS

Despite the technological advances which have occurred throughout the latter part of the twentieth century, including the elucidation of the structure of Deoxyribose Nucleic Acid (DNA), the advent of mobile telecommunications and the propulsion of manned missions into space, there is still no universally accepted definition of what precisely constitutes a clay or clay mineral.

2.1. CLAY MINERALS

One of the earliest attempts at defining a clay mineral was made by Agricola²⁹ (1546), who believed clays to be members of the earth element due to their being cold and dry to the touch. Agricola defined earth elements as being;

“a simple mineral body which can be worked with the hands when it is moistened, and from which a mud can be made when it is saturated with water”

A more recent definition of what exactly constitutes a clay mineral was given by Grim²⁹ (1953);

“In general, the term clay implies a natural, earthy, fine grained material which develops plasticity when mixed with a limited amount of water”

Despite the fact that these definitions are separated by almost four hundred years, they essentially convey the same information. In a geological context, the term clay is used as a reference to particle size, and a clay is considered to have a particle size <4 μm .³⁰ However, more recently, high purity minerals are considered to have a size fraction of <2 μm .³¹

³⁰ R.E. Grim, Applied Clay Mineralogy, McGraw Hill, New York, 1962.

³¹ S. Guggenheim & R. T. Martin, Definition of Clay and Clay Mineral: Joint Report of the AIPEA Nomenclature and CMS Nomenclature Committees, *Clays and Clay Minerals*, **43** (1995) 255 – 256.

As a result of their structural variety and 'unusual' properties, clay minerals have found employment in a vast range of applications throughout the centuries. Indeed, upto 25,000 years ago, these versatile materials were used for making pots and vessels by ancient civilisations. Likewise, the often excellent adsorption properties of clay minerals were recognised and appreciated by the ancient Greeks and Romans. In modern society, clays continue to form an important sub section of materials science. In addition, due to their many advantageous properties such as high resistance to atmospheric conditions, ease of access to geochemically pure material and relatively low cost, clays continue to serve as raw materials in a variety of industrially and commercially viable situations. Table 4 below lists some of the common uses of three of the most economically important classes of clay minerals.³²

Table 4 – Common Uses of Industrially Important Clay Minerals

KAOLINITES	SMECTITES	PALYGORSKITE
Paper Coatings	Drilling Muds	Drilling Fluids
Paper Filling	Foundry Sand Bonding	Paint
Paint Extenders	Pelletising Iron Ores	Agricultural Carriers
Ceramic Ingredients	Sealants	Industrial Floor Adsorbents
Rubber Fillers	Animal Feed Bonds	Tape Joint Compounds
Plastic Fillers	Bleaching Edible Oils	Litter Box Adsorbents
Ink Extenders	Agricultural Carriers	Suspension Fertilisers
Cracking Catalysts	Litter Box Adsorbents	Animal Feed Bondants
Fibreglass	Adhesives	Catalyst Supports
Cement	Pharmaceuticals	Adhesives
Adhesives	Emulsion Stabilisers	Paper
Enamels	Desiccants	Pharmaceuticals
Pharmaceuticals	Catalysts	Anti-Caking Agents
Crayons	Cosmetics	Reinforcing Fillers
Molecular Sieves	Paint	Environmental Adsorbents

2.1.1. THE STRUCTURE OF CLAY MINERALS

As indicated previously, clay minerals are used in a wide range of applications. Examination of the structure of clays provides an insight into the structure - activity relationships of these materials.

³² H. H. Murray, *Applied Clay Science*, **17** (2000) 207 – 221.

The roots of modern clay science can be traced back to the early 1920's, and in particular to the advent of X-Ray Diffraction (XRD). Pioneering XRD studies on clays, carried out by Hadding³³ and Rinnie³⁴ indicated that clay minerals were typically composed of crystalline material. Such observations ran contrary to the belief of the scientific community of the time that clays were amorphous in nature. Subsequent work by Ross³⁵ and Hendricks,^{36,37} along with their respective co-workers confirmed these preliminary findings.

In 1930, Pauling^{38,39} published further XRD work on a range of clay minerals. These results indicated that despite a significant variation in the chemical composition over the range of materials studied, the dimension of their unit cell in the plane of cleavage was very similar in all cases, falling in the range 5.1Å to 8.8Å. These results led Pauling to propose that clays are formed from the joining of individual layers of material to form extensive two dimensional sheets. The occurrence of this sheet type morphology has given rise to the term phyllosilicates in respect of clay minerals. This term translates literally as 'leaf like silicates' and relates to the layered structure observed in clays.

Closer examination of the nature of these sheets confirms that all clay minerals are essentially composed of only two different sheet types. Joining of these sheets in a variety of arrangements gives rise to a range of mineral sub groups.

³³ A. Hadding, Eine Röntgenographische Methode Kristalline und Kryptokristalline Substanzen zu Identifizieren, *Z. Krist.*, **58** (1923) 108 – 112.

³⁴ F. Rinne, Röntgenographische Untersuchungen an Einigen Feinzerteilten Mineralien Kunstprodukten und Dichten Gesteinen, *Z. Krist.*, **60** (1924) 55 – 69.

³⁵ C. S. Ross, The Mineralogy of Clays, *Trans. 1st Int. Congr. Soil Sci.*, Washington, **4** (1927) 555 – 561.

³⁶ S. B. Hendricks, *Z. Krist.*, **71** (1929) 269 – 273.

³⁷ S. B. Hendricks & W. H. Fry, *Soil Science*, **29** (1930) 457 – 478.

³⁸ L. Pauling, *Proceedings of the National Academy of Science U.S.*, **16** (1930) 578 – 582.

³⁹ L. Pauling, *Proceedings of the National Academy of Science U.S.*, **16** (1930) 123 – 129.

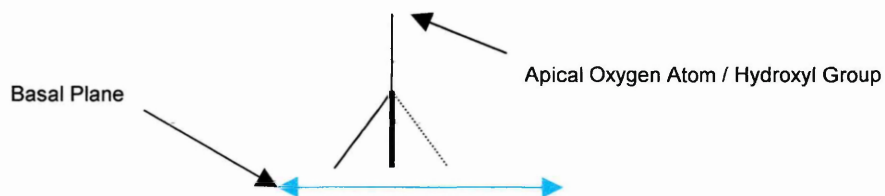
The two types of sheet identified to date can be classified as follows;

1. **TETRAHEDRAL SHEET** = Composed of individual silica or alumina tetrahedra
2. **OCTAHEDRAL SHEET** = Composed of metallic octahedra in which the resident metal ion is a divalent or trivalent cation

2.1.1.1. THE TETRAHEDRAL SHEET

The tetrahedral sheet is formed through the polymerisation of individual silica tetrahedral units (SiO_4^{4-}), such as that illustrated in figure 7.

Figure 7 – Individual Silica Tetrahedron

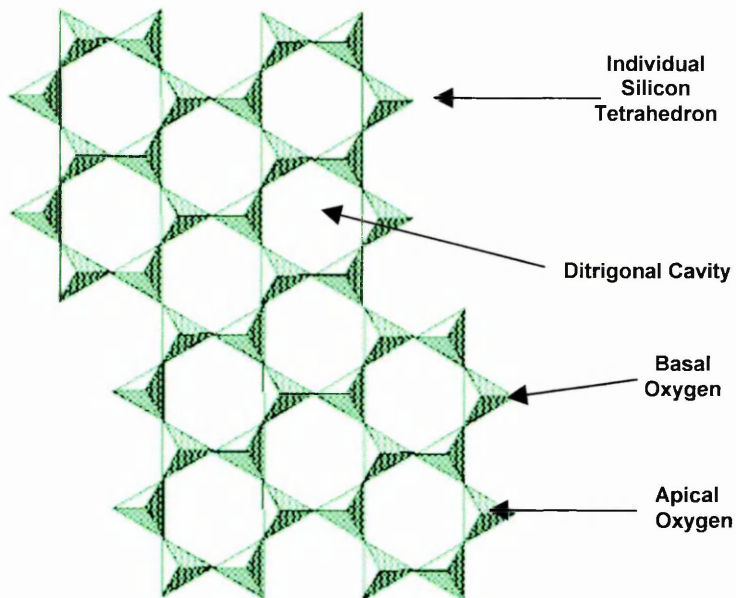


Each individual tetrahedron is composed of a silicon ion which is tetrahedrally coordinated and hence equidistant from four oxygen atoms or hydroxyl groups. In order to effect sheet formation, the basal oxygens of each of the individual tetrahedra are shared between adjacent units, the result of which is the formation of an extensive two dimensional network of silica tetrahedra, in which the apical oxygen of each individual unit is directed perpendicular to the basal plane.

Any number of the tetrahedrally associated oxygen atoms may be replaced by hydroxyl groups depending upon the location of the tetrahedron within the overall sheet structure. For instance, at loci of sheet termination, where there are no adjacent tetrahedra to complete the bonding process, exposed oxygen atoms may take up protons, from interlayer water molecules, and hence form hydroxyl groups (-OH) in order that charge neutrality be maintained over the entire sheet structure.

The result of the tetrahedral polymerisation process is the formation by the basal oxygens of the individual tetrahedral units of a sheet containing hexagonal shaped voids. Such structural voids have become known as hexagonal holes. Although the voids in the structure appear to be hexagonal, many argue that due to the existence of faults within the tetrahedral sheet, the trigonal arrangement of the basal oxygens is not strictly planar. As such, in order to overcome the technical nomenclature for the arrangement, the term 'Ditrigonal Cavity' is often applied. Figure 8 below shows the nature of the polymerisation process, and illustrates the formation and nature of the ditrigonal cavity.

Figure 8 – Ditrigonal Cavity Formation Through SiO_4^{4-} Tetrahedral Polymerisation



In terms of overall chemical composition, the infinite two dimensional polymerised sheet structure of the tetrahedral sheet can be described by the unit formula $\text{Si}_4\text{O}_6(\text{OH})_4$.

2.1.1.2. THE OCTAHEDRAL SHEET

The octahedral sheet is composed of a series of individual octahedral units which are polymerised to form a two dimensional sheet structure. Each octahedral unit has the formula $M_{2-3}(OH)_6$, where M is either a divalent or trivalent cation.

The octahedral sheet basically consists of two parallel planes of closely packed oxygen atoms or hydroxyl groups. These species in turn act as ligands for octahedrally co-ordinated metal ions, typically aluminium (Al^{3+}), magnesium (Mg^{2+}) or iron (Fe^{3+}), which are located centrally within the octahedral co-ordination sphere.

As indicated by the formula for the unit cell, the arrangement of atoms in the octahedral sheet allows for differential occupation of the available octahedral sites.

If aluminium predominates in the octahedral sheet, then on average only two out of every three available octahedral sites are occupied, and the material is said to be dioctahedral. In materials in which the octahedral sheet is rich in either magnesium or iron, all three of the available sites are occupied and the material is referred to as being trioctahedral.

Octahedral sheet residency is determined by a combination of the elements present, in addition to the overall layer structure of the material. The occurrence of oxygen atoms or hydroxyl groups within a structural unit contributes negative charge to the structure as a whole. Such negative charges are compensated for by the octahedral cations. In the case of aluminium, the element is present as the ionic species Al^{3+} , whereas the smaller magnesium ion occurs as Mg^{2+} . Therefore for each aluminium cation present in the layer structure of a clay mineral, a total of 1.5 of the ionic Mg species are required to achieve the same compensating effect, the result of which is differential residency.

2.1.2. THE PHYLLOSILICATES

As indicated previously, the phyllosilicates or layer silicates are formed through the condensation of individual tetrahedral and octahedral sheets to form extensive two dimensional layered structures.

The ratio and arrangement of the differing sheet types provides the basis of the classification system for clay minerals. The combination of tetrahedral and octahedral sheets to form layered materials is facilitated by the fact that the individual component sheets have almost identical dimensions. In addition the individual sheets exhibit symmetry which allows for the sharing of oxygen atoms between the two different sheet types, a process which results in the formation of bonds and hence joining of the sheets to form layers.

2.1.2.1. DIMORPHIC CLAY MINERALS

The joining of an individual silica tetrahedral sheet to an individual octahedral sheet results in the formation of a dimorphic mineral of which Kaolinite is perhaps the most widely studied example. Such minerals are also known as 1:1 or T:O (Tetrahedral : Octahedral) minerals.

2.1.2.2. TRIMORPHIC CLAY MINERALS

In contrast to dimorphic clays, the trimorphic analogues are formed from the condensation of a single octahedral sheet sandwiched between two individual tetrahedral sheets. Such morphology results in the materials being referred to as 2:1 or T:O:T type clays.

Figure 9 below is a diagrammatic representation of the layer structure of a trimorphic clay mineral, and clearly shows the existence of the bonds which allow for joining of the individual sheets to form the layered structure observed in clay minerals.

Figure 9 – The Effect of Sheet Condensation To Effect Layer Formation (2:1 Clay)

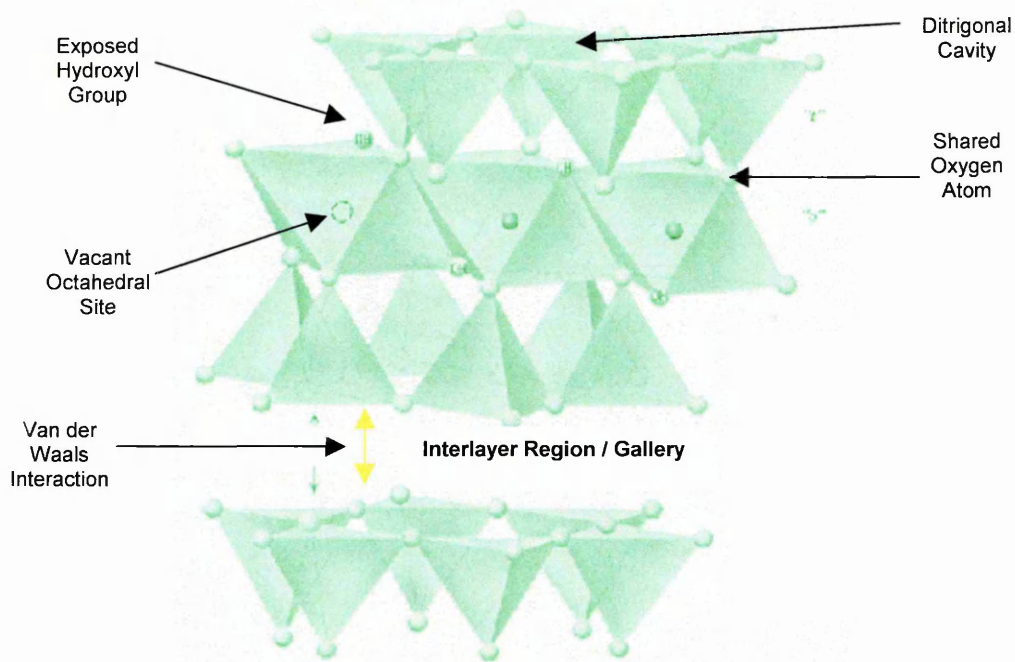


Table 5 – Sub Classification of Trimorphic Clay Minerals

GROUP	SUBGROUP	NAME	SPECIES	CHARGE
Pyrophyllite-Talc	Diocahedral	Pyrophyllites	Pyrophyllite	$\cong 0$
	Triocahedral	Talcs	Talc	$\cong 0$
Smectite	Diocahedral	Smectites or Montmorillonites	Montmorillonite Beidellite Nontronite	$\cong 0.25 - 0.6$
	Triocahedral	Smectites or Saponites	Saponite Hectorite Sauconite	$\cong 0.25 - 0.6$
Vermiculite	Diocahedral	Vermiculites	Dioc. Vermiculite	$\cong 0.6 - 0.9$
	Triocahedral	Vermiculites	Trioc. Vermiculite	$\cong 0.6 - 0.9$
Mica	Diocahedral	Micas	Muscovite Paragonite	$\cong 1$
	Triocahedral	Micas	Biotite Phlogopite	$\cong 1$
Brittle Mica	Diocahedral	Brittle Micas	Margarite	$\cong 2$
	Triocahedral	Brittle Micas	Clintonite	$\cong 2$

As outlined previously, the octahedral sheet of clay minerals can assume either dioctahedral or trioctahedral residency. In reality, due to the phenomenon of isomorphous substitution (2.3.1.), in both the tetrahedral and octahedral sheets, many clay minerals assume a net negative charge which is compensated by the sorption of

exchangeable cations. The magnitude and location of this charge allows for a sub classification system to be applied to trimorphic clays. Table 5 above illustrates the nature of this sub classification.

2.2. SMECTITES

The smectites are by far the most widely studied of the trimorphic class of clay minerals. In addition, the materials are also of significant industrial importance, finding application in a variety of industrial situations. Differentiation between individual smectites is made on the basis of chemical composition, with different members of the group classified according to the species and location of the cations resident in the tetrahedral and octahedral sheets.

2.3. PROPERTIES OF SMECTITES

As highlighted previously, smectites are used in a vast range of commercially viable applications. Such a diverse range of uses can be attributed to the variable properties that they exhibit due to structural variations seen through the smectite mineral class.

2.3.1. ISOMORPHOUS SUBSTITUTION

Variability in chemical composition arises through a process known as isomorphous substitution in which internal substitutions result in the replacement of Al^{3+} in the octahedral sheet by ions of similar size but different and usually lower valency (eg. Mg^{2+} or Fe^{2+}), and to a lesser extent the replacement of Si^{4+} by Al^{3+} in the tetrahedral sheet.⁴⁰ The former process accounts for the transformation of dioctahedral minerals into trioctahedral species. Table 6 gives the idealised formulae for the more important members of the smectite class of clay minerals.

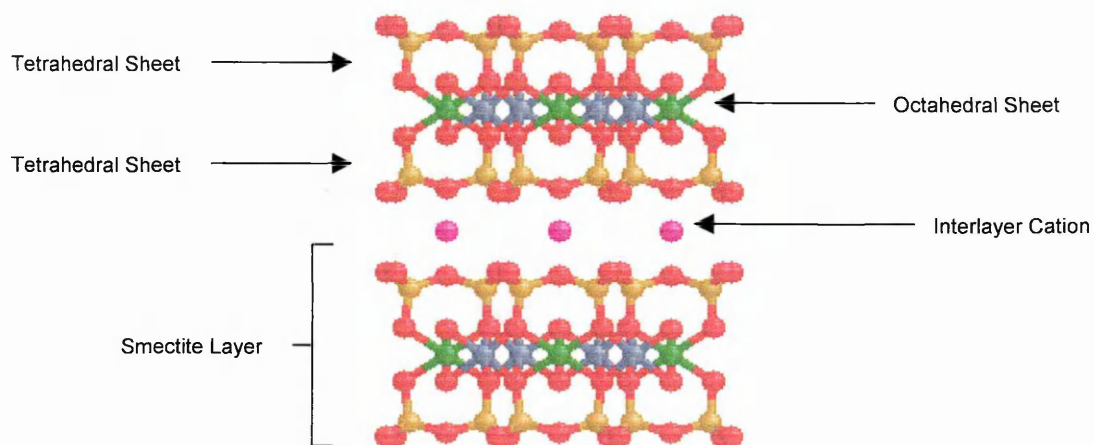
⁴⁰ C. T. Johnston, Sorption of Organic Compounds on Clay Minerals: A Surface Functional Group Approach, 1-44 in: Organic Pollutants in the Environment (ed. B. L. Shawhney) Clay Mineral Society Workshop, Lecture 8, Boulder, CO, USA, 1996.

Table 6 – Theoretical Formulae For Idealised Smectites

Location of Layer Charge	Trioctahedral Smectites	Diocahedral Smectites
Octahedral	Hectorite $(Mg_{6-x}Li_x)(Si_8)O_{20}(OH)_4.xM^+$	Montmorillonite $(Al_{4-x}Mg_x)(Si_8)O_{20}(OH)_4.xM^+$
Tetrahedral	Saponite $(Mg_6)(Si_{8-y}Al_y)O_{20}(OH)_4.yM^+$	Beidellite $(Al_4)(Si_{8-y}Al_y)O_{20}(OH)_4.yM^+$

Such isomorphous substitutions alter the charge balance within the material, and as such, the structures of most smectites have a variable, structure dependant, net negative charge which becomes delocalised over the entire layer accommodating the substitution.⁴¹ This charge is balanced by the adsorption of non structural cations which may associate themselves with the external surfaces of the clay, or be resident in the interlayer region of the material (Figure 10).

Figure 10 – Association of Interlayer Cations and Smectite Structure



⁴¹ R. W. Grimshaw, *Chemistry and Physics of Clays*, Benn, London, 1971.

The compensating cations are not fixed in the mineral structure and as such are exchangeable, typically with ions of higher valency replacing those of lower valency. The higher valency replacement ions are generally associated more tightly to the interlayer exchange sites than the ions they replace, primarily as a consequence of enhancements in the magnitude of the attractive electrostatic forces between the cation itself, and the negatively charged mineral surface. In naturally occurring smectites, Ca^{2+} , Mg^{+} , Na^{+} and K^{+} predominate as charge compensating exchangeable cations.⁴²

2.3.2. CATION EXCHANGE CAPACITY (C.E.C)

As highlighted previously, the charge compensating cations resident in smectites are not fixed in position, and as such are exchangeable. The C.E.C acts as a measure of the cation storage ability of a given mineral, and in doing so provides an indication of the charge imbalance imparted to the mineral structure as a result of isomorphous substitution. High layer charge smectites can exchange in excess of 100 millimoles of M^{+} per 100g of clay.

As highlighted in table 4, smectites play an important role as agricultural carriers in soils by fulfilling crucial roles in the supply of nutrients and water to growing plants. As a result of their cation exchange capabilities, smectites are able to act as negatively charged colloidal bridges, and thus promote the supply of essential nutrients from the weathering of primary minerals within the soil matrix, to plant rootlets, via a process of proton exchange.⁴³

It has been shown that charge compensating cations resident in the interlayer region of a smectite clay are more readily exchangeable than those associated with the

⁴² G. W. Brindley & g. Brown, *Crystal Structure of Clay Minerals and their X-Ray Identification*, Mineralogical Society, London, 1980.

⁴³J. Konta, *Applied Clay Science*, **10** (1995) 275 – 335.

surface exchange sites.⁴⁴ The exchangeability of charge compensating cations of smectite structures in aqueous suspensions containing a secondary cationic species is governed by a number of key factors;

1. The magnitude of the layer charge on the mineral.
2. The properties of the interlayer cation (hydration energy, size, valency).
3. The relative concentration of the secondary cationic species.
4. The population of exchange sites on the clay.

As a general rule, physically small, high valency metal cations are highly effective at displacing and replacing charge compensating cations resident in the interlayer region of smectite minerals.^{45,46}

2.3.2.1. DETERMINATION OF THE C.E.C.

Throughout the years, a variety of methods have been developed to allow for the determination of the C.E.C. of smectites. The following represents some of the more popular methods for the determination of this parameter;

1. Uptake by the clay of the ammonium ion species (NH_4^+).⁴⁷
2. Exchange of the clay with Methylene Blue.⁴⁸
3. The adsorption of the coloured species Cobalt Sulphate.⁴⁹
4. Rapid methods involving the uptake of a Cu-ethylenediamine complex.⁵⁰

⁴⁴R. E. Grim & G. Kulbicki, *American Mineralogist*, **46** (1961) 1329 – 1369.

⁴⁵R. E. Grim & R. H. Bray, *Journal of the American Ceramics Society*, **19** (1936) 307 – 315.

⁴⁶R. W. McCabe, *Clay Chemistry: Inorganic Materials* (eds. D. W. Bruce & D. O'Hare) John Wiley & Sons, England (1996) 314 – 363.

⁴⁷R. H. S. Robertson & R. M. Ward, *Journal of Pharmacy and Pharmacology*, **3** (1951) 27 – 35.

⁴⁸G. W. Brindley & T. D. Thompson, *Israel Journal of Chemistry*, **8** (1970) 409 – 415.

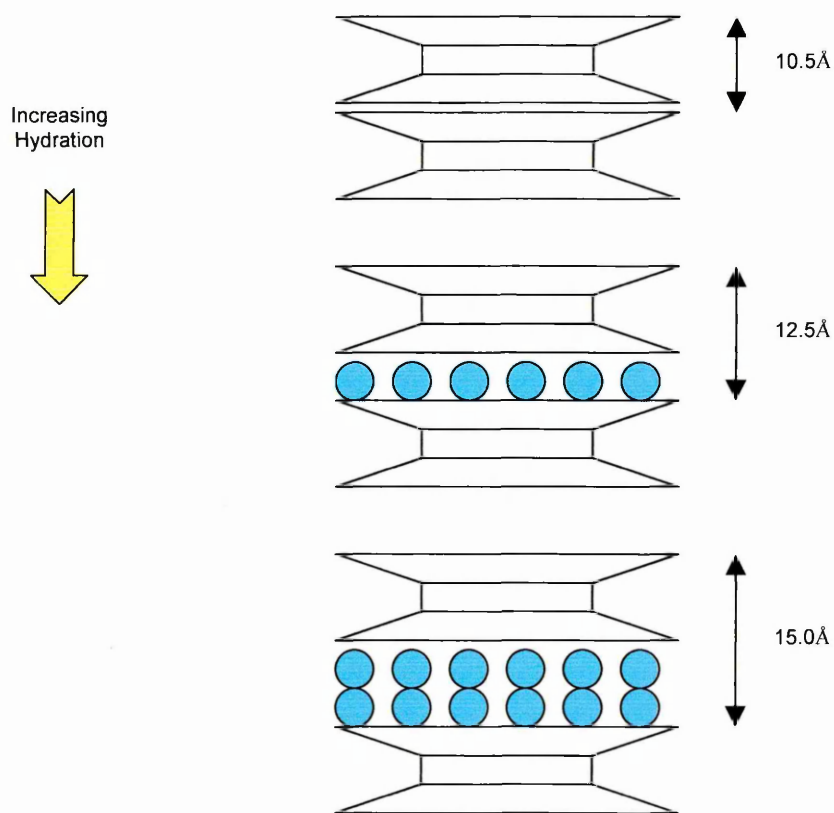
⁴⁹C. N. Rhodes & D. R. Brown, *Clay Minerals*, **29** (1994) 799 – 801.

⁵⁰F. Bergaya & M. Vayer, *Applied Clay Science*, **12** (1997) 275 – 280.

2.3.3. HYDRATION & SWELLING CAPACITY OF CLAYS

The most renowned characteristic of the smectite mineral class is their ability to swell. This process occurs through the intercalation of water molecules into the interlayer or gallery regions of the mineral structure between each of the individual layers. The effect of this water adsorption is an increase in the basal spacing of the material as determined by XRD. Dehydrated smectites typically show basal spacings of 9.6Å to 11.0Å, which when hydrated can be increased to anywhere between 12.5Å and 20.0Å (Figure 11), with the exact value being determined by the type of clay, and the nature, including hydration energy, of the charge compensating cation.^{51,52}

Figure 11 – Swelling States of Smectite Minerals



⁵¹ P. F. Low, I. Ravina & J. L. White, *Nature*, **226** (1970) 445 – 446.

⁵² B. Velde, *Composition and Mineralogy of Clays: Origin and Mineralogy of Clays, Clays and the Environment*, Springer, Berlin, 1995.

The individual T:O:T units in smectite clays are commonly referred to as layers and are held together by weak interlayer electrostatic attractive forces. It is due to these relatively weak electrostatic forces that clay minerals are able to swell. The presence of water molecules in the interlayer region promotes the separation of the individual layers. In cases where the interlayer cation has a significant hydration energy, as is the case with sodium, there is a tendency for the formation of many orientated water layers on lamellar surfaces. In extreme circumstances, the degree of swelling may result in the complete dissociation of the individual layers from each other and thus disintegration of individual tactoids (mineral multi layer stacks). The result of such an event is the formation of a colloidal solution of the clay.⁵³

Interlamellar water in smectites can be divided into 3 distinct regions. Table 7 below identifies the nature of this classification.⁵⁴

Table 7 – Classification of Interlamellar Water in Smectites

CLASSIFICATION	DESCRIPTION
A_m	Water molecules which form the hydration spheres of the interlayer charge compensating cations.
A_o	Water molecules which form clusters which reside in the spaces between the hydrated interlayer cations.
B_{om}	Disordered water molecules filling the gaps between the former two structured regions of water.

⁵³ I. E. Odom, *Phil. Trans. R. Soc. Lond.*, **A311** (1984) 391 – 409.

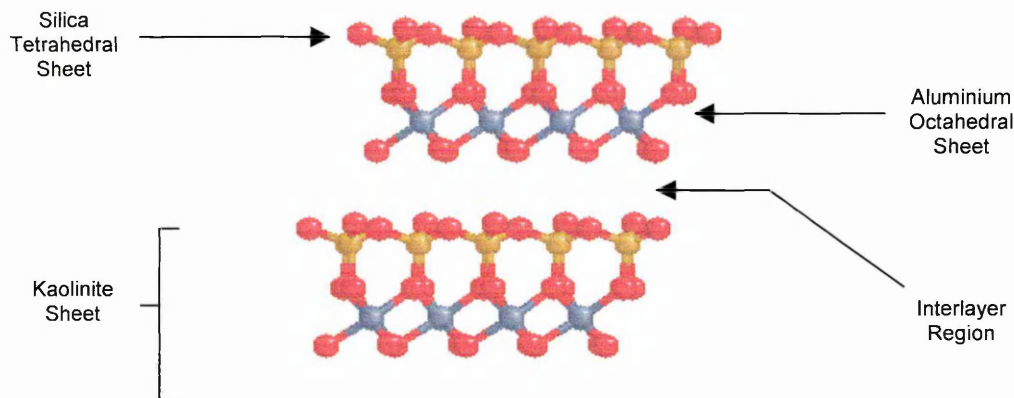
⁵⁴ S. Yariv, *Modern Approaches to Wettability: Theory and Applications* (eds. M. E. Schrader & G. Leob) Plenum Publishing Corporation, New York (1992) 279.

2.4. KAOLINITES

Kaolin or kaolinite is the most widely studied member of the dimorphic class of clay minerals. In fact, the kaolinites represent only one subgroup of this class. Whereas kaolin is a dioctahedral mineral, the other member of the group, the serpentines are trioctahedral, and in contrast to Kaolin have received very little attention.

The idealised formula for kaolin is $Al_4Si_4O_{10}(OH)_8$, and its structure is given in figure 12. Other members of the dioctahedral kaolinites include dickite and nacrite (which exhibit isomorphous substitution in their tetrahedral and octahedral sheets respectively), and it has been shown that throughout the three polytypes, there is little variation in composition, and indeed little variation from the ideal.

Figure 12 – Structural Representation of Kaolin



In contrast to smectites, the ideality of the chemical composition of kaolin infers that the overall structure is electrically neutral. However, in reality, small amounts of isomorphous substitution^{55,56,57} do occur, and this results in the formation of a slight residual negative charge being assumed by the mineral structure. In addition, this substitution imparts a small degree of cation exchange capacity to the clay. While

⁵⁵ R. K. Schofield & H. R. Samson, *Clay Minerals Bulletin*, **2** (1953) 45 – 51.

⁵⁶ R. H. S. Robertson, G. W. Brindley & R. C. Mackenzie, *American Mineralogist*, **39**, (1954) 118 – 1398.

⁵⁷ J. P. Quirk, *Nature*, **188** (1960) 253 – 254.

smectites experience isomorphous substitution in both the tetrahedral and octahedral sheets, it has been proposed⁵⁸ that kaolin only experiences substitution in the tetrahedral sheet, thus inferring that this remains the primary location of the cation exchange sites. Further studies involving electron-optical work have provided support for this view.^{59,60}

As can be seen by reference to the Kaolin structure in figure 12 above, the crystal structure of the mineral results in the exposed aluminol groups (AlOH) on the upper surfaces of the octahedral sheet of one layer, coming into close proximity to the silica tetrahedral sheet of the adjacent layer. This gives rise to an intimate hydrogen bonding situation. As a consequence of this, and in combination with the non specific electrostatic interactions which arise through isomorphous substitution, intercalation of cations or organic molecules into the interlayer region of kaolin is potentially difficult. In this respect, adsorption of species by kaolin usually occurs at the external surfaces of the mineral. As a result, the external surfaces of Kaolin, and in particular the unsatisfied valencies (broken bonds) which occur at loci of sheet termination are of critical importance, as they account for upto 20% of the total surface area of the crystal, some $40 \times 10^3 \text{ m}^2 \text{ kg}^{-1}$.^{57,61} In the case of smectites, such unsatisfied valencies account for only 2-3% of the total surface area (both interlayer and external surfaces), and as such are of significantly less importance.

A kaolin derivative of interest to mineralogists is halloysite, which although structurally similar to kaolin, contains layers of interposed water molecules between each successive kaolin layer.

⁵⁸ U. Hofmann, H. P. Boehm & W. Gromes, *Z. anorg. allgem. Chem.*, **308** (1961) 143 – 154.

⁵⁹ A. Weiss & J. Russow, *Proceeding of the International Clay Conference – Stockholm*, **1** (1963) 203 – 213.

⁶⁰ E. A. C. Follett, *Journal of Soil Science*, **16** (1965) 542 – 545.

⁶¹ G. H. Cashen, *Transaction of the Faraday Society*, **55** (1959) 477 – 486.

2.5. THE THERMAL BEHAVIOUR OF CLAY MINERALS

Clay minerals are hydrous phyllosilicates which by definition have small particle sizes. The magnitude of their particle dimensions is of importance in the study of the thermal behaviour of clays.

The thermal reactions of clay minerals can be separated into three distinct temperature regimes;

1. Low Temperature Reactions (Up to about 400°C)

Typically involves the loss of water composing the hydration spheres of charge compensating cations from the interlayer region of smectite minerals. In the case of kaolin, water molecules hydrogen bonded to the external surfaces of the mineral are removed over this temperature range. Such thermal reactions are grouped and referred to as dehydration reactions.

2. Intermediate Temperature Reactions (400 – 750°C)

Involves dehydroxylation, and the formation of quasi-stable dehydroxylated phases. Pre-dehydroxylation, some minerals experience proton delocalisation,^{62,63} and will be considered under this category.

3. High Temperature Reactions (750°C +)

Typically, recrystallisation reactions occur at such high temperatures, with the resultant formation of new phases. It is not uncommon for reactions classified as intermediate and high temperature reactions to occur simultaneously.

⁶² J. J. Fripiat & F. Toussaint, *Journal of Physical Chemistry*, **67** (1963) 30 – 36.

⁶³ G. C. Maiti & F. Freund, *Clay Minerals*, **16** (1981) 395 – 413.

2.5.1. LOW TEMPERATURE REACTIONS

Until relatively recently, the low temperature reactions of smectites were believed to involve only the removal of water molecules forming the hydration sphere of interlayer and surface exchange site charge compensating cations. Increased understanding of the precise nature of the water environments found in the interlayer region of smectites⁵⁴, led to a renewed interest into the field of mineral dehydration.⁶⁴ Malek et al,⁶⁵ have shown through the use of emanation thermal analysis⁶⁶ that smectite dehydration is in fact a three stage process. Initially, weakly adsorbed, non structured water (zone B_{0m}) is evolved from the interlayer. At higher temperatures, water of hydration is stripped from the charge compensating cations. Finally, it was found that in dioctahedral smectites, the exposed cations undergo migration, through the ditrigonal cavities of the silicate layer and become fixed in the structure. This final stage leads to collapse of the clay structure. The same cation migration is observed in trioctahedral minerals, although the process occurs at much higher temperatures. In addition, it has been shown that the thermal dehydration of smectites with tetrahedral substitutions have higher molar dehydration energies when compared to minerals with little or no such substitution.⁶⁷ This observation was attributed to differences in the surface basicity of the oxygen plane in the smectite structure. Substitution of Al³⁺ for Si⁴⁺ in the tetrahedral sheet increases the basic character of the sheet, and in doing so promotes the formation of hydrogen bonds between the interlayer water molecules and the exposed mineral surfaces, therefore interlayer and hydration waters are held to higher temperature.

⁶⁴ M. Foeldvari, in *Thermal Analysis in the Geosciences* (eds. W. Smykatz-Kloss & S. St. J. Warne) Springer-Verlag, Berlin (1991) 84.

⁶⁵ Z. Malek, V. Balek, D. Garfinkel-Shweky & S. Yariv, *Journal of Thermal Analysis*, **48** (1997) 83 – 92.

⁶⁶ V. Balek, *Thermochimica Acta*, **192** (1991) 1.

⁶⁷ S. Yariv et al, *Thermochimica Acta*, **207** (1992) 103.

2.5.1.1. CATION MIGRATION

It has been shown that when montmorillonites containing charge compensating cations of small radius ($<0.7\text{\AA}$) are heated to temperature between 200 and 300°C, they undergo a reduction in their C.E.C. and have limited expandability when rehydrated. This observation was first made by Hofmann and Klemen⁶⁸ using Li⁺ exchanged clays. These findings were supported by the work of Greene-Kelly⁶⁹ who demonstrated that trioctahedral minerals, with no octahedral vacancies, do not behave in a similar fashion. Likewise beidellite, with its Al³⁺ for Si⁴⁺ tetrahedral substitution does not share this type of behaviour with montmorillonites.

Again using Li⁺ saturated montmorillonites, Calvet and Prost⁷⁰ were able to show that lattice charges arising from octahedral substitutions are probably localised within the sheet at positions of isomorphous substitution. The result of cation migration is to create local trioctahedral configurations, and to induce partial neutralisation of the layer charge, an observation which accounts for the reduction in the C.E.C. of heat treated montmorillonites as recorded previously.⁶⁸

This heat induced relocation of dehydrated interlayer cations, into vacant octahedral sites allows for a degree of control to be achieved over the layer charge and hence the swelling and expansion properties of montmorillonites.

More recently Ertem⁷¹ has suggested that in addition to occupying vacant octahedral sites, post migration, these cations may react with structural hydroxyl groups to yield protons as noted by Russell and Farmer.⁷²

⁶⁸ V. Hofmann & R. Klemen, *Z. Anorg. Allg. Chem.*, **262** (1950) 95 – 99.

⁶⁹ R. Greene-Kelly, *Mineralogical Magazine*, **30** (1955) 604 - 615.

⁷⁰ R. Calvet & R. Prost, *Clays and Clay Minerals*, **19** (1971) 175 – 186.

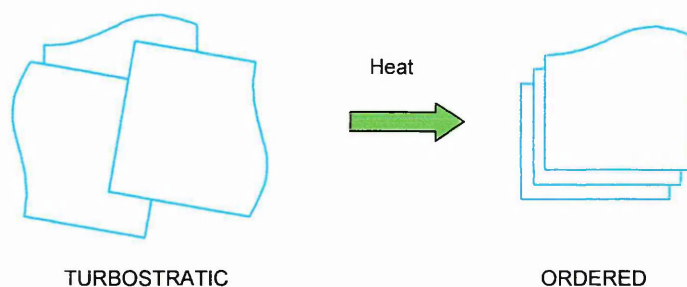
⁷¹ G. Ertem, *Clays and Clay Minerals*, **20** (1972) 199 – 205.

⁷² J. D. Russell & V. C. Farmer, *Clay Mineral Bulletin*, **5** (1964) 443 – 464.

2.5.1.2. STRUCTURAL REORGANISATION

XRD data has indicated⁷³ that cation migration may have the effect of installing ordered layer stacking to smectites. In their natural state, the structure of smectites is turbostratic, a structural orientation which it is believed to allow for more effective local neutralisation of layer charges in contrast to regular ordered stacking. The effect of local sheet neutralisations as a result of cation migration is to reduce the necessity of the mineral to exhibit turbostratic layer orientations. Figure 13 below illustrates the effect on layer stacking of this transformation.

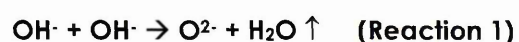
Figure 13 – Structural Reorganisation Resulting from Cation Migration



2.5.2. INTERMEDIATE TEMPERATURE REACTIONS

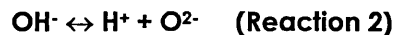
At temperatures above 450°C, clay minerals undergo a structural change known as dehydroxylation. This process involves degradation of the structural integrity of the material through the loss of water molecules formed from the release of hydroxyl groups associated with the octahedral sheet of the mineral.

In the most basic of terms, dehydroxylation can be considered to be a proton transfer event, represented by the following equation;



⁷³ J. Mering & R. Glaeser, *C.r. hebd. Seanc. Acad. Sci.*, Paris, **265** (1967) 1153 – 1156.

In reality, the overall process is more likely to be the result of two separate processes operating independently. Reactions 2 and 3 below illustrate the nature of these processes.



In reaction 2, one structural hydroxyl group dissociates to yield a 'free' proton, and a structural oxygen ion. The second stage (reaction 3) involves the combination of the 'free' proton with a second hydroxyl group to effect the formation of a water molecule which is subsequently lost from the structure as a result of thermal effects. The dehydroxylation process is considered to be homogeneous if reactions 2 and 3 involve the simultaneous reaction of two adjacent structural hydroxyl groups. Johnson and Kessler⁷⁴ have proposed that the rate kinetics applicable to dehydroxylation are defined by the diffusion through and expulsion of water from the mineral structure, as opposed to the rate of formation of water molecules via the proton transfer reactions given in reactions 2 and 3 above.

Bearing the above in mind, it has been proposed independently, that as a result of the ability of protons to diffuse through the mineral structure more readily than water molecules on the grounds of size, that a second dehydroxylation mechanism may exist. In the so called heterogeneous mechanism, reaction 3 may be carried out at favourable active sites on the mineral surface (donor regions). The activity of these donor sites is maintained through a flux of protons to the active sites from locations internal to the mineral structure (acceptor regions) where reaction 2 predominates.^{75,76,77} In order that electrical neutrality be maintained, the proton flux

⁷⁴ H. B. Johnson & F. Kessler, *Journal of the American Ceramics Society*, **52** (1969) 199 – 204.

⁷⁵ M. C. Ball & H. F. W. Taylor, *Mineralogical Magazine*, **32** (1961) 754 – 766.

⁷⁶ H. F. W. Taylor, *Clay Minerals Bulletin*, **5** (1962) 44 – 55.

⁷⁷ G. W. Brindley, *Journal of the Mineralogical Society of Japan*, **5** (1961) 217 – 237.

generates a counter flow of cations (Mg^{2+} , Fe^{2+} , Fe^{3+} , Al^{3+}) from donor towards acceptor regions.

In 1971, Pampuch⁷⁸ proposed that the homogeneous mechanism will predominate in minerals containing hydroxyl groups of differing acidities. The more acidic protons will react with the lesser acidic protons to form water. This process allows for an equal probability of structural water formation throughout the whole mineral crystal structure. This uniform structural disturbance promotes the formation of poorly crystalline post dehydroxylation mineral products. Evidence for the existence of different hydroxyl groups in Kaolinites has been reported through the application of vibrational spectroscopic techniques.^{79,80,81}

In contrast, in minerals in which all of the available hydroxyl groups have the same dissociation potential as detailed by reaction 2, the material is most likely to dehydroxylate via the heterogeneous mechanism, assuming that counter cation migration to the resultant structural oxygen ions is permitted. In this event, the post dehydroxylation mineral will exhibit a high degree of crystallinity relative to the parent mineral.

More recently, while studying the dehydroxylation via surface silanol groups of synthetic and natural beidellites, Kloprogge *et al*⁸² have provided supplementary evidence to the acceptor / donor region theories outlined above. They were able to show that Infra Red Emission Spectroscopy (IES) could be used as a tool to monitor the dehydroxylation of clay minerals. Liberation of hydroxyl groups from the

⁷⁸ R. Pampuch, *Bull. Grpe. Franc. Argiles*, **23** (1971) 107 – 118.

⁷⁹ R. Pampuch, M. Kawalska & W. Patak, *Pol. Acad. Nauk, Oddzial Kradowie, Pr. Kom. Ceram., Ceram.* **17** (1971) 63 – 75.

⁸⁰ P. G. Rouxhet, N. Samudacheata, H. Jacobs & O. Anton, *Clay Minerals*, **12** (1977) 171 – 179.

⁸¹ M. M. Mestdagh, A. J. Herbillon, L. Rodrique & P. G. Rouxhet, *Bull. Mineral.*, **105** (1982) 457 – 466.

octahedral sheet by recombination of two hydroxyl groups to form water, leaves behind a newly formed metal – oxygen bond in the tetrahedral sheet, as evidenced by reduction in the intensity of bands attributed to both OH bending and stretching modes. Concurrently, a new band at 3715cm^{-1} evolves at temperatures above 400°C and is attributed to silanol groups located at edge sites on the tetrahedral sheet. It is proposed that these newly formed silanols behave as active donor regions, in that they act as an intermediate holding point for hydroxyl groups evolved from the octahedral sheet.⁸²

2.5.2.1. PROTON DELOCALISATION

Investigations using vibrational spectroscopy and electrical measurements of hydrous phyllosilicates at points below their dehydroxylation temperatures, have shown that pre-dehydroxylation, these materials exhibit proton delocalisation.⁸³ Definitive evidence for this phenomenon was given when White *et al*⁸⁴ were able to demonstrate an interchange of deuterons for protons in Kaolinite at 300°C .

Subsequently, two distinct mechanisms have been identified for the conduction of protons in clay minerals.⁸⁵ In the first instance, protons which are excess to the structural requirements of the clay and as such are fully delocalised, travel along high lying energy bands known as proton conduction bands. These protons interact and exchange with the protons of structural hydroxyl groups. This represents one possible mechanism of water formation. In the second case, a free proton, known as a defect proton is displaced from the structure. This results in a cascade effect in which adjacent protons jump from one structural hydroxyl group to an adjacent O^{2-} ion. In contrast to the high energy proton conduction bands employed in excess proton

⁸² J. T. Klopogge, S. Komarneni, K. Yanagisawa, R. Fry & R. L. Frost, *Journal of Colloid and Interface Science*, **212** (1999) 562 – 569.

⁸³ J.J. Fripiat & F. Toussant, *Nature*, **186** (1960) 627 – 628.

⁸⁴ J. L. White, A. Laycock & M. Cruz, *Bull, Grpe franc Argiles*, **22** (1970) 157 – 165.

⁸⁵ G. C. Maiti & F. Freund, *Clay Minerals*, **16** (1981) 395 – 413.

conduction, defect proton conduction occurs on intermediate energy levels, and can be described as thermally activated proton tunnelling.

2.5.3. DEHYDROXYLATION PRODUCTS

Diocahedral minerals such as Kaolin and Montmorillonite give rise to quasi-stable dehydroxylated phases, whereas trioctahedral minerals tend to dehydroxylate and recrystallise concurrently.

2.5.3.1. KAOLINITE

Kaolinites have been shown to undergo dehydroxylation at about 400°C, with a resultant weight loss of 14.0%, corresponding to the structural formula $\text{Al}_2\text{Si}_2\text{O}_5(\text{OH})_4$, to yield a material known as Metakaolin. Post dehydroxylation XRD work has suggested that metakaolin is amorphous, although single crystal studies have indicated that some structural integrity is maintained. Brindley and Nakahira⁸⁶ have shown that any residual order remains within the individual layers as opposed to between layers. In addition, despite a 14.0% weight loss associated with dehydroxylation, it has been found that metakaolin differs only slightly from kaolin in respect of density,^{87,88} indicating that the layers must collapse to about the same extent, although be it in a very irregular fashion. Likewise, Brown and Gregg⁸⁸ were able to show that no surface area enhancements were achieved as a result of dehydroxylating Kaolin.

As such, it is widely believed that in metakaolin, the structural integrity of the tetrahedral sheet is maintained. Evidence indicating the relaxation of the tetrahedral sheet has also been published.⁸⁹ Data from X-Ray Fluorescence measurements (XRF)

⁸⁶ G. W. Brindley & M. Nakahira, *Journal of the American Chemical Society*, **42** (1959) 311 – 324.

⁸⁷ R. Rieke & L. Mauve, *Ber. Deut. Keram. Ges.*, **23** (1942) 119 – 151.

⁸⁸ M. J. Brown & S. J. Gregg, *Clay Minerals Bulletin*, **2** (1952) 228 – 235.

⁸⁹ G. W. Brindley & D. L. Gibbon, *Science*, **162** (1968) 1390 – 1391.

have indicated that the residual aluminium in the octahedral sheet is in four fold as opposed to octahedral coordination.^{90,91}

2.5.3.2. SMECTITES

Smectites have been shown to dehydroxylate over a wide temperature range, typically 500 to 700°C.⁹² One reason for such an extensive range of dehydroxylation temperatures is the fact that smectites contain exchangeable charge compensating cations both in their interlayer region and in surface exchange sites. Many authors have postulated that the mechanism of water release is controlled by the interlayer cation, and to a lesser degree, the charge on the outer basal oxygens.^{93,94} The dehydroxylation of certain smectites appears to be controlled by the evolution of water from the octahedral sheet, through the tetrahedral sheet, and finally, diffusion through the interlayer region.⁹⁵ More recently, results from a variety of cation exchanged montmorillonites have indicated that the observed influence of the interlayer cation and the dehydroxylation temperature could be related to thermally induced collapse of the clay. Upon dehydroxylation, small highly charged cations enter the ditrigonal cavities and allow for complete layer collapse, thus providing a restriction of flow to dehydroxylation water through the interlayer region.⁹⁶

Overall, smectite dehydroxylation is a three stage process. (1) Proton Delocalisation, (2) Localised Dehydroxylation, and (3) Loss of structural integrity .

⁹⁰ G. W. Brindley & H. A. McKinstry, *Journal of the American Ceramics Society*, **44** (1961) 506 – 507.

⁹¹ M. C. Gastuche, F. Toussaint, J. J. Fripiat, R. Touilleaux & M. van Meersche, *Clay Minerals Bulletin*, **5** (1963) 227 – 236.

⁹² J. W. Earley, I. H. Milne & W. J. McVeagh, *American Mineralogist*, **38** (1953a) 770 – 783.

⁹³ I. Horvath & L. Galikova, *Chemicke Zvesti*, **33** (1979) 604 – 611.

⁹⁴ A. F. Koster van Groos & S. Guggenheim, *Clays and Clay Minerals*, **34** (1986) 281 – 286.

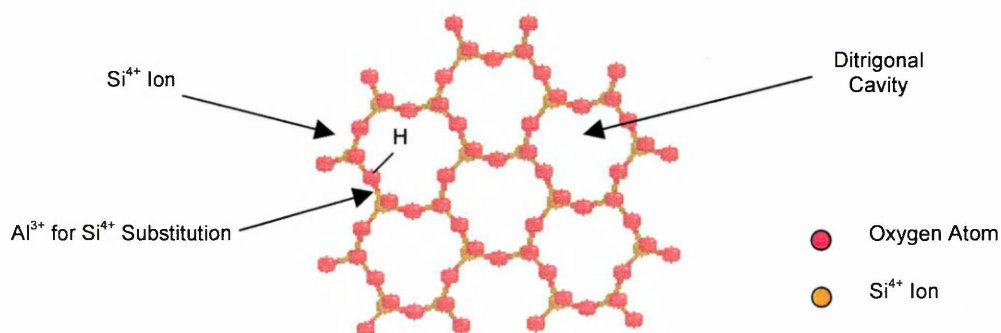
⁹⁵ H. J. Bray, S. A. T. Redfern & S. M. Clark, *Mineralogical Magazine*, **62** (1998) 647 – 656.

⁹⁶ H. J. Bray & S. A. T. Redfern, *Mineralogical Magazine*, **64(2)**, (2000) 337 – 346.

2.6. ACIDITY OF CLAY MINERALS

The basal planes of smectite clays expose the bridging oxygens of the tetrahedral sheet. These oxygen bridges interact with water molecules, and through a process of proton abstraction, structural hydroxyl groups are formed. This is particularly the case for minerals which exhibit Al^{3+} for Si^{4+} substitution in the tetrahedral sheet, such as saponites and beidellites. In these materials, Al^{3+} is forced into tetrahedral coordination, and as a consequence, the ion assumes a formal negative charge, an event which alters the polarisation of the bridging oxide bonds. This results in the formation of siloxane bridges ($\text{Si} - \text{O} - \text{Al}$) which, due to a positive inductive effect exerted by the aluminium ion over the oxygen atom, activates the oxygen in respect of its Brønsted basicity. Once activated by proton uptake, these siloxane groups yield strong Brønsted acidic structural hydroxyl groups,⁹⁷ as illustrated in figure 14 below. In addition, the structural hydroxyl groups of the octahedral sheets are also accessible through the ditrigonal cavities formed through tetrahedral sheet formation, and thus provide a further source of Brønsted acidic protons.

Figure 14 – Siloxane Bridge Formation In Smectites



The Brønsted – Lowry theory of acids and bases regards an acid as a proton donor, and a base as a proton acceptor. The electronic theory of acids and bases as described by Lewis defines an acid as an electron pair acceptor, and likewise, a

⁹⁷ J. F. Lambert & G. Poncelet, *Topics in Catalysis*, **4** (1997) 43 – 56.

base is an electron pair donor. Protons are well defined by the Brønsted theory of acids and bases. However, it should be noted that the proton (H^+) is an excellent electron pair acceptor, and as such is also classified under the Lewis acid theory as an acid. Therefore, to avoid confusion, the terms Brønsted Acid (protionic) and Lewis Acid (aprotic) should be used fully.

The acidity of untreated smectite clays has two principal sources, namely;

- 1. Compensating Cations:** These have a strong polarising effect on co-ordinated water molecules. The effect of this process is to convert these water molecules into efficient Brønsted acid sites. However, the majority of such charge compensating cations are resident in the interlayer and are not readily accessible. In this respect, acidity is dependant upon the water content of the clay and to the positions of the isomorphous substitutions giving rise to the layer charge. Typically, acidity is greatest when the water content of the clay is low, and the charge compensating cations are small and highly charged.^{98,99,100}
- 2. Layer Termination:** At specific locations on mineral layer edges at which structural sheets undergo termination, the resultant broken bonds may be coordinatively compensated by hydroxyl group formation. For instance, the breaking of a structural $\equiv Si-O-Si \equiv$ bond arrangement within the tetrahedral sheet will result in the formation of a Brønsted acid silanol group ($\equiv Si-OH$). Likewise, aluminol ($\equiv Al-OH$) and magnesol ($\equiv Mg-OH$) groups may be formed at loci of sheet termination. However, such groups are considered to be less acidic than the comparative silanol group on the grounds of the relative electronegativities of the metallic elements involved.

⁹⁸ M. M. Mortland & K. V. Raman, *Clays and Clay Minerals*, **16** (1968) 393 – 398.

⁹⁹ M. Frenkel, *Clays and Clay Minerals*, **22** (1974) 435 – 441.

¹⁰⁰ H. A. Benesi & H. C. Winquist, *Advanced Catalysis*, **27** (1978) 98 – 176.

In addition, coordinatively unsaturated Al^{3+} and Mg^{2+} are easily formed at the edges of mineral tactoids, and are capable of behaving as efficient Lewis acid centres.

Despite these factors, the edge surfaces of smectite minerals constitute no more than a maximum of 10% of the total available surface area, and as such these structural acidic features are insufficient to impart significant acidity to smectite minerals in their natural state.

Although not widely perceived, the existence of life on earth is almost certainly connected with clay. It has been proposed within the scientific community that clays played a principal catalytic role in the primordial organic reactions which led to the synthesis of the first basic organisms capable of self reproduction.^{101,102} Bearing this fundamental catalysis in mind, it is ironic that these materials have been exploited by the human race in a variety of ways including application as solid acid catalysts. It is also disheartening that many have disregarded the use of clays as catalysts in favour of employing synthetic materials. Irony again strikes in that for many of these synthetic alternatives, clays have proven to be an effective chemical and structural template.

As highlighted previously, in contrast to some alternatives, clay minerals represent a cheap, widely available raw material. In respect of their natural levels of acidity, they are also ideally suited for application as solid acid catalysts. However, due to the impoverished levels of acidity exhibited by many smectites, their application in some of the more industrially useful applications of solid acid catalysts is limited.

¹⁰¹ A. G. Cairns-Smith & H. Hartman (eds) *Clay Minerals and the Origin of Life*, Cambridge University Press, Cambridge, (1986).

¹⁰² S. Yuasa, *Journal of the Clay Science Society of Japan*, **29** (1989) 89 – 96.

This in turn has led to the development of a variety of treatments which can be employed to enhance the acidity of clay minerals. There are three principal methods of enhancing the acidity of clays which have been developed to promote their widespread application in situations which through factors such as corrosion protection and waste solvent disposal treatments, hold a requirement for the use of solid acid catalysts. These three treatments are listed below;

1. Ion Exchange Activation.
2. Acid Activation.
3. Activation through Pillaring.

2.7. ION EXCHANGE ACTIVATION

In naturally occurring clays, the predominant interlayer and surface exchange site charge compensating cations⁴² are Na⁺, Ca²⁺ and K⁺. Such cations exert little polarising effect on coordinated water molecules, and this accounts for the relatively low levels of acidity exhibited by naturally occurring clay minerals.

One method which allows for the natural acidity of clays to be increased, and therefore for their catalytic activity to be enhanced is through the process of ion exchange activation.

2.7.1. THE PROCESS OF ION EXCHANGE ACTIVATION

The process of exchanging the resident interlayer and surface exchange site charge compensating cations of smectite minerals can be achieved simply by immersing the clay in an aqueous solution containing the appropriate cation, and then washing.

2.7.2. THE EFFECTS OF ION EXCHANGE ACTIVATION

Under standard conditions of temperature and pressure, the interlayer cations of smectite minerals are hydrated (Table 7), despite this, they are readily exchangeable. Those cations found naturally in clays can be removed and replaced with highly charged, small radii cations such as Al³⁺, Cr³⁺ and Fe³⁺,¹⁰³ through the simple process outlined above. Studies involving the use of montmorillonites exchanged with these ions have shown them to possess higher levels of catalytic activity than the naturally occurring mineral.¹⁰⁴ Attribution of this enhanced catalytic activity has been given to the increased polarisation of water molecules in the Am zone of the exchanged cations.^{105,106}

¹⁰³ A. Vaccari, *Catalysis Today*, **41** (1998) 53 – 71.

¹⁰⁴ A. Cornelis & P. Laszlo, *Janssen Chimica Acta*, **8** (1990) 3.

¹⁰⁵ M. P. Atkins, D. J. H. Smith & D. J. Westlake, *Clay Minerals*, **18** (1983) 423 – 429.

¹⁰⁶ R. Gregory, D. J. H. Smith & D. J. Westlake, *Clay Minerals*, **18** (1983) 431 – 435.

2.7.3. APPLICATIONS OF ION EXCHANGED CLAYS

The enhanced acidity of ion exchanged clays arises through the increased polarisation of water molecules comprising the primary co-ordination sphere of hydrated charge compensating cations. As such, the acidity exhibited by these materials is typically Brønsted in nature. This makes ion exchanged clays suitable for application in a wide variety of organic reactions which require proton catalysis, including, in addition to others;

1. Transformation of alkenes^{107,108}
2. Hydration of alkenes¹⁰⁶
3. Esterification of organic acids¹⁰⁹

As outlined previously, the replacement of corrosive liquid acids by solid acid catalysts is driven by a multitude of factors including protection of the environment and ease of separation. However, it should be pointed out, that the replacement of liquid acids with solid acid catalysts has the effect, in certain reactions, of altering the reaction mechanism.¹¹⁰ Reacting species adsorbed by the clay are constrained to diffusion in two dimensional space as opposed to three dimensional volume, thereby increasing the encounter frequencies, and hence the rate of reaction.

As a consequence of the source of Brønsted acidity in ion exchanged clays, they are typically restricted to use in low temperature reactions, where hydration water is retained.¹¹¹

¹⁰⁷ J. M. Adams, A. Bylina & S. H. Graham, *Journal of Catalysis*, **75** (1982) 190 – 195.

¹⁰⁸ J. M. Adams, A. Bylina & S. H. Graham, *Clay Minerals*, **16** (1981) 325 – 332.

¹⁰⁹ J. A. Ballantine, M. Davies, H. Purnell, M. Rayanakorn, J. M. Thomas & K. J. Williams, *Journal of the Chemical Society – Chemical Communications*, 8 – 9 (1981).

¹¹⁰ P. Laszlo, *Pure and Applied Chemistry*, **62** (1990) 2027.

¹¹¹ S. Cheng, *Catalysis Today*, **49** (1999) 303 – 312.

2.8. ACID ACTIVATION

The acid activation of clay minerals is a relatively simple process which has taken place commercially for almost 100 years. The first mass produced materials were manufactured in Germany from 1905 onwards.¹¹² In 1922, the United States of America became an active producer of acid activated clays. During 1923, German manufacturers filed a number of entrants in the patent literature relating to the application of acid treated clays as catalysts for the commercial scale production of petroleum from crude oil feedstocks. The potential commercial, industrial and economic importance of these technologies led to a rapid programme for the building and opening of mineral treatment plants across the industrialised world, including England, Canada, Italy and Spain and Japan.

In their formative years, acid activated bentonites presented excellent activity with regard to the production of fuel applicable hydrocarbons from petrochemical feedstocks, however, these materials suffered from one major drawback. While active for short periods of time, these modified minerals were susceptible to rapid deactivation through hydrocarbonaceous coke deposition when used to carry out hydrocarbon reforming reactions, a factor which lowered the commercial feasibility of these catalysts in industrial scale processes. However, 1938 saw the introduction of the Houdry Process¹¹³ for catalytic cracking. This Process continued to exploit acid activated clays for their hydrocarbon reforming activity, but enjoyed the added advantage of on stream catalyst regeneration, a mechanism which allowed for an extension to the useful lifetime of these materials and therefore an enhancement in their commercial viability.

¹¹² D. R. Taylor & D. B. Jenkins, *Society of Mining Engineers of AIME (Transactions)* **282** (1986) 1901 – 1910.

¹¹³ E. Houdry, W. F. Burt, A. E. Pew Jr. & W. A. Peters Jr., *National Petroleum News*, **48** (1938) R570 – R580.

Acid activated clays have been active in the field of catalytic cracking / reforming in the petroleum industry for over quarter of a century. Their demise was brought about by the development and subsequent introduction of zeolite based materials in 1964. Typically, zeolites exhibit superior activity, selectivity and thermal stability relative to modified clay minerals for the production of commercial transportation fuels from crude oil feedstocks. While structure : activity relationships in zeolites are vitally important for the hydrocarbon reforming mechanisms that they promote, such information remains outside of the scope of this preliminary introduction to the modification processes applied to clay minerals.

In the century connecting today to the introduction of acid activated clays, these versatile materials have established themselves firmly in a number of niche markets, of which the following are some of the more commercially important;

1. 2^o dye developers for carbonless copying paper (Section 2.8.3.1.)
2. Clarification of edible food oils (Section 2.8.3.2.)
3. Alkene removal from BTX hydrocarbon product streams (Section 2.8.3.3.)
4. Catalysis in the speciality organic/ fine chemicals market (Section 2.8.3.4.)

Despite the loss of their more traditional markets, and in light of the applications outlined above, market demand for acid activated clays remains high with world wide requirements for these materials is currently running at in excess of 550,000 tonnes per year.

Rationalisation of the market for acid activated clays over recent years has resulted in the emergence of four key manufacturers who have established themselves in the market for the mass production and supply of these modified clay minerals (Table 8).

Table 8 – The Worlds Major Acid Activated Mineral Producers (By Mass)¹¹²

World Ranking	Organisation	Production Sites
1 st	Sud Chemie AG	Bavaria, West Germany Puebla, Mexico
2 nd	Harshaw Filtrol Partnership	Mississippi, U.S.A. Winnipeg, Canada
3 rd	Mizusawa Industrial Chemicals	Niigata, Japan Yamagata, Japan
4 th	Laporte Speciality Chemicals	Cheshire, England Almeria, Spain

Perhaps the biggest challenge to using clays as catalysts, and particularly for hydrocarbon reforming reactions which are usually carried out at high temperatures, is that the extensive surface areas of raw smectites class ($194\text{m}^2/\text{g}$)¹¹⁴ is typically not available at high temperature due to dehydration effects. At temperatures above 200°C , water molecules associated with the charge compensating, interlayer cations of smectites are driven from the mineral structure. This deprives the material of the physical support keeping each of the individual layers apart. This results in a phenomenon known as layer collapse, in which individual layers within tactoid units come into direct contact (Figure 10), thus eliminating the surface area associated with the gallery region. Likewise, the potential Lewis acidity attributable to the exposed interlayer cations is also lost.

Resolution of this unfortunate consequence of the use of clays as catalysts in high temperature applications can be achieved through the process of acid activation,

¹¹⁴ Y. Z. Yao & S. Kawi, *Journal of Porous Materials*, **6** (1999) 77 – 85.

2.8.1. THE MECHANISM OF ACID ACTIVATION

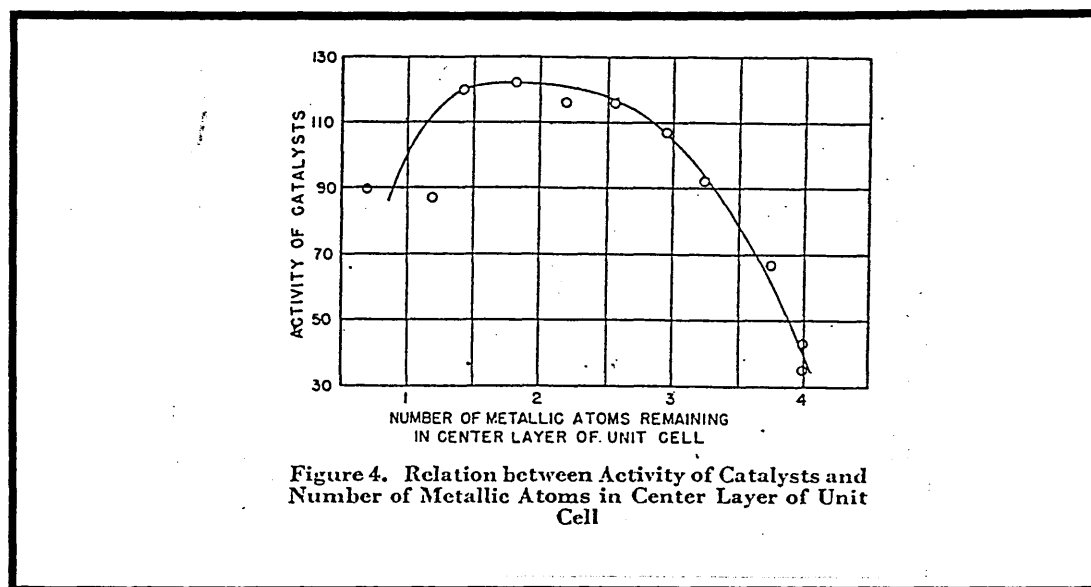
One of the first theoretical attempts to explain the changes occurring within the structures of smectites as a consequence of acid activation was made in 1950 by Thomas, Hickey and Stecker.¹¹⁵ At that time, mineralogists were aware that the charge compensating cations associated with smectite structures in order to balance the negative lattice charges resulting from isomorphous substitution were in fact exchangeable. Replacement of the resident interlayer cations with different species had been shown to occur without any disruption to the mineral structure. Indeed, treatment of raw clays with cold dilute mineral acids, to yield proton exchanged materials, was common practice. Such treatments were shown to be highly effective in the removal of interlayer and surface exchange site cations, and their subsequent replacement with protons from the treatment acid. Repetition of the procedure with hot mineral acids resulted in the loss of a degree of the structural integrity associated with smectites as determined by XRD. In addition, the high temperature treatment also leached structural aluminium from the clay, thus confirming the degradation of the mineral structure in hot mineral acids. In actuality, upto 80% of the ions comprising the octahedral sheet of smectites must be removed from clays to induce significant changes in their X-Ray diffraction patterns.

Thomas *et al*¹¹⁵ illustrated that by varying the extent of the acid treatment it was possible to control the amount of aluminium removed from the octahedral sheet of these materials, and in turn, control the catalytic activity of these clays when applied as cracking catalysts for the process of hydrocarbon reformation.

¹¹⁵ C. L. Thomas, J. Hickey & G. Stecker, *Industrial and Engineering Chemistry* (May 1950) 866 – 870.

Figure 15 shows the results published by Thomas *et al*¹¹⁵, correlating cracking activity to octahedral sheet composition.

Figure 15 – Effect of Octahedral Aluminium Removal on Cracking Activity



As a result of their shape, the types of plot shown in figure 15 are often referred to as volcano plots. The information conveyed by such illustrations suggests that there is an optimum treatment regime for the preparation of Acid Activated Clays (AAC's) for use in pre-defined applications. In this instance, removal of two (or half of the octahedral ions) comprising the unit cell of the smectite results in optimum cracking activity under the test conditions employed. Sub or super removal of ions associated with the octahedral sheet of these minerals reduces the product yield.

In the latter half of the last century, huge advances in understanding the processes occurring during acid activation of clay minerals, and the subsequent effects on mineral structure and resultant catalytic activity were made, thus allowing for the development of structure/activity relationships.

The realisation that the octahedral sheet of both dimorphic and trimorphic clay minerals can be depopulated in a controlled fashion to yield products of enhanced applicability has provided a driving force for the development of a fuller understanding of how minerals become activated.

Four key variables have been identified;

1. Nature of the Starting Mineral (Chemical Composition)
2. Nature of the Treatment Acid (Speciation, Concentration)
3. Activation Temperature
4. Duration of the Activation Procedure

2.8.1.1. NATURE OF THE STARTING MATERIAL

It has been extensively reported in the literature that there are differences in the leaching rates of dioctahedral and trioctahedral minerals. In particular, octahedral sheets containing high proportions of magnesium are much more readily leached than those which are rich in aluminium¹¹⁶ under identical treatment conditions. Such observations have been supported by reports that magnesium rich trioctahedral smectites such as hectorites are subject to depletion of their octahedral sheets when immersed in mineral acids at or near room temperature.¹¹⁷

It is now generally agreed that the ease of removal of structural ions associated with the octahedral sheet of phyllosilicates¹¹⁸ is $Mg^{2+} > Fe^{2+}$ (ferrous) $> Fe^{3+}$ (ferric) $> Al^{3+}$.

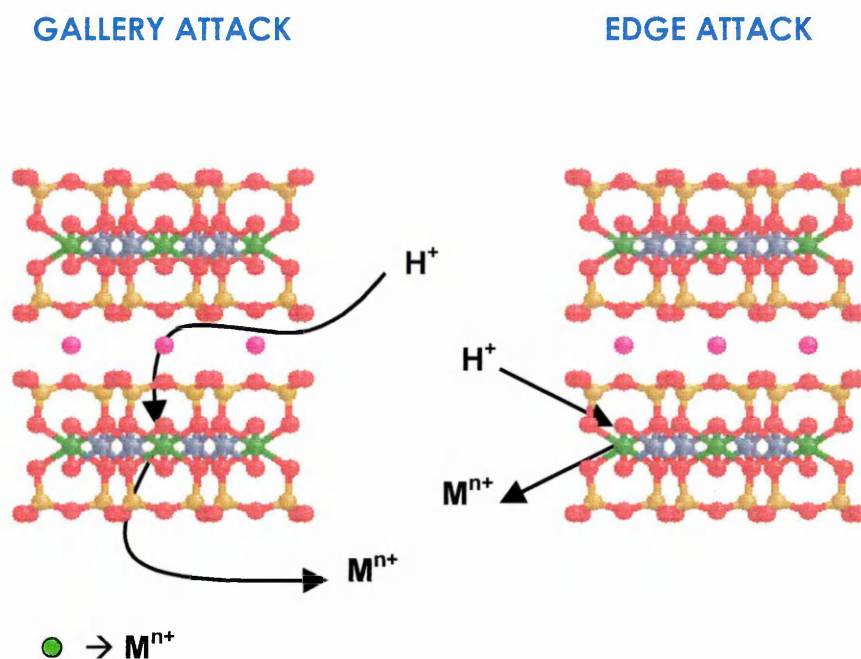
¹¹⁶ (a) C. Breen, J. Madejová & P. Komadel, *Journal of Materials Chemistry*, **5** (1995) 469. (b) C. Breen, J. Madejová & P. Komadel, *Applied Clay Science*, **10** (1995) 219.

¹¹⁷ P. Komadel, J. Madejová, M. Janek, W. P. Gates, R. J. Kirkpatrick & W. J. Stucki, *Clays and Clay Minerals*, **44** (1996) 228.

¹¹⁸ A. Corma, A. Mifsud & E. Sanz, *Clay Minerals*, **22** (1987) 225 – 232.

Typically, octahedral sheet depletion proceeds via a mechanism of proton attack at exposed sheet edges. Evidence for this mode of attack is given by the particle size / hydrolysis rate co-dependence observed in non swelling minerals.¹¹⁹ In the case of swelling minerals, such as smectites, a second possible route for the proton induced leaching of octahedral sheet components exists. The penetration of protons into the gallery regions of swelling minerals by a simple process of ion exchange, allows proton attack through the ditrigonal cavities created as a result of tetrahedral sheet formation. Figure 16 illustrates these two differing modes of attack.

Figure 16 – Comparison of Edge Attack and Gallery Attack of Smectites



Kaviratna and Pinnavaia¹²⁰ were able to demonstrate, using solid state Nuclear Magnetic Resonance (NMR) spectroscopy techniques, that despite the availability of two competing attack mechanisms, swelling clays undergo octahedral sheet depletion through a predominantly edge orientated mechanism during the early

¹¹⁹ H. Cetisli & T. Gedikbey, *Clay Minerals*, **25** (1990) 207 – 215.

¹²⁰ H. Kaviratna & T. J. Pinnavaia, *Clays and Clay Minerals*, **6** (1994) 717 – 723.

stages of attack. During the latter stages of the activation procedure (post 62% octahedral ion depletion), the edge attack mechanism continues to operate, although it is augmented by the initiation of the gallery attack mechanism. Likewise following the removal of 83% of the resident octahedral structural ions, the gallery attack mechanism becomes the more active of the two competing processes.

Kaviratna and Pinnavaia made two assumptions concerning this observation. Firstly, they suggested that the late onset of the gallery attack mechanism may be attributed to structural disorder and to a reduction in the magnitude of the layer charge which accompanies acid activation. A second proposition related to the formation of amorphous silica at the sites of edge attack. Due to the insolubility of silica in the treatment medium, this activation by-product remains intact, and may physically prevent the activation acid from penetrating the edge sites of the clay to promote further enhanced sheet degradation, this event is termed passivation. Although passivation is independent of the nature of the starting material, it is potentially important to the catalytic characteristics of the activated products. Further information pertaining to the occurrence and effects of passivation are given in section 3.8.1.

As a result of its sensitivity to structural modifications in clay mineral structures, vibrational spectroscopy, and in particular Fourier Transform Infra Red (FTIR) Spectroscopy is routinely employed to monitor the evolution of structural changes which accompany the acid activation of clays. Variability in the chemical composition of the octahedral sheets of smectites and kaolinities can be studied in detail as a consequence of the differing infra red band assignments made to the hydroxyl group stretching frequencies associated with the variety of elements which compose the octahedral sheets. As protons infiltrate the layer structure of smectites, they attack ions associated with the octahedral sheet, an event which leads to the

dehydroxylation of the mineral through a loss of the hydroxyl groups bonded directly to the ion being leached. Loss in the spectral intensity associated with the characteristic absorption bands of these hydroxyl groups confirm the loss of the structural ion from the mineral structure.^{121,122}

A second consequence of acid activation which results from the nature of the starting material is acid induced degradation of the tetrahedral sheet. In minerals such as beidellites and saponites (100% Mg in octahedral sheet), which have Al³⁺ for Si⁴⁺ isomorphous substitution in their tetrahedral sheets, treatment with hot mineral acids not only leaches structural aluminium ions from the octahedral sheet, but also induces dealumination of the tetrahedral sheet. This mechanism of attack has been proven through the application of Solid State Cross Polarisation Magic Angle Spinning Nuclear Magnetic Resonance Spectroscopy (CP MAS NMR). Tkáč *et al*^{123,124} have used ²⁷Al MAS NMR to demonstrate that in minerals containing both octahedral and tetrahedral aluminium (Al_{oct} and Al_{tet}) the respective rates of dissolution of aluminium ions in each of the different environments is directly comparable.

As with smectites, ²⁷Al NMR has been successfully employed to study the dealumination of kaolinites.¹²⁵ To date, the acid activation of dimorphic minerals has been restricted almost entirely to pre calcined samples. The calcination product of kaolin is known as metakaolin, and in addition to the hexa coordinated Al seen in kaolin, also contains tetra and penta co-ordinated ions, the relative amounts of which are determined by the calcination temperature. In addition, Macedo *et al*

¹²¹ J. Madejová, J. Bujdák, M. Janek & P. Komadel, *Spectrochimica Acta Part A*, **54** (1998) 1397 – 1406.

¹²² M. A. Vincente-Rodriguez, M. Suarez, M. A. Bañares-Muñoz & J. de Dios Lopez-Gonzalez, *Spectrochimica Acta Part A*, **52** (1996) 1685 – 1694.

¹²³ I. Tkáč, P. Komadel & D. Müller, *Clay Minerals*, **29** (1994) 11 – 19.

¹²⁴ I. Tkáč, P. Komadel & D. Müller in *Eleventh Conference on Clay Mineralogy and Petrology* (ed. Č. Budějovice) (1990) 1993, 273 – 279.

¹²⁵ J. C. D. Macedo, C. J. A. Moita, S. M. C. de Menezes & V. Camorim, *Applied Clay Science*, **8** (1994) 321 – 330.

were able to show that the penta coordinated species are subject to preferential leaching during the acid activation treatment phase.

2.8.1.2. NATURE OF THE TREATMENT ACID

The effect of the chemical nature of the treatment acid on the post activation products generated from a variety of mineral structures has been studied. In particular, Perissinotto and co-workers¹²⁶ were able to illustrate that differences in the mineral acids used for clay activation can lead to differential mechanisms for the leaching of octahedral sheet components. It was found that when Hydrochloric Acid (HCl) was used, that leaching of aluminium was extremely rapid, and that post activation washing did not further increase the surface area enhancements achieved following activation. In contrast, the application of Sulphuric Acid (H₂SO₄) resulted in much lower leaching rates, and surface area enhancements which only became accessible following washing of the activated product with distilled water. These observations, in agreement with others,¹²⁷ were attributed to the ability of the H₂SO₄ anion (SO₄²⁻) to form complexes with the aluminium ions released from the mineral structure, a non viable situation with the HCl anion (Cl⁻). This complexing activity leads to redeposition of the aluminium sulfate species on the surface of the clay, and possibly inhibits further dealumination.

Likewise, Sabu et al¹²⁸ reported differences in the physiochemical properties of acid activated metakaolinites using a variety of mineral acids of varying concentration. The primary conclusion of this work related to the importance of acid strength in defining the properties of the activated products.

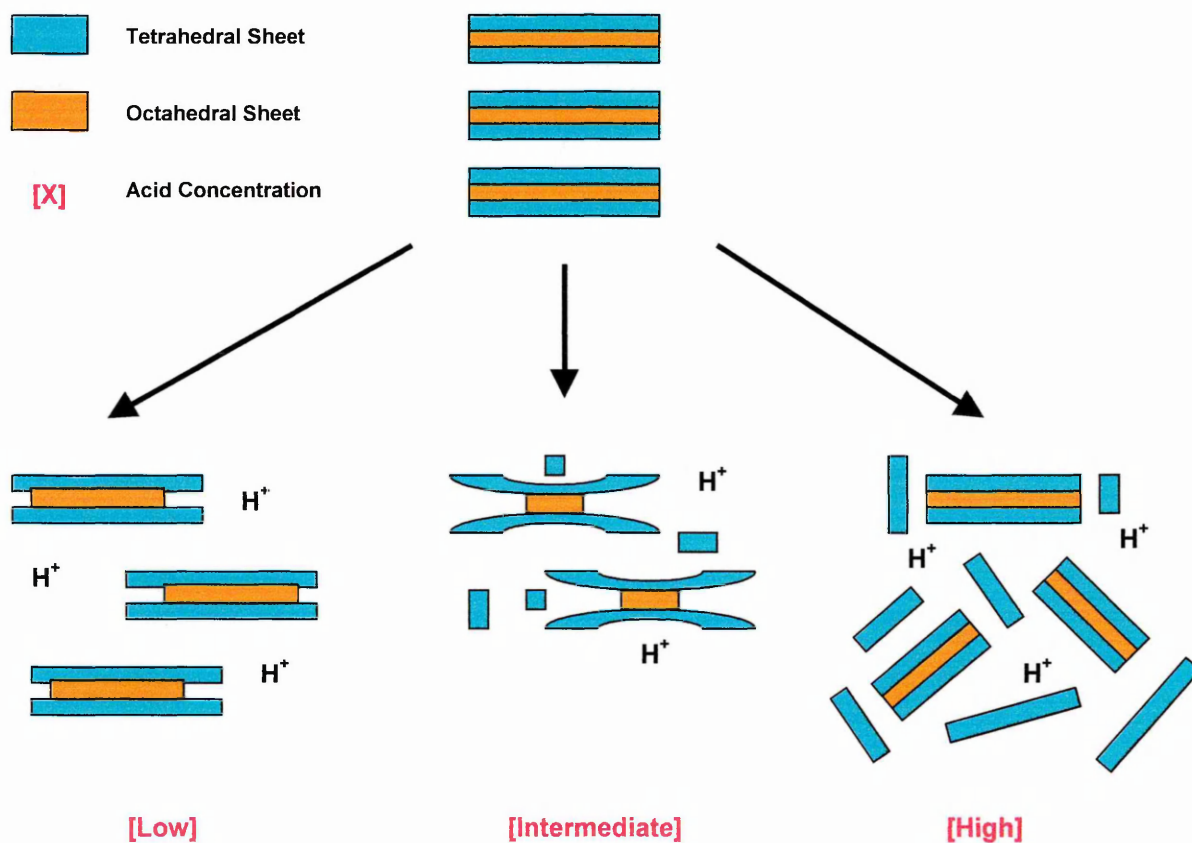
¹²⁶ M. Perissinotto, M. Lenarda, L. Storaro & R. Ganzerla, *Journal of Molecular Catalysis A: Chemical*, **121** (1997) 103 – 109.

¹²⁷ J. Lussier, *Journal of Catalysis*, **129** (1991) 225.

¹²⁸ K. R. Sabu, R. Sukumar, R. Rekha & M. Lalithambika, *Catalysis Today*, **49** (1999) 321 – 326.

Moreover, it has been shown elsewhere that the concentration of the treatment acid plays a significant role in the activation process. Pesquera et al¹²⁹ have reported that for the acid activation of a swelling bentonite with HCl, that the concentration of the acid plays a crucial role in determining the mechanism of activation and consequently the physiochemical properties of the product material. Figure 17 below represents an adaption of a figure presented in the findings of Pesquera and her co-workers.

Figure 17 – Effect of Acid Concentration on the Activation Mechanism of Smectites



¹²⁹ C. Pesquera, F. González, I. Benito, C. Blanco, S. Mendioroz & J. Pajares, *Journal of Materials Chemistry*, **2(9)** (1992) 907 – 911.

The effects of the varying acid concentrations can be briefly summarised as follows;

[Low] (1-3M)

Exchange of interlayer and surface exchange site charge compensating cations with protons from the acidic treatment solution. Preliminary removal of structural octahedral cations at edge sites. Structural integrity associated with the individual tactoid units is retained.

[Intermediate] (4-6M)

Again, tactoid integrity retained, while allowing for proton exchange. Octahedral sheet substantially depopulated, leading to the formation of silica fronds, which are prone to breaking, the result of which is the formation of colloidal free silica.

[High] (7-12M)

Tactoid units become delaminated. Expeditious leaching of the octahedral sheet in the initial stages of activation. Rapid production of large quantities of acid insoluble amorphous silica leads to passivation of the clay structure and inhibits further structural attack.

2.8.1.3. EFFECT OF ACTIVATION TEMPERATURE

The effect of the activation temperature is variable, and depends heavily on the chemical composition of the starting material. Trioctahedral materials such as saponites, which have high levels of readily acid soluble octahedral cations such as Mg^{2+} are prone to leaching at temperatures much lower than required to achieve similar levels of octahedral sheet depletion in dioctahedral minerals. It has been reported,¹³⁰ and is generally accepted that as the temperature of the treatment acid

¹³⁰ F. Kooli & W. Jones, *Clay Minerals*, **32** (1997) 633 – 643.

is increased, the rate of dissolution increases for a given mineral. Estimates suggest that the dissolution rate may double for each 10°C rise in treatment temperature.

2.8.1.4. DURATION OF ACTIVATION

As with activation temperature, the effects of the duration of the activation treatment is highly dependant on the nature of the starting material. For a given mineral subjected to activation in a known concentration of acid at a defined temperature, increasing the duration of the treatment serves to enhance the depopulation of the octahedral sheet. In particular, the extent of dealumination is improved.¹³¹

2.8.2. THE EFFECTS OF ACID ACTIVATION

The effects of acid activation on the structural and physiochemical properties of clay minerals have been of continuing interest to both industry and academia. One of the primary driving forces is to attain a fuller understanding of the observed activity of acid activated clays in a wide range of industrially important applications.

There are four predominant effects which arise through the application of acid activation treatments to phyllosilicates;

1. Ion Exchange
2. Increases in Acidity
3. Surface Area Enhancements
4. Alteration of the Structural Chemistry

¹³¹ M. A. Vicente Rodriguez, M. Suarez Barrios, J. D. Lopez Gonzalez & M. A. Bañares Muñoz, *Clays and Clay Minerals*, **42(6)** (1994) 724–730.

2.8.2.1. THE EFFECTS OF ION EXCHANGE

As highlighted in previous sections, the acid activation of clay minerals is essentially a two stage process. In the first instance, the interlayer and surface exchange sites cations are eliminated from the clay structure and are replaced by protons from the treatment solution. In the second stage, structural cations associated with the octahedral, and to an equal extent the tetrahedral, sheets are leached from the mineral structure.

Proton exchanged clays are not stable, and once formed undergo a spontaneous change to a condition of Al, Mg and Fe saturation.¹³² This process is termed autotransformation, and it occurs in two stages. Firstly, charge compensating protons undergo exchange with metallic cations associated with the surface of the treated mineral. Secondly a decomposition – exchange mechanism operates in which the charge compensating protons migrate through the ditrigonal cavities of the minerals tetrahedral sheet, and displace structural cations resident in the octahedral sheet. Through a process of back exchange, the liberated ions assume residency as the charge compensating cations of the activated mineral structure.

It should be noted in respect of ion exchange that one effect of the acid activation procedure is a reduction in the C.E.C. of the clay.

2.8.2.2. INCREASE IN ACIDITY

The increase in acidity observed in acid treated clays is too readily attributable to the introduction of protons into the gallery region and into the surface exchange sites associated with swelling minerals in the case of the former, and to isomorphously substituted materials in the case of the latter. However, as outlined above, proton

¹³² E. Bednářiková, P. Komadel & B. Čičel, in *Eleventh Conference on Clay Mineralogy and Petrology* (ed. Č. Budějovice) (1990) 1993, 93 – 97.

exchanged clays are highly unstable, and undergo spontaneous autotransformation in order to enhance stability. This process, which involves the migration of protons into the lattice structure effectively prevents these species being available to contribute to the acidity of these materials. Indeed, in a study relating to the elucidation of the mechanism responsible for the adsorption of chlorophyll from edible food oils by acid activated clays, Mokaya *et al*¹³³ were able to illustrate that the vast majority of the Brønsted acidity associated with acid treated smectites is present as a consequence of the activation procedure, and relates to the installation of Brønsted active sites into the structural clay matrix.

The depopulation of the octahedral sheet of clay minerals which accompanies the acid activation process has the result of breaking the $M^{x+}-OSiO_3$ bond joining the octahedral and tetrahedral sheets together. The unsatisfied valency created in the tetrahedral sheet is fulfilled by the uptake of protons from the treatment acid. This results in the formation of Brønsted acidic structural silanol groups on the exposed surface of the mineral structure ($Si-O^{\delta-}H^{\delta+}$). Furthermore, particularly in the case of minerals with Al^{3+} for Si^{4+} substitution in their tetrahedral sheets, the protonation of the siloxane bridges can form a second type of Brønsted acidic structural hydroxyl groups during the activation procedure.^{97,134} In addition to Brønsted acidic sites these groups can also exhibit Lewis Acidity, once deprotonated.¹³⁵

¹³³ R. Mokaya, W. Jones, M. E. Davies & M. E. Whittle, *Journal of Solid State Chemistry*, **111** (1994) 157 – 163.

¹³⁴ P. Falaras, I. Kovanis, F. Lezou and G. Seiragakis, *Clay Minerals*, **34** (1999) 221 – 232.

¹³⁵ D. Haffad, A. Chambellan & J. C. Lavalley, *Catalysis Letters*, **54** (1998) 227 – 233.

In addition, internal structural hydroxyl groups (aluminol, magnesol, silanol) also become available as potential catalytically active Brønsted acid centres due to the opening up of mineral tactoids as a result of activation in hot mineral acids.¹³⁶

A further source of the additional acidity in activated clays may relate to the formation of coordinatively unsaturated metallic cations within the octahedral sheet. It has been suggested that following the leaching of octahedral sheet components along with their associated hydroxyl groups, the resident cations of the octahedral sheet may assume tetrahedral coordination with the four remaining oxygen atoms.^{137,138,139} The forcing of Al^{3+} into such a coordination environment induces the formation of a formal negative charge on the species, and thus promotes the possibility of proton uptake.

A further source of Brønsted acidity arises as a consequence of the autotransformation process. The intra-structural migration of exchanged protons into the mineral lattice, and their replacement in the gallery region and in the surface exchange sites by Al^{3+} , Mg^{2+} , Fe^{2+} and Fe^{3+} ions liberated from the damaged octahedral sheets of the activated product matrix furnishes these accessible locations within the mineral structure with highly polarising cations. Upon exposure to the atmosphere, the interaction of water with these cations installs a degree of Brønsted acidity.

¹³⁶ U. Flessner, D. J. Jones, J. Rozière, J. Zajac, L. Storaro, M. Lenarda, M. Pavan, A. Jiménez-López, E. Rodríguez-Castellón, M. Trombetta & G. Busca, *Journal of Molecular Catalysis A: Chemical*, **168** (2001) 247 – 256.

¹³⁷ P. Kumar, R. V. Jasra & T. S. G. Bhat, *Industrial Engineering Chemistry Research*, **34** (1995) 1440 – 1448.

¹³⁸ S. Mendioroz, J. A. Pajares, I. Benito, C. Pesquera, F. González & C. Blanco, *Langmuir*, **3** (1987) 676 – 681.

¹³⁹ A. Vaccari, *Applied Clay Science*, **14** (1999) 161 – 198.

In terms of the formation and introduction of active centres exhibiting Lewis acidity in acid treated minerals, these typically have a single source. The erosion of the octahedral sheet of phyllosilicates by the edge attack mechanism installs coordinatively unsaturated Al^{3+} and Mg^{2+} structural cationic centres at edge sites. In the absence of structural bonding elements to fulfil their valency requirements, these ions adopt trigonal coordination, and as such exist as highly efficient Lewis acid centres.

A second source of Lewis acidity, not attributable to the acid activation treatment, resides in the availability of transition metal ions in high valency states within the tetrahedral sheets.¹⁴⁰

A further potential source of Lewis acidity in acid activated clays becomes available when the materials are used in high temperature applications. Post dehydration, interlayer and surface exchange site cations are converted from effective Brønsted acid sites into highly efficient Lewis acid centres. However, it should be noted that due to the phenomenon of layer collapse, significant amounts of these Lewis acid centers are no longer available for active involvement in catalysis, particularly of non polar species.

Note that total acidity of acid activated clays will not increase indefinitely with increases in the harshness of their activation treatments. The Brønsted acidic groups arising as a result of the formation of tetrahedrally coordinated aluminium in the octahedral sheet rises to a maximum, but post 50% removal of octahedral cations, these potentially active acidic centers are lost from the structural matrix, as a result of leaching, along with their associated acidity.¹³⁷ Therefore, independent of the activation parameter altered (temp., acid concentration, duration) to promote

¹⁴⁰ D. H. Solomon, *Clays and Clay Minerals*, **16** (1968) 31 – 39.

enhanced structural degradation, acidity will always peak prior to undergoing decline. Therefore it is important to optimise treatment parameters for a given mineral system in order to achieve the level of structural and chemical alteration required.¹⁴¹

2.8.2.3. SURFACE AREA ENHANCEMENTS

It is now widely accepted that the very early stages of the activation of clay minerals with hot concentrated acids is accompanied by a rapid increase in surface area. The primary reason for this is the opening up of the structural lamellae as a consequence of the abstraction of the interlayer and surface exchange site charge compensating cations along with the water molecules composing their respective hydration spheres. In addition, the acidic treatment solution promotes elimination of impurities such as free oxides and carbonates which may contribute to aggregation of individual clay particles.¹³⁸

As with acidity, the increased surface areas associated with activated minerals undergo a reduction when the harshness of the treatment variables are increased. Although highly dependant on the nature of the starting material, these observed reductions have been attributed to factors, including loss of structural order and eventual complete degradation of the acid soluble components of the mineral.¹⁴²

Under severe or prolonged treatment conditions, both of which have been shown to induce passivation^{129,138} the formation of free silica, and subsequent precipitation of this material as a result of the saline conditions induced by the leaching of

¹⁴¹ C. Breen, F. D. Zahoor, J. Madejová & P. Komadel, *Journal of Physical Chemistry B*, **101** (1997) 5324 – 5331.

¹⁴² S. Narayanan & K. Deshpande, *Recent Advances in Basic and Applied Aspects of Industrial Catalysis : Studies in Surface Science and Catalysis*, **113** (1998) (ed's. T. S. R. Prasada & M. Dhar) Elsevier Science B. V.

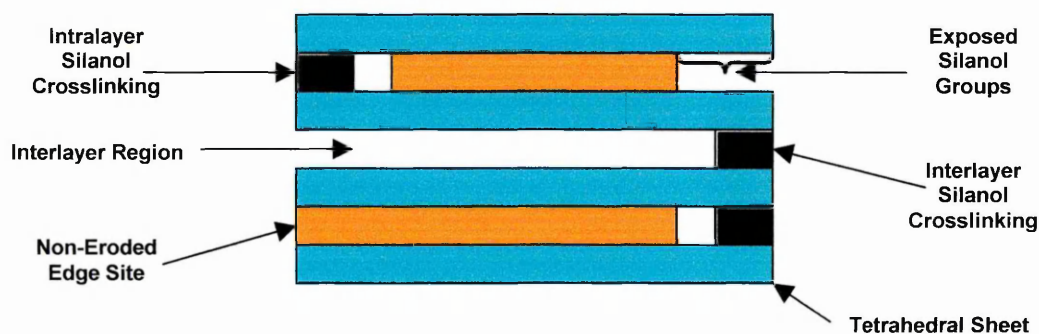
octahedral sheet components,¹⁴³ also adversely affects surface area. The deposition of this material on the surface of the remaining clay particles not only physically blocks the available pores, but also inhibits further structural attack. Both effects result in lower than expected surface areas.

2.8.2.4. ALTERATION OF STRUCTURAL CHEMISTRY

Obvious changes to the structural chemistry of acid activated clays accompany the removal of the acid soluble components of both the octahedral and tetrahedral sheets of clay minerals.^{121-124,131,135,141} The results of these structural changes, and in particular the formation of structural silanol groups in the tetrahedral sheets (to fulfil the unsatisfied valencies formed following the leaching of octahedral sheet) can lead to the occurrence of side reactions which ultimately affect the physiochemical properties of the product material.

These structural silanol groups on adjacent tetrahedral sheets within individual tactoid layers can become involved in condensation reactions to yield a three dimensional silica framework. Tkáč *et al*¹²³ also presents data suggesting that in addition to intralayer crosslinking, interlayer crosslinking is also a possibility. These possibilities are presented in figure 18.

Figure 18 – Intralayer and Interlayer Crosslinking In Acid Activated Smectites



¹⁴³ R. K. Iller in *The Chemistry of SiO₂*, Wiley Interscience: New York (1979)

2.8.3. MAJOR USES OF ACID ACTIVATED CLAYS

The data in table 4, shows that clay minerals are used in a vast range of applications. The modification of clay minerals, by acid activation, is carried out to enhance certain properties of these versatile materials, and therefore their fields of application are rather more specialised than those for unmodified minerals. Following the demise of acid activated clays as hydrocarbon reforming / cracking catalysts for application in the petroleum industry, these materials are established in a range of commercially important applications of which the following are the more important;

1. 2^o dye developers for carbonless copying paper.
2. Clarification of edible food oils.
3. Alkene removal from BTX hydrocarbon product streams.
4. Catalysis in the speciality organic/ fine chemicals market.

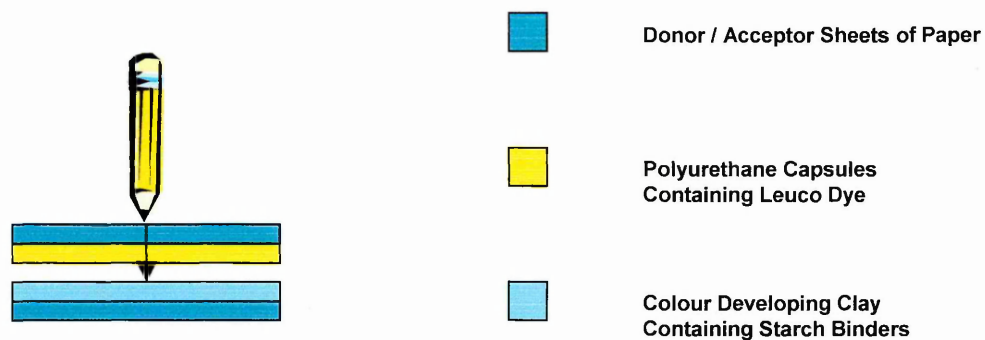
2.8.3.1. CARBONLESS COPYING PAPER

Carbonless copying paper is used in a range of applications where permanent records of written information are required for distribution to a second party. An example may be registration forms in universities. Carbonless copying paper allows duplicate copies of the registration details to be retained by both the university and the student. The elimination of the need for a sheet of insertable carbon coated material, saves both time and mess, especially in cases where the exchange of the recorded information must be completed efficiently and rapidly.

The mode of operation of carbonless copying paper is detailed in the literature.¹⁴⁴ The assembly used is illustrated in figure 19;

¹⁴⁴ R. Fahn & K. Fenderl, *Clay Minerals*, **18** (1983) 447 – 458.

Figure 19 – Mode of Operation for Carbonless Copying Paper Systems



Compression on the upper sheet of paper with a writing implement causes the polyurethane capsules coated on the underneath to be ruptured with the release of their contents, the dye precursor. The leuco dye contacts the acid treated clay coated on the lower sheet, and undergoes a chemical reaction. One of the most widely used dye precursors employed in carbonless copying paper systems is Crystal Violet Lactone (CVL).

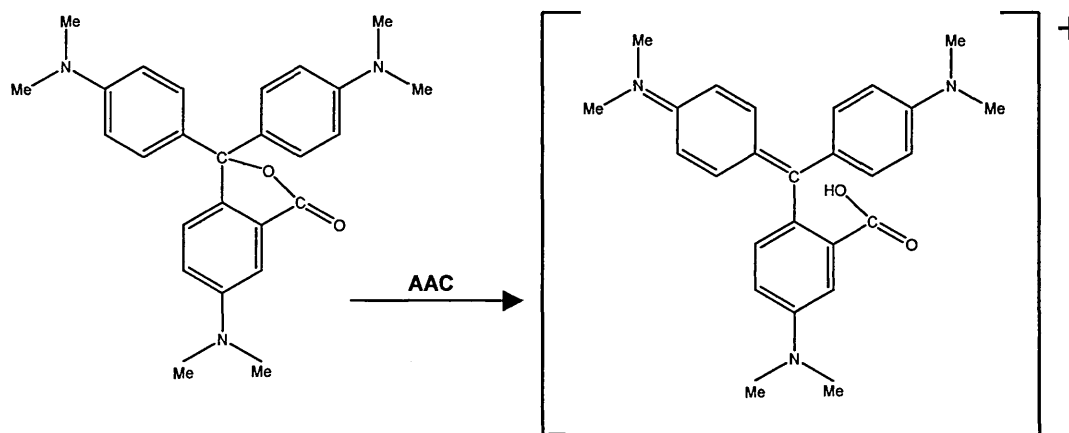
The commercial importance of acid activated clays for application in carbonless copying paper systems is illustrated by the fact that most major clay processors now produce acid activated clays which are marketed solely for use in this role. Table 9 below shows the major manufacturers and their branded acid activated clay products.

Table 9 – Secondary Dye Developing Branded Clays and Their Manufacturers

Manufacturer	Brand	Country of Origin
Laporte Adsorbents	Fulacolor™	United Kingdom
Sud Chemie	Tonsil™	Germany
	Copisil™	Germany
Mizusawa	Silton™	Japan

The clays operate by protonating the dye precursor to generate a charged species. The resultant molecular ion contains an active chromophore which allows for the development of a long lasting coloured species which is stabilised by adsorption onto the clay surface. Figure 20 below illustrates the reaction mechanism for this process using CVL as the secondary dye precursor. The coloured ion formed is Crystal Violet (CV).

Figure 20 – Protonation of CVL To Generate CV on Acid Activated Clays



2.8.3.2. CLARIFICATION OF EDIBLE FOOD OILS

Another major market sector for acid activated clays is in the clarification of edible food oils. Post extraction, many edible oils contain naturally occurring materials such as chlorophyll, fatty acids, and tocopherols.^{133,134} The presence of the latter is advantageous as they possess good antioxidant activity, and help to prevent auto oxidation of the oil.¹⁴⁵ In contrast, fatty acids are undesirable as they promote putrification of the oil, and therefore their removal is of importance to extend the shelf life of edible oils intended for human consumption.

¹⁴⁵ K. Boki, M. Kubo, T. Wada & t. Tamura, *Journal of the American Oil Chemists Society*, **69(3)**, (1992) 232 – 236.

Although acid activated clays have enhanced adsorptive properties relative to the untreated minerals, their strongly acidic Brønsted sites can promote the formation of free fatty acids within the oil by the acid catalysed hydrolysis of glyceride ester linkages which occur within other components of the oil.¹⁴⁶ In respect of the chlorophyll content, although not detrimental to the oil, these coloured pigments do impart a significant off colour to the oil which would deter possible consumers.

Recent attempts at enhancing the adsorptive capabilities of these materials have involved the addition of iron chlorides and copper sulphates while ensuring low levels of activation so as to inhibit the formation of strongly Brønsted acidic structural silanol groups which promote fatty acid formation.¹⁴⁷ In respect of chlorophyll adsorption, both Pillared Interlayered Clays (PILC's) and Pillared Acid Activated Clays (PAAC's)^{148,149} have been studied.

2.8.3.3. ALKENE REMOVAL (BTX HYDROCARBONS)

Benzene, Toluene and Xylene (BTX) hydrocarbons are typically formed during modern catalytic reforming processes. In addition to being valuable octane rating boosters for blending commercial fuels, these aromatic hydrocarbons are subject to extensive utilisation in the manufacture of plastics and synthetic fibres.

Large scale catalytic reforming at refinery sites produces a multitude of hydrocarbonaceous products from the crude oil feedstocks supplied. Although BTX hydrocarbons are usually formed in good yield, their removal and isolation from the overall product stream is complicated by the fact that many of the other

¹⁴⁶ D. R. Taylor & C. B. Ungermann, *Journal of the American Oil Chemists Society*, **61(8)**, (1984) 1372 – 1379.

¹⁴⁷ F. K. Hymore, *Applied Clay Science*, **10** (1996) 379 – 385.

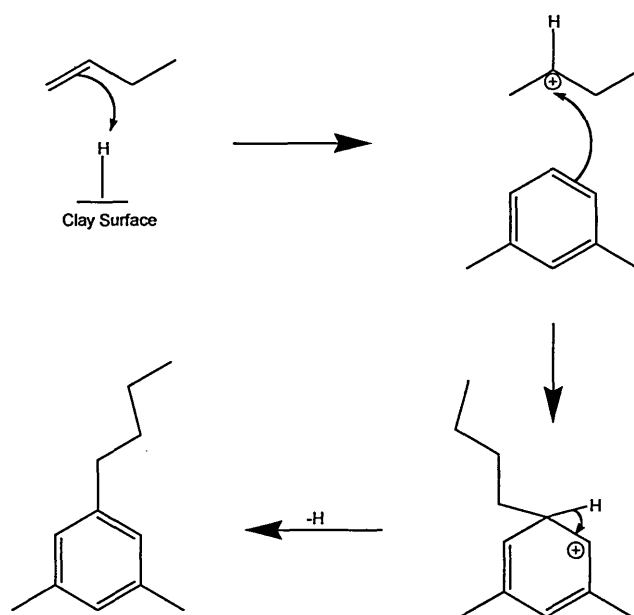
¹⁴⁸ R. Mokaya, W. Jones, M. E. Davies & M. E. Whittle, *Journal of the American Oil Chemists Society*, **70(3)**, (1993) 241 – 244.

¹⁴⁹ R. Mokaya & W. Jones in: *Multifunctional Mesoporous Inorganic Solids*, (eds. C. A. C. Sequeira & M. J. Hudson) (1993) Kluwer Academic Publishers.

hydrocarbon components of the product stream may share similar boiling points to the cyclic compounds required. As a consequence, thermal stripping of the BTX hydrocarbons produced during catalytic reforming often removes significant quantities of other hydrocarbons, particularly unsaturated species such as alkenes.

The Brønsted and Lewis acidity of acid activated clays means that they are routinely employed to reduce the quantity of free alkene in BTX hydrocarbon streams.¹⁵⁰ This is achieved by catalysing the alkylation of the BTX hydrocarbons with the alkenes present through utilisation of the Brønsted acidic protons on the clay surface to protonate the free alkenes, thereby increasing their susceptibility to attack by the nucleophilic aromatic. The reaction scheme given in figure 21 shows how this procedure occurs mechanistically.

Figure 21 – Alkylation of m Xylene By 1-Butene To Yield 3-Butyl, 5-Methyl Toluene



¹⁵⁰ L. T. Novak & K. F. Petraitis, *Industrial Engineering Chemistry Research*, **28** (1989) 1567 – 1570.

Although the product hydrocarbon is not strictly a BTX material, its octane rating is significantly higher than the free alkene, thus enhancing the octane rating of the fuel.

A clear comparison can be drawn between the hydrocarbon reforming activity of acid activated clays and zeolites because of the similarity of reactions which occur over their respective surfaces. β - zeolites have been successfully engaged as catalytically active materials for the generation of alkyl benzenes from benzene and short chain linear alkenes precursors.¹⁵¹ This work confirmed the mechanism outlined in figure 21 as being the most likely, thus dismissing benzene adsorption as an intermediate step in the process.

2.8.3.4. PRODUCTION OF SPECIALITY CHEMICALS

In addition to the use of AAC's as aromatic alkylation catalysts as outlined above, AAC's are also routinely used in many more speciality chemical manufacturing processes, some of the more important of which are detailed below.¹⁵²

ACYLATION REACTIONS

Many iso-ketones have pleasant smelling odours which allow them to be used in the perfumery industry. Their preparation by acylation of the appropriate alkene with acetic anhydride can be catalysed over AAC's. Although conversion is generally good, the rate of reaction is sometimes slow, therefore AAC's are not always the material of choice for this particular synthetic application.

¹⁵¹ S. Siffert, L. Gaillard & B. L. Su, *Journal of Molecular Catalysis A: Chemical*, **153** (2000) 267 – 279.

¹⁵² S. R. Chitnis & M. M. Sharma, *Reactive & Functional Polymers*, **32** (1997) 93 – 115.

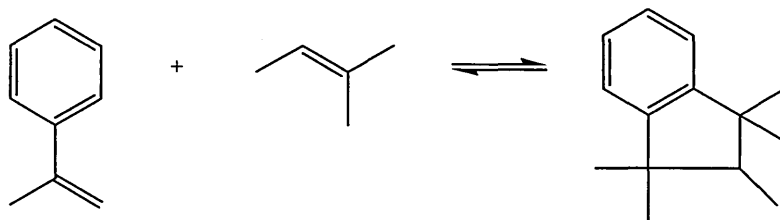
DIMERISATION REACTIONS

The acid catalysed dimerisation of α -methylstyrene has been shown to produce a variety of products, including 2,4-diphenyl-4-methyl-1-pentene and 2,4-diphenyl-4-methyl-2-pentene. These materials are of commercial interest as they act as molecular weight regulators in the manufacture of certain polymers including polystyrene.

CROSS DIMERISATION REACTIONS

Again, important for the perfumery industry, the cross dimerisation of α -methylstyrene (AMS) with isoamylene yields products which have musk like fragrances. Figure 22 below illustrates the nature of these cross dimerisation reactions.

Figure 22 – The Cross Dimerisation of AMS with Isoamylene



OLIGOMERISATION REACTIONS

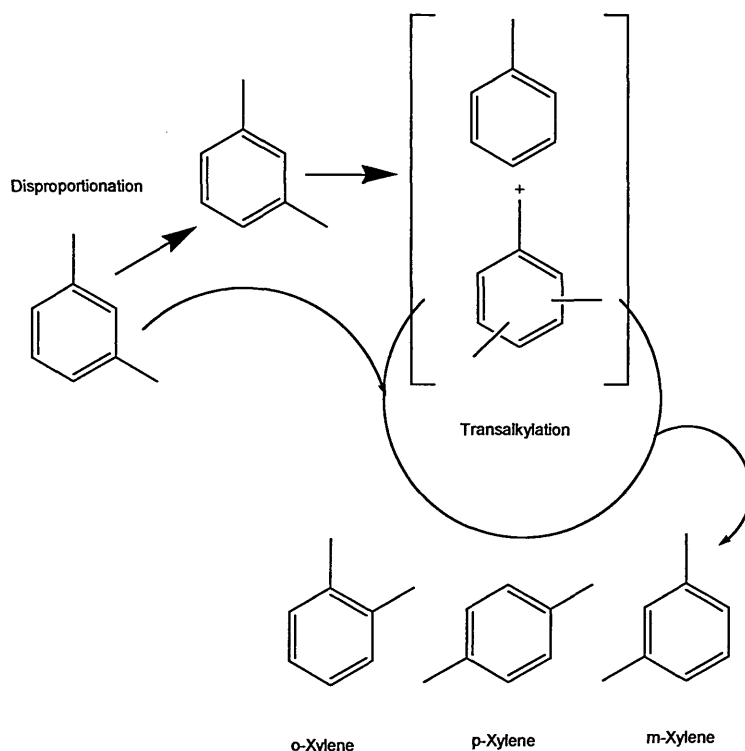
Oligomerisation of intermediate length 1-alkenes ($C_{10} - C_{24}$) is a convenient route for the preparation of synthetic lubricants. Much of the literature in this field remains patented, and the area of study remains active.

ISOMERISATION REACTIONS

Isomerisation reactions are useful when a reaction mixture contains a number of isomers of a given substance, and in particular when one of those isomers has a greater degree of commercial or industrial significance than the others. A good example of this is the petrochemical xylene. Industrially, there is a huge demand for p-xylene, for use in the manufacture of polyesters. Demand for o-xylene and m-

xylene is much lower, and their occurrence in the C₈ aromatic cut from hydrocarbon processing is undesirable. The application of solid acid catalysts, including AAC's and zeolites for the disproportionation and subsequent transalkylation of the primary reaction products to yield p-xylene is now common practice. Figure 23 below shows the operation of these two complimentary processes in the manufacture of all three xylene isomers from the meta precursor.¹⁵³

Figure 23 – m-Xylene Isomerisation (Bimolecular Reaction)



ETHERIFICATION REACTIONS

Methyl-tertiary-butyl ether (MTBE) is a widely used chemical, the tonnage use of which is growing annually. Since the elimination of lead as an anti-knocking agent, MTBE has played a crucial role in its replacement in commercial grade fuels.

¹⁵³ M. Guisnet, N. S. Gnep & S. Morin, *Microporous and Mesoporous Materials*, **35-36** (2000) 47 – 59.

Currently, manufacture is achieved by the use of polymeric cation exchanged resins. However, the direct preparation of MTBE from *t*-butanol and methanol using HF modified montmorillonite clays as catalysts has recently been reported.¹⁵²

ESTERIFICATION REACTIONS

ACC's are used to catalyse the anhydrous esterification of fatty acids with olefins. The product esters are used as pharmaceutical delivery agents for topically applied medications.

CONDENSATION REACTIONS

Barbituric Acid derivatives find application in the field of medicine as both sedatives and anesthetics. Their preparation through the condensation of barbituric acid and arylcarboxyaldehydes is catalysed by AAC's with yield in excess of 85%.

2.9. ACTIVATION BY PILLARING

Pillared Interlayered Clays (PILC's) represent one of the most active areas of research in the field of microporous materials. The principal method used in PILC synthesis is via the intercalation and exchange of bulky inorganic polyoxymetallic cations into the interlayer region of smectites via elimination of the resident interlayer charge compensating cations. Calcination of the resultant pillared clay precursor promotes conversion of the polyoxymetallic cations into thermally stable metal oxide clusters through processes of dehydration and dehydroxylation. The ensuing clusters are referred to as pillars, and reside between individual smectite layers thereby acting as a permanent support to prop the layers apart.

The effect of pillaring is the generation of an interlayer space of molecular dimensions, a two dimensional porous network and the incorporation of new potentially catalytically active sites.

The synthesis of PILC's was first detailed in the early 1970's. The instability in the oil industry and its effect on the price of crude oil, which led to a requirement for the processing of lower quality crudes than were typically dealt with at the time. PILC's were developed to meet this challenge.

Prior to their advent, all of the aspects associated with the preparation of pillared clays had been studied in detail. The intercalation chemistry of clays was well documented, In addition, the ability to incorporate large organic molecules into the gallery region of smectites was also an established process.¹⁵⁴

¹⁵⁴ A. Gil & L. M. Gandia, *Catalysis Reviews – Sci. and Eng.*, **42(1&2)** (2000) 145 – 212.

2.9.1. PREPARATION OF PILLARED CLAYS

Pillared Interlayered Clays, to give them their full and correct title, currently have few large scale industrial applications. Their evolution, during a time at which zeolites were coming to prominence, has severely limited their use. In addition, whereas surface areas and acidities of AAC's can be controlled relatively easily, control over the porosity and acidity of PILC's is extremely difficult due to the turbostratic nature of clay layers, and the charge inhomogeneity in mineral structures.¹⁵⁵ Despite these negative aspects, this unusual class of materials remain an academic curiosity, with research into their preparation and characterisation remaining an active field of investigation.

PILC's can be prepared from polyoxymetallic clusters of various metallic elements. Recent reports have shown tantalum,^{156,157} titanium,¹⁵⁸ chromium,¹⁵⁹ manganese¹⁶⁰ and in particular aluminium^{161,162,163,164,165} to be effective candidates.

In addition, there have been many reports in the literature pertaining to the preparation and characterisation of a range of mixed or even multi metal oxide pillars.

¹⁵⁵ D. J. Pruisen, P. Čapková, R. A. J. Driessen & H. Schenk, *Applied Catalysis A: General*, **165** (1997) 481 – 488.

¹⁵⁶ G. Guiu, A. Gil, M. Montes & P. Grange, *Journal of Catalysis*, **168** (1997) 450 – 462.

¹⁵⁷ G. Guiu & P. Grange, *Journal of Catalysis*, **168** (1997) 463 – 470.

¹⁵⁸ H. L. Del Castillo & P. Grange, *Applied Catalysis A: General*, **103** (1993) 23 – 34.

¹⁵⁹ T. Mishra & K. Parida, *Applied Catalysis A: General*, **166** (1998) 123 – 133.

¹⁶⁰ T. Mishra & K. Parida, *Journal of Materials Chemistry*, **7(1)** (1997) 147 – 152.

¹⁶¹ S. Moreno, R. Sun Kou & G. Poncelet, *Journal of Physical Chemistry*, **101** (1997) 1569– 1578.

¹⁶² S. Chevalier, R. Franck, J. F. Lambert, D. Barthomeuf & H. Suquet, *Applied Catalysis A: General*, **110** (1994) 153 – 165.

¹⁶³ S. Chevalier, R. Franck, H. Suquet, J. F. Lambert & D. Barthomeuf, *Journal of the Chemical Society – Faraday Transactions*, **90(4)** (1994) 667 – 674. Part 1.

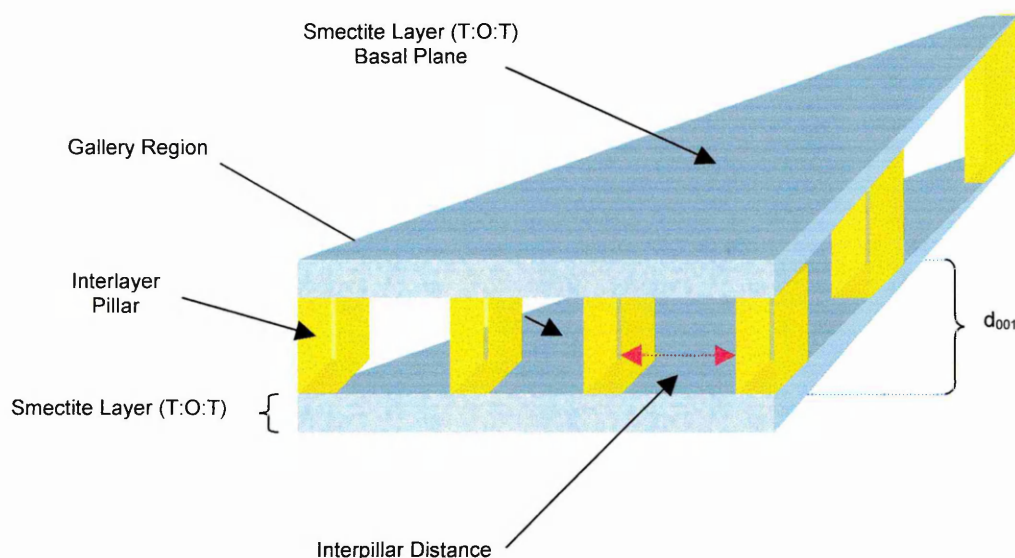
¹⁶⁴ J. F. Lambert, S. Chevalier, R. Franck, H. Suquet & D. Barthomeuf, *Journal of the Chemical Society – Faraday Transactions*, **90(4)** (1994) 675 – 682. Part 2.

¹⁶⁵ L. Bergaoui, J. F. Lambert, R. Franck, H. Suquet & J. L. Robert, *Journal of the Chemical Society – Faraday Transactions*, **91(14)** (1995) 2229 – 2239. Part 3.

Examples of this work have included the combination of aluminium with cerium,¹⁶⁶ chromium,^{167,168} copper¹⁶⁹ and a variety of other transition metals¹⁷⁰ (including cobalt, nickel, zinc and magnesium). The addition of the second species is typically used as a way of enhancing the thermal, adsorptive or catalytic properties of the PILC.¹⁵⁴

Independent of the species used to effect the pillaring of smectites, the overall process and ultimate result are the same, in that post calcination, the product is a thermally stable acidic solid with pores of molecular geometry. Figure 24 below is a 3-dimensional representation of the nature of a pillared interlayered clay.

Figure 24 – Representation of the Structure of a Pillared Interlayered Clay (PILC)



¹⁶⁶ J. Pires, M. Machado & M. Brotas de Carvalho, *Journal of Materials Chemistry*, **8(6)** (1998) 1465 – 1469.

¹⁶⁷ I. Pálinkó, K. Lázár & I. Kiricsi, *Journal of Molecular Structure*, **410 – 411** (1997) 547 – 550.

¹⁶⁸ R. Toranzo, M. A. Vicente & M. A. Bañares-Muñoz, *Chemistry of Materials*, **9** (1997) 1829 – 1836.

¹⁶⁹ K. Bahranowski, M. Gasiór, A. Kielski, J. Podobinski, E. M. Serwicka, L. A. Vartikian & K. Wodnicka, *Clays and Clay Minerals*, **46(1)** (1998) 98 – 102.

¹⁷⁰ C. Flego, L. Galasso, R. Millini & I. Kiricsi, *Applied Catalysis A: General*, **168** (1998) 323 – 331.

Two individual stages can be identified in the process used to generate PILC's:

1. Intercalation of the Pillaring Species – to yield a Precursor Pillared Clay.
2. Calcination of the Precursor Pillared Clay – to yield the Pillared Clay.

2.9.1.1. INTERCALATION OF THE PILLARING SPECIES

This procedure operates along a simple cation exchange process which arises as a consequence of the C.E.C. associated with smectites as a result of isomorphous substitution in both their tetrahedral and octahedral sheets.

To effect exchange and replacement of the resident charge compensating interlayer cations with the intended pillaring species, an aqueous suspension of the clay to be pillared is mixed with a solution of the pillaring species.¹⁷¹ Prior to mixing the solution containing the pillaring species is hydrolysed and aged, by heating (80°C), to induce polymerisation of the chosen cation to form the required multivalent cation.

Pillaring solutions are typically prepared through the addition of an aqueous solution of a base (0.1 – 0.4M NaOH) to a solution containing the appropriate cation (X^{N+}).¹⁷² Under the strongly acidic conditions promoted by free cation in solution, the species will exist in its monomeric form $[X(H_2O)_6]^{N+}$. Following the addition of the base, the free cations undergo successive dimerisations and polymerisations to yield the pillaring precursor.⁹⁷ Combination of the solution containing the polycationic species with that containing the clay promotes a cation exchange process. Filtration of this solution yields a material known as a precursor pillared clay (PPC).

¹⁷¹ S. Moreno, E. Gutierrez, A. Alvarez, N. G. Papayannakos & G. Poncelet, *Applied Catalysis A: General*, **165** (1997) 103 – 114.

¹⁷² R. A. Schoonheydt *et al*, *Clays and Clay Minerals*, **41(5)** (1993) 598 – 607.

2.9.1.2. CALCINATION OF THE P.P.C.

Following intercalation of the pillaring species, the PPC is subjected to calcination. The purpose of this high temperature treatment is to fix the pillars in place by anchoring them to the basal planes of the smectite sheets. Calcination is typically carried out at temperatures of 500°C. At temperatures in excess of 500°C (773K) for pillared montmorillonites and 750°C (1023K) for pillared saponites, pillared clays become thermally unstable, and are subject to collapse.⁹⁷

As with the acid activation of clays, there are a number of variables which can effect the physiochemical properties of the products obtained from the process of pillaring. The major contributing factors can be summarised as follows;

1. Nature of the Starting Material.
2. Nature of the Pillaring Species.
3. Concentration of the Pillaring Species.
4. Drying / Conditioning of the P.P.C.

2.9.1.3. NATURE OF THE STARTING MATERIAL

One of the primary reasons for pillaring a clay is to make available, for potential catalytic use, the surface area of the mineral associated with the gallery region of the clay. This requires the intercalation of pillaring precursors which are much larger than the resident interlayer charge compensating cations and their associated hydration spheres. It is therefore critical to determine the magnitude and location of layer charge of the mineral under investigation, as these factors greatly influence the expansion properties of smectites,¹⁷³ and therefore their ability to act as hosts for large intercalates.

¹⁷³ T. Sato, T. Watanabe & R. Otsuka, *Clays and Clay Minerals*, **40(1)** (1992) 103 – 113.

It can be seen by reference to figure 24 that following their introduction and calcination, pillars become anchored to the tetrahedral sheet of the host mineral, and in no way interact directly with the octahedral sheet. While studying the effect of pillaring on smectites with and without tetrahedral substitution, beidellite and montmorillonite respectively, Plee *et al*¹⁷⁴ were able to illustrate that the tetrahedral location of the layer charge in the beidellite had the effect of requiring higher concentrations of the pillaring species to achieve the same level of basal spacing expansion seen for the montmorillonite. This may arise as a consequence the elevated levels of sheet / compensating cation interactions in the former material. In addition, it was also seen that the presence of aluminium in the tetrahedral sheet of the beidellite results in the installation of a higher degree of ordering to the resultant pillar distribution as a result of aluminium / pillar interactions in the anchoring process.

Likewise, catalytic studies involving the use of montmorillonite and beidellites pillared with the same species show the materials to have different activities.¹⁷⁵ It has been shown that in cumene cracking, pillared beidellites are much more selective, and are less readily coked than their montmorillonitic counterparts. This was attributed to the enhanced acidity of beidellites which results from the Al³⁺ for Si⁴⁺ substitution in their tetrahedral sheets. Pillaring exposes these groups to the cumene, and therefore reduces the necessity of the feedstock molecule to undergo reaction with sites associated with the pillars themselves.

The host clay also has a significant effect on the thermal stability of the PILC.¹⁷⁶ Thermal stability tends to follow the trends observed for dehydroxylation temperatures of the host clays, with structure degradation severing clay / pillar interactions.

¹⁷⁴ D. Plee, L. Gatinéau & J. J. Fripiat, *Clays and Clay Minerals*, **35(2)** (1987) 81 – 88.

¹⁷⁵ R. Swarnakar, K. B. Brandt & R. A. Kydd, *Applied Catalysis A: General*, **142** (1996) 61 – 71.

¹⁷⁶ F. Kooli, J. Bovey & W. Jones, *Journal of Materials Chemistry*, **7(1)** (1997) 153 – 158.

In a further study by Moreno *et al*,¹⁷⁷ the effect of tetrahedral substitutions in minerals other than beidellites have been examined with respect to catalytic activity. Again, enhanced rates and levels of conversion and selectivity over pillared saponites relative to montmorillonites was accounted for on the basis of strongly acidic silanol groups (siloxane bridges) which arise through the isomorphous substitutions outlined previously for beidellites, and which limit the activity of the sites associated directly with the pillars.

2.9.1.4. NATURE OF THE PILLARING SPECIES

It has been shown that certain tri-component pillared clays have higher levels of acidity and thermal stability than those pillared with a mono or bi-elemental species. In addition, differences in both the relative number and distribution of different types of acid site were also seen to differ as a consequence of the nature of the third element used in pillar construction.¹⁷⁰

Even with mono-component pillared clays, the nature of the Lewis acidity imparted to the PILC is highly dependant upon the pillaring species. In addition, interaction between atoms in the pillar, and atoms in the tetrahedral sheet at the point of anchoring also appear to effect the resultant acidic properties of pillared clays.¹⁷⁸

The potential catalytic activity installed in clay minerals as a result of pillaring can be refined by post calcination activation of the pillars. It has recently been depicted that impregnation of aluminium pillared clays with hydrogenation-dehydrogenation active metal functions such as palladium, can aid in refining the selectivity of the material in the execution of hydroisomerisation reactions.¹⁷⁹

¹⁷⁷ S. Moreno, R. Sun Kou & G. Poncelet, *Journal of Catalysis*, **162** (1996) 198 – 208.

¹⁷⁸ S. A. Bagshaw & R. P. Cooney, *Chemistry of Materials*, **5** (1993) 1101 – 1109.

¹⁷⁹ R. Issaadi, F. Garin, C. Eddine Chitour & G. Maire, *Applied Catalysis A: General*, **207** (2001) 323 – 332.

Mention should be made of the most studied of all pillaring species. The Al_{13} species, or so called Keggin Ion is an aluminium tridecamer with the formula $[Al_{13}O_4(OH)_{24}(H_2O)_{12}]^{7+}$. The species consists of 12 octahedral aluminiums, arranged in four groups of three octahedra around a central AlO_4 tetrahedron. The $[Al_{13}]$ polycation can be seen to exhibit 12 terminal water groups, all of which should impart protonic acidity to the moiety.⁹⁷

2.9.1.5. CONCENTRATION OF THE PILLARING AGENT

The primary effect of altering the concentration of the pillaring agent is to induce changes in the porosity of the product material.¹⁶⁶ Note has also been made of the poor thermal stability of PILC's pillared with high concentrations of pillaring agents.¹⁷² Clays containing high density pillaring configurations have also been shown to exhibit poor skeletal isomerisation activity in respect of hydrocarbon reforming reactions.¹⁸⁰ This could be attributed to changes induced in the chemistry of the tetrahedral sheet which arises during the anchoring process. It has been postulated that aluminium tetrahedra in the tetrahedral sheets of some smectites may become inverted as a result of fragilisation of the siloxane linkages which form as a result of their presence. This inversion may be the mechanism by which pillars become irreversibly intercalated into the gallery regions of P.P.C. which have been calcined at high temperature.⁹⁷

2.9.1.6. CONDITIONING OF THE P.P.C.

Contrary to literature speculation, PILC's are not strictly thermally stable.¹⁷⁶ Artificial aging tests (heat treatment) carried out on pillared saponites have revealed that over time, these materials can lose up to 40% of their surface area as a

¹⁸⁰ M. Trombetta, G. Busca, M. Lenarda, L. Storaro, R. Ganzerla, L. Piovesan, A. J. Lopez, M. Alcantara-Rodríguez & E. Rodríguez-Castellón, *Applied Catalysis A: General*, **193** (2000) 55 – 69.

consequence of gallery disorganisation.¹⁶² This unfortunate effect has the potential to limit the application of these materials in high temperature applications.

2.9.2. EFFECTS OF THE PILLARING OF SMECTITES

As with acid activation of clays, the process of pillaring is carried out with the intention of enhancing or installing certain key attributes to the activated material.

There are four key properties installed as a result of pillaring smectites, these being;

1. Increasing Thermal Stability.
2. Increasing Acidity.
3. Increasing Surface Area.
4. Installing Defined Porosity.

2.9.2.1. INCREASING THERMAL STABILITY

As highlighted previously, the introduction of pillars into the gallery region of smectites does eliminate the layer collapse phenomenon outlined for acid activated clays when these materials are used in high temperature applications. However, as also shown, PILC's show limited long term thermal stability. The suggestion that these materials are not thermally stable is inaccurate, but when selecting suitable clays for pillaring, care should be taken to ensure that the resultant PILC will have sufficient thermal stability for the intended application.

2.9.2.2. INCREASING ACIDITY

The nature of the acidity associated with PILC's is defined ultimately by both the nature of the clay being pillared, and by the chemistry of the pillaring species. An in depth study of the origin of acidity in pillared clays remains beyond the scope of this introductory chapter, and therefore the acidity enhancements associated with pillaring will be presented in general terms only.

In terms of Brønsted acidity, there is extensive vibrational spectroscopic evidence to support the existence of various types of protonic sites in pillared clays (hydroxyl groups associated with the metallic component of the pillaring species). Many of the species used to promote pillaring are in fact Brønsted acidic polyacids, including the widely employed Keggin ion. Post intercalation, these pillaring species retain the ability to furnish protons in the presence of suitable acceptor sites, with such sites perhaps being provided by the host clay matrix. In the case of dioctahedral smectites such as montmorillonites, these minerals possess vacant octahedral sites to which protons released by the pillars may migrate, and be stored. In trioctahedral smectites, such vacant octahedral sites are not available. However, isomorphous substitutions in the tetrahedral sheets of these minerals does allow for the formation of siloxane bridges as described earlier, which due to their formal negative charge can accept protons to form structural Brønsted acidic groups. These groups remain available for active catalysis due to the opening up of the gallery regions of clays which results from the pillaring process. The aforementioned hydroxyl groups associated with certain pillaring species such as the Keggin ion may also provide Brønsted acidic protons, although such groups are prone to dehydroxylation during the calcination process.

In terms of Lewis acidity, limited levels are provided by broken bonds at loci of sheet termination in the mineral structure. In PILC's additional Lewis acidity is provided by the pillars. As a result of dehydroxylation during calcination, the metallic components of the pillars are able to act as efficient Lewis acid centres. In light of the potential of the pillars to rehydrate when stored under atmospheric conditions, such Lewis acidity may only be made available when the PILC's are employed in high temperature applications, or are preconditioned at elevated temperatures.

In addition, due to the turbostratic nature and inhomogeneous charge distribution of clay layers, control over the location of installation of pillars is something of a black art, and therefore accurate control over the acidity imparted to PILC's is very difficult to replicate on both an inter and intra batch level.

2.9.2.3. INCREASING SURFACE AREA

The potential surface area of pillared clays is comparable to that of moderately acid treated clays at around 400m²g⁻¹. The majority of the surface area increase, relative to the raw clay, is attributable to the opening up of the gallery region, in addition to the available surface area of the pillars themselves. Surface area can be controlled to some degree by selecting the appropriate concentration of the pillaring species. High concentrations lead to dense pillar configuration, with detrimental effects on the accessible surface area of the material.

2.9.2.4. INSTALLING DEFINED POROSITY

Again controlled to a certain degree by the nature of the substitution of the host clay matrix and by the size and concentration of the pillaring species, pore size in PILC's is notoriously difficult to regulate. Controlling the chemistry of the resultant pores is more practical and has received attention.¹⁸¹

2.9.3. APPLICATION OF PILLARED CLAYS

Due to their peculiarities, PILC's have been slow to receive acceptance as industrially useful materials. The original intended application of PILC's, to be used as cracking catalysts for low quality crude oil feedstocks, remains an active field of research, despite the fact that zeolites remain active in the field and fulfil this role adequately.

The potential benefits of PILC's over zeolites have been explored, including larger pore opening, to install the ability to handle larger feedstock molecules, and also low

¹⁸¹ J. W. Johnson, J. F. Brody, S. L. Soled, W. E. Gates, J. L. Robbins & E. Marucchi-Soos, *Journal of Molecular Catalysis A: Chemical*, **107** (1996) 67 – 73.

hydrogen transfer capability, in order to limit the occurrence of hydrogenation reactions.¹⁸² Zeolites should not feel unduly threatened as some academic researchers are of the opinion that despite the potential activity of pillared interlayered clays as pre-cracking matrices for heavy oils, acid activated clays possess comparable activity and are not only significantly cheaper, but are also easier to produce and to attain control over the properties of the activated products.¹⁸³

More recently, attempts have been made to use PILC'S of defined composition to catalyse specific industrially important reactions such as the conversion of the petrochemical ethylbenzene into the polymer monomer styrene. Currently, this process uses α -Fe₂O₃ based catalysts. The transition metal ion pillared clays studied have shown many selectivity advantages over materials currently in use.¹⁸⁴

Finally, mention should be made to a hybrid class of materials which are referred to as pillared acid activated clays (PAAC's). These are manufactured by subjecting pre-acid activated clays to the pillaring processes outlined above. The materials present many of the advantageous properties associated with the respective products from which they are formed. Although this class of activated clays remains outside the scope of this investigation, they are of prime academic and industrial importance, and as such are the subject of extensive literature.^{185,186,187}

¹⁸² F. González, C. Pesquera, I. Benito, E. Herrero, C. Poncio & S. Casuscelli, *Applied Catalysis A: General*, **181** (1999) 71 – 76.

¹⁸³ H. Suquet, R. Franck, J. F. Lambert, F. Elsass, C. Marcilly & S. Chevalier, *Applied Clay Science*, **8** (1994) 349 – 364.

¹⁸⁴ G. Perez, A. De Stefanis & A. A. G. Tomlinson, *Journal of Materials Chemistry*, **7(2)** (1997) 351 – 356.

¹⁸⁵ R. Mokaya & W. Jones, *Journal of the Chemical Society – Chemical Communications* (1994) 929 – 930.

¹⁸⁶ R. Mokaya & W. Jones, *Journal of Catalysis*, **153** (1995) 76 – 85.

¹⁸⁷ J. Bovey, F. Kooli & W. Jones, *Clay Minerals*, **31** (1996) 501 – 506.

CHAPTER
THREE

Analytical Theory

3. INTRODUCTION TO ANALYTICAL THEORY

A range of analytical techniques have been used to generate the data presented in this thesis. This chapter offers an insight to the theoretical aspects associated with each of these techniques and provides elementary information regarding the appropriateness of each technique with respect to the information required.

The following techniques will be discussed;

- | | | | |
|----|--|-----------------------------------|----------|
| 1. | Synergic Chemical Analysis: | <i>Thermogravimetric Analysis</i> | (TGA) |
| | | <i>Infra Red Spectroscopy</i> | (IR) |
| | | <i>Organic Trap Module*</i> | (OTM) |
| | | <i>Gas Chromatography</i> | (GC) |
| | | <i>Mass Spectrometry</i> | (MS) |
| 2. | x-ray Fluorescence Spectrometry | | (XRF) |
| 3. | x-ray Diffraction Analysis | | (XRD) |
| 4. | Gas Chromatography – Mass Spectrometry | | (GC-MS) |
| 5. | Inductively Coupled Plasma Spectrometry | | (ICP) |
| 6. | Fourier Transform Infra Red Spectroscopy | | (FTIR) |
| 7. | Diffuse Reflectance Infra-Red Fourier Transform Spectroscopy | | (DRIFTS) |

3.1. SYNERGIC CHEMICAL ANALYSIS

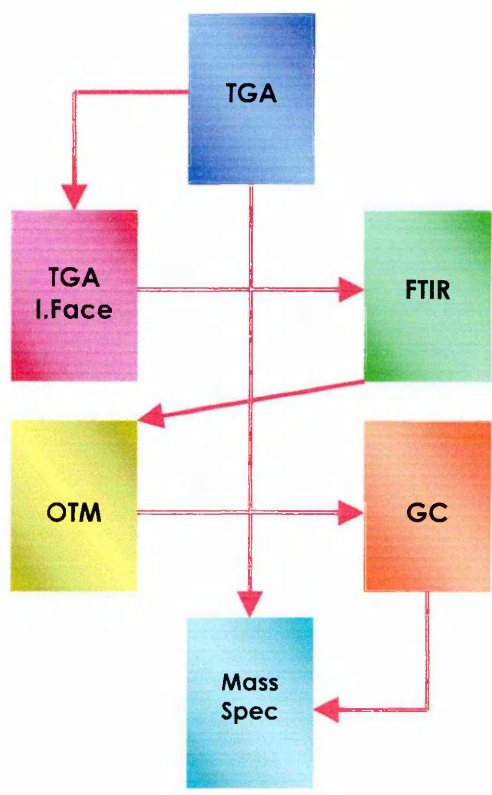
Synergic Chemical Analysis (SCA) is a versatile analytical technique, which makes significant use of Evolved Gas Analysis (EGA). The system comprises a number of traditional analytical instruments, each of which represents a powerful analytical technique in its own right.

* Organic Trap Module (OTM) – Not Strictly An Analytical Technique In Its Own Right, But Comprises An Important Component Of The Post Run Capability Of The Synergy System.

Figure 25 illustrates a diagrammatic representation of the instrumental components of the system. The red arrows represent possible analysis routes for gases generated by heating samples in the TGA. The power of the system resides in the fact that each of the instrumental components can be used individually or in any number of combinations as summarised by the following;

- a. TGA Only (Real Time)
- b. TG – FTIR (Real Time)
- c. TG – MS (Real Time)
- d. TG – FTIR / MS (Real Time)
- e. TG – OTM – GC – MS (Real Time / Post Run Analysis)
- f. TG – FTIR – OTM – GC – MS (Real Time / Post Run Analysis)

Figure 25 – Layout of the Synergic Chemical Analysis System



Interest in the application of EGA has grown considerably, and the technique is now widely accepted as an effective method for analysing a wide range of materials. In particular, the technique has proven useful in polymer science where the approach is routinely put to use to ascertain polymer decomposition products.^{8,188,189,190,191,192} Likewise, EGA is rapidly becoming the preferential method in catalyst screening programmes.^{8,193,194,195,196,197,198} Reports of novel derivatives of EGA have also appeared.^{199,200,201,202,203,204} Furthermore, EGA is becoming a recognised method for the direct study of mineral behaviour.^{205,206}

The EGA system used in this work is known as a Synergic Chemical Analysis (SCA) System, and it is composed of several analytical instruments (figure 25). The following sub sections will briefly identify these instruments, their mode of operation and the theory behind the analysis.

-
- ¹⁸⁸ M. Webb, P. M. Last & C. Breen, *Thermochimica Acta*, **326** (1999) 151 – 158.
- ¹⁸⁹ J. Mullens, G. Reggers, M. Ruysen, R. Carleer, J. Yperman, D. Franco & L. C. Van Poucke, *Journal of Thermal Analysis*, **49** (1997) 1061 – 1067.
- ¹⁹⁰ J. D. Van Dyke & K. L. Kasperski, *Journal of Polymer Science Part A: Polymer Chemistry*, **31** (1993) 1807 – 1823.
- ¹⁹¹ X. Xiao, W. Zmierczak & J. Shabtai, *Division – Fuel Chemistry*, **40** (1995) 4 – 8.
- ¹⁹² T. Faravelli, G. Bozzano, C. Scassa, M. Perego, S. Fabini, E. Ranzi & M. Dente, *Journal of Analytical and Applied Pyrolysis*, **52** (1999) 87 – 103.
- ¹⁹³ C. Dossi, A. Fusi, S. Recchia, S. Calmotti & R. Psaro, *Analyst*, **120** (1995) 2353 – 2356.
- ¹⁹⁴ P. A. Barnes, G. M. B. Parkes, D. R. Brown & E. L. Charsley, *Thermochimica Acta*, **269/270** (1995) 665 – 676.
- ¹⁹⁵ P. G. Smirniotis & W. Zhang, *Industrial Engineering Chemistry Research*, **35(9)** (1996) 3055 – 3066.
- ¹⁹⁶ W. Zhang & P. G. Smirniotis, *Applied Catalysis A: General* **168** (1998) 113 – 130.
- ¹⁹⁷ D. P. Serrano, J. Aguado & J. M. Escola, *Applied Catalysis B: Environmental*, **25** (2000) 181 – 189.
- ¹⁹⁸ C. Breen, P. M. Last, S. Taylor & P. Komadel, *Thermochimica Acta*, **363** (2000) 93 – 104.
- ¹⁹⁹ F. Cheng-Yu Wang & B. Gerhart, *Analytical Chemistry*, **68(22)** (1996) 3917 – 3921.
- ²⁰⁰ F. D. Kopinke & M. Remmler, *Thermochimica Acta*, **263** (1995) 123 – 139.
- ²⁰¹ R. Ocha, H. Van Woert, W. H. Lee, R. Subramanian, E. Kugler & P. C. Eklund, *Fuel Processing Technology*, **49** (1996) 119 – 136.
- ²⁰² A. A. Garforth, Y. –H. Lin, P. N. Sharratt & J. Dwyer, *Applied Catalysis A: General*, **169** (1998) 331 – 342.
- ²⁰³ J. Walendziewski & M. Steininger, *Catalysis Today*, **65** (2001) 323 – 330.
- ²⁰⁴ F. Cheng-Yu Wang, B. Gerhart & C. G. Smith, *Analytical Chemistry*, **67(20)** (1995) 3681 – 3686.
- ²⁰⁵ R. Carleer, G. Reggers, M. Ruysen & J. Mullens, *T. Acta*, **323**(1998) 169 – 178.
- ²⁰⁶ C. Breen, J. Forsyth & J. Yarwood, *Physical Chemistry and Chemical Physics*, **2(17)** (2000) 3887 – 3892.

The red arrows shown in figure 25, represent glass lined heated transfer lines. They connect the individual pieces of instrumentation and allow for passage of gas samples from one instrument to another without the possibility of condensation. The system operates using a series of valves, which allow or prevent the passage of gas down each of the transfer lines illustrated depending upon the mode of operation and analysis selected.

3.1.1. THERMOGRAVIMETRIC ANALYSIS (TGA)

TGA provides a means for the continuous measurement of the mass of a sample as it is subjected to a linear heating rate under a controlled reaction atmosphere. Hence, the resultant thermogram is a plot of mass or mass percent as a function of time, with the appropriate temperature profile being superimposed for comparative purposes.

TGA is useful in investigating the thermal behaviour of clay minerals, in particular, those used in high temperature applications such as the hydrocarbon reforming processes investigated in this work. Information can also be realised in respect of the rate of polymer decomposition, and subsequent flow rate of the product gases through the catalyst bed.

The Synergy system is equipped with a Cahn TG131 TGA unit. Unless otherwise stated, all TGA data presented was recorded using this instrument. A Mettler-Toledo TG50 thermobalance equipped with a TC10A processor was also used as noted.

3.1.2. INFRA-RED ANALYSIS (IR)

Infra red represents a useful analytical technique which, due to its non destructive nature, provides a beneficial addition to the SCA system. The synergy system is fitted with a TGA-IR interface containing an infra red gas cell which is coupled directly to an ATI Mattson Infinity Series FTIR spectrometer.

The availability of an infra red analytical capability on the synergy system permits the accumulation of real time vibrational spectroscopic data from the species thermally evolved from samples within the TGA. In the catalyst screening work in this thesis, the number of species evolved from a sample over any given time interval were numerous, making definitive identification by infra red difficult due to band overlap, in addition to the presence of common signals attributable to a variety of different species.

As with all spectroscopic techniques, infra red analysis relies upon the interaction of electromagnetic radiation with matter, the analyte. Infra red radiation contains insufficient energy to break intermolecular bonds or to induce the type of electronic transitions observed in UV/Vis spectroscopy. Only polar bonds are infra red active. As a consequence of their asymmetric charge distribution, the vibrations associated with polar bonds are restricted to certain quantum levels, a situation which gives rise to regular fluctuations of the dipole moment associated with the bond. When molecules are irradiated with infra red radiation which contains individual components which are equal in energy to that of the bond vibration, a net energy transfer takes place. This results in a change in the amplitude of the bond vibration, thus promoting absorption of certain components of the incident radiation. Infra red techniques report those component wavelengths of the incident radiation which have been absorbed by the molecules under investigation. As a result of quantisation, these absorption's are common for given functional groups and thus

characteristic spectra are obtained. Further information relating to the design and operation of Fourier Transform infra red spectrometers will be given in section 3.6.

3.1.3. ORGANIC TRAP MODULE (OTM)

Although the OTM provides no direct analytical information, it represents an important component of the synergy system's post run capability. The OTM houses an interchangeable adsorbent trap, which can be substituted with traps for the specific absorption of the materials under investigation. During real time analysis, gases evolved from the TGA are extracted from the furnace under negative pressure by an appropriately named 'sniffer tube'. These gases travel along a heated transfer line and pass directly into the infra red gas cell, at which point infra red analysis is performed. The gas stream is extracted from the infra red gas cell by a pump attached to the exit port of the trap contained within the OTM. The gas stream passes down a second heated transfer line before being immobilised on the adsorbent trap, which is maintained at room temperature. Post run, the trapped gases are desorbed from the trap by heating the assembly, and by passing a rapidly flowing stream of pre-heated helium through the trap. The contents are thus desorbed into the injection port of the associated GC and are subject to separation and analysis by GC-MS.

3.1.4. GAS CHROMATOGRAPHY (GC)

Ordinarily, methods for chemical analysis are usually selective, with very few, if any, being truly specific. It is therefore generally advantageous, in the case of mixtures to employ pre-analysis separation. Such separations are routinely carried out by one of many chromatographic methods.

Gas chromatography (GC) promotes separation by 'combining' the analyte mixture with a mobile phase (inert carrier gas) which is then passed through an immiscible stationary phase constrained within a column. Modern capillary columns for use in Gas Liquid Chromatography are coated with a high boiling point, thermally stable liquid stationary phase which is incompatible with the intended analyte. Partition equilibrium between components in the analyte and the mobile and stationary phases effects separation. In analyses in which the analyte comprises a range of species with a broad scope of boiling points, temperature programming of the oven housing the column can be used to enhance separation efficiency. High temperature separations may repress resolution.

The SCA system is equipped with an ATI Unicam 615GC. For purposes of hydrocarbon analysis, the instrument is fitted with a fused silica, wall coated open tubular (WCOT) capillary column with an external diameter of 0.25mm and a length of 30m.

3.1.5. MASS SPECTROMETRY (MS)

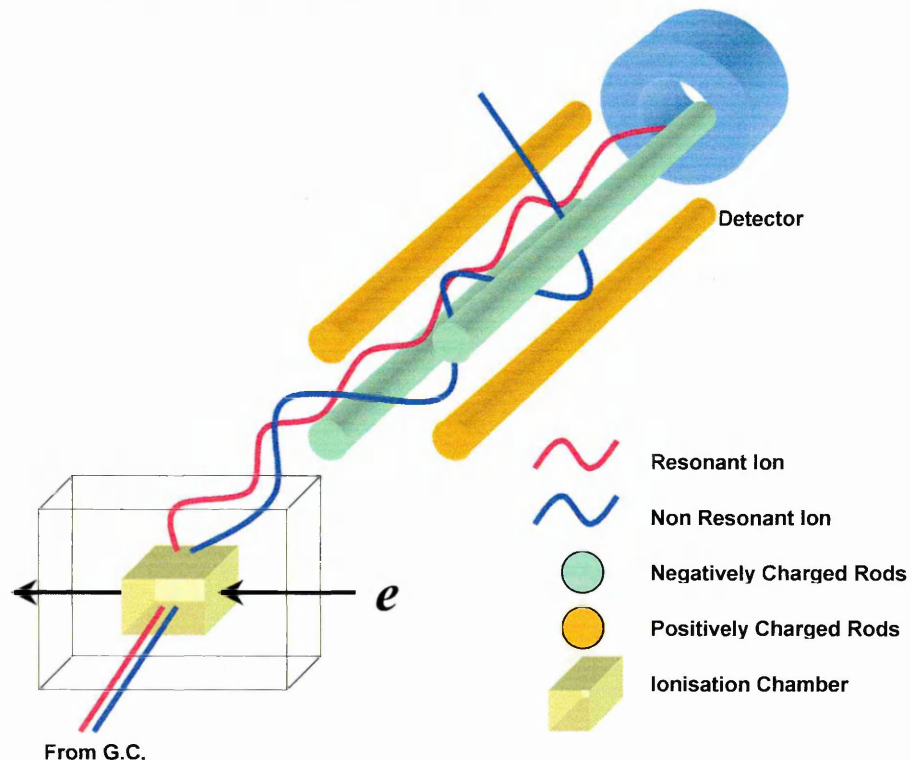
The major detection instrument on the synergy system is a mass spectrometer, which can be used in real time (TG-MS) or post run ((TG-(FTIR)-OTM-GC-MS). The system is fitted with an ATI Unicam Automass System 2 benchtop quadrupole mass spectrometer.

Mass spectrometry is concerned with the formation, separation and subsequent decomposition of ions from neutral compounds. Requiring only picograms (10^{-12} g) of material to perform an analysis, the technique relies upon the execution of a chemical reaction, and as such the analyte is not recoverable.

Mass spectrometric analysis (GC-MS) admits the effluent gas stream from a GC column into the ion source of the spectrometer. The analyte molecules are ionised

by one of two methods, electron ionisation (EI) or chemical ionisation (CI). The SCA system is configured for the former. Figure 26 illustrates the assembly which composes the ion source and quadrupole.

Figure 26 – Ion Source / Quadrupole Arrangement for the Automass System 2



The entire arrangement is maintained under vacuum. Electrons generated by a heated filament are directed across the ionisation chamber with a defined energy, measured in electron volts (eV). By convention, spectra are recorded at 70eV as this represents maximum ion yield and reproducibility. Inside the ionisation chamber, the electrons pass in close proximity to analyte molecules causing a mutual distortion of the electron wavefunction and the electric field of the analyte molecule. Although electron capture and electronic excitation of the analyte are possible, the desired outcome for MS is electron abstraction as illustrated by reaction 4 below;



The resultant molecular ions (M^+) are typically unstable, and as a consequence of their excess internal energy, imparted by the energy associated with the incident electrons, undergo fragmentation. The resultant ions are separated and experience sequential detection on the basis of their mass to charge ratio.

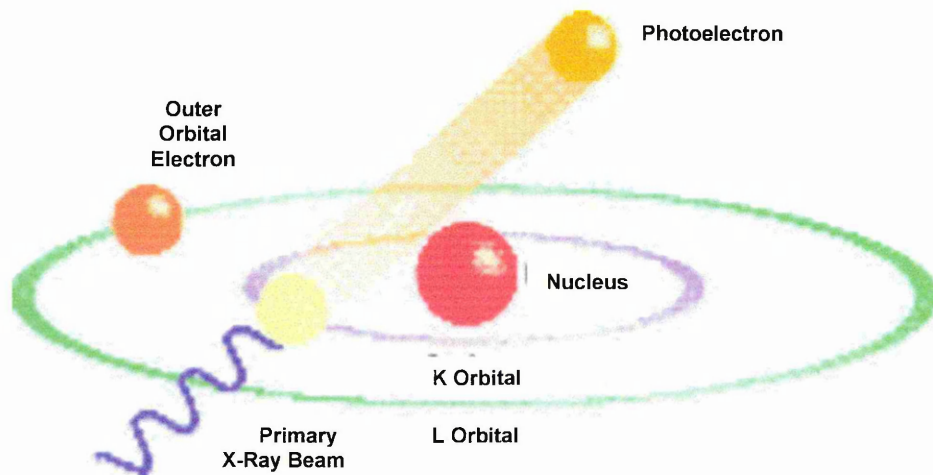
The quadrupole mass filter consists of a set of four cylindrical rods held in a square array. Between each set of opposite and electrically connected rods is applied a direct current (DC) voltage, superimposed upon which is a radiofrequency (RF) potential. This forms crossed, oscillating electric fields within the quadrupole arrangement, which are perpendicular to the direction of travel of the ions introduced into the quadrupole via acceleration from the ionisation chamber. Under the influence of these combined electric fields, the ions follow complex trajectories. If the oscillation motion of the ion is out of resonance, the ion strikes the quadrupole and is not detected. The application of known voltages and RF potentials to the quadrupole can control the 'stable' ion trajectories and thus filter the ion stream to limit those charged species reaching the detector. Scanning RF and DC voltages allows ions to be transmitted through the quadrupole mass filter in a sequential fashion in order of increasing mass to charge (m/z) ratio with constant resolution, therefore permitting multi ion analysis. Quadrupole mass filters were originally developed for the removal of unstable nuclei from waste streams destined for elution into the environment by the nuclear industry.

3.2. X-RAY FLUORESCENCE SPECTROMETRY (XRF)

Wavelength dispersive x-ray fluorescence spectrometry is a non / destructive analytical technique which is routinely employed to identify and quantify the elements present in a sample. XRF can handle solids, powders and liquids, and can be used to efficiently identify and measure all elements from beryllium to uranium.

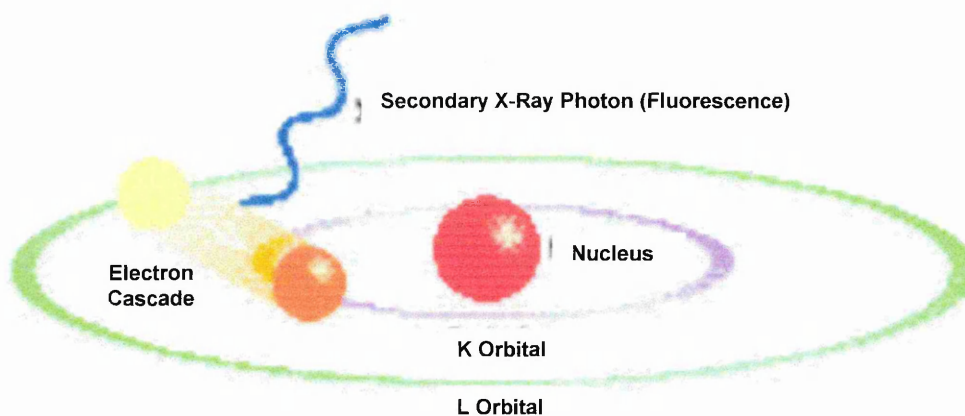
Samples for analysis are irradiated with a high energy polychromatic x-ray beam. Assuming that the energy associated with the incident beam is greater than the binding energy of the core electrons of the elements under investigation, this irradiation results in the ejection of core electrons from the sample in the form of photoelectrons. This creates electron 'holes' in the core atomic orbitals of the element, and thus its conversion into a highly unstable ion. The nature of this process is illustrated in figure 27.

Figure 27 – Sample Irradiation and Photoelectron Ejection in XRF Spectrometry



In an attempt to restore stability, the holes generated in the inner orbitals of the elemental ions, are filled, via a cascade of electrons from outer atomic orbitals. These transitions are accompanied by the emission of secondary (2°) X-Ray photons, this being the process known as fluorescence. Figure 28 illustrates this stabilisation process. The wavelengths of these 2° X-Ray photons are characteristic of individual elements. Elemental concentrations are determined through examination of the intensity of the secondary radiation observed.

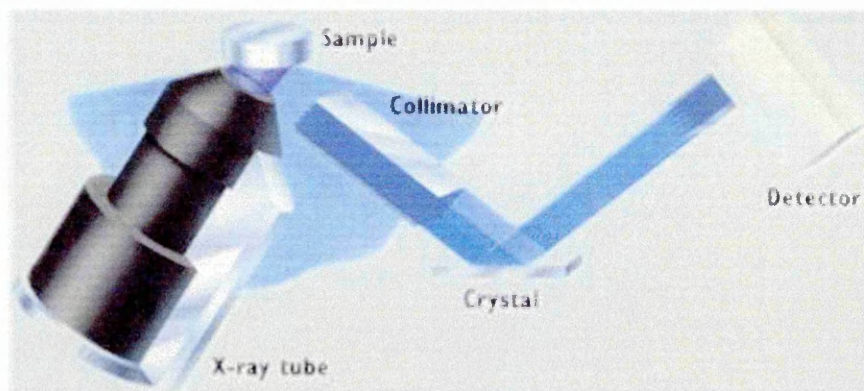
Figure 28 – Fluorescence Emission During Electron Cascade in XRF Spectrometry



XRF analysis were performed using a Phillips PW2400 high performance sequential wavelength dispersive x-ray spectrometer operating with a 3kW close coupled x-ray tube (Rh). The sampling arrangement for this type of spectrometer is illustrated in figure 29. A goniometer permits sequential, multi element determination by rotating the analysing crystal, while the detector rotates to intercept the diffracted beam.

XRF readily reports the elemental composition of clays and identifies the nature of the interlayer and surface exchange site cations. In addition, information can also be accumulated with regards to the potential of isomorphous substitution in both the octahedral and tetrahedral sheets.

Figure 29 – Sampling Arrangement for Sequential XRF Spectrometer



3.3. X-RAY DIFFRACTION (XRD)

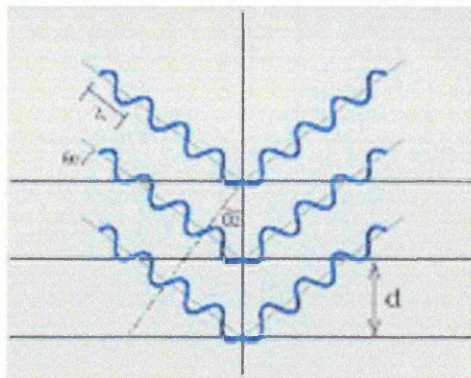
X-ray diffraction (XRD) represents a versatile, non destructive technique for the identification of various crystalline phases in solid materials and powders. Identification is made by comparison of sample diffractograms to databases containing reference patterns.

Crystalline materials contain a regular three dimensional distribution of their atoms in space, resulting in a series of repeating parallel planes separated by a distance defined by as d , which is variable, and material dependant. Diffraction is governed by Bragg's Law (equation 5);

$$n \lambda = 2d \sin \theta \quad (\text{Equation 5})$$

Irradiation of a sample with monochromatic x-rays of known wavelength at an angle theta (θ), promotes diffraction when Bragg's law is fulfilled. This occurs when the distance travelled by the x-ray beam reflected from successive planes differs by a complete number of wavelengths (n). Variation of θ allows for the satisfaction of the requirements of Bragg's Law for a variety of d -spacings. By plotting the angular positions and intensities of the resultant diffracted peaks, a pattern (diffractogram) which is characteristic of the sample is produced. Figure 30 illustrates the satisfaction of the Bragg equation, with the resulting coherent diffraction.

Figure 30 – Satisfaction of Bragg's Law to Promote Total Diffraction



XRD represents an invaluable tool for the study of clay minerals. Indeed, it was XRD data³³⁻³⁹ which led to the realisation that clay minerals are crystalline materials. In the case of modified clay minerals, XRD provides evidence pertaining to the loss of structural integrity associated with acid activation (via reduction in the intensity of the d_{001} signal). Likewise, in the case of pillaring processes, increases in the d_{001} spacing for a material are indicative of successful intercalation of the pillaring species. XRD data presented was recorded using a Phillips PW1130 diffractometer.

3.4. GAS-CHROMATOGRAPHY/MASS-SPECTROMETRY

The usefulness in the speciation of chemical analytes has led to its association with a range of chromatographic techniques. The coupling of gas chromatographs to mass spectrometers is now common practice. Descriptions of gas chromatography and quadrupole based mass spectrometry techniques are given in sections 3.1.4. and 3.1.5. respectively.

3.5. INDUCTIVELY COUPLED PLASMA/MS (ICP-MS)

ICP is a straight forward elemental determination technique in which samples for analysis are ionised by introduction into a high temperature plasma. Plasma conditions are achieved through the ionisation of reagent argon gas molecules. The resultant ions and their associated electrons subsequently interact with magnetic fields generated by a radio frequency powered induction coil. This results in ohmic heating as the ions resist their induced motion paths. Temperatures achieved typically fall in the range 4000 to 8000K.

Samples for analysis are usually aspirated into the plasma, and ionised as a consequence. In the case of ICP-MS, these ions are directed into a mass spectrometer for analysis and identification. ICP-MS analysis measurements were made using a Spectro Analytical ICP-MS.

3.6. FOURIER TRANSFORM INFRA RED SPECTROSCOPY

Fourier Transform Infra Red spectroscopy (FTIR) was originally developed by astronomers in the 1950's in order to study the infra red spectra of stars. FTIR has three main advantages over the use of more traditional dispersive methods, these can be summarised as follows.

Throughput Advantage (Jaquinot Advantage)

FTIR spectrometers have no slits and fewer optical components than dispersive instruments. Therefore, the power of the radiation reaching the detector is much greater than dispersive spectrometers, resulting in a higher signal to noise (S/N) ratio.

High Wavelength Accuracy

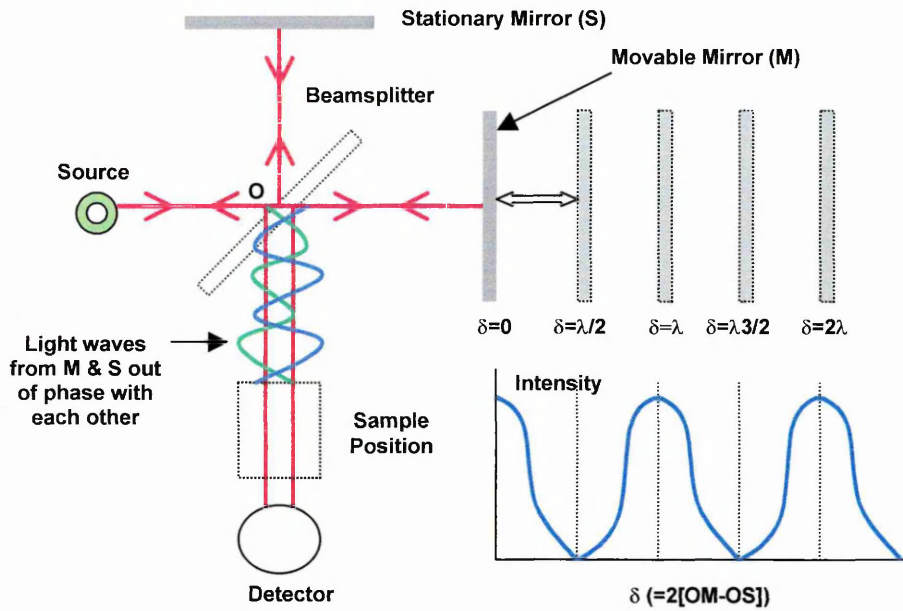
As a consequence of their high level of wavelength accuracy and precision, FTIR spectrometers allow for signal averaging, a process which again enhances S/N ratios.

Multiplex Advantage (Fellgett Advantage)

In FTIR spectrometers, all elements from the source reach the detector simultaneously, thus allowing an entire spectrum to be recorded very rapidly. This allows multiple measurements to be made over a short period of time, a factor which generates enhancements in spectral resolution.

These advantages are achieved primarily through the use of interferometry. Figure 31 shows the arrangement of the components which forge the Michelson Interferometer.

Figure 31 – Component Arrangement within the Michelson Interferometer



Radiation from the source is directed towards the beamsplitter, a device which transmits some of the incident radiation to the stationary mirror, and some to the moving mirror. Rays reflected from each of these mirrors return to the beamsplitter, where half of each ray is transmitted, and half is reflected. One combined ray travels back to the source while the second passes through the sample 'en route' to the detector. As a result of the motion of the moving mirror, the recombined waves are generally not in phase, and therefore interfere destructively. The difference in pathlength, resulting from mirror motion, travelled by the two waves within the interferometer can be described by the formula $2(OM-OS)$, the product being referred to as the retardation (δ). Constructive interference takes place when δ is an integral multiple of the wavelength. Total destructive interference occurs when δ is a half integral multiple of the wavelength of the light. As a result of the motion of the moving mirror, at constant speed, radiation reaching the detector goes through a steady sequence of maxima and minima as the interference alternates between constructive and destructive phases. A chart plotting output light intensity against retardation is known as an interferogram.

In FTIR the sample absorbs certain wavelengths of the recombined ray of light, and as such, the interferogram contains the infra red spectrum of the source minus the infra red spectrum of the sample. To conclude, the resultant spectrum is the Fourier transformation of the recorded interferogram.

The mathematics behind the Fourier transformation determine how the interferogram is sampled. The closer the spacings of the data points, the wider the wavelength range which can be studied. In turn, the sampling interval relates to mirror motion, and mirror speed determines the rate of collation of data points, for a given resolution.

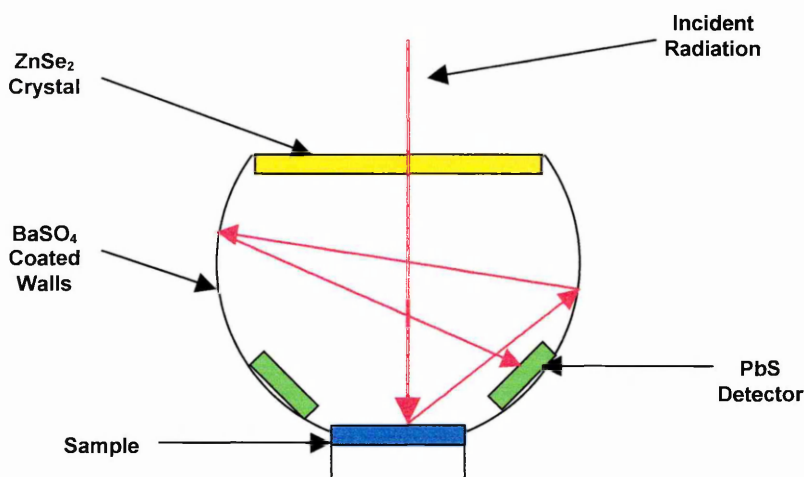
All stand alone infra red analysis was performed using an ATI Mattson Genesis series FTIR spectrometer.

3.7. DIFFUSE REFLECTANCE (IR) (FT) SPECTROSCOPY

Diffuse Reflectance Infra Red Fourier Transform Spectroscopy (DRIFTS) is an accessory technique used in FTIR procedures. The technique relies upon the penetration of the surface of the sample by an incident beam of radiation. This results in the excitation of the vibrational modes of the analyte molecules by the radiation, which is then scattered in all directions, giving rise to both true diffuse reflectance, but also to specular reflectance. The sampling arrangement used in DRIFTS procedures is shown in figure 32.

The interior walls of the sampling accessory are coated with a material (BaSO_4) which promotes total diffuse reflectance. Radiation scattered by the sample ultimately reaches the detector after several reflections.

Figure 32 – Sampling Arrangement Found in the DRIFTS Accessory



All DRIFTS data was recorded using a Mattson Polaris FTIR spectrometer fitted with a Graseby Specac DRIFTS accessory.

All variable temperature (VT) DRIFTS analyses were performed using the instrument detailed above. For the execution of VT-DRIFTS work, a specialised heating stage is used, the temperature of which is controlled externally. Appropriate temperature ramps were selected, and samples given 30 minutes to equilibrate to the chosen temperature prior to recording the appropriate data. The heated sample cell is fitted with an exhaust which with the aid of a dry nitrogen purge is vented into a fume cupboard, thus permitting the removal of desorbed gases from the sample cell.

CHAPTER
FOUR

Experimental

4. EXPERIMENTAL

The aim of this chapter is to define the materials and experimental methodologies employed to generate the data presented in this thesis.

4.1. CLAY MINERALS EMPLOYED

The following materials have been used in the course of these investigations;

4.1.1. PILLARED SAPONITE

These materials were prepared using a base saponite from the Yuncillos deposit in Toledo, Spain. The materials were pillared using, aluminium, chromium and aluminium-chromium oligomers. The products were a range of materials with variable pillar composition (table 10).

Table 10 – Nomenclature for a Series of Pillared Saponites

Notation	Pillar Composition (% Al / Cr)
R1	No Pillars
R2	100 : 0
R3	90 : 10
R4	80 : 20
R5	50 : 50
R6	20 : 80
R7	10 : 90
R8	0 : 100

These materials were provided by the Department of Inorganic Chemistry, Faculty of Chemical Sciences, University of Salamanca, Spain. Details pertaining to the preparation of these materials has been detailed elsewhere.¹⁶⁸

For comparison, the un-pillared source saponite was calcined at 500°C prior to its use in the transformation reactions.

4.1.2. ACID ACTIVATED STEBNO (ST)

Stebno is an iron rich beidellite taken from deposits in the Czech Republic (Breen *et al*¹⁴¹) and it was acid activated in 6M HCl at 60°C for selected treatment times. Table 11 shows the nomenclature applied to these materials.

Table 11 – Nomenclature Applied to a Series of Acid Activated Stebno Derivatives

Notation	Duration of Activation Treatment (Mins)
ST00	No Activation
ST30	30
ST120	120
ST240	240

These materials were prepared and supplied by the Institute of Inorganic Chemistry, Slovak Academy of Sciences, SK-842-36, Bratislava, Slovakia.

4.1.3. ACID ACTIVATED JELSOVY POTOK (JP)

Jelsovy Potok is a sodium montmorillonite taken from the Kremnica mountains in central Slovakia,¹⁴¹ and it was activated in 6M HCl at 95°C for selected periods of time (Table 12).

Table 12 - Nomenclature Applied to a Series of Acid Activated JP Derivatives

Notation	Duration of Activation Treatment (Mins)
JP00	No Activation
JP120	120
JP240	240
JP360	360

These materials were prepared and supplied by the Institute of Inorganic Chemistry, Slovak Academy of Sciences, SK-842-36, Bratislava, Slovakia. The transformation data recorded using these materials as catalysts is not presented in this thesis as the activity

of these activated materials was lower than seen with other modified minerals of montmorillonite origin.

4.1.4. ACID ACTIVATED SWY-2

SWy-2 is a sodium montmorillonite mined from deposits in Wyoming, U.S.A. The material was supplied by the Source Clay Minerals Repository of the Clay Minerals Society and used as received.

SWy-2 was acid activated at Sheffield Hallam University as described in section 4.2.1. As with the ST and JP treatments, SWy-2 was activated in 6M HCl at 95°C for selected periods of time. Preliminary experiments indicated that 95°C represented the most effective treatment temperature. The resultant products were named according to the length of the activation procedure (table 13).

Table 13 - Nomenclature Applied to a Series of Acid Activated SWy-2 Derivatives

Notation	Duration of Activation Treatment (Hours)
SWy-2-0A	No Activation
SWy-2-2A	2
SWy-2-4A	4
SWy-2-6A	6
SWy-2-8A	8

The ending A infers 'Actual' to distinguish these samples from the test samples prepared to optimise the treatment parameters.

4.1.5. COMMERCIALY AVAILABLE AAC'S

A range of commercially available acid activated clays were screened to determine their effectiveness as transformation agents for the catalytic transformation of the gases evolved during the thermal decomposition of HDPE. The materials chosen are listed in table 14 along with their manufacturers and commercial applications.

Table 14 – Selected AAC's, Their Manufacturers and Commercial Applications

Product	Manufacturer	Use
Fulacolor™	Laporte Additives	Carbonless Copying Paper
Fulcat 22B™	Laporte Additives	Adsorbent
Fulcat 40™	Laporte Additives	Adsorbent
K10™	Sud Chemie	Solid Acid Catalyst

Fulacolor™

Fulacolor is manufactured from a beidellitic clay mined at Los Trancos in south east Spain (Almeria). The deposit contains smectites which have developed as a result of hydrothermal alteration of a homogeneous volcanic tuff with an acidic composition.

The material is activated in 6M HCl at 95°C. The duration of the activation procedure is determined by the precise composition of the starting minerals.

Originally classified as montmorillonites, the smectites in the Los Trancos deposit have variable composition and depletion of the montmorillonite type clays has led to a predominance of beidellitic minerals.²⁰⁷ To counteract the loss of the montmorillonitic components of the base clay, Fulacolor contains a 10% w/w addition of a turkish montmorillonite, which is added prior to the activation process.

Samples were supplied by Laporte Additives, Widnes, Cheshire and used as received.

Fulcat 22B™ & Fulcat 40™

Fulcat 22B and Fulcat 40 are both derivatives of the same refractory base mineral. Some of the more important ceramic and mineralogical properties of these types of clays have been detailed elsewhere.²⁰⁸

²⁰⁷ J. Cuadros, A. Delgado, A. Cardenete, E. Reyes & J. Linares, *Clays and Clay Minerals*, **42(5)** (1994) 643 – 651.

²⁰⁸ G. L. Chàvez & W. D. Johns, *Applied Clay Science*, **9** (1995) 407 – 424.

Samples for analysis were supplied by Laporte Additives, Widness, Cheshire and used as received.

K10

K10 is one of a range of solid acid catalysts manufactured from a montmorillonite mined at Bavaria in Germany. Activation is performed for a variable length of time, in boiling HCl, the concentration of which is dictated by the chemical composition of the starting material, and that required in the product.^{114,136}

Samples for analysis were supplied by Sud Chemie, Bavaria Germany and used as received.

In addition to the modified smectites outlined above, a series of acid modified Kaolin Amorphous Derivatives (KAD's) have been studied.

4.1.6. KAOLIN AMORPHOUS DERIVATIVES (KAD's)

The base Kaolin used in the preparation of the acid leached KAD's was supplied by ECC International. The material was ground and sieved to attain the <2 μ m fraction prior to treatment.

Samples for analysis were prepared according to the procedure outlined in section 4.2.2. Post calcination, the resultant metakaolin was activated in HCl of varying concentration for 3 hours at 80°C. Samples were named according to the strength of the treatment acid. Table 17 illustrates the nomenclature of these activated materials.

Notation	[Treatment Acid](M HCl)
Kaolin	No Activation
MK (Metakaolin)	No Activation
AAMK3.1	1
AAMK3.2	2
AAMK3.3	3
AAMK3.6	6

AAMK3.2 = Metakaolin acid activated for 3 hours in 2M HCl.

4.2. SAMPLE PREPARATION

The following sections outline the treatment procedures employed to generate the transformation agents screened during the course of the work outlined hereafter.

4.2.1. PREPARATION OF ACID ACTIVATED SWY-2

250ml of 6M hydrochloric acid, prepared by a 1.44:1 w/v dilution of a fuming 37% aqueous solution of hydrogen chloride in water was heated to 95°C. 5g of SWy-2 was added and the reaction mixture stirred continuously both during and after addition. Following activation, the hot acid / clay suspensions were rapidly filtered under vacuum to remove excess acid and inhibit further structural attack. The resulting filter cakes were dispersed in ice cold distilled water (10ml aliquots), agitated and refiltered. The procedure was repeated until the conductivity of the supernatant fell below 30 μ S. The resulting solids were air dried and ground prior to use.

4.2.2. PREPARATION OF ACID ACTIVATED KAD's

Metakaolin was prepared by calcining the base kaolin at 600°C under air for 15 hours. The resultant metakaolin was cooled, ground and acid leached with constant stirring at 80°C for 3 hours using aqueous HCl concentrations of 1, 2, 3 and 6M. The leached samples were rapidly filtered under vacuum to remove the excess acid and

prevent further structural attack. Filtered samples were not washed because as detailed by Perisinnotto *et al*,¹²⁶ no surface area enhancements are achieved through this process due to the solubility of alumina in HCl.

4.2.3. ION EXCHANGE ACTIVATION

1g of the clay was fully exchanged by washing the material three times with a 0.5M solution containing the appropriate metal cation (Table 18).

Table 18 – Cations Used in Ion Exchange Activation, and Their Source.

Cation	Source (aq)
H ⁺	HCl
Na ⁺	NaCl
Ca ²⁺	CaCl ₂
Mg ²⁺	MgCl ₂
Al ³⁺	AlCl ₃
Co ²⁺	CoSO ₄
Zn ²⁺	ZnSO ₄

Post exchange, the solids were filtered and washed with ice cold de-ionised water (10ml aliquots) until the conductivity fell below 30 μ S. The resultant solids were air dried, ground and stored in air tight containers prior to use.

In cases where only part exchange was required, metal cation was supplied in a single exchange procedure. Following immersion, the solution was stirred overnight, prior to filtering. Post activation, the washing and drying procedures outlined above were used.

4.3. MATERIAL CHARACTERISATION

The primary aim of this work relates to the screening of a range of modified minerals to determine their potential effectiveness as transformation agents for the catalytic transformation of the thermally generated off gases produced as a result of waste

polymer pyrolysis. As such, this procedure forms the basis of the material characterisation process. In addition, a variety of other techniques have been used to attain the appropriate chemical and structural information about the materials screened. More information regarding the uncatalysed process is given in chapter 5.

4.3.1. SYNERGIC CHEMICAL ANALYSIS

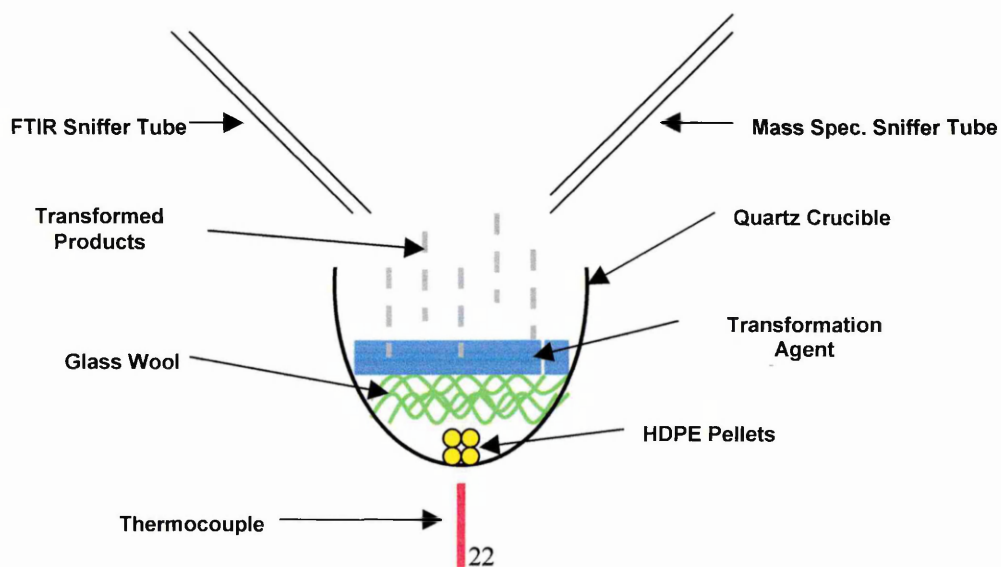
As the primary investigative tool, the SCA system has been used in a variety of configurations, namely

1. TG-OTM-GC-MS
2. TG-(FTIR)-MS

TG – OTM – GC – MS (Isothermal)

This configuration accumulates real time TG data together with post run GC-MS data. Preliminary studies had shown that due to the large number of co-evolving species, identification by either real time FTIR or MS was not realistic. Therefore, the OTM, which allows for collection and subsequent separation and identification of the components in these complex mixtures was used. The sampling arrangement used for catalyst screening is illustrated in figure 33 below.

Figure 33 – Sampling Arrangement For Catalyst Screening Work



Separation, as opposed to intimate contact, of the polymer and transformation agent was chosen to reduce the already numerous variables.

HDPE pellets (\approx 30-60mg, Aldrich) were placed in the crucible and covered with silanised glass wool (\approx 70mg, Phase Separations). The appropriate transformation agent (100 – 200mg) was spread evenly over the exposed surface of the glass wool. The furnace was purged with dry nitrogen before ramping to 420°C at 10°C / min⁻¹, and finally holding isothermally at 420°C for 60 minutes. The heating programme was performed under atmospheric pressures with a dry nitrogen purge (50ml / min⁻¹).

The transformed products in the gas stream were directed down a heated transfer line, held at 250°C, and collected on an adsorbent trap held at room temperature (VOCARB 4000®, Supelco). On completion of the heating programme, the contents of the trap were thermally desorbed (four minutes at 250°C) under a positive helium flow (60ml / min⁻¹), onto the GC capillary column (DB-1, 30m x 0.25mm I.D.) for separation, and subsequent identification. Products were identified by mass spectrometry on the basis of their individual characteristic fragmentation patterns. Temperature programming (35 – 250°C at 5°C / min⁻¹) was employed to assist the efficiency of the separation process. All traps were baked at 300°C for 24 hours prior to use to eliminate any potential contamination.

Blank procedures, in the absence of the transformation agent, were also carried out to identify the polymer decomposition products, and hence to determine the chemical composition of the feedstock gas provided to the catalysts screened.

The amount of polymer used was optimised during the experimental programme.

Initial studies by Breen and Last⁸ identified a range of products that were common over a variety of modified minerals. Routine observation for both aromatics (table 19) and linear alkanes (table 20). These materials were identified in the post run Total Ion Chromatograms (TIC's) by their characteristic fragmentation patterns under the ionisation conditions employed. The amount of each component was determined by manual integration of the base peaks for the appropriate ions in the Single Ion Chromatograms (SIC's).

Table 19 – Aromatic Species Analysed for in Product Gas Streams

Species	Molecular Ion (m/z)	Base Peak (m/z)
Toluene	92	91
Xylene	106	105
Trimethylbenzene	120	105
Tetramethylbenzene	134	119
Ethylbenzene	106	105
Ethylmethylbenzene	120	119
Naphthalene	128	128
Methylnaphthalene	142	142
Dimethylnaphthalene	156	156
Trimethylnaphthalene	170	170
Tetramethylnaphthalene	184	184

Table 20 – n-Alkane Species Analysed for in Product Gas Streams

Species (No ^r Carbons)	Molecular Ion (m/z)	Base Peak (m/z)
6	86	43
7	100	43
8	114	43
9	128	43
10	142	43
11	156	43
12	170	57
13	184	43
14	198	57
15	212	57
16	226	57
17	240	57
18	256	57
19	270	57
20	284	57
21	298	57
22	312	57

For presentation purposes, TIC's have been transformed into normalised TIC's (nTIC's) by extracting the data recorded between 5 and 35 minutes from the TIC, isolating the most intense signal and normalising the remaining signals over this time interval to this value. Analysis of linear alkanes was carried out in an identical fashion.

TG – OTM – GC – MS (Dynamic)

As for the isothermal process. In this case, the temperature ceiling was 650°C, with no isothermal segment.

TG – (FTIR) – MS

The thermal desorption of nitrogen containing bases from solid acid materials remains an invaluable technique for the determination of the surface acidity associated with these materials.^{209,210} In particular, the desorption of basic species such as cyclohexylamine from the surface of acidic solids, such as modified clay minerals, is an invaluable technique for surface acidity determination which can be monitored using the SCA system in this configuration.

Samples for analysis are exposed to cyclohexylamine vapour for at least 48 hours prior to analysis. Again, the furnace is purged prior to analysis, to remove physisorbed material. Samples ($\approx 50\text{mg}$) were heated to 800°C at 15°C /min⁻¹. Evolved gases were directed down a heated transfer line (250°C) into the infra red gas cell (10cm pathlength). A second portion of the sample was directed down a second heated transfer line (250°C) directly into the mass spectrometer. Analyses were performed at atmospheric pressure under a flow of dry nitrogen (50ml / min⁻¹).

²⁰⁹ C. Breen, A. T. Deane & J. J. Flynn, *Clay Minerals*, **22** (1987) 169 – 178.

²¹⁰ C. Breen, *Clay Minerals*, **26** (1991) 473 – 486.

4.3.2. X-RAY FLUORESCENCE SPECTROMETRY

Samples were analysed as 40mm fused beads using a Philips PW2400 XRF spectrometer. The dispersion medium was lithium tetraborate, and the mixing ratio was 10:1 w/w (lithium tetraborate : clay). Beads were analysed using a 3kW close coupled rhodium x-ray tube. Platinum ware was used throughout the bead preparation process.

4.3.3. X-RAY DIFFRACTION ANALYSIS

XRD profiles were recorded for pressed powder samples using Cu-K α radiation ($\lambda = 1.5418 \text{ \AA}$), with the diffractometer (Philips PW1130) operating at 40kV and 40mA at a 2θ scan rate of 2° min^{-1} .

4.3.4. GAS-CHROMATOGRAPHY/MASS-SPECTROMETRY

Direct injection GC-MS (615GC, Unicam-Automass System 2, Unicam) was achieved via separation using a GC capillary column (DB-1, 30 m x 0.25 mm I.D.) and by using a $5^\circ\text{C} / \text{min}^{-1}$ temperature ramping regime (35 – 250°C). A split injection port was used to ensure comparability of the results.

4.3.5. INDUCTIVELY COUPLED PLASMA/MS

Samples for analysis were aspirated into the plasma. Calibration was achieved through the dilution of stock ICP elemental standards (Analar grade, Aldrich) in dilute HCl. A Spectro Analytical XXX was used for these determinations.

4.3.6. FOURIER TRANSFORM INFRA RED SPECTROSCOPY

FTIR analysis was performed using the pressed disk method. The sample (2% w/w) was diluted in KBr. The resultant mixture was pressed under pressure and a vacuum applied. Spectra were recorded over the wavelength range $4000 - 500\text{cm}^{-1}$, and at a resolution of 4cm^{-1} . In all cases, an ATI Mattson Genesis series FTIR was used.

4.3.7. DIFFUSE REFLECTANCE (IR) (FT) SPECTROSCOPY

As with the FTIR analysis, prior to recording spectra, the sample was dispersed in KBr at a 5% w/w value. Spectra were recorded over the wavelength range 4000 – 500 cm^{-1} with a 4 cm^{-1} resolution. Spectra were recorded using a Mattson Polaris FTIR spectrometer fitted with a DRIFTS accessory (Graseby Specac). Variable temperature (VT) DRIFTS was performed using the same instrument and sampling arrangement, with the temperature of the sample cell under thermostatic control.

4.3.8. THERMOGRAVIMETRIC ANALYSIS

TG alone can be used to characterise the thermal behaviour of clay minerals. TG provides data relating to the dehydration and dehydroxylation behaviour of minerals in their modified and unmodified states. Samples for analysis ($\approx 25\text{mg}$) were placed in a dry flow of nitrogen for 15 minutes. The furnace was ramped (35-800 $^{\circ}\text{C}$) at a rate of 15 $^{\circ}\text{C} / \text{min}^{-1}$. TG analysis was carried out using a Mettler Toledo TG50 thermobalance equipped with a TC10A processor.

4.3.9. DETERMINATION OF CATALYST COKE VALUES

As with most materials employed in hydrocarbon reforming reactions, the transformation agents used in the work were subject to coking on stream. The extent of the coke deposition can be determined using TGA (TG131, Cahn). Samples for analysis (50mg) were placed in a quartz TG sample crucible and heated from 25 to 650 $^{\circ}\text{C}$ at a rate of 10 $^{\circ}\text{C} / \text{min}^{-1}$ under a flow of dry nitrogen (50ml / min^{-1} .) At 650 $^{\circ}\text{C}$, the nitrogen flow was replaced by a flow of dry air (50ml / min^{-1}) at atmospheric pressure and held at 650 $^{\circ}\text{C}$ for 30 minutes to oxidise deposited coke on the surface of the catalyst. The coke content was determined via calculation of the weight loss under the air treatment, and the normalisation of the weight loss to the amount of clay from which the weight loss occurred (final weight value).

CHAPTER FIVE

-Results & Discussion-
Polymer Characterisation

5. POLYMER PYROLYSIS IN RECYCLING

Polymer recycling can be performed in a number of ways, each one claiming advantages over the others. However, the diverse nature of polymer waste streams affords the potential to exploit a combination of recycling methodologies.

For many years, polymer pyrolysis was the favoured method for the treatment of waste plastics isolated from post consumer waste streams. In reality, the diverse mixture of plastic types mean that adequate control over the nature of the products derived from the pyrolysis of spent polymers, from such a source, is difficult and costly to achieve. To overcome this problem, focus has been applied to the pyrolysis of polymer mixtures on a laboratory scale.

In a comprehensive study, Pinto *et al*²¹¹ found that the composition of the product stream arising from the pyrolysis of mixed waste plastics was highly dependant upon the chemical nature of the polymers used to fuel the process. In particular, high levels of polyaromatics, such as polystyrene, were found to be effective in increasing the RON of the resultant hydrocarbon mixture, and therefore its potential applicability as a fuel blend. High quantities of polyolefinic materials such as polyethylenes adversely effected the RON. Likewise, Kiran *et al*²¹² showed that the pyrolysis of polyaromatics was an effective way of producing monoaromatic species, whereas the pyrolysis of polyolefins was much less efficient, resulting in a series of saturated and unsaturated linear hydrocarbons. In both cases, the formation of aromatics associated with the pyrolysis of polystyrene was attributed to direct thermally induced depolymerisation to yield the monomer.

²¹¹ F. Pinto, P. Costa, I. Gulyurtlu & I. Cabrita, *Journal of Analytical and Applied Pyrolysis*, **51** (1999) 39 – 55.

²¹² N. Kiran, E. Ekinici & C. E. Snape, *Resources, Conservation and Recycling*, **29** (2000) 273 – 283.

Likewise, Kaminsky²¹³ and others²¹⁴ have reported low levels of aromatics formed during polyolefin pyrolysis. One novel solution to this problem involves hydrogenation of the alkenes which result from polyolefin pyrolysis, to yield a synthetic diesel fuel, low in aromatics but rich in linear alkanes.²¹⁵

The high polyolefinic content of waste plastics has led to multi pyrolysis processes, in which plastic mixtures undergo stepwise pyrolysis, with each incremental increase in temperature being applied to induce pyrolysis of a single component of the feedstock waste.²¹⁶ Under such a scheme undesirable components of the product streams can be disregarded at the point of pyrolysis.

While the potential for refinement of these processes remains an active field of research, the high polyolefinic content of waste polymers in domestic waste streams (upto 70%²¹⁷) necessitates the implementation of procedures which allow for the attainment of a greater degree of selectivity over the composition of intermediate hydrocarbon mixtures attained from the pyrolysis of polyolefinic materials.

5.1. CHARACTERISATION OF HDPE

HDPE was selected as it is representative of the waste plastics found in post consumer waste streams. Prior to use, characterisation was performed to determine the pyrolytic degradation products which would ultimately compose the feedstock gases provided to the transformation agents screened during this investigation.

²¹³ W. Kaminsky & J. S. Kim, *Journal of Analytical and Applied Pyrolysis*, **51** (1999) 127 – 134.

²¹⁴ P. T. Williams & E. A. Williams, *Journal of Analytical and Applied Pyrolysis*, **51** (1999) 107 – 126.

²¹⁵ N. Horvat & F. T. T. Ng, *Fuel*, **78** (1999) 459 – 470.

²¹⁶ H. Bockhorn, A. Hornung & U. Hornung, *Journal of Analytical and Applied Pyrolysis*, **46** (1998) 1 – 13.

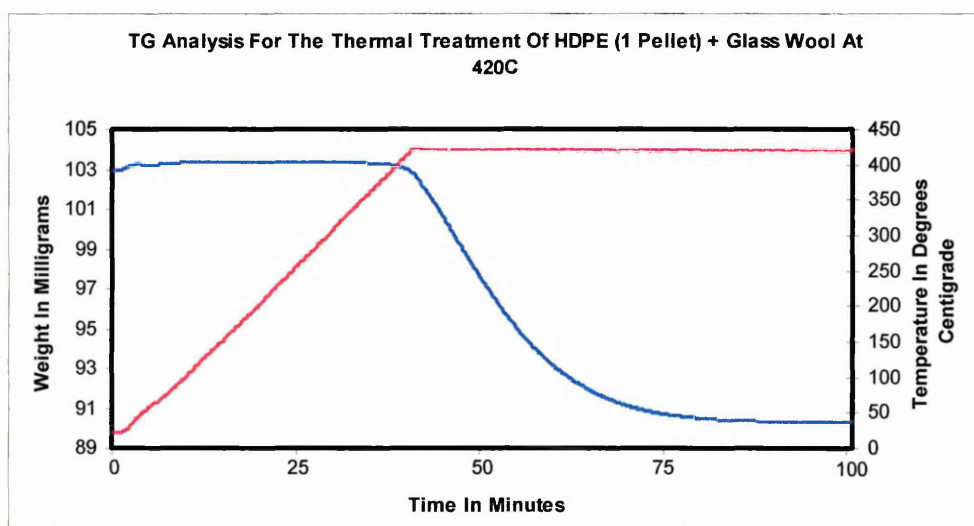
²¹⁷ F. Pinto, P. Costa, I. Gulyurtlu & I. Cabrita, *Journal of Analytical and Applied Pyrolysis*, **51** (1999) 57 – 71.

5.1.1. THERMOGRAVIMETRIC ANALYSIS

In previous studies involving the pyrolytic decomposition of HDPE, temperatures in the range 400-460°C have proven effective in generating high levels of hydrocarbon oils.²¹⁵ In contrast, above 500°C, the product gas stream generated as a consequence of HDPE pyrolysis becomes predominantly gaseous in nature.^{212,218,219}

HDPE was heated up to 420°C and the TG furnace held at this temperature for 1 hour. The resultant TGA trace is illustrated in figure 34.

Figure 34 – TGA Trace for High Density Polyethylene Pyrolysis at 420°C (Isothermal)



Clearly, decomposition begins at 400°C, and continues throughout the isothermal segment of the treatment. In order to ensure that this approach was sufficient to induce complete volatilisation of the polymer sample, the crucible and glass wool were re-run, but no discernable weight loss was observed, thereby confirming the complete volatilisation of the polymeric material over the thermal and time scales employed.

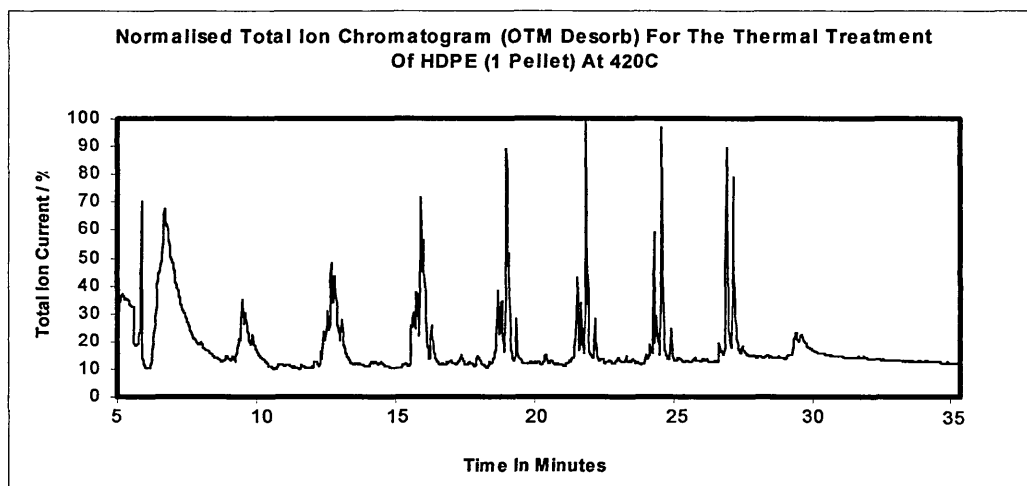
²¹⁸ T. P. Wampler & E. J. Levy, *Analyst*, **111** (1986) 1065 – 1067.

²¹⁹ D. S. Scott, S. R. Czernik, J. Piskorz & St. A. G. Radlein, *Energy & Fuels*, **4** (1990) 407 – 411.

5.1.2. EVOLVED GAS ANALYSIS

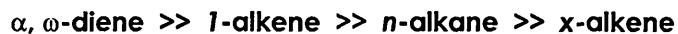
The nature of the species resulting from HDPE pyrolysis under these conditions was determined using TG-OTM-GS-MS. Figure 35 shows the resultant nTIC for this investigation.

Figure 35 – nTIC for the Pyrolysis of HDPE AT 420°C



The general character of the distribution is in agreement with published data for the thermal degradation of HDPE.^{9,10,16,19,24,215,218} The data shows that the major products are eluted as quartets of peaks. Mass spectrometric analysis of each individual peak showed that the product gases were a mixture of *n*-alkanes, 1-alkenes, *x*-alkenes, α , ω -dienes and a range of branched aromatic and polyaromatic species.

In order of increasing retention time, the four major components comprising the quartets of peaks were;



with the alkane representing the most abundant species across each homologous series. It should be noted that the distribution achieved under dynamic conditions was almost identical in terms of species content and relative quantities.

The product distribution arising from the pyrolytic decomposition of HDPE can be explained by an examination of the processes which result in the breakdown of the polymer chains.

5.2. THERMAL DECOMPOSITION OF POLYOLEFINS

There are three types of thermal degradation mechanisms which are characteristic of polyolefins²²⁰;

1. Nonchain scission
2. Random Chain Scission
3. Depropagation

Nonchain Scission

The process involves the removal of pendant groups associated with the main polymer backbone, which itself remains intact. Such reactions are not applicable to HDPE as a consequence of the linearity of the main polymer chains.

Random Chain Scission

Random chain scission involves homolytic bond cleavage reactions at loci of weakness in the main polymer chains. Complex degradation products arising from radical transfer reactions are typically the result (figure 36).

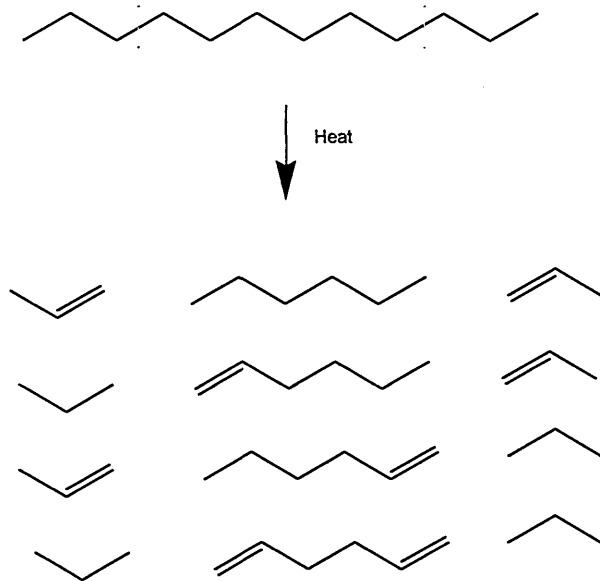
Figure 36 – Radical Transfer Reaction in Thermal Polyolefin Decomposition



²²⁰ M. P. Stevens, Polymer Chemistry – An Introduction (3rd Edition) Oxford, 1999.

Such decompositions are responsible for the range of saturated and unsaturated linear hydrocarbons which are the major breakdown products of HDPE. Figure 37 demonstrates the randomness of this process. Random chain scission is common to all vinyl polymers, but is particularly prolific in HDPE because of the low levels of branching along the polymer backbones.

Figure 37 – Random Chain Scission in Polyethylene



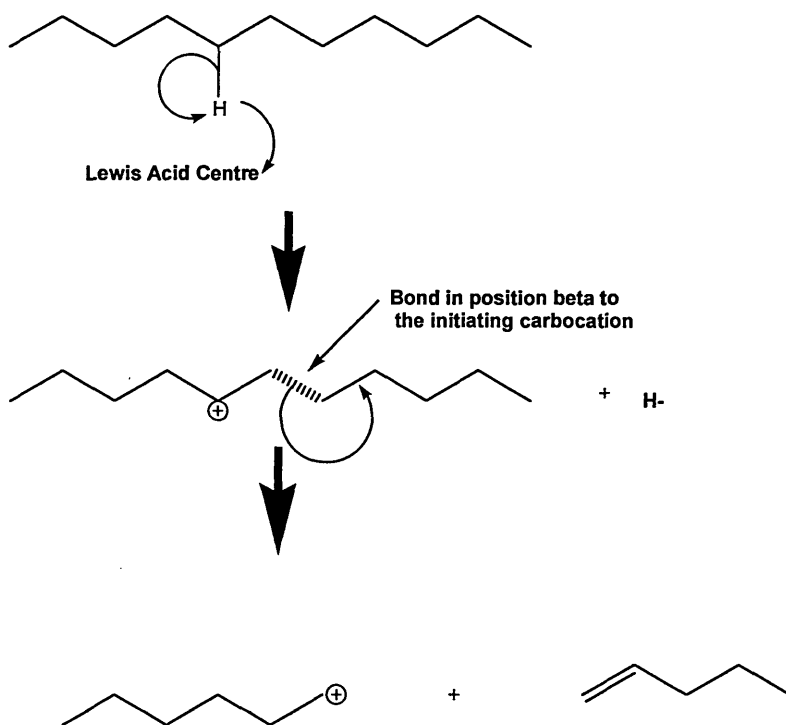
Depropagation

Depropagation (depolymerisation) to yield the original monomer, is a primary decomposition mechanism in polymeric materials which exhibit significant substitution along the lengths of the main polymer chains. The process has little influence on the thermal decomposition of HDPE which has little or no such substitutions.

5.3 MECHANISTIC ASPECTS OF POLYMER CRACKING

In the case of catalytically assisted polymer cracking, it is generally agreed that the first event to take place during the cracking of the integral hydrocarbon chains of polyolefins is the formation of a carbocation on the carbon backbone. Following formation of the cation, cracking proceeds according to the β rule to generate a smaller adsorbed carbocation and an olefin which is released to the gas phase. The β rule is so called as it infers the cleavage of the carbon carbon bond which is in a location beta in relation to the carbon atom holding the formal charge installed during the initiation step. Figure 37A illustrates the concept of polymer cracking as dictated by the β rule. In the presence of strong Lewis Acid Centres, carbocation formation is facilitated by the abstraction of a hydride ion from the saturated carbon chain forming the polymer backbone. The instability associated with the installation of a formal positive charge generates the driving force which causes the molecule to crack.

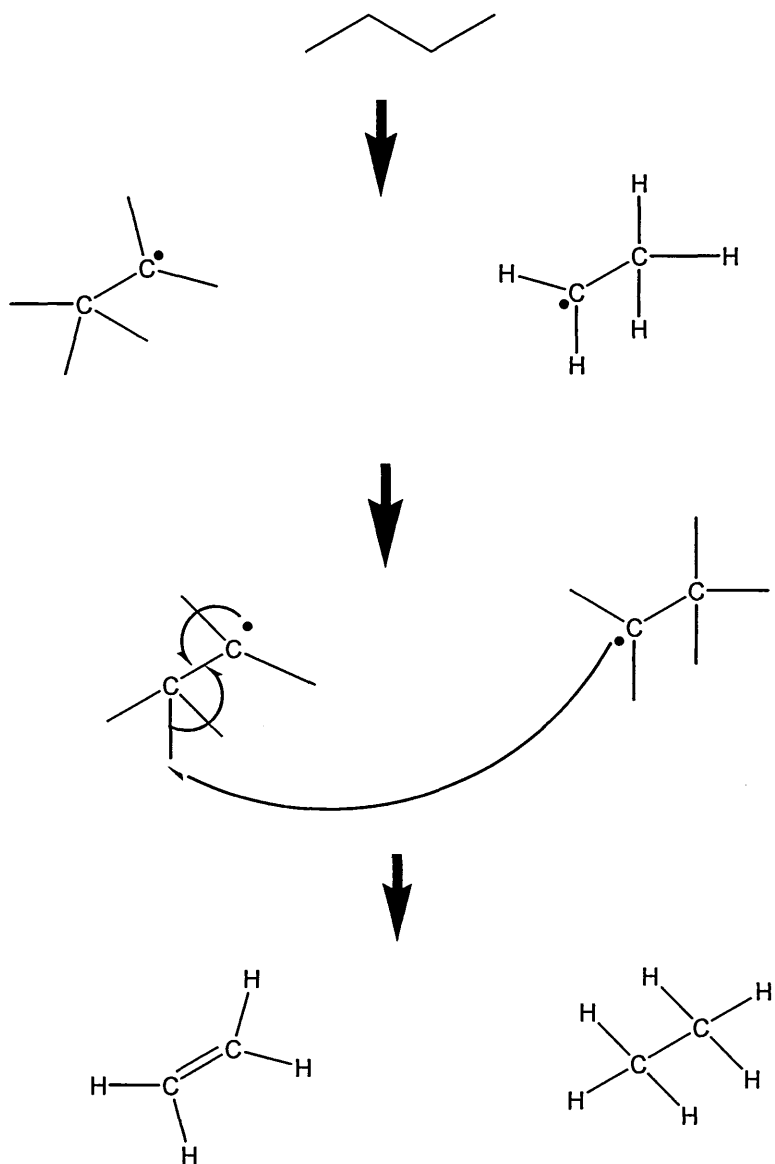
Figure 37A – Polymer Scission According to the β Rule



Generally,²⁹ it is agreed that catalytically assisted polymer cracking proceeds through the occurrence of a series of reactions in which free radicals do not play a part, as highlighted by the mechanistic sequence given in figure 37A. In contrast, the difference in product distribution observed when polymers are thermally cracked as opposed to catalytically cracked, suggests that the two possibilities proceed through different reaction mechanisms, thereby suggesting that thermal cracking involves the intervention of free radicals in a sequence of chain reactions.

In the absence of an active solid acidic transformation agent, thermolysis of polyolefins has been shown to produce product streams rich in unsaturated hydrocarbons²⁷, which are predominantly linear in nature. In contrast, catalytically assisted cracking typically provides a means of promoting skeletal isomerisation reactions, with aromatic and branched aliphatics with minimal unsaturation being prominent.²⁰³ This observation would appear to provide supplementary evidence to the hypothesis that the thermal and catalytic cracking of polymers occur via different mechanisms, although in the case of the latter, post cracking isomerisation plays a key role in the determination of the species present in the final product stream. As detailed in section 5.2, thermal cracking of polymers occurs through three primary mechanisms, with Random Chain Scission being the most prevalent.

Figure 37B illustrates the mechanism of random chain scission using the butane molecule as a representative hydrocarbon chain. In this instance, thermally induced bond cleavage produces two free radicals which subsequently interact in the fashion indicated to yield one saturated and one unsaturated product.



The pair of free radicals formed in the initiation step as a consequence of thermally induced homolytic bond cleavage of one of the integral carbon carbon bonds of the main polymer chain undergo further interaction in order to promote stability. One of the unstable intermediates abstracts a hydrogen atom from the second with the resulting electronic rearrangement shown. The products of the process are more thermally stable than the starting materials, although in the case of long hydrocarbon chains may undergo further cracking to further promote stability.

5.4. CONSTRUCTIONAL ARRANGEMENT OF RESULTS

A range of materials have been studied during the practical work associated with this thesis. These materials can be grouped and assigned to one of three categories of modified minerals, namely

1. Pillared Smectites
2. Acid Activated Smectites
3. Acid Activated Kaolin Amorphous Derivatives

Given the similarities in structure and acidity of each member in a given class, it is realistic to assume that several modified minerals may exhibit similar catalytic behaviours under the test conditions used. This is particularly the case for the acid activated smectites which were by far the largest group of modified materials investigated. Therefore, the results and discussion section for each of the groups above will take the following formats.

Pillared Smectites

All characterisation results will be presented including the catalytic activity data. Subsequently, attempts will be made to relate these results to those present in the literature for materials of this type, if used in similar applications.

Acid Activated Smectites

In view of the similarities in the catalytic behavior of materials modified from a variety of base clays, the discussion aspects associated with each individual class of materials will be agglomerated into a single discussion forum which will form a separate chapter detached from the main characterisation chapters. The effects of acid activation on smectites will be discussed in terms of the effects on the catalytic activity of the transformation agents. Likewise, attempts will also be made to

correlate the activity of these modified minerals to that of other potential catalysts for application in this role, notably zeolites and synthetic silica aluminas.

Acid Activated Kaolin Amorphous Derivatives

As a separate class of mineral, these materials will be discussed in isolation. Again relevant current literature will be used to highlight the potential benefit of these materials for a range of acid catalysed reactions.

5.5. INTERPRETATION OF NORMALISED TIC'S (nTIC's)

While mass spectrometric analysis of individual nTIC traces is imperative for the determination of the relative quantities of each of the product species generated over the surfaces of the transformation agents used, visual examination of these traces can provide information relating to the hydrocarbon reforming activity of these modified minerals.

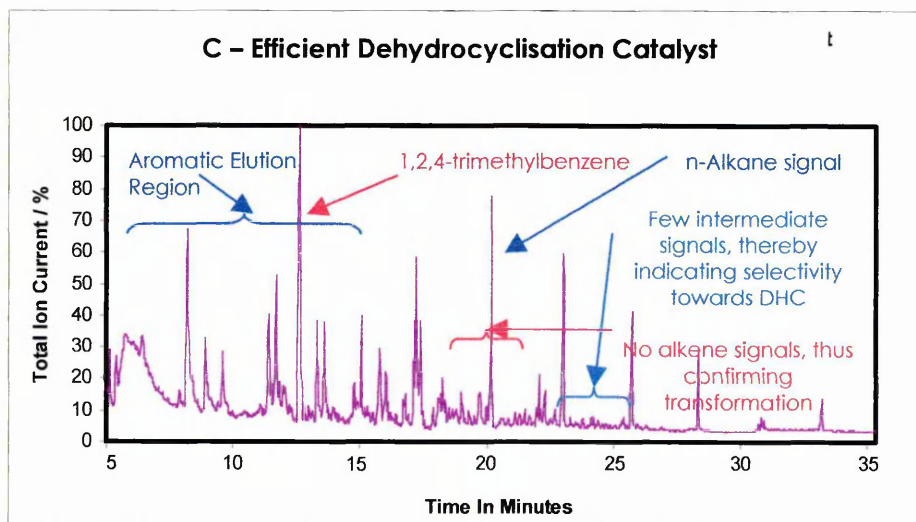
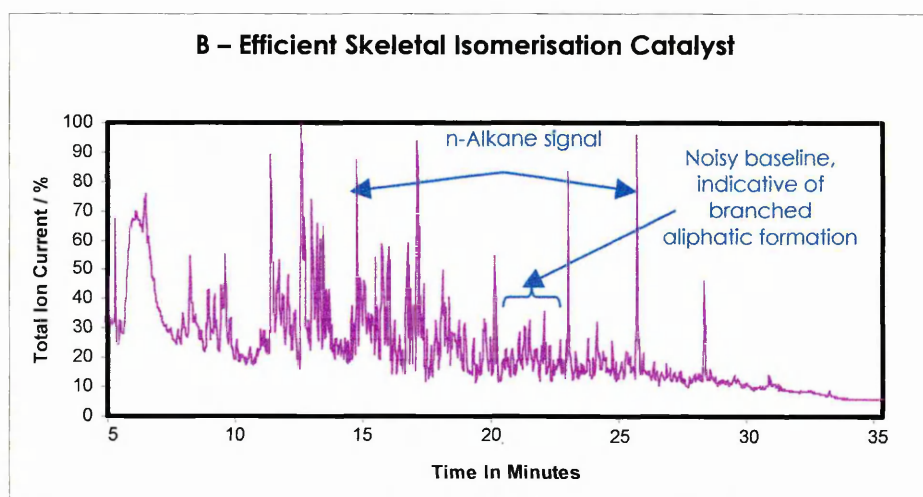
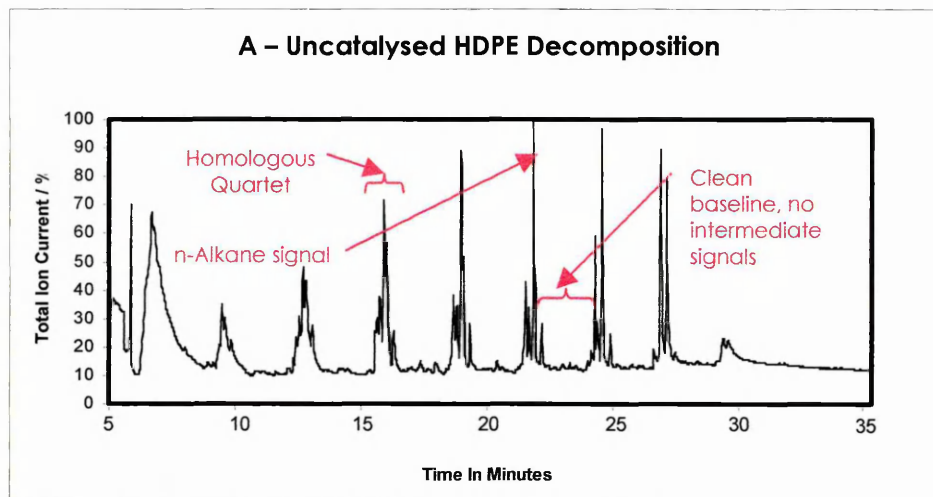
This section will briefly highlight how visual examination of an nTIC can allow informed assumptions to be made regarding the catalytic behaviour of the transformation agents screened.

Figure 38 shows three nTIC's recorded in this work;

- A. High Density Polyethylene.
- B. A transformation agent active in executing dehydrocyclisation reactions.
- C. A transformation agent active in executing skeletal isomerisation reactions.

Figure 38 will aid in interpretation of these traces and allow the reader to differentiate between the presence of a variety of different species.

Figure 38 – nTIC's for Catalysed (B & C) and Uncatalysed (A) HDPE Decompositions



While not exhaustive, this information does provide an elementary tutorial in nTIC visual analysis, which will prove useful in understanding results in the ensuing chapters.

CHAPTER SIX

-Results & Discussion-
Al/Cr Pillared Spanish Saponites

6. INTRODUCTION

The potential exploitation of acidic solids as transformation agents in the catalytic recycling of spent polymeric materials is a relatively new area of investigation, arising from the concerns of many over some of the traditional waste disposal methodologies applied to these versatile, yet durable materials.

To date, particular attention has been paid to the employment of zeolites in this role, because of their controlled microporosity and acidity. In addition, zeolites have a proven track record in the field of commercial fluidised catalytic cracking and are known to be effective hydrocarbon reforming media.

Many zeolites, among them ZSM-5, suffer from the unfortunate consequence of limited pore geometry, with pore size openings of $5.5\text{\AA} \times 5.1\text{\AA}$ ²²¹ being typical. This results in two negative aspects in respect of their use in hydrocarbon processing.

1. Aromatic precursors (unsaturated aliphatics) can enter the channel network of zeolites and undergo addition / dehydrocyclisation reactions within the channel intersections of the material. The resultant cyclic species become trapped internally, and thus are lost from the reaction system.
2. Large hydrocarbon molecules such as those found in 'heavy' feedstocks are often not handled efficiently by zeolites of restricted pore geometry due to the presentation of diffusional barriers relating to the entry of the feedstock molecules in to the pore channel network in order to contact internally available active sites.

²²¹ A Garforth, S. Fiddy, Y.-H. Lin, A. Ghanbari-Siakhali, P. N. Sharratt & J. Dwyer, *Thermochimica Acta*, **294** (1997) 65 – 69.

The development of PILC's in the early 1970's arose from the need of oil companies to process 'heavy' feedstocks, and therefore to overcome the problems outlined in the point two above.

Due to the difficulty of controlling the acidity and porosity of pillared clays, primarily as a consequence of the turbostratic nature and charge inhomogeneity associated with smectite structures,¹⁵⁵ the use of pillared clays in hydrocarbon processing applications has been restricted to specialised procedures.^{175,177,179} The observed activity of these materials for HDPE transformation will be discussed in relation to the known activity of these materials for these specialised procedures.

6.1. MATERIALS CHARACTERISATION

The materials employed in this investigation were a series of Al and Cr pillared saponites. The materials were prepared and supplied by the Department of Inorganic Chemistry at the university of Salamanca. Prior to supply, the materials were fully characterised by the group responsible for their preparation, and their findings have been disclosed elsewhere.¹⁶⁸

6.1.1. THERMOGRAVIMETRIC ANALYSIS

The group performed TGA on both the raw saponite and the range of PILC's prepared through the intercalation of Al and Cr pillaring precursors. The saponite was seen to exhibit a slight initial, low temperature weight loss (centered at 145°C) attributed to dehydration of the mineral. This was followed by a gentle weight loss over the temperature range 200 to 800°C, followed by dehydroxylation at 840°C. The total weight loss was 20 wt/%.

It has been assumed that mixed (Al/Cr) oxide pillars are not present.

The thermal behaviour of the samples pillared entirely (R2) or predominantly with Al (R3&R4) was similar to that for the raw saponite. Dehydration and dehydroxylation effects attributable to the pillars were insignificant when compared to the thermal events associated with the clay. Total weight loss was 22%, with R2 (Al pillared) being stable to temperatures above 800°C.

For those materials containing exclusively (R8) or predominantly (R6&R7) Cr, differential thermal analysis (DTA) of the post intercalation calcined products has provided evidence for exothermic events (320 & 530°C) and an endothermic event (385°C) not seen with the base clay. Such occurrences have been assigned to thermal alteration of the Cr oligomers composing the pillars. Total weight loss was 20% , with these materials showing limited thermal stability above 200°C, this temperature being well below the transformation temperatures used in this work.

6.1.2. ELEMENTAL ANALYSIS

These materials were supplied externally, and were in short supply. As such, XRF analysis was not performed due to the destructive nature of the bead forming process used to execute this technique. Elemental data, determined by ICP spectrometry¹⁶⁸ is presented in terms of the number of Al and Cr pillars per unit cell of the saponite, and is illustrated in table 21.

Table 21 – Pillar Concentration for Series of Al/Cr Spanish Pillared Saponites

Sample	Al:Cr Ratio	$[Al_{13}O_4(OH)_{24}(H_2O)_{12}]^{7+}$	$[Cr_2(OH)_4(H_2O)_8]^{4+}$
R1	No Pillaring	n/a	n/a
R2	100:0	0.1356	n/a
R3	90:10	0.1392	No Data
R4	80:20	0.1314	No Data
R5	50:50	0.0618	0.408
R6	20:80	0.0260	0.492
R7	10:90	0.0166	0.478
R8	0:100	n/a	0.548

The calculated values given in table 21 assume that all Al and Cr in the intercalating solution is oligomerised into the pillaring species. The Al and Cr pillaring ions were prepared by hydrolysis of $\text{AlCl}_3 \cdot 6\text{H}_2\text{O}$ and $\text{Cr}(\text{NO}_3)_3 \cdot 9\text{H}_2\text{O}$ with aqueous NaOH respectively. In the case of R3 and R4 no pillar concentration is given for the Cr species, as other characterisation data indicates that Cr does not polymerise in these materials. The Cr content of these products has been attributed to the adsorption of this species on the surface of the saponite and onto the Al pillars.¹⁶⁸

6.1.3. X-RAY DIFFRACTION ANALYSIS

X-ray diffraction analysis was performed by the group responsible for the preparation of these materials. Table 22 illustrates the calcination temperature for each of the PILC's used in this investigation, along with their recorded basal (d_{001}) spacings.

Table 22 – Basal Spacings & Calcination Temperature for Pillared Spanish Saponites

Sample	Al:Cr Ratio	Calcination Temperature (°C)	D_{001} (Å)
R1	No Pillaring	n/a	9.8
R2	100:0	500	18.4
R3	90:10	500	17.1
R4	80:20	500	15.3
R5	50:50	400	16.6
R6	20:80	300	16.6
R7	10:90	300	12.0
R8	0:100	300	12.1

These results indicate that the basal spacings for R2, prior to calcination increases by 9.0Å relative to the parent saponite (R1). It has been shown previously that the dehydrated Al_{13} cation (the Keggin ion) has a length of 5.4Å which increases to 9.8Å when the species is hydrated. Intermediate values have been reported for the species following its intercalation into smectites.

In contrast, the size of the Cr polycation dimer is 4Å . Sizes for the trimer and tetramer are 5.0Å and 6.5Å respectively. This has led to speculation that the observed

increase in basal spacing for the 100% Cr treated material (R8) occurs as a result of the superposition of two Cr oligomers (R8 d_{001} post pillaring = 18.1 Å). Reduction of this value to 12.1 Å following calcination confirms the low thermal stability of those clays pillared with Cr rich pillaring solutions.

6.1.4. FTIR ANALYSIS

FTIR data reported by the group responsible for the preparation of these materials highlighted that very few differences were evident between the FTIR spectra for the raw saponite, and those for the pillared materials. One notable effect was a shift of the 1011 cm^{-1} band in the saponite sample to 1024 cm^{-1} in the pillared samples. This band is indicative of Si-O-Si vibrations in the tetrahedral sheet. Similar shifts, 659 cm^{-1} to 671 cm^{-1} and 448 cm^{-1} to 466 cm^{-1} for the Mg-OH and Mg-O bending modes were also observed. Such band shifts may be the result of the increased anchoring efficiency of the pillars observed in tetrahedrally substituted minerals.⁹⁷

6.2. CATALYTIC ACTIVITY

As outlined above, two temperature regimes have been employed to investigate the transformation process, 420°C for 1 hour (isothermal) and a 650°C (dynamic). Given the data recorded for acid activated clays operating under dynamic conditions¹⁹⁸ (see later) and in view of the limited thermal stability associated with these Al/Cr PILC's¹⁶⁸, these materials were investigated under the isothermal regime only. However, preliminary studies were undertaken to determine the effect of temperature on the transformation activity of these materials under the standard test conditions. Likewise, these samples were also used to determine the effect of flowrate of the feedstock gas to the transformation agent. This was achieved by reducing the mass of HDPE employed, so as to reduce the amount of polymer handled by the catalyst. Again, the findings of these background studies are presented below.

Previous studies by Breen and Last⁸ using EGA to investigate the catalytic transformation activity of smectites modified by a variety of means was carried out using 4 pellets of HDPE ($\approx 60\text{mg}$) and 200mg of catalyst to give a polymer to catalyst ratio of 1:3.3. In addition, two temperature regimes were employed;

1. **Isothermal** – 10°C / Min to 420°C, then 1 hour isothermal at 420°C.
2. **Dynamic** – 10°C / Min to 650°C

This section will present results obtained over a series of optimisation trials carried out to determine the most suitable sampling arrangements for this work.

It was noted from previous results that when the low temperature regime was employed, independent of the catalyst, significant levels of both aromatic and polyaromatic species were generated, relative to the thermal, non catalysed process. This is in contrast to runs performed using the same catalytic materials under dynamic conditions, where aromatic yields were significantly lower than under isothermal conditions. This observation was previously related to the residence times of the feedstock gas molecules in the catalyst bed. It can therefore be assumed that there is a temperature point between 420°C and 650°C at which the generation of cyclic materials reaches a maximum and then decreases to the levels seen at 650°C. Therefore a preliminary investigation was carried out to determine the effects of temperature on the distribution of products generated by a particular catalyst.

For the purpose of this investigation, the catalyst R3 was selected as it represented an active material of which a good supply was available. As 420°C was the more favourable of the two original temperature regimes, a temperature range of 100°C, centering on 420°C was selected for the purpose of the investigation. The following

temperatures were employed under isothermal conditions; 380 / 400 / 420 / 440 / 460 & 480°C.

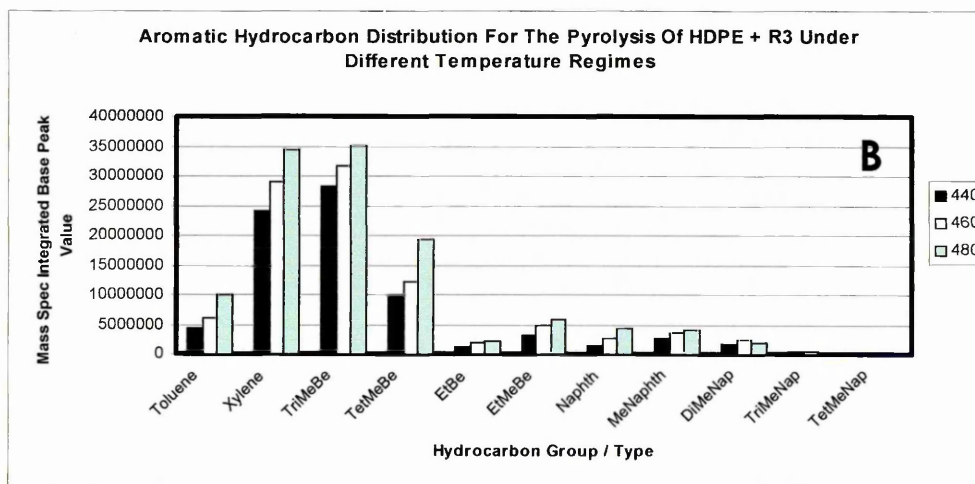
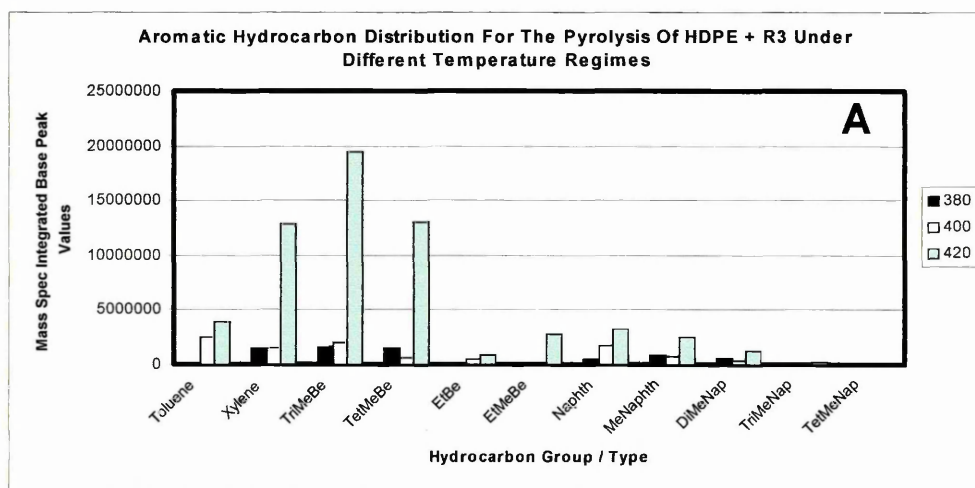
Examination of data relating to the n-alkane distribution achieved over R3 over the six temperature regimes given above showed that the overall aliphatic hydrocarbon distribution for each of the six runs is not significantly different. Although the data is not quantitative, the fact that in all cases, the general trend is the same, indicates that the catalyst is not active enough, in terms of acidity, to crack the long chain alkanes present.

With regards to the generation of aromatic and polyaromatic materials, the data recorded for these products is semi quantitative in that the values plotted represent actual values which are directly comparable between runs, assuming all instrumental parameters remain unchanged. Figures 39 a and b illustrate the aromatic and polyaromatic hydrocarbon distributions recorded for the variable temperature processes outlined above. It should be noted that charts 39a and 39b are plotted on different scales. As indicated in figure 39a, at temperatures below 420°C, the generation of cyclic products is very low. This is most likely due to the fact that the pyrolysis of the polymer is incomplete due to insufficient thermal energy to induce degradation. As such, the catalyst is starved of feedstock gas, and therefore despite the fact that it may be able to carry out transformation reactions at temperatures below 420°C, the lack of feedstock gas prevents this. Confirmation of this has been made through examination of the weight loss profile for these runs in which the weight loss attributable to polymer volatilisation is lower than seen with runs performed at 420°C.

Figure 39b indicates that as the process temperature is increased, so too is the aromatic yield, and considerably so. In addition to the observation that polymer

degradation is incomplete at temperatures below 420°C, there are a further two explanations which could account for these low aromatic yields. As the temperature is increased, the mechanisms by which the polymer breaks down is possibly subject to slight variations, which in turn alters the composition of the feedstock gas, thereby providing higher concentrations of those species able to undergo cyclisation reactions.

Figure 39 :- Aliphatic And Aromatic Hydrocarbon Distribution For The Thermal Treatment Of HDPE + R3 Under Various Temperature Regimes



A second possibility is that as the temperature is increased, the rate of feed of polymer degradation products to the catalyst bed is also increased. This allows for rapid formation of cyclic products on the edge sites of the catalyst, before these

active sites become physically coked up and hence inaccessible to the feedstock gas molecules. During an isothermal run carried out at 420°C, it is possible that the DHC sites become coked up over time. Due to the physical barrier presented, and the slower rate of feed of the feedstock gas to the bed, it may be that these observations account for the lower levels of aromatic products generated by the catalysts at the lower temperatures.

However, as the temperature is increased further, to 650°C, the generation of cyclic products is severely reduced. As indicated, this is most probably due to kinetic restrictions being imposed due to the very short residence times of the polymer degradation molecules in the catalyst bed. This data provides justification for the use of 420°C as the isothermal operating temperature. Although temperatures of 440-480°C appear to be more effective in facilitating the production of aromatics than 420°C, a decision was made not to use the higher temperatures, as such conditions promote gaseous product formation, and inhibit skeletal isomerisation reactions.²⁹ In addition, such temperatures require higher energy inputs at the processing stage, thereby reducing the efficiency of the overall process. These situations have the potential to yield liquid product mixtures unsuitable for low grade fuel applications, and as such, 420°C was retained as the isothermal reaction temperature.

When this project was started, all analyses were carried out using 4 pellets and 200mg of catalyst. During the course of the project, the mass spectrometer employed as a component of the synergy system underwent a major overhaul, which resulted in a significant increase in the sensitivity of the instrument. As such, all subsequent analysis carried out with 4 pellets resulted in saturation of the instrument detector due to the massive amount of materials entering the instrument. Therefore, a decision was made to screen four pellets, two pellets, and a single pellet for purposes of comparison.

Following each experimental run, the % conversion of HDPE is recorded through examination of the appropriate TG trace. It was observed that as the initial polymer mass was reduced, then the % conversion of the starting material was seen to increase. This finding is evidence that the rate of flow of the polymer degradation products is of critical importance in the conversion process. When four pellets are employed, the amount of feedstock gas hitting the catalyst at any given time is extensive, perhaps to the degree that the catalyst is subjected to a degree of local saturation. This in turn requires that the gas molecules are forced to queue up on the surface of the catalyst until such time that an appropriate active site becomes available. It is therefore possible that these unstable species react to form macromolecules on the surface of the catalyst, which due to their nature are not removed at the relatively low pyrolysis temperatures employed.

As the number of pellets is reduced, so too is the amount of material which initially strikes the catalyst. It would appear that as this initial flow rate is reduced, then the catalyst is better able to handle the quantity of degradation product molecules released from the polymer, and therefore all work presented subsequently has been carried out using a single HDPE pellet ($\cong 15\text{mg}$). Bearing in mind the original polymer to catalyst ratio (1:3.3), this would require a catalyst mass of 50mg. However, such a quantity is insufficient to spread evenly over the surface of the glass wool used to separate the polymer and catalyst. As such, 100mg of catalyst has been used in all experiments performed, thereby giving a polymer to catalyst ratio of 1:6.6.

6.2.1. HDPE CATALYTIC TRANSFORMATION ACTIVITY

For ease of presentation of results, the samples used to accumulate the catalytic activity data presented in this chapter have been sub-divided into two groups, namely;

1. **R1 → R4 = Al rich Pillars** (R1 has no pillars)
2. **R5 → R8 = Cr rich Pillars** (R5 has 50:50, Al:Cr pillars)

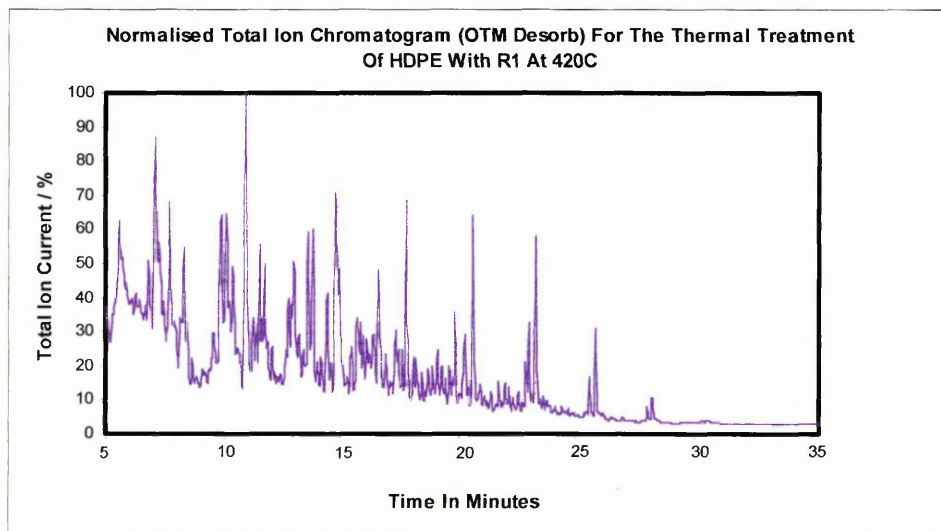
R1 → R4

Two key aspects have been chosen to evaluate the ability of these materials to transform the thermally generated off gases from HDPE pyrolysis. These are (1) the ability of these materials to produce a pre-defined series of aromatic and polyaromatic molecules (2) the effects of the catalysts on the linear alkane distribution found in the product gas stream. Visual confirmation of activity can also be made by reference to the resultant nTIC which provides evidence of transformation behavior.

R1

Pillar Composition = This material is the natural saponite and has no pillars.

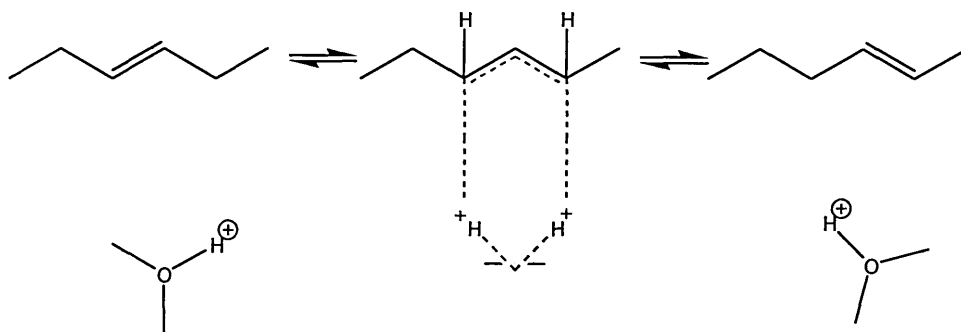
Figure 40 – nTIC for the Thermal Treatment of HDPE + R1 at 420°C (Isothermal)



Clearly, this trace is very different from that for the treatment of HDPE alone under the same conditions (figure 5). In particular the characteristic quartets have been subject to alteration. Mass spectrometric examination of the data confirmed the disappearance of both the α - ω -dienes and the terminal alkenes across the entire homologous series analysed. It should be noted that the n-alkane component of each quartet remains intact, as does the alk-x-ene. This strongly implies that the untreated mineral has limited or inaccessible numbers of mildly Brønsted acidic protons, such sites being highly efficient in promoting double bond shift reactions in unsaturated hydrocarbons. Such an event is illustrated in figure 41 for the isomerisation of 3-hexene to 2-hexene through interaction with a structural hydroxyl group on the surface of a solid acid catalyst.²⁹

Examination of the n-alkane distribution reveals that the maximum signal has shifted from C₁₅ for HDPE to C₁₁ following transformation over R1. Such an observation could result from catalytic cracking and recombination of long chain alkanes, or alternatively from hydrogenation of the linear alkenes which are no longer observed in the product gas stream.

Figure 41 - Brønsted Acidic Proton Catalysed Double Bond Shift Reaction in Alkenes



Examination of the trace also confirmed the presence of branched aliphatic species upto and including C₁₄, which again, are not present in the thermally generated off gases resulting from HDPE pyrolysis. Branched alkanes result from the skeletal

isomerisation of linear materials. As highlighted above, there was evidence for the retainment of alk-x-enes from the feedstock gas in the product gas stream. Such species may be those originally present, but may also represent the products of a range of double bond shift reactions catalysed by the inherent acidity of the parent saponite, arising from isomorphous substitution in the tetrahedral sheet of the mineral. A reaction which has been shown to compete with double bond shift is that of complete proton transfer to generate an adsorbed carbocation intermediate, although this requires sites of greater protonic strength.²⁹ There was no direct evidence to support a change in the relative quantity of alk-x-enes in any of the transformed product mixtures.

Protonation of the terminal double bonds found in 1-alkenes yields 2° carbocations according to the mechanism outlined in figure 42. These species are highly unstable, and readily undergo charge isomerisation in order to enhance stability. Such processes occur through the execution of hydrogen shift reactions which result in the movement of charge along the hydrocarbon chain to a position of greater stability.

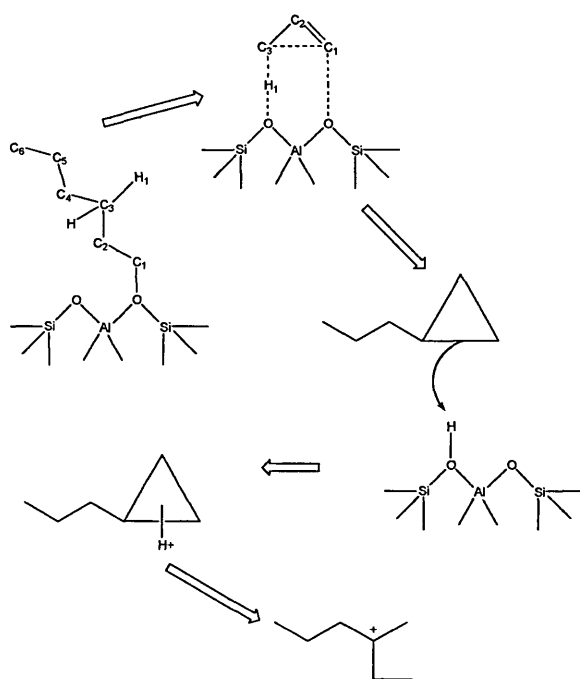
Figure 42 – Secondary Carbocation Formation via the Protonation of 1-alkenes



A more advantageous process involves the conversion of the 2° carbocation into a 3° species. Such conversions are the result of skeletal isomerisation reactions. The monomolecular skeletal isomerisation of olefins begins with the formation of a carbocation via total proton transfer from the acidic surface across the double bond of the olefin. Assuming a sufficient number of carbon atoms, the hydrocarbon ion transforms into a cyclopropyl intermediate, a process requiring back donation of a proton to the catalyst surface. Subsequent reopening of the ring occurs through

protonation of another bond in the ring system^{29,222} to yield the branched product. Figure 43 illustrates the overall mechanism for this process. Evidence for the existence of the protonated cyclopropyl intermediate has come from proton scrambling and product distribution studies²⁹. In the case of the latter, experimentally observed products relate to those in which the intermediate proceeds through the formation of secondary carbocations, and in which the product carbocation is secondary in nature.

Figure 43 – Skeletal Isomerisation via Protonated Cyclopropyl Intermediate

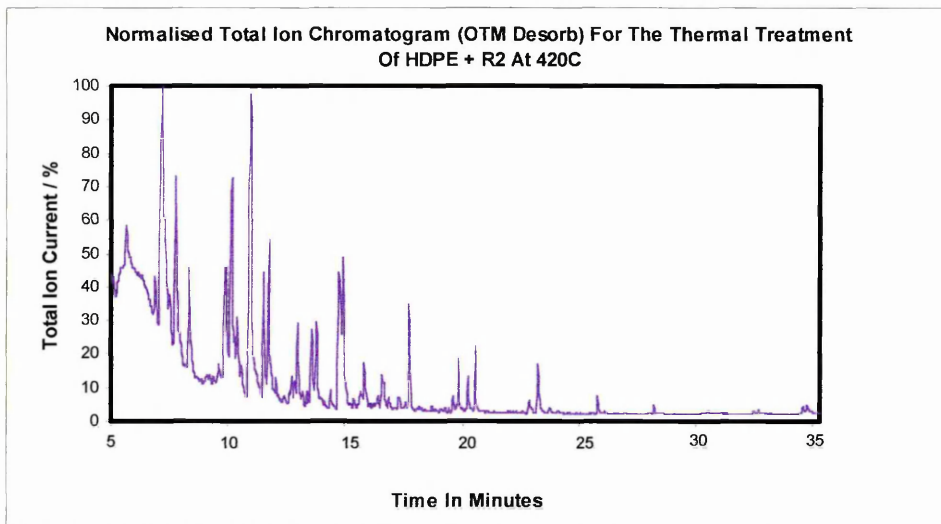


Reaction termination results from hydride abstraction by the product cation from a saturated molecule in the reaction mixture. Aromatisation activity and the effect of this material on the n-alkane distribution will be discussed later.

R2

Pillar Composition = 100% Al

²²² V. B. Kazansky, *Catalysis Today*, **51** (1999) 419 – 434.



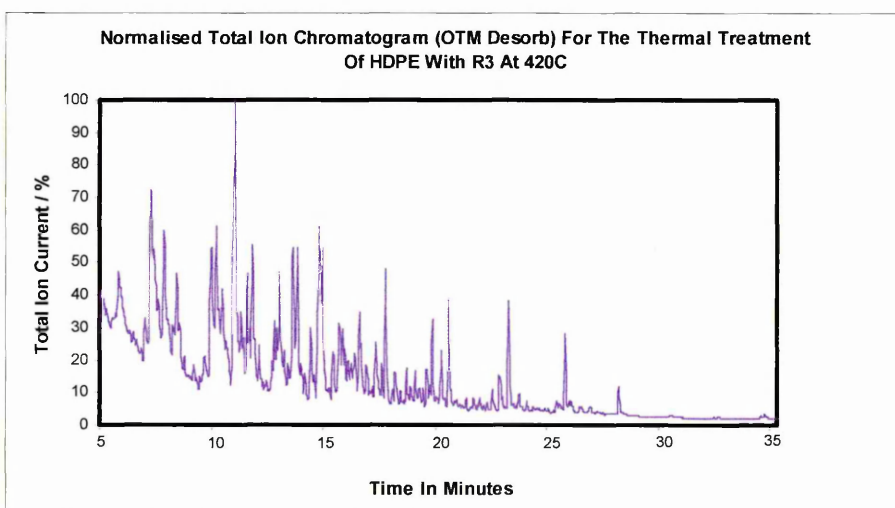
No branched alkanes were produced over this transformation agent which suggests that the pillars have become the predominant active sites in respect of reforming the unsaturated components of the feedstock gas. In addition, all of the alkenes in the original quartet have been removed, indicating a higher catalytic activity over this material when compared to the natural saponite. There is also evidence to suggest that the n-alkanes have been affected by passage over this material. This can be seen by reference to the nTIC in figure 44 in which the characteristic parabolic shape for the linear alkane distribution is no longer evident.

Note also that fewer products were generated over this material in comparison to the parent saponite.

R3

Pillar Composition = 90% Al and 10% Cr. The characterisation data for this material, provided no direct evidence for the existence of Cr pillars, and any Cr present is believed to be deposited on the exposed surfaces of the mineral tactoids, or on the resident Al pillars. Figure 45 shows the nTIC recorded for the transformation of the HDPE off gases over this material.

Figure 45 – nTIC for the Thermal Treatment of HDPE + R3 AT 420°C (Isothermal)



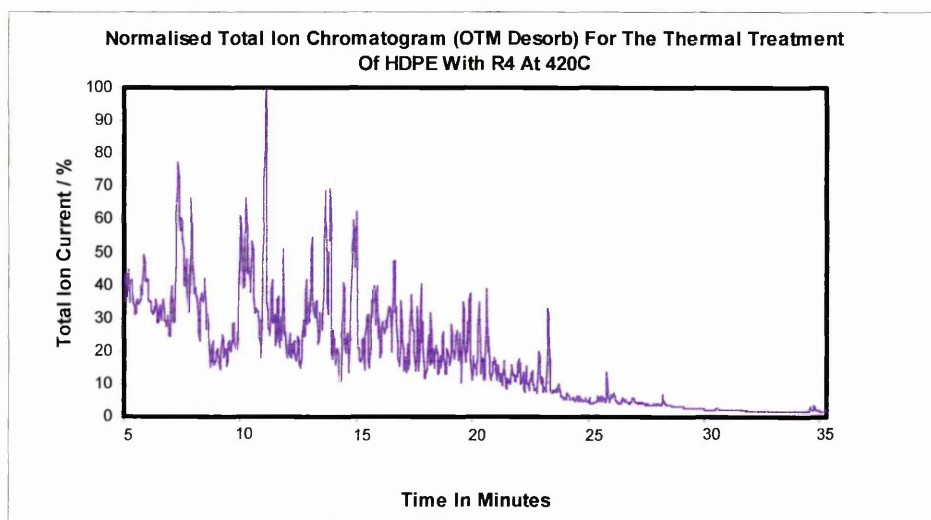
This trace shares many similarities with that recorded for R1. In particular, the parabolic n-alkane distribution is retained. However, in this case, there is no evidence for any of the linear alkenes highlighting the efficiency of the material in transforming these types of hydrocarbons. In addition, the trace contains evidence for the generation of branched aliphatics. Taken together, these observations may suggest that the presence of Cr arduously inhibits the activity of the pillars in respect of alkane cracking, or shields the relevant active sites, thus encouraging transformation reactions to occur on the surface of the mineral tactoids, as is the case for R1. The complete removal of linear alkenes in the product gas stream is indicative of some activity by the pillars.

In particular, long chain alkanes have been subject to depletion possibly as a consequence of the radical transfer mechanism of thermal cracking.²⁹

R4

Pillar Composition = 80% Al and 20% Cr. As with R3 there is no direct evidence for the formation of pillars containing Cr ($[\text{Cr}_3(\text{OH})_4(\text{H}_2\text{O})_8]^{5+}$), hence, the entire Cr content is considered to be located on the surface of the mineral structure or associated with the Al pillars. Figure 46 shows the nTIC trace associated with the reaction of HDPE with R4.

Figure 46 – nTIC for the Thermal Treatment of HDPE + R4 at 420°C (Isothermal)



As with R3 there is evidence for the formation of branched aliphatics over R4, in larger quantities than seen in the former. This could be considered as further evidence for the enhanced deactivation of the pillars as a consequence of Cr deposition, with more free Cr being present in the R4 sample. Once again, there is no evidence for the incidence of unsaturated aliphatic species, suggesting that despite the increased potential Cr deposition on the exposed surfaces of the pillars, they are still accessible to some degree to the feedstock gases. A certain degree of n-alkane distribution retainment is achieved relative to the trace recorded for HDPE alone (figure 5). As with R3 the long chain alkanes ($>C_{17}$) appear to have undergone

depletion. However, the prevalence of these species observed over R1 would seem to eliminate thermal cracking as the cause of their depletion over the pillared analogues.

Isolation of the appropriate single ion chromatograms from the product TIC allows for integration of the base peak area for each of the n-alkanes of interest. The effect of this distribution can then be monitored as a function of the modification treatment. Figure 47 illustrates this type of analysis for the first four members of the R series of pillared clays.

Figure 47 – Aliphatic Hydrocarbon Distribution Achieved Over R1 – R4 (Isothermal)

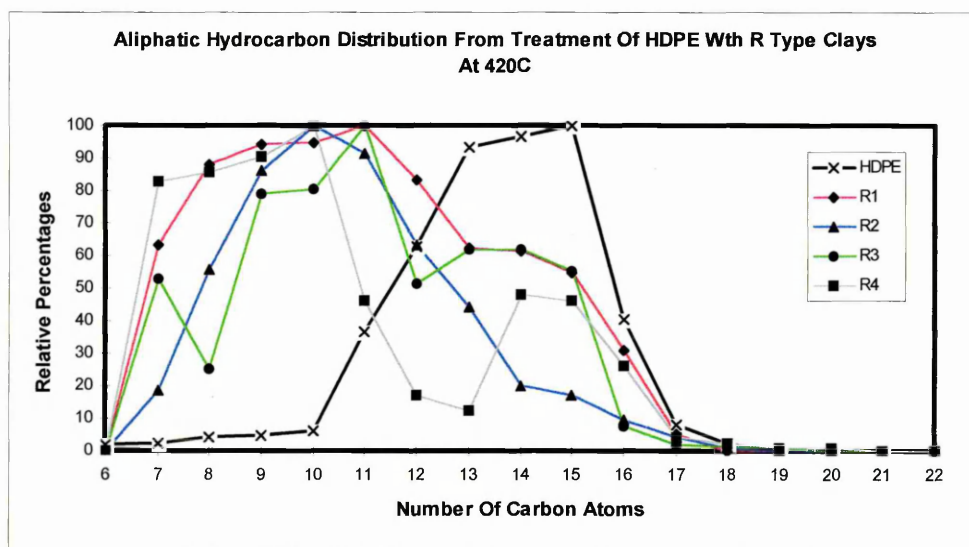


Figure 47 shows that the relative n-alkane distributions achieved over R1-R4 are very similar. This contradicts the visual evidence provided by the respective nTIC's for these transformation agents. However, it should be noted that the analysis leading to the generation of the data in figure 47 only compares these materials relatively and is not a fully quantitative analysis.

Two main observations can be drawn from the data presented in figure 47. Firstly, there is a dramatic shift towards a predominance of shorter chain alkanes in the

transformed product mixtures generated over all four modified clays relative to that seen for HDPE. Secondly, the overall distribution becomes wider, encompassing a greater range of carbon chain lengths. Such a shift could be attributed, in part to the operation of catalytic cracking mechanisms. Thermal cracking, which proceeds through the formation of free radical intermediates can be discounted on the basis that such reactions are only kinetically significant at temperatures above 800K (527°C) which are not covered by this work.²²³

Catalytic cracking of alkanes is a three step process involving initiation, propagation and termination.²²⁴

Initiation

The initiation step responsible for the catalytic cracking of alkanes remains an active field of discussion. It is generally agreed^{29,224,225} that in the case of gas phase reactions this step involves protonation of an olefin to generate an adsorbed carbonium ion. As shown previously, once formed, this cation can undergo both charge or skeletal isomerisations. A third possibility relates to the direct cracking of the carbocation without further reaction. The C-C bond which succumbs to cleavage is that located in a position β with respect to the carbon atom accommodating the formal positive charge installed as a consequence of protonation, this process being well documented and referred to as β scission. The products of such an event are an alkene which is released into the gas phase as well as an adsorbed carbocation. Given the potential for the occurrence of skeletal isomerisation reactions, the possibility of forming 1° carbocations is avoided in ions containing more than 8 carbon atoms.

²²³ S. Kotrel, H. Knözinger & B. C. Gates, *Microporous and Mesoporous Materials*, **35 – 36** (2000) 11 – 20.

²²⁴ A. Corma & A. V. Orchilles, *Microporous and Mesoporous Materials*, **35 – 36** (2000) 21 – 30.

²²⁵ P. Govind Menon & Z. Paal, *Industrial Engineering Chemistry Research*, **36** (1997) 3282 – 3291.

More recent propositions by Haag and Dessau^{223,224} claiming that alkanes can be cracked directly by protonic addition to C-C bonds have subsequently proven controversial on the basis of work carried out using solid acid catalysts. The potential role of Lewis acid centres has also been considered. Hydride ion abstraction from alkanes by structural Lewis acid sites could account for the formation of olefins capable of propagating the cracking process.

Conclusive evidence has remained elusive, but it is postulated that in all probability traces of alkene are required to initiate alkane cracking, via the processes outlined above.

Propagation

In catalytic cracking of gaseous molecules using solid acid catalysts, the carbonium ion formed during the initiation step goes on to abstract a hydride ion from a reactant alkane. The abstracting species subsequently desorbs from the catalyst surface as an alkane, with the reactant molecule undergoing conversion to a carbonium ion that, following adsorption, can either isomerise or crack. This series of events accounts for the high levels of branched alkanes found in catalytic cracking product streams, and thus affords the possibility of being the major mechanism for the cracking of alkanes over R1, R3 and R4. The almost complete absence of branched alkanes generated over R2 indicates the predominance of protolytic cracking reactions resulting from the direct addition of protons to the reactant alkanes, rather than isomerisation of adsorbed feedstock gas molecules on less strongly acidic sites. Such an event could be accounted for on the basis of the enhanced acidity of Al pillared clays produced from materials exhibiting Al³⁺ for Si⁴⁺ substitution in their tetrahedral sheets, as is the case here. Evidently, the presence of Cr oligomers lowers this effect perhaps by physically blocking access to the strong protonic sites required.

The interaction between adsorbed carbocation and reactant alkane has been shown²²⁶ to yield stable carbocation intermediates. This species represents a C-H-C bond which is bielectronic and tricentric, and the geometry of which changes according to the nature of the carbon atoms involved. The decomposition of this intermediate results in the formation of a gas phase alkane and a carbocationic derivative of the reactant alkane as described above. This secondary event is bimolecular in nature and therefore is termed a bimolecular chain transfer reaction.

Termination

Chain transfer termination occurs when surface carbonium ions back donate protons to the catalytic surface to regenerate the original Brønsted acid site. This process represents the opposite of the initial olefin adsorption step.

Thermal cracking (figure 37) is known to proceed through the participation of free radicals in a series of chain mechanisms. It has been noted²⁹, that the product distribution achieved in catalytic cracking systems is significantly different to that in thermally cracked systems, with aromatisation and skeletal isomerisation being prevalent in the latter, with main chain and ring side chain cracking being dominant in the former.

In work by Breen *et al*⁸ using Al pillared clays as HDPE transformation catalysts, such an extreme shift towards the appearance of shorter chain aliphatics in the product stream was also observed. The author noted similarities to previous results from others using rare earth exchanged zeolite-Y.²⁴

An important aim of this investigation is to encourage, through modification, the ability of these transformation agents to generate aromatic species from the HDPE

²²⁶ M. Boronat, P. Viruela & A. Corma, *Journal of Physical Chemistry. A*, **101** (1997) 10069.

decomposition products. As such determination of the aromatic content of the product streams is important to elucidate the DHC activity of these materials.

As outlined in table 19, preliminary studies by Breen *et al*⁸ had shown that certain simple aromatics and polyaromatics were prevalent dehydrocyclisation products over Al pillared clays in particular. Figure 48 illustrates the aromatic product distribution, which was performed through integration of the areas associated with the base peaks of the relevant ions from the mass spectrometric data.

Figure 48 – Aromatic Hydrocarbon Distribution Achieved Over R1 – R4

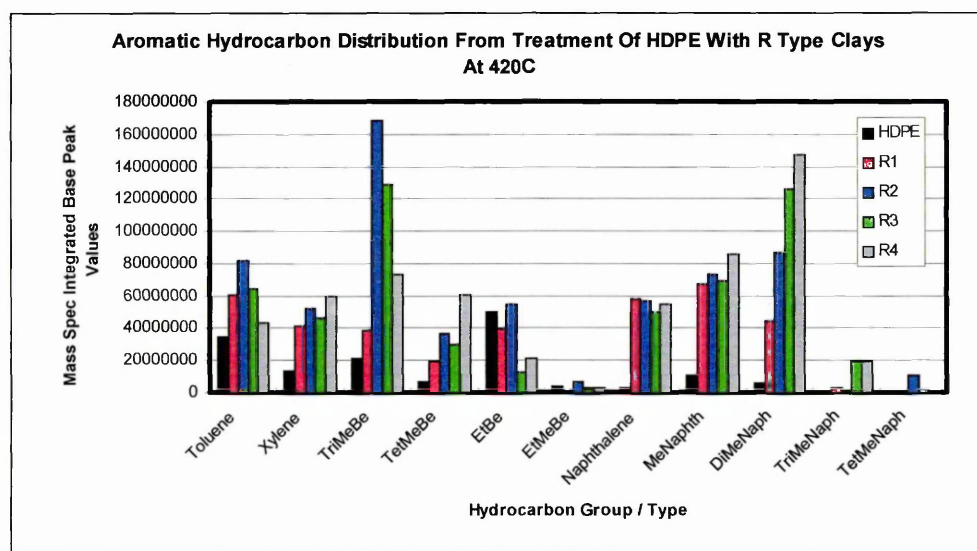


Figure 48 shows that the materials studied did enhance the aromatic yield in the product gas stream relative to that for the uncatalysed process. No other aromatics, other than those noted were identified in the product gas stream. In particular, no single ring aromatics larger than ethylbenzene were identified, and this could be attributed to the relative stability of the methylaromatics.²⁰ Such findings are in agreement with Uemichi¹⁶ when using SA, but disagree with other studies using the zeolite ZSM-5.^{17,26,227,228} In the latter cases, benzene was also identified, although that

²²⁷ G. de la Puente & U. Sedran, *Applied Catalysis B: Environmental*, **19** (1998) 305 – 311.

²²⁸ S. Vitolo, B. Bresci, M. Seggiani & M. G. Gallo, *Fuel*, **80** (2001) 17 – 26.

was not the case in this work. Certainly, catalytic transformation over ZSM-5 favours the formation of large quantities of low molecular weight gases as a consequence of the small pore openings of the zeolite, which present diffusional barriers to carbon chains greater than C₄. Despite this, ZSM-5 does exhibit some secondary aromatisation behavior when molecules cracked externally subsequently diffuse into the pore channel network.²¹ Ohkita et al¹⁷ was able to demonstrate that ZSM-5 produces upto three times more aromatics than the most active SAs when polyethylene decomposition gases are directed over their surfaces. As such the enhanced aromatic yield observed over R2 may arise as a consequence of the availability of large numbers of strongly protonic sites such as those found on zeolites.

Songip et al^{229,230} have demonstrated that H⁺ZSM-5 is not a suitable material for the reforming of oils derived from polyethylene. Despite producing high quality fuels, with limited coke deposition, liquid product yield was low (20%) when compared to gas generation (68%). In contrast, proton exchanged (HY) and rare earth exchanged (REY) zeolite-Y generates fuels of comparable quality, but with significantly less gas. HY is much more acidic than REY, thus the former is subject to lower liquid fuel yields (27% vs. 49%) and is deactivated more readily by heavy coke deposition (6% vs. 3%). Such findings are in agreement with others.²³¹

Bearing the above in mind, the activity of R1 – R4 is analogous to that of the REY samples, as pillared clays are known to accommodate a large number of milder acid sites than most zeolites.¹⁶² In addition, pillared clays exhibit predominantly Lewis acid sites following activation at high temperature.^{232,233,234,235} Accordingly, the large

²²⁹ A. R. Songip, T. Masuda, H. Kuwahara & K. Hashimoto, *Applied Catalysis B: Environmental*, **2** (1993) 153 – 164.

²³⁰ A. R. Songip, T. Masuda, H. Kuwahara & K. Hashimoto, *Energy and Fuels*, **8** (1994) 136 – 140.

²³¹ Y.-H. Lin, P. N. Sharratt, A. A. Garforth & J. Dwyer, *T. Acta*, **294** (1997) 45 – 50.

²³² H. Ming-Yuan, L. Zhongui & M. Enze, *Catalysis Today*, **2** (1988) 136.

²³³ S. A. Bagshaw & R. P. Cooney, *Chemistry of Materials*, **5** (1993) 1101.

²³⁴ S. Bodoardo, F. Figueras & E. Garrone, *Journal of Catalysis*, **147** (1994) 223.

²³⁵ S. Perathoner & A. Vaccari, *Clay Minerals*, **32** (1997) 123.

unsaturated molecules present in the polymer degradation feedstock gas were cracked into smaller molecules, some of which were subject to dehydrocyclisation to produce aromatics. Over cracking such as that over zeolites is discounted on the basis of insufficient acidic strength.

Examination of figure 48 shows a reduction in the levels of aromatics generated as a function of increasing Cr content, perhaps suggesting that the primary DHC capability of the materials is associated directly with the pillars. However, this decrease is offset by an apparent increase in the formation of polyaromatic species. It should be noted that in the case of toluene, levels of production in the catalysed processes are only slightly higher than seen with the non catalysed process. In addition, ethylbenzene levels are actually lower than in the uncatalysed reaction. As can be seen later by reference to the results for AAC's, the levels of aromatics generated over these materials are much lower. As such, the levels of polyaromatics are in all probability low, and may arise as a consequence of the thermal removal of polyaromatic coke precursors deposited on the pillars.

The depletion in ethylbenzene levels may occur as a consequence of side chain cracking reactions to yield toluene. Alternatively, transalkylation reactions may be in operation as Al pillared clays have proven effective in this role.^{236,237}

There is clear evidence to correlate the production of aromatics to the presence of branched aliphatics in the catalysed product gas stream. The relationship is inverse, and is highlighted in later sections with data presented for the AAC's. This is evidence for a competitive process for the types of reactions leading to the formations of each type of product. Other factors including active site accessibility, residence time and feedstock flow rate may also be important.

²³⁶ T. Matsuda, M. Matsukata, E. Kikuchi & Y. Morita, *Applied Catalysis*, **21** (1986) 297 – 306.

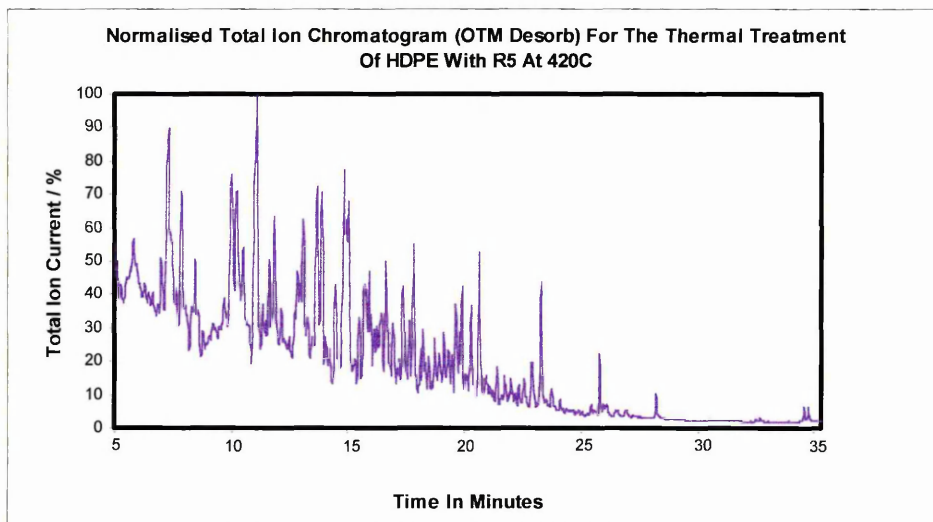
²³⁷ E. Kikuchi, T. Marsuda, J. Ueda & Y. Morita, *Applied Catalysis*, **16** (1985) 401 – 410.

R5

Pillar Composition = 50% Al and 50% Cr

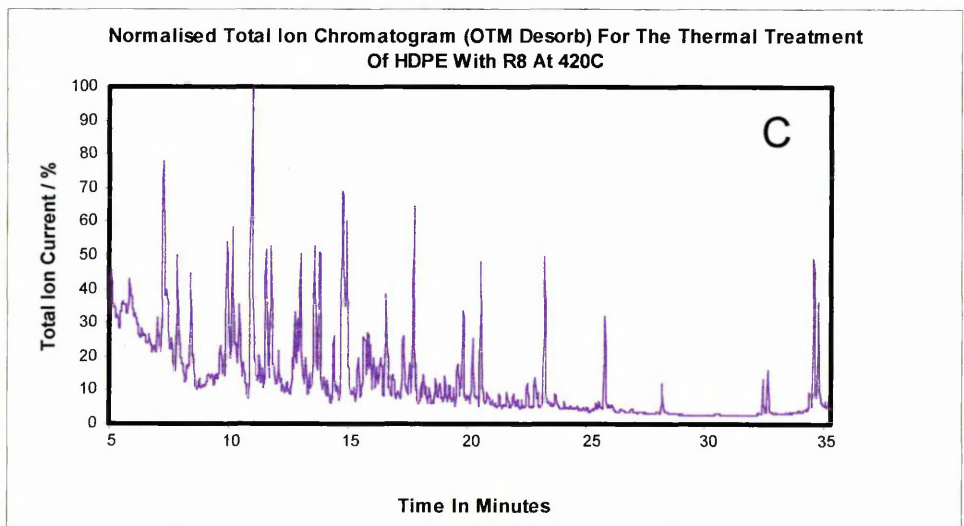
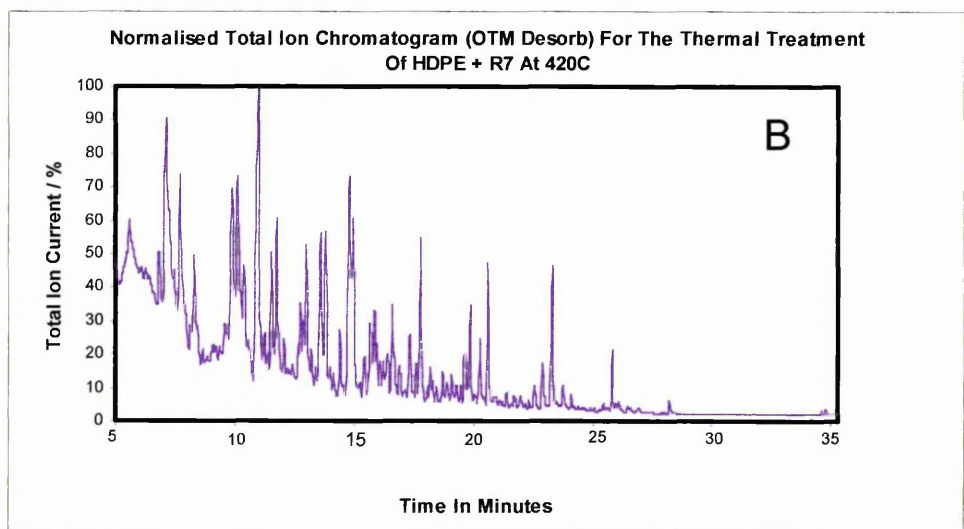
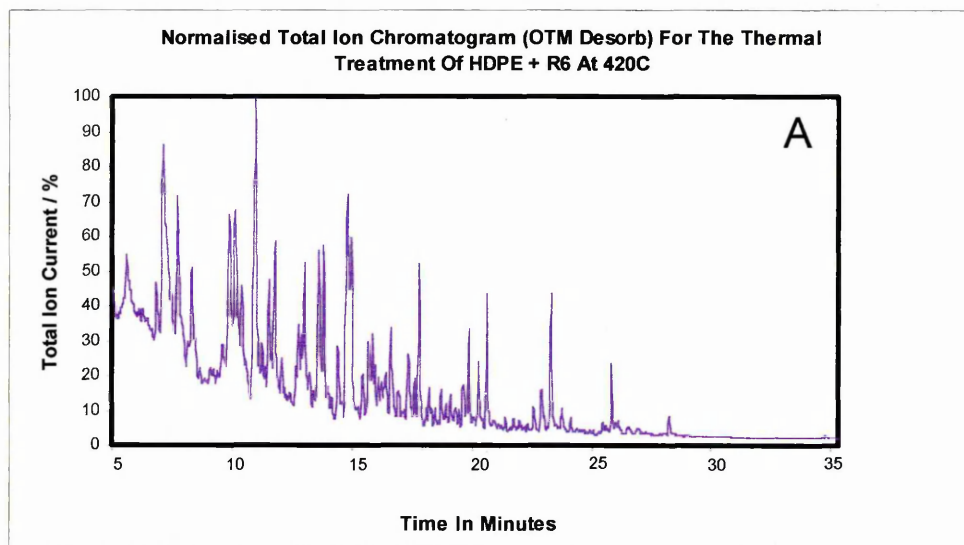
Figure 49 below shows the nTIC recorded using R5 as a transformation agent for the HDPE decomposition products.

Figure 49 – nTIC for the Thermal Treatment of HDPE + R5 at 420°C (Isothermal)



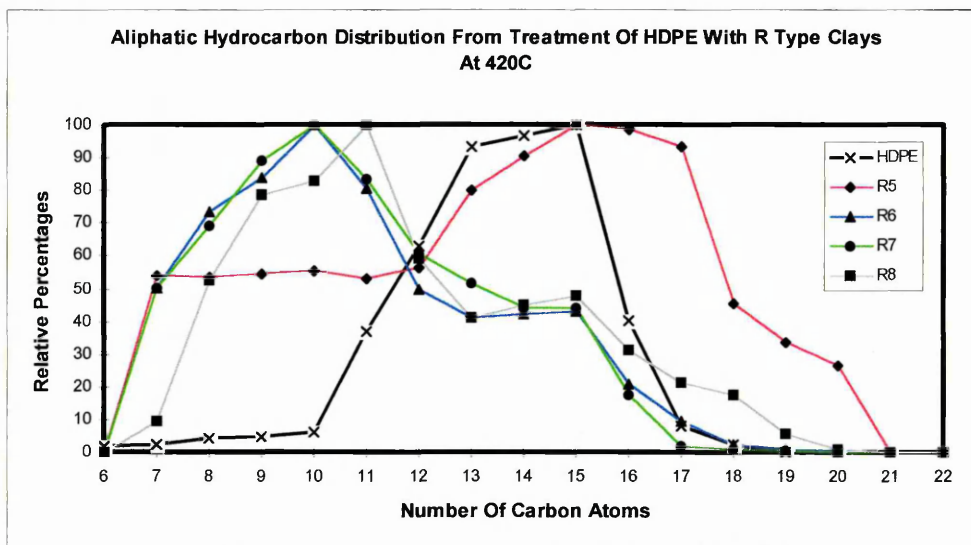
The trace presented in figure 49 possesses many similar features to those shown for PILC's R2 – R4, including retention of the parabolic n-alkane distribution, and the appearance of numerous branched aliphatic products. Indeed, the traces obtained for the Cr rich pillared clays are all very similar in nature, and those for R6-R8 are given in figure 50 (A. R6, B. R7, C. R8) for comparative purposes.

In terms of the production of branched alkanes, the relative number and quantities of each present little deviation through the series. In addition, there appears to be excellent agreement in the nature of these materials, possibly highlighting selectivity factors in respect of the skeletal isomerisation reactions promoted by these materials. This selectivity could be accounted for on the basis of shape or size constraints imposed by the pillaring process.



Closer examination of the n-alkane distribution highlights an anomaly, as can be seen by reference to (figure 51).

Figure 51 – Aliphatic Hydrocarbon Distribution Achieved Over R5 – R8



While the distributions for R6 – R8 resemble those for the Al rich pillared clays, in that there is a shift towards shorter chain alkanes in the product stream relative to the uncatalysed process, that for R5 is significantly different. While the relative amounts of shorter chain alkanes (<C₁₁) can be seen to increase relative to HDPE alone, the most abundant products remain those of higher carbon chain length (>C₁₁) which levies greater resemblance to the HDPE distribution. The overall effect is that R5 presents a very wide range distribution of linear alkanes, including the apparent production of materials with chain lengths greater than C₁₇.

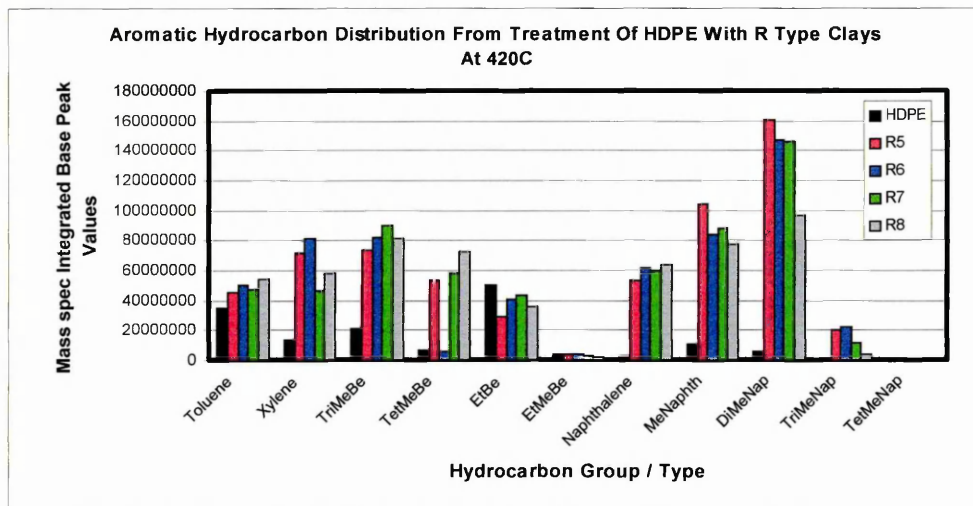
The PILC's prepared from Cr rich pillaring solutions demonstrated little thermal stability at temperatures above their calcination temperature (200°C).¹⁶⁸ As such, it is reasonable to assume that this latter series of modified clays (R5-R8) may have undergone total or partial layer collapse under the experimental conditions employed here. This would render the gallery region and indeed the exposed surfaces of the pillars inaccessible to the feedstock gas molecules, thus forcing any

hydrocarbon reformation reactions to occur on the outer surfaces of the saponite tactoids. This would explain the similarities seen in the nTIC for the predominantly Cr pillared clays, and that for the natural saponite (figure 40).

Given the poor thermal stability of the Cr pillared clays, it is plausible that the Brønsted acid sites available on the surface of saponites as a consequence of their Al³⁺ for Si⁴⁺ isomorphous substitution may be actively involved in the feedstock reformation.

In light of the impoverished aromatic yields relative to certain AAC's (see later), the apparent shift towards the generation of shorter chain alkanes is actually a consequence of the skeletal isomerisation of linear alkenes in the feedstock gases on the protonic sites presented by the mineral matrix. Chain propagation through hydride abstraction allows for the formation of branched alkanes in the product gas stream. The insufficient acidity of these groups to effect direct protonation of the alkanes present would account for the retention of the parabolic paraffinic distribution through this series of materials.

In terms of DHC activity, aromatic yield was disappointing and resembled that over R1 on all cases (Figure 52). As with the previous series, polyaromatic yield was much higher than over AAC's. Again this could be attributed to the removal of carbonaceous residues from the catalyst surfaces at the temperatures employed. Bearing in mind the low levels of aromatic species, these figures appear artificially inflated relative to their actual occurrence in the product gas streams.

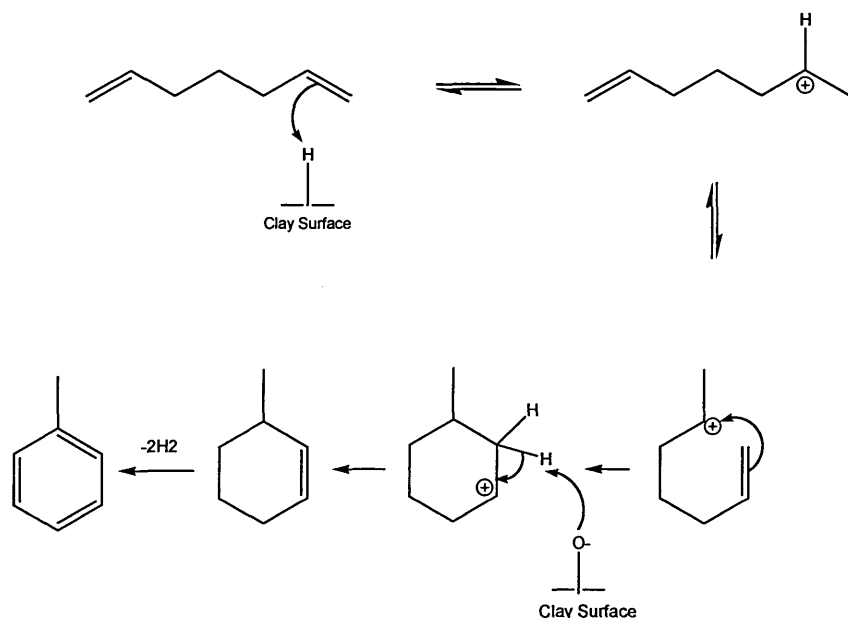


In view of these results, it could be postulated that the aromatics seen in the product streams generated over R1 and R5 – R8 occur as a result of a series of proton catalysed DHC reactions involving the α,ω -dienes generated during the pyrolysis of HDPE. Such materials are absent from the product stream in all cases, including R1, despite the fact that this product mixture retains some of its unsaturated components.

Figure 53 illustrates the mechanism of this proton catalysed reaction, using 1,6-heptadiene as the feedstock molecule. The catalytic proton is furnished by a surface siloxane group present in tetrahedrally substituted minerals such as saponites. It should be noted that the formation of Benzene from a C_6 terminal diene is unlikely as the transition state involves the formation of a highly unstable 1° carbocation. This could account for the complete absence of benzene from all of the analysed product gas streams. Terminal dienes of chain length greater than C_7 could also be involved in such a reaction, although as highlighted by Takuma et al²³⁸ alkylaromatics with substituent chain lengths greater than C_3 are subject to side chain cracking under hydrocarbon reformation conditions, hence their absence in this work. This can be accounted for by electronic stabilisation by the delocalised π electrons of the ring.

²³⁸ K. Takuma, Y. Uemichi & A. Ayame, *Applied Catalysis A: Gen.*, **192** (2000) 273 – 280.

Figure 53 – Proton Catalysed Dehydrocyclisation of 1,6-heptadiene to Yield Toluene



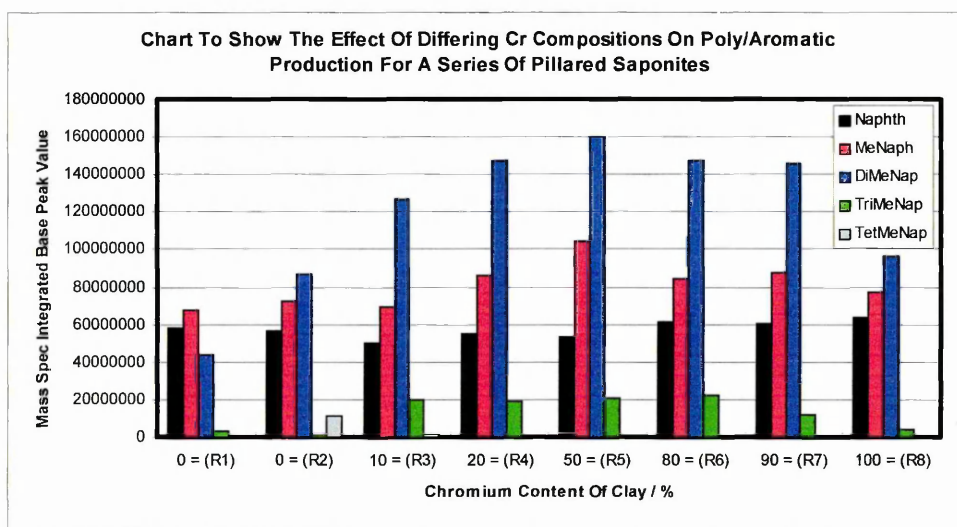
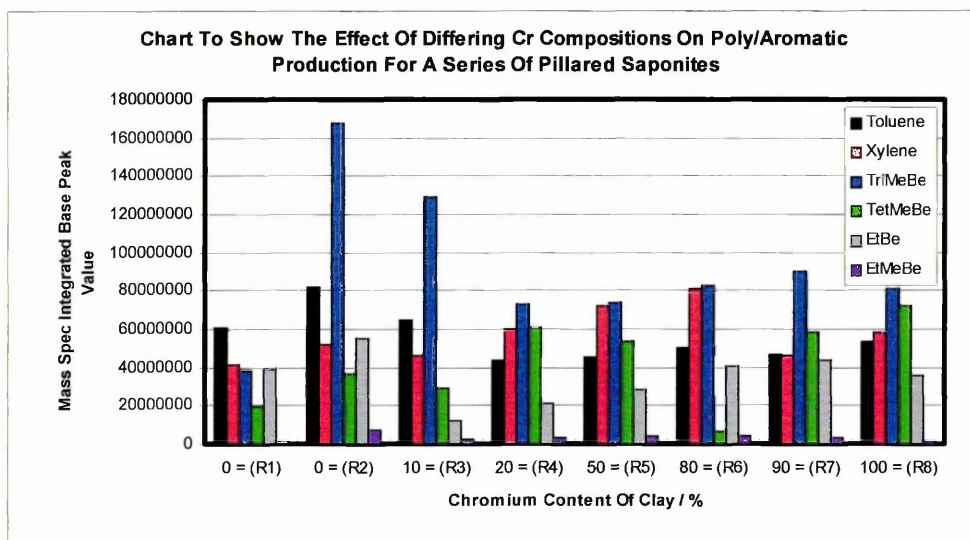
In respect of the data recorded for the aromatisation activity of R2 – R8, and in light of work by Auer and Hoffman,²³⁹ a secondary analysis was performed to determine the effect of the pillar composition on the ability of these materials to fabricate aromatic molecules.

Auer and Hoffman demonstrated that the passage of toluene over Cr pillared clays resulted in disproportionation to effect the formation of xylenes. They found that Cr pillared clays were more active than Al pillared clays for this type of transformation, attributing the observation to the increased levels of both Brønsted and Lewis acidity associated with the former. As a transition metal, Cr is well equipped to function efficiently as a Lewis acid centre. Zeolites were found to promote dealkylation reactions as a consequence of their extensive integral acidity.

Figure 54 presents the results of this analysis, with the individual aromatic and polyaromatic species identified plotted as a function of the Cr content of the pillars.

²³⁹ H. Auer & H. Hoffman, *Applied Catalysis*, **97** (1993) 23.

Figure 54 – Aromatic Hydrocarbon Distribution as a Function of Pillar Cr Content



The results above suggest the operation of different mechanisms of alkylaromatic formation depending on the composition of the pillars. In the case of R1 (100% Al), there is a relatively high selectivity towards the formation of trimethylbenzene. In contrast, as the Cr content on the materials is increased, there develops an apparent equilibrium between the various alkylaromatics. Such results are indicative of the operation of transalkylation mechanisms, proven previously by passing alkylaromatics over the acidic solid catalyst SAPO-5, acidity of which is lower than traditional zeolitic materials.²⁴⁰

²⁴⁰ V. Hulea *et al*, *Microporous Materials*, **8** (1997) 201 – 206.

Likewise, large pore zeolites including dealuminated steam treated mordenite has also been shown to be effective in promoting the transalkylation of alkylaromatics, while its more acidic counterparts H-omega and H-beta were less active.²⁴¹

6.2.2. DETERMINATION OF COKE

Table 23 lists the coke values determined for each of the spent catalysts employed in this investigation.

Table 23 – Determination of Coke Content for R1 – R8 Spent Transformation Agents

Material	Weight %
R1	1.52
R2	2.06
R3	2.93
R4	3.37
R5	3.06
R6	2.74
R7	2.63
R8	2.88

As can be seen from the data in table 23, the introduction of Cr as a pillaring species has a dramatic effect on the levels of associated coking. The process of coking is heavily dependant upon the nature of the process used to perform the catalysis with factors such as flow rate, temperature and time on stream being of critical importance. It is therefore unreasonable to draw conclusions from the work of others. However, Breen et al⁸ have shown that using the experimental conditions employed herein, pillared clays are subject to elevated levels of coking relative to AAC's. In particular, those containing transition metal pillars are particularly susceptible to deactivation by coke.

²⁴¹ Y-K. Lee, S-H. Park & H-K. Rhee, *Catalysis Today*, **44** (1998) 223 – 233.

The apparent reduction in coke as a function of increased Cr content could be attributed to the thermal instability of these materials, and the entrapment of the Cr oligomers within the gallery region following collapse.

6.3. SUMMARY OF CATALYTIC BEHAVIOUR

Across the series of materials studied, none have proven particularly active in respect of the execution of DHC reactions to yield aromatic hydrocarbons. Impoverished aromatic yields over those materials containing high levels of Cr oligomers suggests that the associated thermal instability of these materials has the effect of limiting or preventing access by the feedstock gas molecules to the clay gallery, and indeed to the pillars themselves at the temperatures employed herein, as a consequence of thermally induced layer collapse. Only in the case of R2 in which there are no Cr related ambiguities is DHC both active and selective towards the formation of trimethylbenzene. In addition, skeletal isomerisation is depressed in this case.

In contrast, over R1 and all materials with a Cr content, skeletal isomerisation is prevalent, DHC efficiency is low, with the alkylaromatic product distribution suggesting the operation of transalkylation reactions. All such processes are proton catalysed, thus affording the possibility that the saponitic matrix is responsible, in part, for the observed activity. Likewise, although cracking activity is inferred from the data, the shift in n-alkane distribution is almost certainly the consequence of protonation and subsequent hydride abstraction reactions involving short chain olefins present in the feedstock gases, as evidenced by similar activity over R1 which would be expected to contain no acid sites of sufficient strength to induce alkane cracking.

CHAPTER SEVEN

-Results & Discussion-
Acid Activated Metakaolin (AAMK's)

7. INTRODUCTION

The primary focus of this investigation was to determine the relative effectiveness of a series of acid activated metakaolin derivatives to act as transformation agents for the conversion of HDPE pyrolysate gases into potentially useful hydrocarbons, and in particular aromatic species.

Recent foundation studies focusing on the use of pillared clays, acid activated bentonites and smectites have shown that these materials are capable of producing respectable quantities of important petrochemicals including toluene, xylenes and trimethylbenzenes from the gases produced during the thermal pyrolysis of HDPE.^{8,198} Given the recent return of interest in acid activated kaolins as solid acid catalysts¹²⁸, it was decided to compare the activity of these clay based materials with those derived from bentonites and smectites.

Kaolin is a 1:1 type clay mineral in which an octahedral alumina sheet is fused to a silica tetrahedral sheet. The individual 1:1 layers are held together by hydrogen bonding between the hydroxyl groups on the gibbsite surface and the oxygens on the adjacent siloxane surface. This hydrogen bonding prevents the ready adsorption of molecules into the interlayer region, a situation which arises in swelling minerals such as montmorillonites and hectorites. Moreover, the nitrogen surface area of kaolin is small (10-30m²g⁻¹) and its C.E.C. is also low. Despite this, acid leached kaolins and smectites were among the first solid acid materials to find employment in the Houdry process for catalytic cracking in the petroleum reforming industry.²⁴² The high octahedral aluminium content of kaolin makes the material resistant to dealumination through the process of acid activation.^{127,243}

²⁴² J. M. Adams, *Applied Clay Science*, **2** (1987) 309.

²⁴³ E.F. Aglietti, J. M. P. Lopes & E. Pereira, *Applied Clay Science*, **3** (1988) 155.

Metakaolin, generated through the calcination of kaolin in air at temperatures > 450°C, is much more susceptible to acid activation to yield catalytically active materials with similar activity to acid activated montmorillonites, despite exhibiting only half of the fresh surface area.¹²⁷ As such, acid activated metakaolin is a material which offers both enhanced surface area and acidity compared with either kaolin or metakaolin.^{126,127}

7.1 MATERIALS CHARACTERISATION

Analysis was performed using the Synergic Chemical Analysis system outlined previously. In this case, FTIR and 'real time' MS data were not collected for the transformation processes. Initial investigations had shown that due to the complexity of the product gas stream, in terms of the number of individual species present, identification and analysis of the individual components by FTIR and 'real time' MS was potentially difficult due to the phenomena of band overlap and co-elution respectively. As such 100% of the product gas stream evolved from the reaction chamber was passed directly to the OTM and trapped using the purge trap identified. One HDPE pellet (15mg, Aldrich) was placed in the quartz crucible and covered with silanised glass wool (70mg, Phase Separations). Finally, a 100mg portion of the selected transformation agent was spread evenly over the glass wool. Samples were heated at 10°C min⁻¹ from room temperature to 420°C and held isothermally for 1 hour. Despite the problems encountered using real time TG-MS, the technique was used to evaluate the surface of these materials. As detailed elsewhere,²⁰⁶ the thermal desorption of basic species from clays minerals can be used as a semi qualitative evaluation of the types of acid sites present on the surface of clay minerals. The results of these studies are given in section 7.1.1 of this chapter.

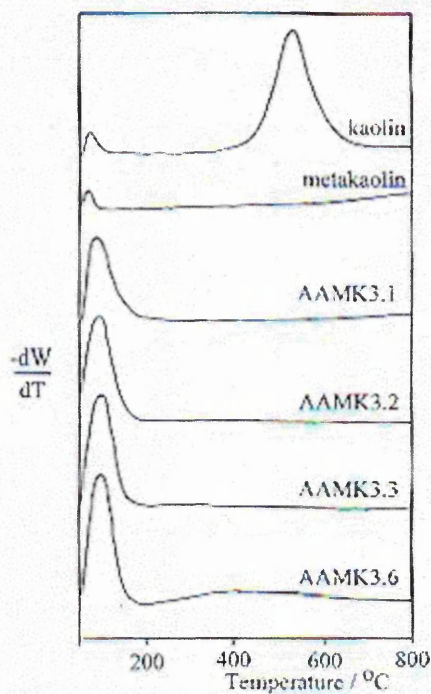
The resultant 'post run' MS data was interrogated to determine the relative amounts of aromatic hydrocarbons produced over each of the transformation agents through

the integration of base peak signals, identified through known fragmentation pathways for the type of ionisation employed.

7.1.1. THERMOGRAVIMETRIC ANALYSIS

Kaolin was found to lose 16wt% by 800°C, with the corresponding derivative thermogram being dominated by layer dehydroxylation above 450°C, as illustrated in figure 55. This 16% weight loss is primarily due to the dehydroxylation of the kaolin structure which appears as a maximum in the derivative thermogram at 520°C as illustrated below.

Figure 55 – Derivative Thermograms For Acid Activated Metakaolin (AAMK) Samples



Following the production of metakaolin, the 16% weight loss seen with kaolin is reduced to 4% over the same temperature range. These reduced overall weight losses, combined with the lack of dehydroxylation features in the above derivative thermograms confirm the dehydroxylation of the kaolin structure during calcination to yield metakaolin. There is no evidence of the aforementioned dehydroxylation

maximum in any of the metakaolin derived samples. As the concentration of the acid used in the activation treatments was increased, the weight loss attributed to the loss of sorbed water ($\geq 200^\circ\text{C}$) also increased (Table 24) from 0.1% for metakaolin to 3.1% for AAMK3.1 and then to 7.5% for AAMK3.3 and AAMK3.6.

Table 24 – Weight Loss and Acidity Data for Acid Activated Metakaolin Samples

Sample	Treatment Time (H)	[HCl]/mol dm ⁻³	Weight Loss to 800°C / wt%	Acidity mmol/g ⁻¹ clay
Kaolin	n/a	n/a	16	n/a
MK	n/a	n/a	4	0.01
AAMK3.1	3	1M	7	0.22
AAMK3.2	3	2M	10	0.31
AAMK3.3	3	3M	12	0.34
AAMK3.6	3	6M	13	0.49

These materials are also referred to as Acid Leached Metakaolins (ALMK's) in some of the figures presented in this chapter

The weight loss above 200°C varied in a systematic manner, but was not as marked and occurred at a constant rate thus providing no features in the derivative thermogram. The increase in the loss of sorbed water at temperatures $< 200^\circ\text{C}$ can be attributed to an increase in available surface area for water adsorption following acid activation.

The total acidity of each of the AAMK's was determined as the number of millimoles of cyclohexylamine-derived products desorbed over the temperature range 290-420°C. These values were normalised to the amount of AAMK present, and are represented in table 24. The total acidity increased as the strength of the treatment acid used to prepare each AAMK was increased. Apparently, raising the concentration of the treatment acid from 2M to 3M has significantly less effect on total acidity than increasing from 1M to 2M. Overall, the results were low when compared to those obtained by Breen *et al*¹⁴¹ for a series of acid activated smectites. However, acid treated smectites are able to sorb appreciable quantities of cyclohexylamine between their layers, where it can undergo interaction with

exchangeable cations. This does not occur with the AAMK's in which the layer structure is destroyed by calcination.

The use of evolved gas analysis to determine the nature of the thermally desorbed products arising from adsorbed amines is a well established technique. Indeed, it has been found²⁴⁴ that when heated, adsorbed alkylammonium ions undergo thermal C-N bond cleavage producing ammonia and the corresponding alkene.

The range of products observed using TG-OTM-GC-MS along with the characteristic mass to charge (m/z) ratio used to identify each of the hydrocarbons from their resultant Total Ion Chromatogram (TIC) are given in table 25. Such products are inkeeping with previous work by Breen *et al*²⁰⁶ in which EGA was used to determine the range of decomposition products achieved for the desorption of cyclohexylamine from cation exchanged smectites.

Table 25 – Cyclohexylamine Degradation Products Generated Over AAMK's

Species	Ion (m/z ratio)
Ammonia	17
Methylcyclopentene	53
Cyclohexene	54
Cyclohexadiene	77
Benzene	78
Aniline	93
Cyclohexylamine	99

The formation of benzene and ammonia during cyclohexylamine desorption agrees with the work of Huang and co-workers.²⁴⁵ Similarly, the formation of ammonia, cyclohexene and aniline was reported by Sokoll,²⁴⁶ and attributed to the interaction of cyclohexylamine with strong Lewis acid centres. Breen *et al*²⁰⁶ have recently

²⁴⁴ A. K. Ghosh, *Journal of Catalysis*, **96** (1985) 288 – 291.

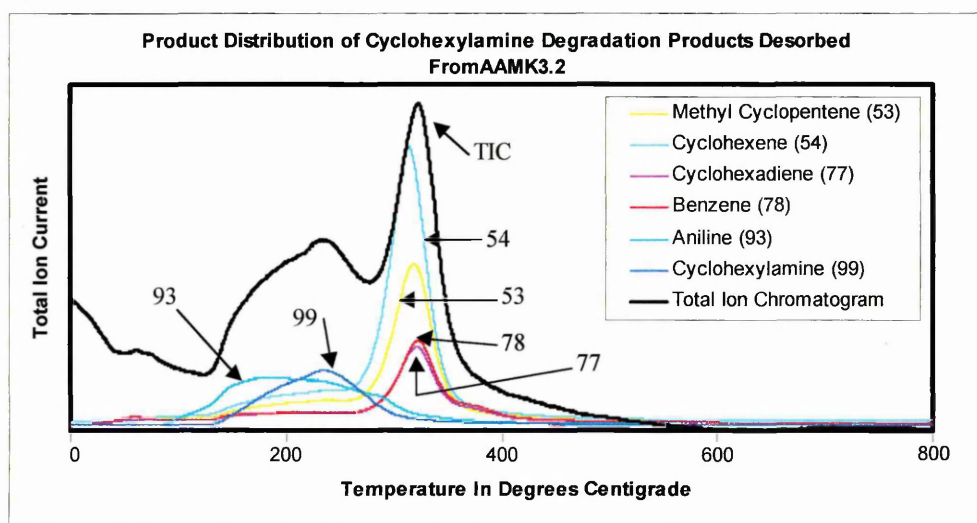
²⁴⁵ S. X. Huang & J. L. Gland, *Journal of Physical Chemistry*, **100** (1996) 2206 – 2212.

²⁴⁶ R. Sokoll, H. Hobert & I. Schmuck, *Journal of Catalysis*, **125** (1990) 276 – 284.

observed different decomposition routes for cyclohexylamine desorbed from Al^{3+} and Ni^{2+} bentonites which exhibit Brønsted and Lewis acid sites respectively.²⁰⁶

The mass spectral single ion chromatograms (SIC), collected in real time, together with the TIC show which of the individual species desorb over a particular temperature interval (Figure 56). Such desorption events occurred at temperatures of 90, 215, 245 and 320°C. The most prominent event was that occurring over the temperature range 300-400°C.

Figure 56 – R.T. Determination of Cyclohexylamine Degradation Products (AAMK3.2)



7.1.2. ELEMENTAL ANALYSIS

As anticipated, the acid activation of metakaolin results in structural dealumination (Table 26). Clearly, appropriate activation parameters (acid strength, temperature, time) can be selected to control the degree of structural degradation and hence the physical and chemical attributes of the activated products.

With respect to the starting material, relatively low levels of both magnesium and iron suggest that the octahedral residency of the kaolin structure is predominantly aluminium, thus confirming that the parent mineral is a dioctahedral kaolinite. The

effect of this lack of isomorphous substitution yields a material with an almost zero layer charge, a factor which accounts for the extremely low levels of typical clay mineral interlayer and exchange site cations such as sodium and calcium found in the untreated samples. In contrast to trioctahedral serpentines and trioctahedral smectites (saponites) which contain a larger proportion of octahedral magnesium and iron, the aluminium rich structure of the octahedral sheet of kaolin is relatively resistant to acid attack. The enhanced acid solubility of both magnesium and iron relative to aluminium accounts for the harsh treatment conditions required to achieve the structural depletion seen in this work when compared to other studies involving trioctahedral minerals.¹⁴¹

Table 26 – XRF Data for the Acid Activated Metakaolin Samples

%	Kaolin	MK	AAMK3.1	AAMK3.2	AAMK3.3	AAMK3.6
Al ₂ O ₃	43.73	43.69	36.54	26.94	23.60	12.34
SiO ₂	54.06	54.06	61.41	71.14	74.57	86.05
Fe ₂ O ₃	0.80	0.79	0.76	0.65	0.59	0.47
MgO	0.19	0.19	0.17	0.16	0.14	0.12
Na ₂ O	0.08	0.08	0.09	0.09	0.06	0.07
CaO	0.06	0.06	0.04	0.04	0.03	0.03
K ₂ O	1.04	1.03	1.02	1.00	1.01	1.01
Others	0.04	0.1	-0.03	-0.02	0.00	-0.09
TOTAL	100	100	100	100	100	100

The relative amounts of dealumination agree with the results of Perissonotto *et al*¹²⁶ in that the Si/Al ratio after treatment with 6M HCl are the same at 12.6 ± 0.1 .

7.1.3. X-RAY DIFFRACTION ANALYSIS

Figure 57A and 57B show the XRD traces obtained for both kaolin and metakaolin respectively. Figure 57A in particular illustrates the intense characteristic d_{001} and d_{002} reflections indicative of kaolin at 2θ values of 12.29° and 25.03° . These reflections are no longer present following the thermal dehydroxylation process which yield

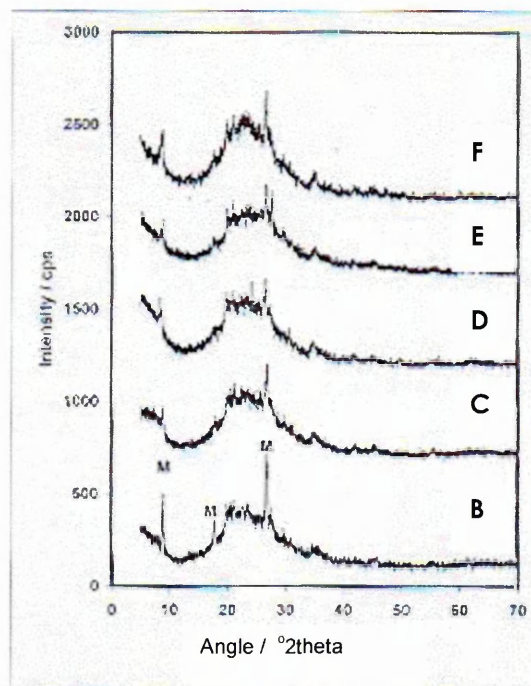
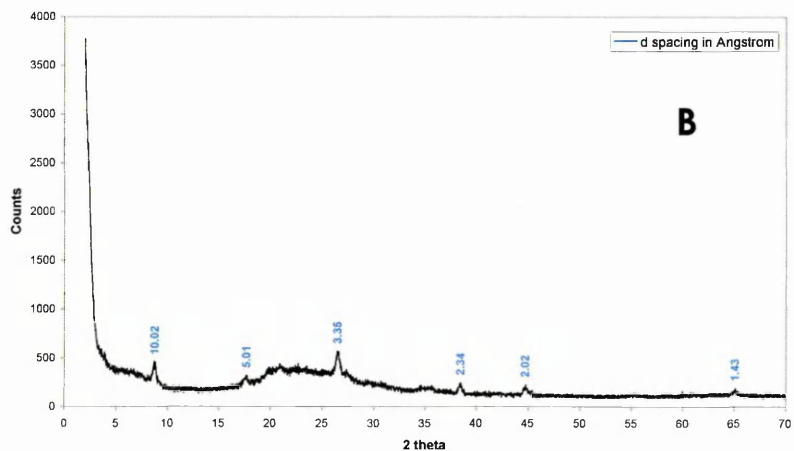
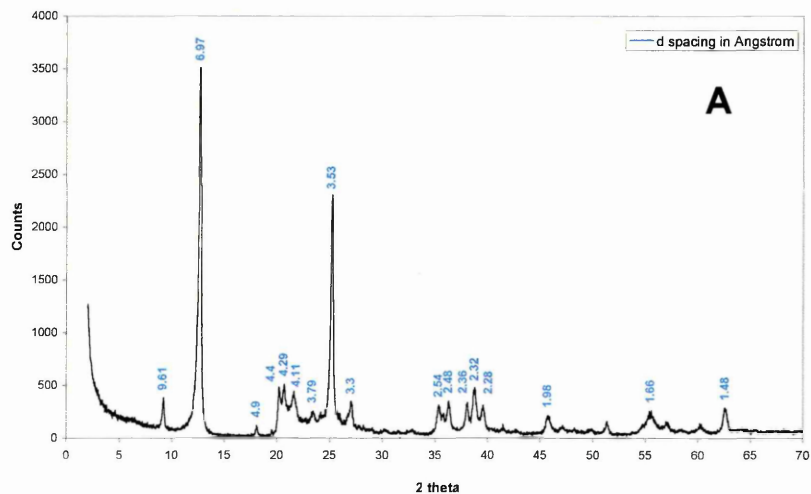
metakaolin (figure 57B) thus confirming the loss of structural integrity of the parent mineral. In addition these signals are absent from those traces recorded for the acid treated samples (Figure 57 (C) AAMK3.1, (D) AAMK3.2, (E) AAMK3.3 & (F) AAMK3.6). This together with the broad hump in the range 16-32° 2θ, which increased with the severity of the activation treatment, confirms the loss of structural integrity and the presence of an amorphous product.²⁴⁷

Figure 57A also shows a small signal with a 2θ value of 26.93° (3.31Å). This can be attributed to a small amount of a mica impurity in the sample. The occurrence of the same signal in figure 57B confirms that the impurity is unaffected by the thermal process leading to the formation of metakaolin. In addition, the XRD traces for each of the acid treated transformation agents retain this feature, thereby possibly indicating the acid insolubility of this inclusion.

With respect to the acid treated minerals, the most notable feature of each of the traces is the appearance of a broad signal over the 2θ range 16-32°, and can be attributed to the amorphous product. The intensity of this broad signal increases as the concentration of the treatment acid is increased, the result of which is enhanced dealumination. Such observations are in line with those reported by others.^{39,43}

²⁴⁷ C. Breen, J. Madejová & P. Komadel, *Applied Clay Science*, **10** (1995) 219 – 230.

Figure 57 – X-Ray Diffraction Analysis For AAMK Transformation Agents



7.1.4. FTIR ANALYSIS (DRIFTS)

The saturation of clay mineral surfaces with vapour phase pyridine results in a variety of interactions which occur primarily through the availability of the lone pair of electrons on the nitrogen atom of the pyridine ring system.²¹⁰ Infra red spectroscopic investigation of pyridine treated acidic solids can readily distinguish between Brønsted and Lewis acid sites on the surface and provide semi quantitative estimates of the number of each type. The room temperature DRIFTS spectrum for pyridine saturated AAMK3.2 (Figure 58A) exhibits bands due to Brønsted bound pyridine at 1634 and 1541 cm⁻¹ and for Lewis bound pyridine at 1616 cm⁻¹ together with a shoulder on the higher wavenumber side of the 1445 cm⁻¹ band. The 1445 cm⁻¹ band in combination with the 1596 cm⁻¹ band was assigned to hydrogen bonded pyridine, HPYR.²⁴⁸ The 1490 cm⁻¹ band is attributable to pyridine bonded to both Brønsted and Lewis acid sites, although the Brønsted bound species is known to contribute a greater intensity.

Raising the sample temperature to 150°C (Figure 58B) resulted in a significant reduction in the intensity of the bands at 1445 and 1596 cm⁻¹ attributed to hydrogen bonded pyridine. The reduction in the 1445 cm⁻¹ band revealed the 1452 cm⁻¹ band previously assigned to Lewis bound pyridine. The intensity of the 1540 cm⁻¹ band increased and the width decreased as the hydrogen bonded pyridine bands became less intense. This suggests that some of the hydrogen bonded pyridine was actually forming a hydrogen bond with the proton on the Brønsted bound pyridine as observed in Al³⁺ exchanged²⁴⁹ and acid treated smectites.²¹⁰ However, the strong 1540 cm⁻¹ band seen at room temperature suggests that there was some Brønsted bound pyridine that could not form hydrogen bonds with excess pyridine due to steric

²⁴⁸ R. Buzzoni, S. Bordiga, G. Ricciardi, C. Lamberti, A. Zecchina & G. Bellussi, *Lanmuir*, 12 (1996) 930.

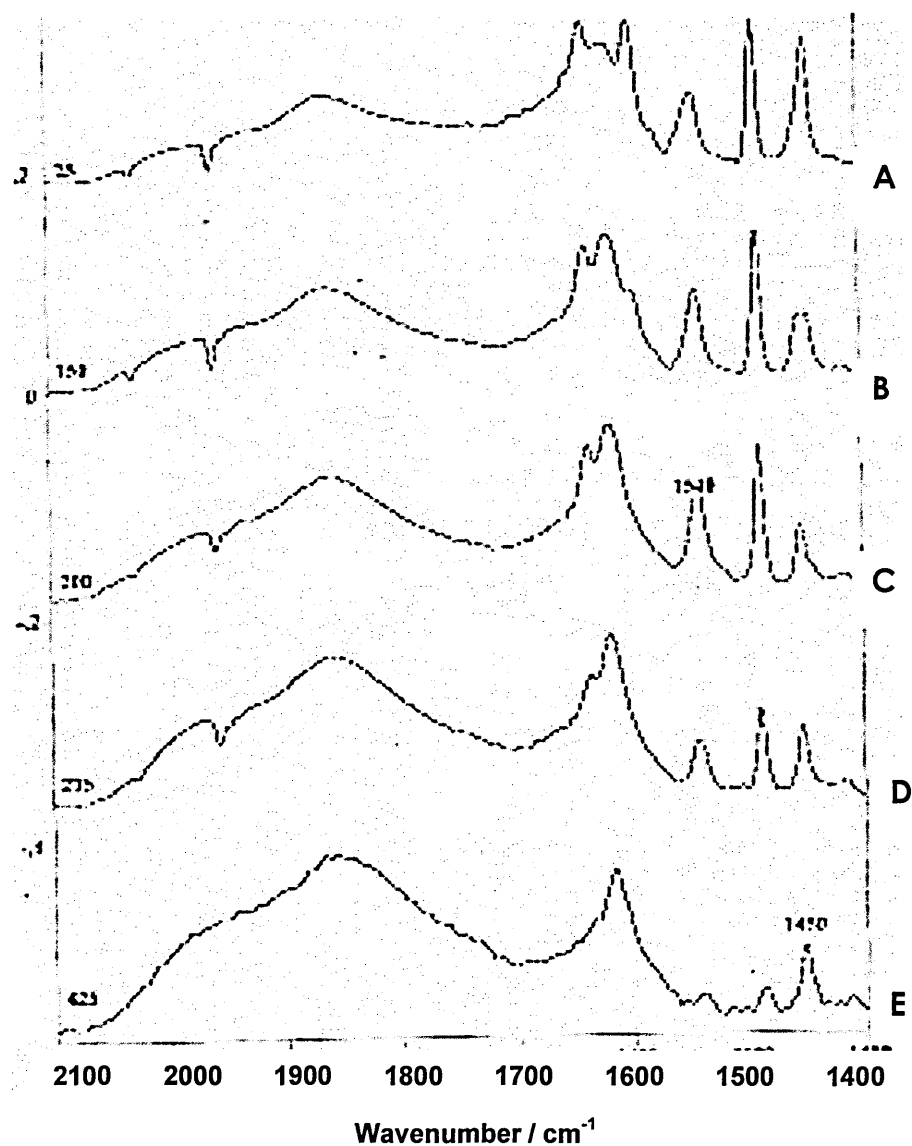
²⁴⁹ J. Rocha & Klinowski, *Angew. Chem. Int. Ed. Engl.*, 29 (1990) 553.

constraints, insufficient excess pyridine or inefficient pyridine adsorption due to pore size constraints.

At 200°C (Figure 58C) the bands for hydrogen bonded pyridine had completely gone and the intensity of the Lewis and Brønsted bands in relation to the AAMK combination bands at 1856cm⁻¹ and 1923cm⁻¹ had diminished a little. At 275°C (Figure 58D), the intensity of the bands for Brønsted bound pyridine had significantly reduced whereas the bands for Lewis bound pyridine remained relatively constant. At 425°C, the majority of pyridine remaining on the sample was bound to Lewis acid sites, although there were weak contributions from Brønsted bound pyridine at 1539cm⁻¹ and 1636cm⁻¹ (Figure 58E).

This apparent loss of Brønsted acidity can be explained on the basis of dehydration effects. As the material is heated, it undergoes dehydration. This includes the loss of water molecules associated with the surface charge compensating cations. The interaction of water molecules which compose the hydration sphere of these ions, with the cation itself, results in polarisation of the water molecules, and thus their ability to impart Brønsted acidity to the material. Dehydration of these surface cationic species results not only in the loss of their associated Brønsted acidity, but also a conversion of these ions to Lewis acid sites. In addition, dehydroxylation of the surface aluminol and silanol groups would also yield efficient Lewis acid centres.

By 425°C (figure 58E), only traces of Brønsted acidity are apparent as indicated by the low intensity band at 1539cm⁻¹ and by the shoulder at 1636cm⁻¹. At this temperature, the acidity of the materials appears to be predominantly Lewis in nature. However, such observations are not inkeeping with the apparent catalytic activity of these materials, and their ability to carry out dehydrocyclisation reactions using alkene feedstocks.



The first step in the formation of aromatics from alkenes involves the protonation of the alkene to yield a carbocation. Evidently, this small quantity of thermally stable Brønsted acid sites facilitate the dehydrocyclisation reactions involving the alkenes produced during the thermal pyrolysis of HDPE. Although carbocations can be formed through Lewis acid site promoted hydride ion abstraction from alkanes, this process does not account for the removal of unsaturated materials from the feedstock gases passed over these acid treated clay minerals.

Figure 58A shows that when exposed to vapour phase pyridine, AAMK3.2 is capable of forming the pyridinium ion. The formation of this species requires the direct and total transfer of a proton from the transformation agent to a gas phase pyridine molecule, with the newly formed bond being co-ordinate in nature. Acid strength, and in particular Brønsted acidity is determined by the ability and relative ease of the site to furnish its proton to a basic molecule, the overall process also being governed by the relative basic strength of the proton accepting species. Increases in acid strength enhance the probability that the site will promote direct protonation as opposed to becoming involved in interactions involving adsorption of the base to the acidic active site. It can thus be summarised that the formation of the pyridinium ion is the result of the availability of strong Brønsted acid sites on the surface of the transformation agent. The acid sites which participate in Brønsted bound pyridine interactions can be considered to be of overall lower acid strength than those promoting total proton transfer, on the basis that the available basic molecule is the same for all exposed sites. Post protonation, the resultant conjugate base is only slightly basic, and is therefore unlikely, on these grounds alone, to re-accept the proton from the pyridinium ion. Electrostatic interaction between the pyridinium ion and the resultant conjugate base is the most likely explanation for the relatively high temperatures to which the pyridinium ions are held.

Under transformation conditions, these strong Brønsted acid sites (structural silanol, aluminol and magnesol) are available to act upon the feedstock gases, on the basis that they are fresh structural acid sites which have not previously been exposed to basic species, and thus their protons remain intact.

The VT-DRIFTS spectra for the other pyridine treated samples revealed similar behaviour in that the Lewis acid sites predominated at the reaction temperature of >400°C. Incidentally, the amount of HPYR at low temperatures increased as the

severity of the acid activation treatment was increased. This pyridine was either bonded to weakly acid hydroxyls or formed hydrogen bonds to the proton of the pyridinium cation on the AAMK surface. It is well established that the diagnostic band for the pyridinium cation (1540cm^{-1}) is significantly reduced and broadened when it is hydrogen bonded to another pyridine molecule.²⁴⁸ Nevertheless, the 1540cm^{-1} band increased in intensity as the HPYR was lost at temperatures above 150°C .

7.2. CATALYTIC ACTIVITY

As with the pillared clays described in the previous chapter, the primary aim of this work was to ascertain the ability of these materials to generate commercially important aromatic hydrocarbons from the gases evolved during the thermal decomposition of HDPE in addition to determining other aspects of the catalytic reforming behaviour of these materials.

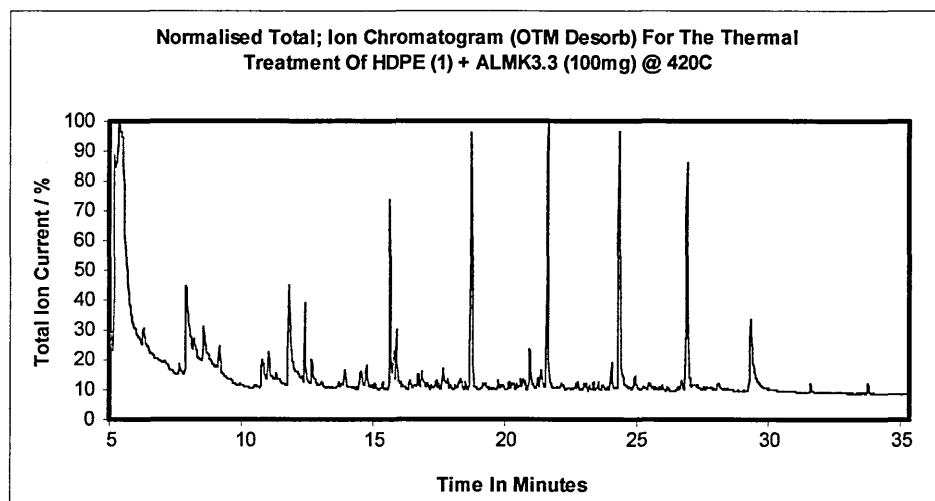
As reported previously by several authors,^{8,9,10,198} the pyrolysis of HDPE yields an homologous series of saturated and unsaturated hydrocarbons, which were shown by this work, and in agreement with previous studies^{8,198} to consist, in order of increasing retention time, of the following species: α,ω -dienes, alk-1-enes, n-alkanes and alk-x-enes.

Figure 5 (section 1.2.3.2, chapter 1) illustrates the normalised total ion chromatogram (nTIC) obtained for the pyrolysis of HDPE at 420°C in an inert nitrogen atmosphere. The characteristic quartets, attributed to the species outlined above, can clearly be seen, although no evidence of branched aliphatic species or even low levels of aromatic products was found, although this observation is in agreement with others.^{8,9,198}

7.2.1 HDPE CATALYTIC TRANSFORMATION ACTIVITY

As anticipated, inclusion of a post pyrolysis transformation agent significantly altered the composition of the products, both in terms of the species present and their relative quantities. Figure 59 shows a nTIC recorded for a TG-OTM-GS-MS run carried out in the presence of AAMK3.3 as the post pyrolysis transformation agent.

Figure 59 – nTIC for the Thermal Treatment of HDPE + AAMK3.3 at 420°C

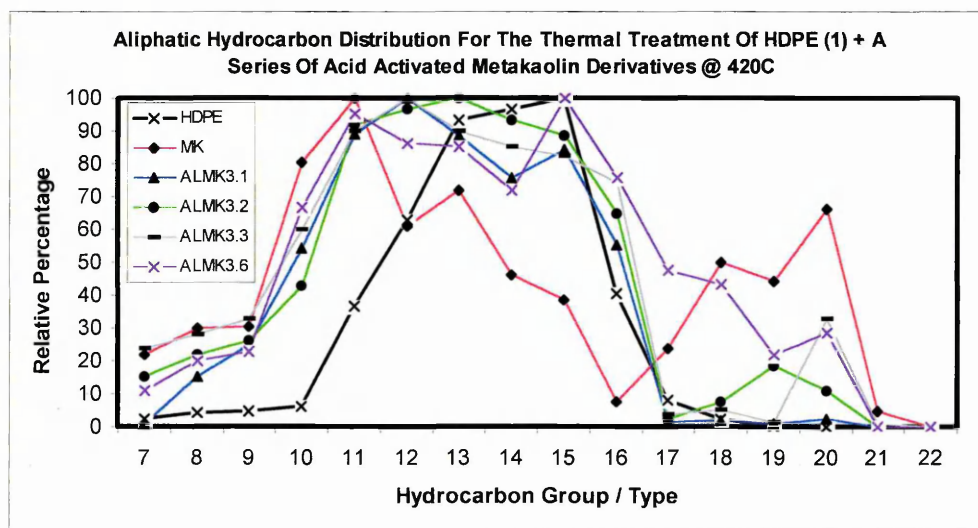


The prominent peaks between 15 and 30 minutes are indicative of n-alkanes, and represent an homologous series over the carbon range $C_{10} - C_{15}$. Further examination of the trace reveals an overall n-alkane distribution over the range $C_7 - C_{21}$, which contrasts slightly with the distribution for HDPE alone. Figure 60 shows that in the presence of any of the acid activated transformation agents, there is a broadening of the linear alkane distributions, with the relative amounts of the short chain ($C_6 - C_{10}$) and the longer chain ($C_{17} - C_{22}$) products increasing relative to the uncatalysed process.

The three peaks for the unsaturated aliphatics were not present after contact with the transformation agent AAMK3.3 (figure 59). The TIC's obtained in the presence of

AAMK3.1 and AAMK3.2 were virtually identical to that shown in figure 59, but the TIC's obtained in the presence of MK and AAMK3.6 exhibited significant differences. In the presence of AAMK3.6 both the number and relative quantities of branched aliphatic products generated (identified from their fragmentation patterns) increased compared to the products over AAMK3.1, 3.2 and 3.3. (Figure 61)

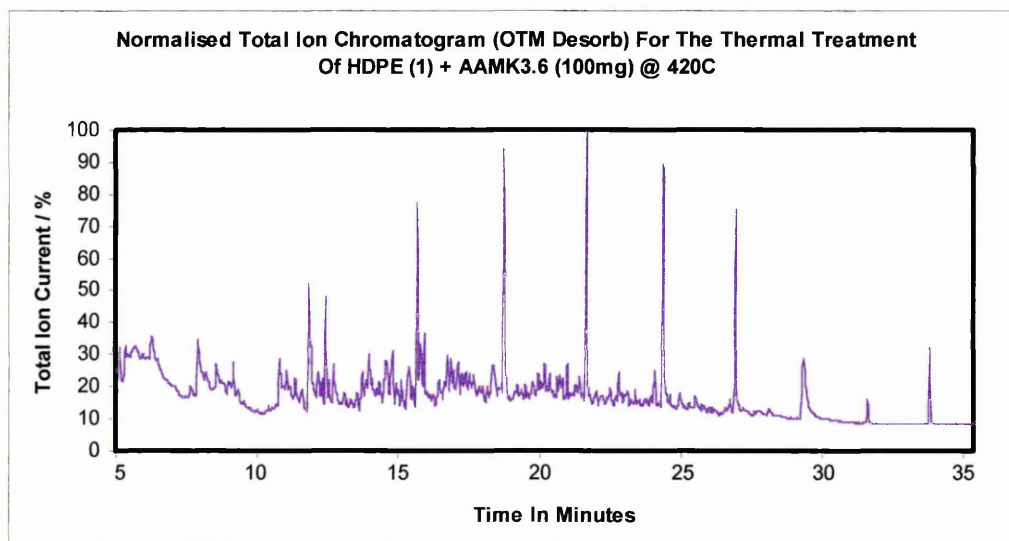
Figure 60 – Aliphatic Hydrocarbon Distribution Achieved Over the AAMK's



Direct protonation of an alkene by a Brønsted acid site is one possible route for the formation of branched aliphatics from linear alkenes. The resultant carbocation is unstable, and it rearranges through a series of methyl group shift reactions, to a conformation in which the formal positive charge is stabilised. Carbon scrambling studies by others suggest that the methyl shift reaction occurs through the formation of protonated cyclopropyl intermediates. The formation of branched aliphatics from linear alkanes is also possible in the presence of strong Lewis acid centres, on which the n-alkanes undergo hydride ion abstraction. Once again, the resultant carbocation is unstable and isomerises to a more stable form.

The distribution of alkanes in the presence of the AAMK's shifts towards lower carbon numbers (except over AAMK3.6), in addition, the distribution was broadened (figure 60). HDPE yields a greater quantity of C₁₅ than any other linear alkane species, whereas over AAMK3.1, 3.2 and 3.3, the most abundant n-alkanes were C₁₁- C₁₂. In all cases, the n-alkane distribution became broader indicating the occurrence of a combination of cracking and recombination reactions.

Figure 61 – nTIC for the Thermal Treatment of HDPE + AAMK3.6 at 420°C

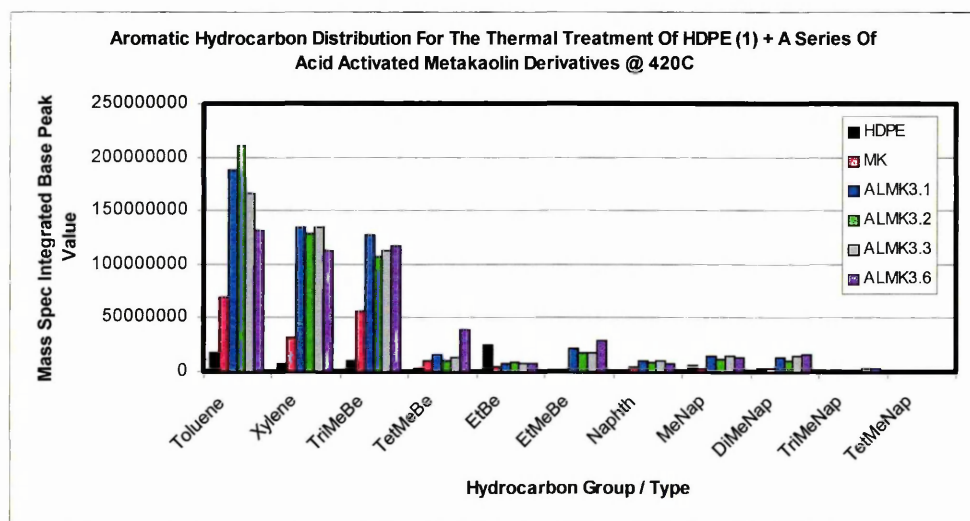


An important aim of this work was to employ the AAMK modified clay minerals as transformation agents to enhance the aromatic content of the hydrocarbonaceous product mixture produced during the pyrolysis of post consumer HDPE plastic waste. Figure 62 shows that relative to HDPE, all of the AAMK's used gave an enhanced aromatic composition in the product gas stream. The sites required to promote dehydrocyclisation reactions were present even after the mildest acid treatment used. This is shown in that AAMK3.1 was as active, as the other transformation agents with respect to the generation of single ring aromatic hydrocarbons. In addition, the activity and or availability of these sites to the feedstock gas molecules was not

affected as the severity of the acid activation process was increased. None of the AAMK's produced significant quantities of polyaromatics.

One plausible explanation of this could be the formation of Brønsted acidic silanol, aluminol and magnesol groups formed by the protonation of exposed Si-O⁻, Al-O⁻ and Mg-O⁻ respectively at loci of bond cleavage in the octahedral sheet as it undergoes structural disruption during acid activation. The apparent dehydrocyclisation capability of metakaolin could be explained in the same way. Structural alteration during the calcination process yields similar co-ordinatively unsaturated structural components within the transformed mineral. Upon rehydration, adsorbed water molecules undergo dissociation, with the resultant protons and hydroxyls being used in the formation of the Brønsted acidic structural sites detailed above.

Figure 62 – Aromatic Hydrocarbon Distribution Achieved Over AAMK's



The complete absence of benzene in the product stream may reflect the relative instability of linear primary carbocations derived from a C₆ alkene compared with the much easier formation of toluene from the more stable secondary carbocation formed from a C₇ alkene. Alkylbenzenes of higher carbon number would also be

produced through a stable, secondary carbocation. The amount of ethylbenzenes produced was significantly lower than seen under thermal conditions alone (figure 62). This result suggests a capability of the transformation agents to effect side chain cracking of alkyl substituted aromatics to yield toluene. While levels of toluene were relatively high in all of the catalysed reactions, when compared to the thermal process, generation of polymethyl substituted single ring aromatics such as dimethylbenzenes (xylenes) and trimethylbenzenes also achieved respectable levels.

The respectable levels of xylene and trimethylbenzenes suggests that catalytic methylation occurred after cyclisation / aromatisation or that structural isomerisation of the protonated alkene occurred prior to cyclisation. The former is more likely because under cracking conditions, alkylaromatics undergo total or partial dealkylation to yield benzene or short chain alkyl aromatics such as methyl or ethyl benzenes. The absence of benzene from the product streams in this case suggests that the latter two products are preferentially formed during dehydrocyclisation reactions involving carbocations originating from linear alkenes of carbon chain length greater than C₇. The methyl substituent on toluene is an activating group which enhances the reactivity of toluene towards electrophilic aromatic substitution reactions compared to benzene. The foregoing suggests that the following mechanism occurs. The first step is the protonation of a linear alkene by strong Brønsted acid sites on the exposed surface of the AAMK, possibly a structural silanol group. The resultant carbocation then undergoes dehydrocyclisation in order to stabilise the positive charge. The resultant alkyl aromatic may undergo side chain cracking to yield toluene. In parallel, a series of cracking reactions produce gas phase alkenes and adsorbed carbocations. The newly formed toluene molecule may undergo an electrophilic aromatic substitution reaction. The adsorbed carbocation attacks the toluene ring system and in doing so eliminates a proton. This free proton is taken up by the site vacated by the adsorbed carbocation, the result

of which is the re-formation of the original Brønsted acid group, the overall process therefore being truly catalytic.

Although the AAMK's are capable of cation exchange, Brønsted acidity attributable to polarised water on, for instance Al^{3+} , is discounted on the basis of dehydration.

With respect to the formation of polyaromatics, none of the materials screened exhibited appreciable activity in this respect. Selectivity towards polyaromatics was low in all cases, with the di and tri methyl substituted derivatives being the most abundant polyaromatic products seen in all cases.

Commercially available acid activated and pillared smectites generally produce more of the trimethylbenzenes than either the xylenes or toluene.^{8,198} Thus, the AAMK's were unusual in that toluene was the preferred product, but they were less active than the commercially available acid activated clays for which direct comparisons were meaningful. For example, freshly prepared acid activated smectites produced similar quantities of xylene, 60% more trimethylbenzene and 50% less toluene.

The observed activity of metakaolin (MK) in the production of aromatics was much higher than anticipated. However, Perissonotto *et al*¹²⁶ reported that MK was able to promote double bond shift reactions in 1-butene to give a 55% conversion. However, the material was found to be inactive towards the dehydration of 2-propanol to yield olefins and ethers. The groups equivalent to AAMK3.2 and AAMK3.6 were able to convert 33% and 70% of 2-propanol respectively, under the same conditions. Perissonotto also reported that their acid activated metakaolin derivatives were active in the isomerisation of 1-butene. Such transformations require relatively strong Brønsted acid sites when compared to that required to promote double bond shift reactions.

Macedo and co-workers¹²⁵ prepared metakaolin by calcination at different temperatures. After leaching these MK's under identical conditions, cumene cracking at 370°C was used to investigate the catalytic activity of their AAMK's. They reported that the activity for cumene cracking followed total acidity of the samples in a volcano type plot which was optimised in samples calcined at 800°C prior to leaching. They also reported a linear relationship between the activity and the sum of the four and five fold co-ordinate aluminium nuclei (determined from ²⁷Al MAS NMR). A number of workers have reported the presence of four and five fold coordinate Al in MK's produced either thermally^{250,251} or through mechanical grinding for extended periods.²⁵² These four and five fold co-ordinate sites are usually removed upon contact with the treatment acid. This was not apparent in the work of Macedo, although they did report that calcination at 550°C for three hours after acid leaching increased the amount of five fold co-ordinate aluminium with respect to the four and six fold co-ordinate species. It is probable that the AAMK's produced in this work also contained four and five fold co-ordinate aluminium because the temperature ramp to the process temperature of 420°C would be sufficient to promote the conversion of post activation six fold species to afore mentioned lower co-ordination environments.

7.2.2. DETERMINATION OF COKE

Table 27 shows the coke values determined for each of the acid activated metakaolin derivatives employed as transformation agents in this investigation.

²⁵⁰ K. J. D. McKenzie, R. H. Meinhold, A. K. Chakravorty & M. H. Dafadar, *Journal of Materials Chemistry*, **6** (1996) 833.

²⁵¹ J-F. Lambert, w. s. Millman & J. J. Fripiat, *Journal of the American Chemical Society*, **111** (1989) 3517.

²⁵² H. Kodama, L. S. Kotlyar & J. A. Ripmeister, *Clays and Clay Minerals*, **37** (1989) 364.

Table 27 - Determination of Coke Content for R1 – R8 Spent Transformation Agents

Sample	Weight %
Metakaolin	1.40
AAMK3.1	1.17
AAMK3.2	1.19
AAMK3.3	1.27
AAMK3.6	1.38

The coke values reported in table 27 are intermediate between pillared and acid activated clays as reported elsewhere.⁸

7.3. SUMMARY OF CATALYTIC BEHAVIOUR

The thermal decomposition of HDPE is a well documented process. Beginning at around 290°C, the degradation proceeds via β scission, the result of which is the formation of a variety of saturated and unsaturated hydrocarbons as outlined in previous sections. This process is known to be non random in nature, and the rate of decomposition is enhanced through increases in temperature. The low levels of aromatic species seen in the HDPE pyrolysis gas are in all probability the result of a series of dehydrocyclisation reactions proceeding via thermal effects.

Under the experimental conditions employed, the transformation agents are fully dehydrated prior to the delivery of the volatile HDPE decomposition products, thus ensuring the accessibility of the available active sites to the feedstock gases. Protonation of feedstock gas alkenes by surface active Brønsted acid sites, yields conjugate bases with formal negative charges on the oxygen atom of the original site.

Such sites thus become available for interaction with short chain gas phase carbocations produced as a result of concurrent cracking reactions. The resultant

adsorbed carbocations are thus available for participation in post dehydrocyclisation catalytic alkylation of aromatic rings.

When the pyrolysis product gases were directed over the transformation agents at temperatures in the range 360 to 420°C, the unsaturated hydrocarbons were transformed into both aromatics and branched aliphatic species. In addition, the linear alkane distribution was broadened and the maximum shifted from C₁₅ for HDPE alone to C₁₁ – C₁₂ over the AAMK'S. Toluene was the most abundant aromatic product followed by xylene and trimethylbenzene. The severity of the activation treatment did not significantly influence the aromatic product distribution.

This latter observation is in contrast to data reported previously by Breen *et al*⁸ for a series of acid activated smectites. These materials gave rise to a systematic decrease in aromatisation behaviour as the severity of their acid activation treatment was increased. In addition, Toluene was never the most abundant mono / poly methyl substituted aromatic formed, with both xylene and trimethylbenzene exhibiting higher levels of production. Such variations in the relative distributions of the methyl substituted aromatics could be attributed to the variable promotion of both disproportionation and transalkylation reactions on the active surfaces of these structurally different minerals.

CHAPTER EIGHT

-Characterisation Results-
Acid Activated Stebno

8. INTRODUCTION

In view of the results determined over R1 (unmodified saponite) and the apparent transformation activity associated with minerals exhibiting isomorphous substitution in their tetrahedral sheets, a decision was made to undertake a systematic evaluation of materials possessing this feature. While saponites are classified as such because of their Al^{3+} for Si^{4+} tetrahedral substitution, as shown previously¹⁴¹, an unfortunate consequence of their high octahedral Mg residency, is that they are readily leached under even the most mild acid activation conditions. As shown with the acid activated metakaolin samples, activation of mineral structures results in materials with enhanced activity in respect of polymer transformation activity. The low tolerance of saponites to activation in mineral acids was taken as an indication that other tetrahedrally substituted minerals may be more suitable for use in this role. Therefore beidellites were selected as a key mineral for investigation. Beidellites are dioctahedral smectites, and while their occurrence in nature is low compared to other smectites several synthetic analogues have been produced, although none have been used in this work. The first to be investigated was a beidellite of Czech origin already well documented in the mineralogy literature.^{129,141}

Stebno is an iron rich beidellite mined in the Czech republic, the Brønsted acidity and associated catalytic activity of which has been demonstrated previously¹⁴¹ using the conversion of 2,3-dihydropyran and methanol to produce tetrahydropyranyl ether as a test reaction. In this investigation a series of acid treated Stebno derivatives were used to convert HDPE pyrolysate gases into potentially useful hydrocarbons, with particular focus being applied to the ability of these materials to execute DHC reactions to yield aromatic species.

Stebno has an octahedral sheet rich in ferric iron, and as a consequence of tetrahedral Al^{3+} for Si^{4+} isomorphous substitution, Stebno has approximately 57% of its

charge character associated with these sheets. Stebno contains about 21% of total iron bound in geothite¹⁹⁸ which is present as an admixture in the <2 μ m fraction. This admixture is readily soluble under the acidic treatment conditions employed and therefore is of no consequence in this work.

8.1 MATERIALS CHARACTERISATION

Analysis was performed using the Synergic Chemical Analysis system. One HDPE pellet (15mg, Aldrich) was placed in the quartz crucible and covered with silanised glass wool (70mg, Phase Separations). Finally, a 100mg portion of the selected transformation agent was spread evenly over the glass wool. Samples were heated at 10°C min⁻¹ from room temperature to 420°C and held isothermally for 1 hour (isothermal process). In the case of this material, a second series of analyses were performed to determine the effect of temperature on the process. In this instance, samples were heated directly from 35°C to 650°C at a rate of 10°C min⁻¹, with no isothermal segment being employed (dynamic process). Note that due to the sampling arrangement within the synergy system, it is not possible to change the temperature of the catalyst and polymer independently, therefore the HDPE degradation mechanisms are temperature dependant.

The resultant 'post run' MS data was interrogated to determine the relative amounts of aromatic hydrocarbons produced over each of the transformation agents under both the isothermal and dynamic temperature regimes pursued.

8.1.1. THERMOGRAVIMETRIC ANALYSIS

These materials have been fully characterised elsewhere,¹⁴¹ therefore extensive thermogravimetric evaluation was not undertaken. However, the relative acidities of materials were determined using to the thermal desorption of cyclohexylamine, (Table 28).

Table 28 – Acidity Data and Treatment Conditions for Acid Activated Stebno Samples

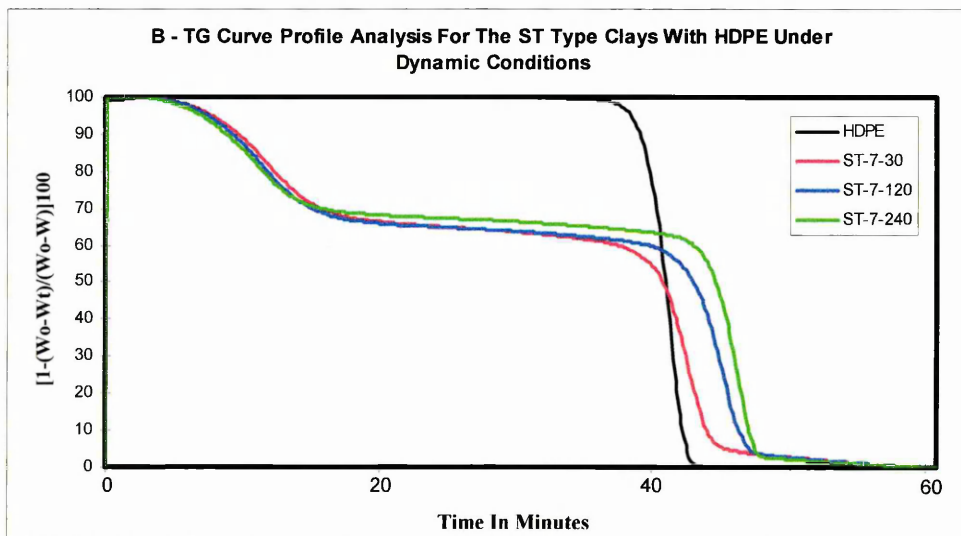
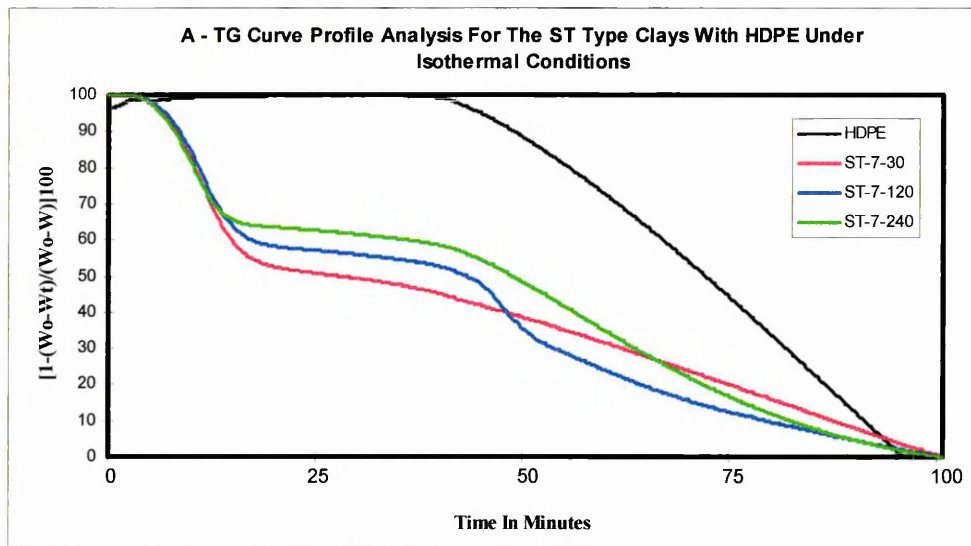
Sample	Treatment Time (mins)	[HCl]/mol dm ⁻³	Acidity mmol/g ⁻¹ clay
ST00	n/a	n/a	n/a
ST30	30	6M	1.05
ST120	120	6M	0.97
ST240	240	6M	0.80

The total acidity of each of the Stebno samples was determined as the number of millimoles of cyclohexylamine-derived products desorbed over the temperature range 290-420°C. These values were normalised to the amount of clay present, and are represented in table 28. The total acidity of these materials decreased as the activation time increased. As highlighted in the previous chapter, acid activated smectites are able to sorb appreciable quantities of cyclohexylamine between their layers, where it can undergo interaction with exchangeable cations. This may have the effect of defining acidity values to these materials which are unrealistic when it is considered that in HDPE transformation applications, these materials are fully dehydrated, and the acidity associated with these cations is no longer available due to layer collapse.

Comparison of the TG plots for each of the transformation agents employed under both isothermal and dynamic conditions can provide information relating to the rate of conversion of the HDPE pyrolysate gases into transformed products. Figure 63 illustrates these results for ST30/120/240 under both isothermal (A) and dynamic (B) conditions.

The weight loss versus temperature curve for the thermal decomposition of HDPE under a linear heating rate (figure 63B) shows that the decomposition was a single step process with onset and end temperatures of 380°C and 470°C respectively during which 98.53% of the initial polymer mass was lost.

Figure 63 – Weight Loss Curves for Stebno Samples (a) Isothermal (b) Dynamic



The traces in figure 63 clearly illustrate the differences which exist between the feedstock gas flow rates for the two processes outlined. In both cases, the curves exhibit three distinct regions. The first low temperature event relates to the dehydration of the clay structures at temperatures below which the thermal decomposition of HDPE begins. The second portion of the curves shows few thermal events and most probably relates to the loss of unstable hydroxyl groups from the clay or loss of those water molecules associated with interlayer and surface and exchange site cations. As polymer decomposition begins, the third portion of the

curves relates to the polymer volatilisation combined with passage of these decomposition products through the catalyst bed.

Comparison of the isothermal and dynamic regimes reveals clear differences in the rate of passage of the feedstock gas through the catalyst bed. In the case of the latter, this event is much more rapid, thus reducing the time during which these gases can be acted upon catalytically by the transformation agents. This reduction in residence time has a negative effect on aromatic hydrocarbon yield.

The third region of each set of curves also suggest differences which provide information pertaining to the transformation process. Under isothermal conditions, this latter portion indicates a gradual reduction in mass, inferring that the pyrolysate gases experience a relatively slow but constant rate of passage through the catalyst bed. Under dynamic conditions, this event is much more rapid perhaps highlighting the fact that the feedstock gas molecules have insufficient residency in the catalyst bed to undergo DHC transformation reactions over the surfaces of the modified minerals applied herein.

8.1.2. ELEMENTAL ANALYSIS

As anticipated, the acid activation of the Stebno base clay results in structural dealumination (Table 29). Clearly, appropriate activation parameters (acid strength, temperature, time) can be selected to control the degree of structural degradation and hence the physical and chemical attributes of the activated products.

Confirmation of potassium as the primary exchange cation is provided in that almost all of this species is removed under the least severe of the acid treatments used. As a consequence of acid activation, clays undergo a reduction in their C.E.C. That

remaining and requiring compensation is fulfilled by either protons from the treatment solution and/or polyvalent cations leached from the octahedral sheet.

Table 29 – XRF Data for the Acid Activated Stebno Samples

%	ST00	ST30	ST120	ST240
Al ₂ O ₃	17.92	16.71	14.79	12.63
SiO ₂	53.85	62.27	68.04	74.02
Fe ₂ O ₃	19.42	15.42	11.99	8.52
MgO	2.78	2.21	1.56	1.11
Na ₂ O	0.04	0.02	0.01	0.01
CaO	0.31	0.00	0.00	0.00
K ₂ O	2.95	0.31	0.25	0.18
Others	2.73	3.06	3.36	3.53
TOTAL	100	100	100	100

The substantial decreases seen for Al, Mg and in particular Fe are indicative of the fact that the parent structure has undergone extensive structural degradation as a consequence of the acid activation treatments employed. As a beidellite, Stebno will also contain >10% Al³⁺ for Si⁴⁺ substitution in its tetrahedral sheet, and as dissolution rates for octahedral and tetrahedral Al are comparable,¹²³ it is expected that this species will also undergo depletion during the activation process.

The results in table 29 suggest that the acid treatments used were successful in producing a range of materials in which the depletion of the octahedral sheet was controlled in a stepwise fashion.

8.1.3. X-RAY DIFFRACTION ANALYSIS

As outlined in the experimental section, these materials were supplied externally and were not available in sufficient quantities to perform meaningful in house XRD analysis, but these materials have been characterised fully by Breen *et al* in previous work.¹⁴¹ X-ray diffraction confirmed the existence of few crystalline impurities, and as

expected, intensity of the d_{001} signal, attributable to ordered layer stacking, is reduced, thereby confirming the loss of structural integrity which accompanies the activation process.

8.2. CATALYTIC ACTIVITY

The principal aim of this work was to establish the transformation behaviour of these materials in respect of their ability to create commercially important aromatic hydrocarbons from the gases evolved during the thermal decomposition of HDPE. In addition, determination of other aspects of the catalytic reforming behaviour of these materials is also an important aspect of the work.

As reported previously by several authors,^{8,9,10,198} the pyrolysis of HDPE yields an homologous series of saturated and unsaturated hydrocarbons, which were shown by this work, and in agreement with previous studies^{8,198} to consist, in order of increasing retention time, of the following species: α,ω -dienes, alk-1-enes, n-alkanes and alk-x-enes.

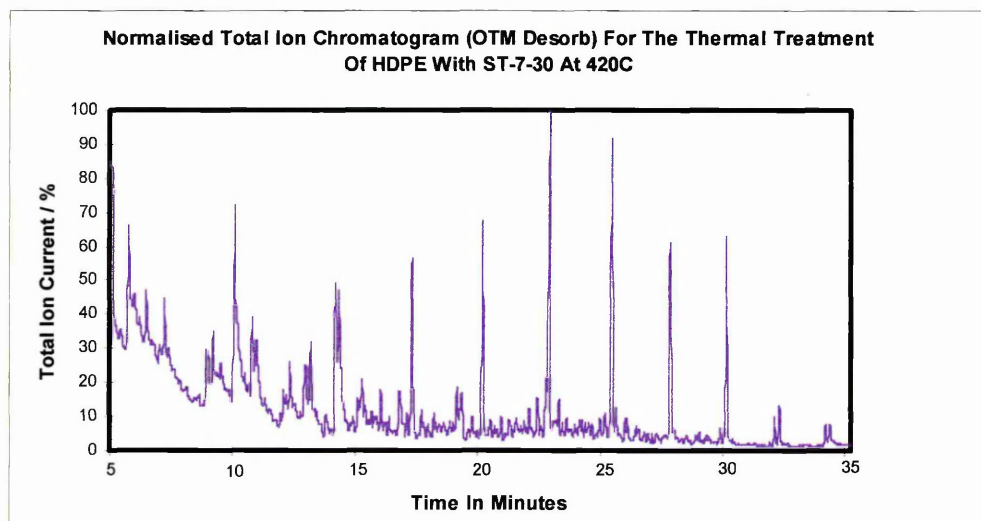
Figure 35 (section 5.1.2, chapter 5) illustrates the normalised total ion chromatogram (nTIC) obtained for the pyrolysis of HDPE at 420°C in an inert nitrogen atmosphere. The characteristic quartets, attributed to the species outlined above, can clearly be seen, although no evidence of branched aliphatic species or even low levels of aromatic products was found, although this observation is in agreement with others.^{8,9,198}

8.2.1 HDPE CATALYTIC TRANSFORMATION ACTIVITY

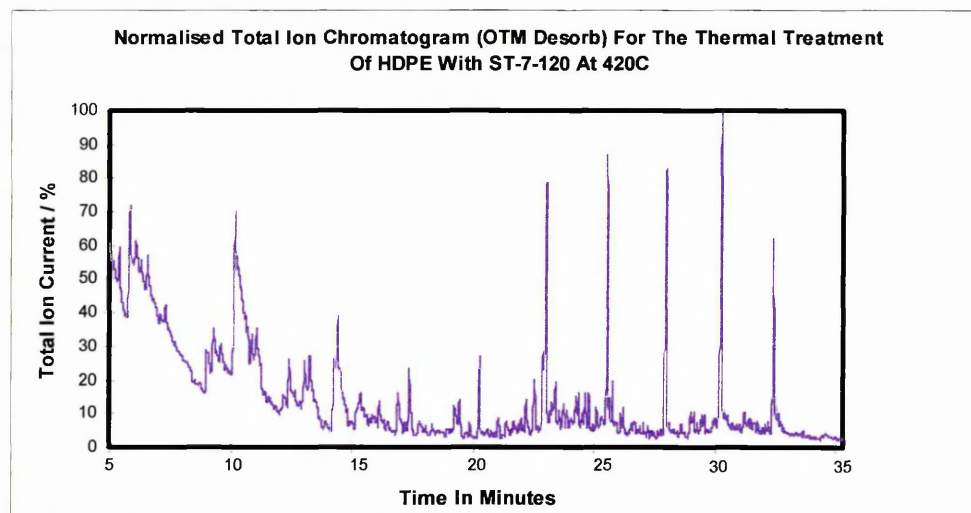
As expected, incorporation of a post pyrolysis transformation agent was successful in altering the chemical composition of the product gas stream, both in terms of the species present and their relative quantities. Figure 64 shows a nTIC recorded for a

TG-OTM-GC-MS run carried out in the presence of ST30 as the post pyrolysis transformation agent operating under an isothermal temperature regime. The trace retains the characteristic n-alkane distribution seen with HDPE alone, although evidence supporting the presence of unsaturated species is absent.

Figure 64 – nTIC for the Thermal Treatment of HDPE + ST30 (Isothermal Conditions)



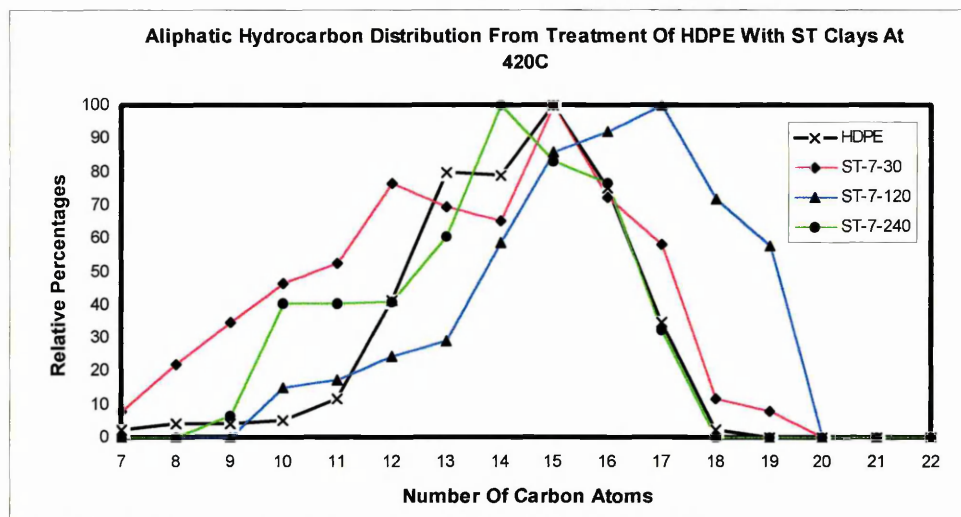
This trace is significantly different to those recorded for an identical procedure executed in the presence of ST120 or ST240 as the transformation agent, the traces for which are markedly different to that given above for the lessor treated analogue. As illustrated in figure 65, there is an obvious disruption in the n-alkane distribution achieved over ST120 under isothermal conditions. ST240 presented similar data.



This apparent shift towards a predominance of n-alkanes with carbon chain lengths greater than that seen in the uncatalysed process contrasts significantly with the pillared clays and acid activated metakaolins, both of which exhibited a shift towards shorter carbon chain lengths relative to HDPE alone. Analysis of the relative quantities of these various n-alkanes confirms this visual observation (figure 66). In the presence of ST120, there is a shift towards n-alkanes with carbon chain lengths greater than recorded for the uncatalysed process. Direct comparison of the actual amounts of these species, determined from the raw data for the catalysed and uncatalysed processes, confirms that the longer chain alkanes are unaltered by the transformation process, while the shorter chain species $<C_{16}$ undergo a severe reduction. Such observations are indicative of the occurrence of cracking reactions which are selective to alkanes in the chain length range $C_9 - C_{16}$. The limited alteration of the actual quantities of the $>C_{16}$ alkanes suggests that recombination reactions are not in operation.

The three peaks for the unsaturated aliphatics were not present after contact with any of the transformation agents derived from Stebno and none of the acid treated Stebno clays were active in the generation of branched aliphatic products.

Figure 66 – Aliphatic Hydrocarbon Distribution Achieved Over ST Clays (Isothermal)



Again, in contrast to the results for the pillared saponites and acid activated metakaolins, these materials did not significantly broaden the aliphatic hydrocarbon distribution to any extent, although there are slight shifts away from the HDPE distribution pattern. This suggests that post cracking, alkanes passing over ST120 and ST240 are not involved in hydride abstraction processes to yield product alkanes in the range $C_6 - C_{10}$ which are efficiently trapped employing the methodologies used herein. The yield of these alkanes, which have chain lengths shorter than the those of the starting material, but longer than those normally associated with the light gases ($C_1 - C_5$) is not greatly enhanced. This leaves two possibilities:

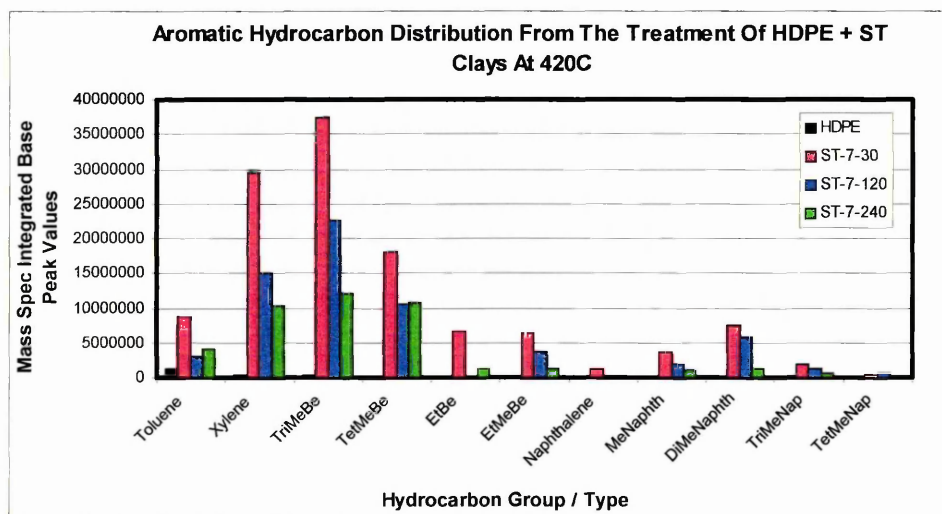
1. The cracking reactions are excessive, resulting in $C_1 - C_5$ carbocations, which following hydride abstraction are released into the product gas stream as light gases which are not detected using the analytical methods employed in this work.
2. The second possibility relates to a series of reactions which occur over the surface of transition metal impregnated zeolites which are active in the dehydrocyclopolymerisation of light gases. Biscardi and Iglesia²⁵³ have

²⁵³ J. A. Biscardi & E. Iglesia, *Catalysis Today*, **31** (1996) 207 – 231.

demonstrated that Ga loaded ZSM-5 forms C₆+ aromatics from propane precursors. The Ga is believed to function as a hydrogen recombination centre through its ability to operate as a Lewis acid site in its dehydrated form. Similarly, Guisnet and Gnep²⁵⁴ demonstrated that other zeolitic frameworks were suitable matrices for similar reactions. More recently, Xu and Lin²⁵⁵ have shown that Mo loaded ZSM-5 is able to catalyse the non oxidative formation of aromatics from lower light gases, and in particular methane.

The likely occurrence of dehydrocyclopolymerisation reactions can be determined by establishing the aromatic output over each of the modified Stebno clays. Figure 67 illustrates the relative aromatic yield over each of these materials.

Figure 67 – Aromatic Hydrocarbon Distribution Achieved Over ST Clays (Isothermal)



Once again, the absence of benzene is indicative of the relative instability of a linear primary carbocations derived from a C₆ alkene compared with the much easier formation of toluene from the more stable secondary carbocation formed from a C₇ alkene.

²⁵⁴ M. Guisnet & N. S. Gnep, *Catalysis Today*, **31** (1996) 275 – 292.

²⁵⁵ Y. Xu & L. Lin, *Applied Catalysis A: General*, **188** (1999) 53 – 67.

None of the materials screened exhibited appreciable activity in the formation of polyaromatic species. The di and tri methyl substituted derivatives were the most abundant polyaromatic products seen in all cases.

These materials share a common feature with commercially available acid activated smectites in that they generally produce more of the trimethylbenzenes than either the xylenes or toluene.⁸

It is of particular interest to note that the DHC activity of these materials diminished as the extent of their acid activation increased. This pattern can be shown to correlate directly with the acidity values determined for these modified minerals (table 28), and suggests that the ability to form monomethyl substituted aromatics may be related to the formation of small pores and high relative acidities, both of which are installed as a consequence of mild activation of suitable minerals.

Again, acidity arising from the polarised hydration spheres of exchange site cations is unlikely on the basis of dehydration of these species at the operating temperatures.

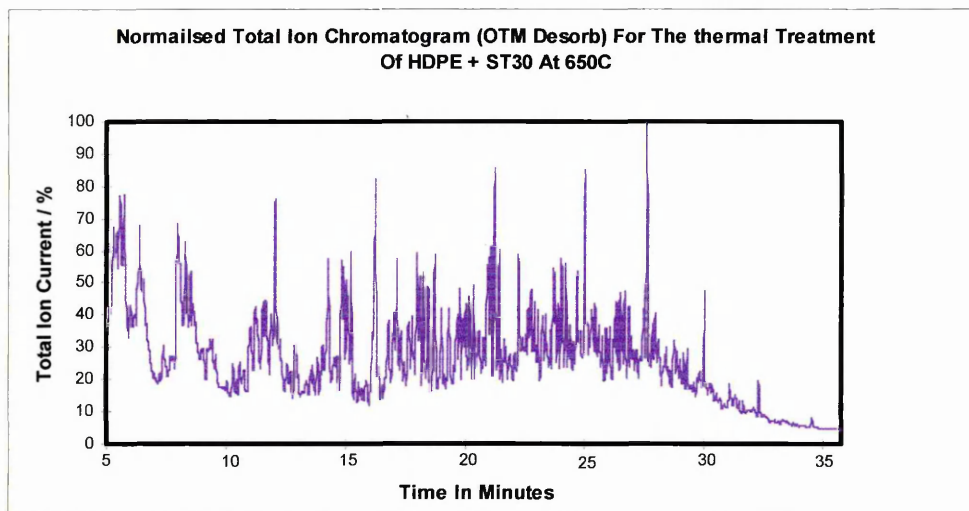
Another possible explanation may relate to the availability of those sites responsible for the catalytic promotion of the DHC reactions which yield aromatic hydrocarbons. As outlined in chapter two (2.8.2), one of the primary consequences of acid activation is an increase in surface area and acidity arising from edge attack mechanisms operating during the activation process. Such mechanisms promote the formation of Brønsted acidic silanol, aluminol and magnesol groups as the mineral structure undergoes degradation from the outside inwards.⁹⁷ The formation of these groups may account for the increase in acidity observed in the activated materials relative to the parent clay. However, as the extent or duration of the treatment process is extended, these groups will be lost, as the structural ions from which they

are formed are leached from the mineral matrix. Nevertheless, they will be replaced by similar groups formed from other structural octahedral resident cations located more centrally within the mineral arrangement. The apparent loss of acidity associated with increases in the harshness of the activation process may be attributable to the poor accessibility of these sites to the probing species. This may arise due to the location of these groups within the mineral structure, whereas, as opposed to being located on the edge sites of the structure where they are freely available to both the probing species and the feedstock gas molecules.

Another explanation which may account for the apparent loss of acidity in the more severely treated samples, resulting in an associated loss of DHC capability, is the possible passivation of the mineral structure.¹²⁹ This presents a physical barrier to the interaction of feedstock gas molecules with the acidic sites thereby causing a reduction in the ability of these samples to effect the formation of alkyl substituted aromatic species. In addition, passivation lowers the level to which the clays become delaminated during its activation stage. The occurrence of intralayer silanol crosslinking limits separation of tactoid layers, thus limiting access to the potentially catalytically active siloxane bridges believed to be resident on these surfaces.

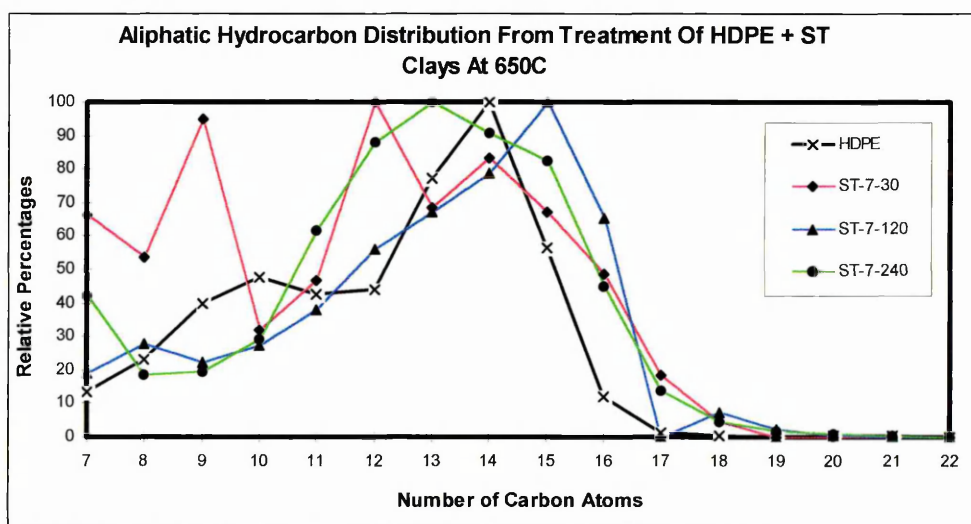
The data for the transformation activity of these materials under dynamic conditions show significant differences to that seen for the same materials under isothermal (includes dynamic heating segment) conditions. Figure 68 shows the nTIC recorded when ST30 was employed as the transformation under dynamic conditions upto 650°C.

Figure 68 – nTIC for the Thermal Treatment of HDPE + ST30 upto 650°C (Dynamic)



Direct comparison of the trace above with that in figure 64 clearly demonstrates that the activity of this material is substantially different in that the distribution and relative number of products are greater under the dynamic conditions than under isothermal treatments. Figure 69 illustrates that there was very little change in the aliphatic hydrocarbon distribution data determined for this sample/temperature combination.

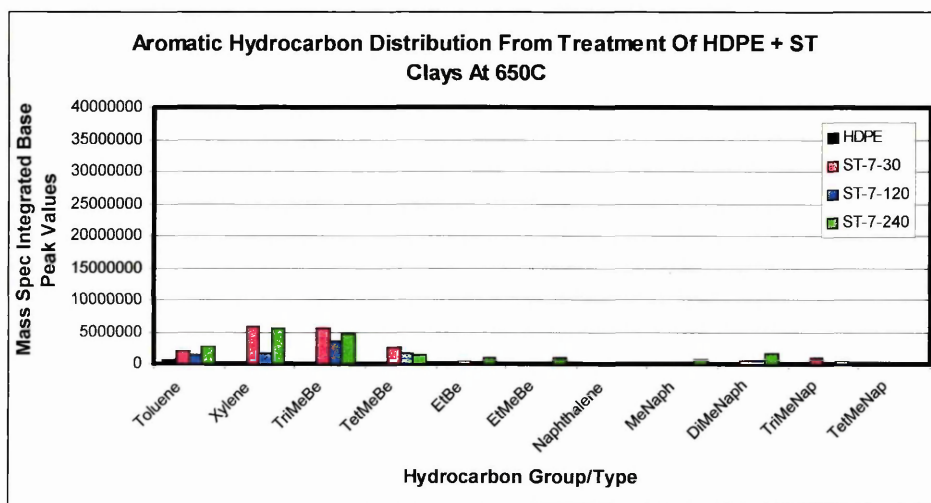
Figure 69 – Aliphatic Hydrocarbon Distribution Achieved over Stebno Clays (Dynamic)



This could be accounted for on the basis of feedstock gas delivery rate to the catalyst surface. As shown in figure 63B, this passage is rapid, which may indicate that the residence time is insufficient for catalytic cracking reactions to occur.

The apparent increase in the number of individual products identified at higher temperatures was shown to arise from the generation of branched aliphatic species. The formation of aromatic species was not instantly obvious from a simple visual examination of the trace, and so the appropriate analysis was performed (Figure 70) Note that for direct comparison purposes, this figure is plotted with the same y scale as that for the same analysis under isothermal conditions (figure 67).

Figure 70 – Aromatic Hydrocarbon Distribution Achieved for Stebno Clays (Dynamic)

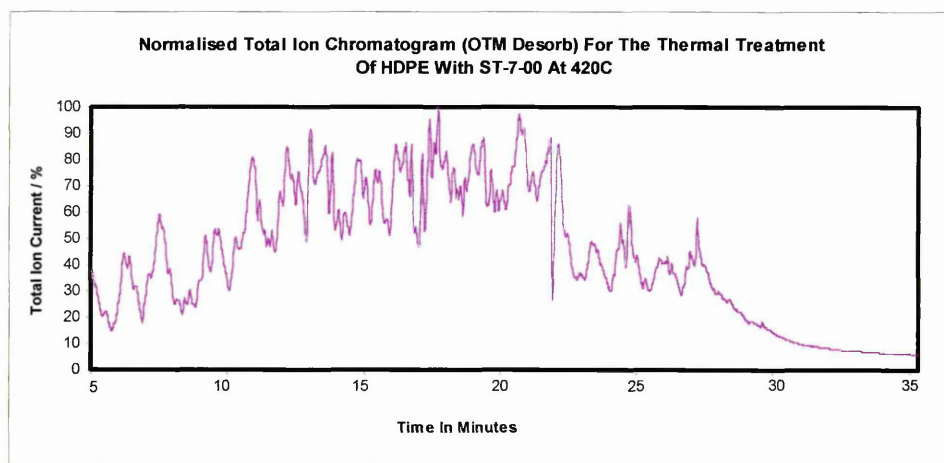


Clearly, DHC activity is greatly reduced under dynamic conditions. Aromatic yields are extremely low, and no real pattern emerges regarding the extent of acid activation and aromatisation behaviour during this higher temperature process. It is highly plausible that any aromatics formed are the result of thermally induced DHC reactions, and that DHC transformations attributable to the modified clays are of little consequence in this respect under dynamic conditions.

Clearly, rapid transit of the feedstock gas molecules through the catalyst bed has the effect of reducing aromatic yield in favour of branched alkanes. These findings are in agreement with Uemichi *et al*²⁰ where an aromatic/aliphatic ratio temperature dependence was also noted. However, light gas formation is also enhanced when using high temperature regimes to promote polymer degradation.²⁰

Returning to the isothermal conditions, ST00 was employed to determine the ability of the unmodified clay, with tetrahedral substitution, to promote DHC, skeletal isomerisation and catalytic cracking reactions. Figure 71 illustrates the nTIC recorded for the procedure carried out under isothermal conditions in the presence of ST00. This process allowed for comparison of the resultant data to that recorded in the presence of R1 (unmodified saponite) for the same transformation process.

Figure 71 nTIC for the Thermal Treatment of HDPE + ST00 (Isothermal Conditions)



Evidently, the trace does not resemble those for HDPE alone or those recorded when using acid activated Stebno derivatives as the transformation agent. Mass spectrometric examination of the trace confirmed that unsaturated materials were still present, although they were different in nature to those found in the uncatalysed reaction process, consisting of species with low level branching and different double

bond positions. This suggests that the unmodified mineral is active in promoting double bond shift reactions, and to a lesser extent, the skeletal isomerisation of some of the feedstock gas molecules. There was no evidence for the formation of any cyclic species, and the n-alkane distribution remained unchanged. The double bond shift and skeletal isomerisation reactions noted here are Brønsted catalysed reactions and may result as a consequence of the beidellitic character of this mineral. Formation of Brønsted acidic surface siloxane bridges is possible due to the Al³⁺ for Si⁴⁺ isomorphous substitution in the tetrahedral sheet of this mineral. These surface species may be of sufficient acidity to promote these types of reaction.

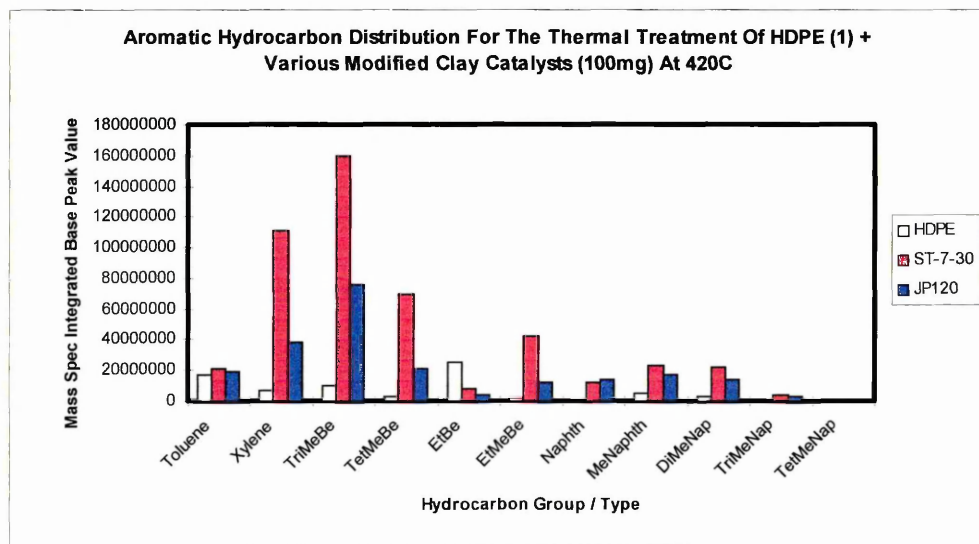
By way of validating the decision to study those materials exhibiting tetrahedral substitution as the most effective candidates for employment in the role of polymer transformation, a secondary study was performed in which ST30, the most active material in the Stebno range (in terms of DHC behaviour) was analysed alongside an acid activated clay described in the literature^{141,247}, and having been shown to possess similar physicochemical properties, including acidities, to those of ST30.

The material chosen was Jelsový Potok, a hydrothermal aluminium rich montmorillonite mined in the Kremnica mountains in the Czech Republic. The Brønsted acidity and associated catalytic activity of this material, along with its acid activated counterparts has been demonstrated previously²⁴⁷ using, respectively, the desorption of cyclohexylamine and the conversion of 2,3-dihydropyran and methanol to produce tetrahydropyranyl ether as a test reaction. JP120 (activated for 120mins in HCl at 95°C) was chosen as it most closely resembled ST30 predominantly in respect of acidity. Figure 72 illustrates the result of this investigation.

Clearly, the production of single ring aromatics over JP120 is much lower than seen over ST30 under identical conditions. Examination of the nTIC for the JP120 catalyst

process (not shown) suggests that the material is an excellent aromatisation catalyst, as the signals for such products dominate the trace. The data in figure 72 confirms that the visual suggestion of enhanced aromatisation behaviour over JP120 is actually due to a disruption in the n-alkane distribution in the product gas stream, and not to elevated levels of DHC activity.

Figure 72 – Aromatic Hydrocarbon Distribution Achieved Over ST30 & JP120



This data clearly provides evidence highlighting the potential advantage of employing modified smectites with tetrahedral substitution. However, in order to confirm these observations, and in the absence of a suitable series of materials, a range of modified montmorillonites (SWy-2) were generated in house and analysed to determine their activity in this transformation role. The results of these investigations are given in chapter 9.

8.2.2. DETERMINATION OF COKE

Table 30 shows the coke values determined for each of the acid activated Stebno derivatives employed as transformation agents in this investigation.

Table 30 - Determination of Coke Content for Stebno Spent Transformation Agents

Sample	Weight % (Isothermal)	Weight % (Dynamic)
ST30	1.0	0.6
ST120	1.0	0.4
ST240	0.9	0.4

The coke values reported in table 30 are low compared to those quoted for other pillared and acid activated clays as reported elsewhere.⁸ In addition, they are also comparatively low in contrast to the values determined for the acid activated metakaolin samples detailed in the previous chapter. Likewise, these values are particularly low when compared to the 7% reported for the zeolite US-Y,²⁵⁶ 6% over silica alumina²⁵⁷ and upto 19% on Ca-exchanged zeolite-X²⁰ when the catalyst was ground together with the polymer. Note should be made of the fact that in the cases detailed, polymer / catalyst ratio's differed to those used here.

Secondly, the relative acidity of each of these materials decreased as the severity of the acid treatment increased. This behaviour is mirrored to some degree by the coke deposition data, in which the more extremely activated samples exhibited lower levels of coke deposition, although only slight differences were apparent. This contrasts significantly with the pillared clays in which those materials with higher levels of acidity were subject to lower levels of coke deposition. This may infer that the type of acidity found in the pillared clays is different in nature to that found in the acid activated materials. As the latter can be shown to present predominantly Brønsted acidity, it may be the case that as postulated, the acidity of pillared clays is heavily biased in favour of Lewis acidity.

²⁵⁶ Y.-. Lin, P. N. Sharrat, A. A. Garforth & J. Dwyer, *Thermochimica Acta*, **294** (1997) 45.

²⁵⁷ Y. Ishihara, H. Nanbu, T. Ikemura & T. Takesue, *Fuel*, **69** (1990) 978.

CHAPTER NINE

-Characterisation Results-
Acid Activated SWy-2

9. INTRODUCTION

SWy-2 is a Na montmorillonite mined in Crook County, Wyoming, U.S.A. The material was subjected to acid activation in 6M hydrochloric acid for selected time intervals. The materials were investigated to determine their relative effectiveness as transformation agents for the conversion of HDPE pyrolysate gases into potentially useful hydrocarbons, and in particular aromatic species. Comparisons will be drawn to the materials screened previously and those presented in the later chapters.

9.1 MATERIALS CHARACTERISATION

Analysis was performed using the Synergic Chemical Analysis system outlined previously operating in the TG-OTM-GC-MS configuration. One HDPE pellet (15mg, Aldrich) was placed in the quartz crucible and covered with silanised glass wool (70mg, Phase Separations). Finally, a 100mg portion of the selected transformation agent was spread evenly over the glass wool. Samples were heated at 10°C min⁻¹ from room temperature to 420°C and held isothermally for 1 hour.

The resultant 'post run' MS data was analysed to determine the relative amounts of aromatic hydrocarbons produced over each of the transformation agents through the integration of base peak signals, identified through known fragmentation pathways for the type of ionisation employed. Attention was also paid to the effect on the n-alkane distribution present in the product gas stream after passing over the acid activated SWy-2 derivatives.

9.1.1. THERMOGRAVIMETRIC ANALYSIS

Thermogravimetric analysis was performed to determine the effect of the various acid activation treatments on the thermal behaviour of the activated SWy-2 derivatives (Table 31).

Table 31 – Weight Loss Data for Acid Activated SWy-2 Samples

Sample	Treatment Time (H)	[HCl]/mol dm ⁻³	Weight Loss to 800°C / wt%
SWy-2-0A	n/a	n/a	10
SWy-2-2A	2	6M	12
SWy-2-4A	4	6M	15
SWy-2-6A	6	6M	18
SWy-2-8A	8	6M	21

The weight loss below 200°C was variable, and increased despite a corresponding decrease in the cation exchange capacity of the material as a function of the severity of the acid activation process. These weight losses are associated with dehydration of the mineral matrix through the loss of sorbed water associated with interlayer and surface exchange site cations.

The weight loss above 200°C varied in a systematic manner, but was not as marked and occurred at a constant rate thus providing no features in the derivative thermogram. As with the metakaolin samples, the increase in the loss of sorbed water at temperatures <200°C can be attributed to an increase in available surface area for water adsorption following acid activation.

9.1.2. ELEMENTAL ANALYSIS

As anticipated, the acid activation of SWy-2 results in structural dealumination (50% in SWy-2-8A) in addition to losses of both Mg and Fe from the octahedral sheet (Table 32). In keeping with previous observations, selection of appropriate activation parameters (acid strength, temperature, time) allows control of the degree of structural degradation and hence the physical and chemical attributes of the activated products.

The relatively low levels of both magnesium and iron suggest that the octahedral residency of the SWy-2 structure is predominantly aluminium, thereby confirming that the parent mineral is a montmorillonite (dioctahedral smectite). The level of isomorphous substitution yields a material with a low layer charge, and hence low levels of exchangeable Na and Ca.. In particular, table 32 indicates that all Ca²⁺, Na⁺ and some of the Mg²⁺ has been removed from the samples with only low level activation (SWy-2-2A)

Table 32 – XRF Data for the Acid Activated SWy-2 Samples

%	Swy-2-0A	SWy-2-2A	SWy-2-4A	SWy-2-6A	SWy-2-8A
Al ₂ O ₃	20.31	18.80	16.39	13.41	11.04
SiO ₂	68.35	74.68	77.78	81.68	84.79
Fe ₂ O ₃	4.08	3.33	2.86	2.33	1.87
MgO	2.83	2.04	1.72	1.36	1.07
Na ₂ O	1.75	0.29	0.30	0.30	0.30
CaO	1.72	0.05	0.09	0.06	0.06
K ₂ O	0.69	0.62	0.64	0.64	0.65
Others	0.27	0.19	0.22	0.22	0.22
TOTAL	100	100	100	100	100

The results indicate that the treatments selected were successful in achieving controlled levels of dealumination. Similarly, Na and Ca (the resident interlayer cations) were also seen to undergo depletion, although some Na remained even after the most severe of treatments. Ca was effectively removed in totality. Residual levels of Fe and potassium are likely to be the result of inclusions which are either acid insoluble or resistant to attack under the conditions employed. Such hypothesis will be confirmed by XRD analysis. Indeed, there is some evidence from the XRD data for these samples (figure 73) that the residual Na may be present as albite (28.05°2θ) or feldspar (27.94°2θ) impurities.

9.1.3. X-RAY DIFFRACTION ANALYSIS

Figure 73 presents the XRD traces obtained for the entire series of acid activated SWy-2 derivatives in addition to that for the parent mineral. The traces clearly illustrates the intense characteristic d_{001} reflection indicative of smectites at 2θ values of around 12.29° for the SWy-2-8A trace (purple). The traces presented in figure 73 are slightly misleading as they appear to suggest that the d_{001} reflection is subject to an increase in intensity as the severity of the activation treatment is increased. This arises as a consequence of the technique used to stack the individual traces. Examination of the figure confirms that progression through the series, d_{001} intensity decreases in favour of the enhanced predominance of other signals in the traces relating to mineral impurities, notably the albite and feldspar inclusions identified already.

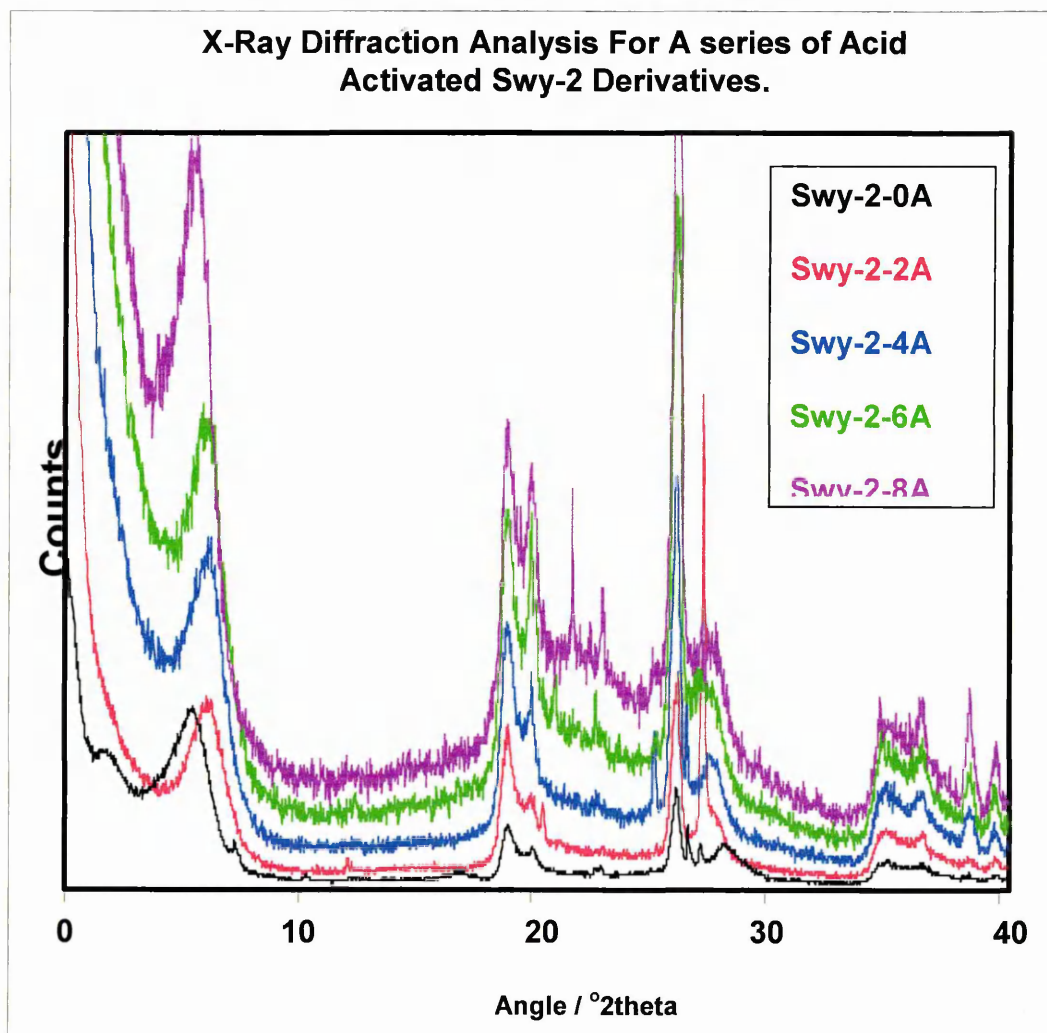
All traces subsequent to that for SWy-2-0A show a slight shift in the actual position of the primary d_{001} reflection for the smectite structure. The parent mineral exhibits a reflection at a 2θ value of 6 (14\AA) which is seen to shift to slightly lower spacings following even the least severe of the activation treatments. This may be a consequence of the removal of the resident interlayer exchange cations, and thus a reduction of the primary electrostatic forces holding the mineral structure together.

Figure 73 provides little evidence of serious delamination of the tactoidal assemblage of SWy-2. In addition, whereas acid activation has been shown previously to be effective in increasing the amorphous character of clays, figure 73 offers little evidence for an increase in the amorphous nature of the activated products in. This infers that while the mineral has been elementally depleted, structurally, it remains virtually in tact.

These materials do not give rise to a distinct broad hump in the range $16-32^\circ 2\theta$, which was observed in the metakaolin traces. This feature was seen to increase with

the severity of the activation treatment, confirming the loss of structural integrity and the presence of an amorphous product.²⁴⁷ The absence of this feature in the traces illustrated in figure 73, and the retention of intensity associated with the d_{001} reflection may suggest that while the activation treatments selected were successful in promoting dealumination of the parent mineral, delamination of the mineral tactoid was not achieved to any significant degree.

The trace for SWy-2-2A contains an intense signal at a 2θ value of 31.72 (2.82Å) which can be accounted for on the basis of NaCl deposition on the surface of the activated product. Confirmation of this observation can be made by reference to the secondary signals at 2θ values of 27.37 (3.26Å) and 45.48 (1.99Å) which are also characteristic of this salt. The natural form of SWy-2 is a predominantly Na but also Ca^{2+} exchanged mineral. Liberation of these ions during the activation process and their subsequent combination with Cl anions provided by the treatment acid account for this observation. This by-product was successfully removed by washing the activated minerals in deionised water according to the method outlined in the experimental section.



9.1.4. FTIR ANALYSIS (DRIFTS)

The exposure of clay mineral surfaces to vapour phase pyridine results in a diverse range of interactions which reflect the availability of the lone pair of electrons on the nitrogen atom of the pyridine ring system.²¹⁰ Infra red spectroscopic investigation of pyridine treated acidic solids can readily distinguish between Brønsted and Lewis acid sites on the surface and provide semi quantitative estimates of the number of each type.

There are a number of difficulties associated with probing the available acidity of swelling minerals through exposure to vapour phase bases such as pyridine. In this work, and in the absence of specialised equipment for in situ dosing, the mineral under investigation is exposed to pyridine vapours at ambient temperature. This allows the assumption to be made that in addition to the freely available surface acid sites, the probe molecule may also gain access to the gallery region of the mineral tactoid. During the desorption process, probe species are lost from these sites. However, in the case of the work presented here, transformation activity is executed at 420°C, a temperature at which swelling minerals are dehydrated, and as such, the acid sites within the gallery region are not available for participation in hydrocarbon transformation reactions. Therefore, using the probe technique employed here, a definitive determination of the types of acid sites available at the transformation temperatures can not be made. In addition, structural changes during dehydroxylation may provide or regenerate structural acid sites, and thus the surface acidity of swelling minerals at the transformation temperatures used here must be considered as dynamic.

The room temperature DRIFTS spectrum for pyridine saturated SWy-2-4A (Figure 74) exhibits bands due to Brønsted bound pyridine at 1632 and 1537cm⁻¹ and for Lewis bound pyridine at 1612cm⁻¹ together with a shoulder on the higher wavenumber side

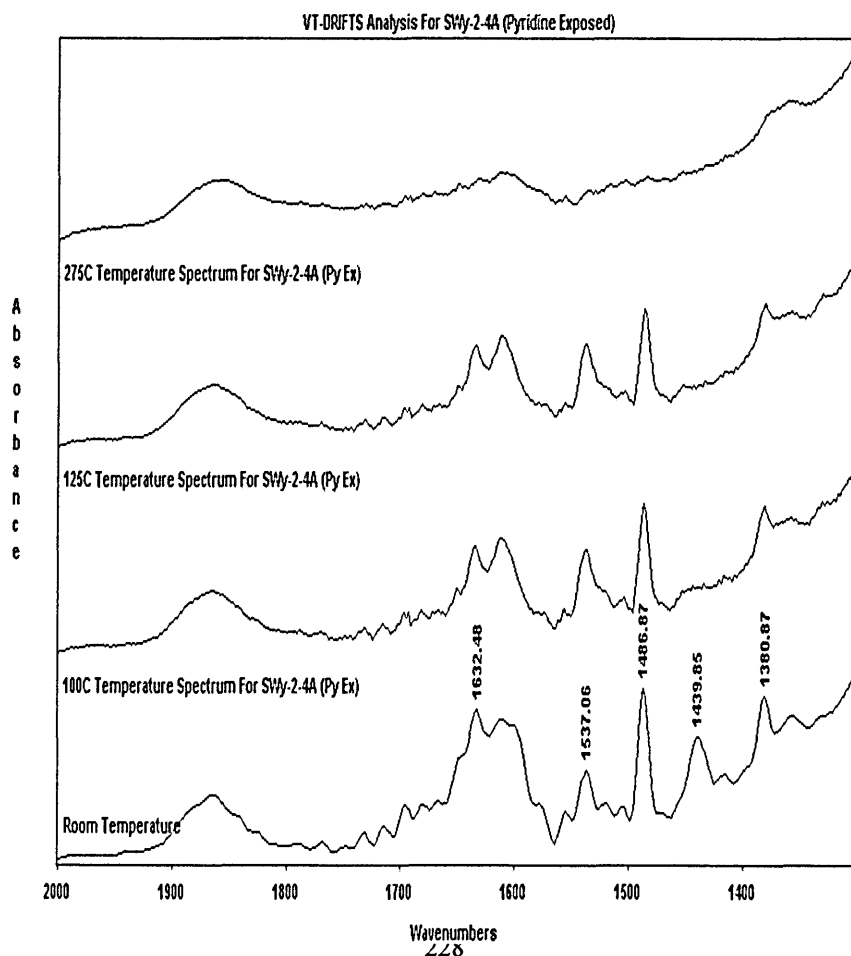
of the 1439cm^{-1} band. The 1439cm^{-1} band in combination with the 1596cm^{-1} band can be assigned to hydrogen bonded pyridine, HPYR.²⁴⁸ The 1486cm^{-1} band is attributable to pyridine bonded to both Brønsted and Lewis acid sites, although the Brønsted bound species is known to contribute a greater intensity. Increasing the sample temperature to 100°C completely removes the bands at 1439 and 1596cm^{-1} attributed to hydrogen bonded pyridine, thereby indicating a complete loss from the surface of the mineral of hydrogen bonded pyridine. The intensity of the 1537cm^{-1} band increased and the width decreased as the hydrogen bonded pyridine was removed. This may suggest that some of the hydrogen bonded pyridine actually forms a hydrogen bond with the proton on the Brønsted bound pyridine as observed in Al^{3+} exchanged²⁴⁹ and acid treated smectites.²¹⁰ As seen with the metakaolin samples, the strong 1537cm^{-1} band seen at room temperature suggests that there is some Brønsted bound pyridine that can not form hydrogen bonds with excess pyridine due to the effects of surface chemistry or topography of the mineral.

At temperature above 125°C the bands for hydrogen bonded pyridine had completely gone, and between 125°C and 275°C , the intensity of the bands for Brønsted bound pyridine had significantly reduced as had those bands for Lewis bound pyridine. By 275°C , and at the transformation temperature of 425°C (not shown), there was little evidence of pyridine remaining on the sample, although at the lower temperature, there were weak contributions from Brønsted bound pyridine at 1486cm^{-1} and 1632cm^{-1} . As outlined previously, this apparent loss of Brønsted acidity can be explained on the basis of dehydration effects. The apparent loss of Lewis acidity may be a consequence of the sampling technique employed. Samples for analysis were exposed to pyridine at room temperature, allowing for interaction of pyridine molecules with sites, particularly in the interlayer, which may not be accessible at the transformation temperatures employed. Dehydration of smectites during heating can allow for the evolution of Lewis acidity through loss of hydration

sphere water and subsequent exposure of surface exchange site charge compensating cations.

By 425°C, only traces of Brønsted acidity are apparent. Once again, such observations are not inkeeping with the apparent catalytic activity of these materials, and their ability to carry out dehydrocyclisation reactions using alkene feedstocks. One plausible explanation to account for this observation may be the mechanism by which smectites dehydroxylate, described elsewhere⁸² and detailed in chapter three. Liberation and subsequent recombination, to form water molecules, of hydroxyl groups from the octahedral sheet provides a means by which dehydroxylated surface silanols can act as temporary holding sites for the evolved water, thereby mimicking the behaviour of surface silanol, aluminol and magnesol groups.

Figure 74 – VT – DRIFTS Spectra for Pyridine Treated Acid Activated SWy-2 Samples



The VT-DRIFTS spectra for the other pyridine treated samples revealed similar behaviour in that the Lewis acid sites predominated at the reaction temperature of >400°C.

9.2. CATALYTIC ACTIVITY

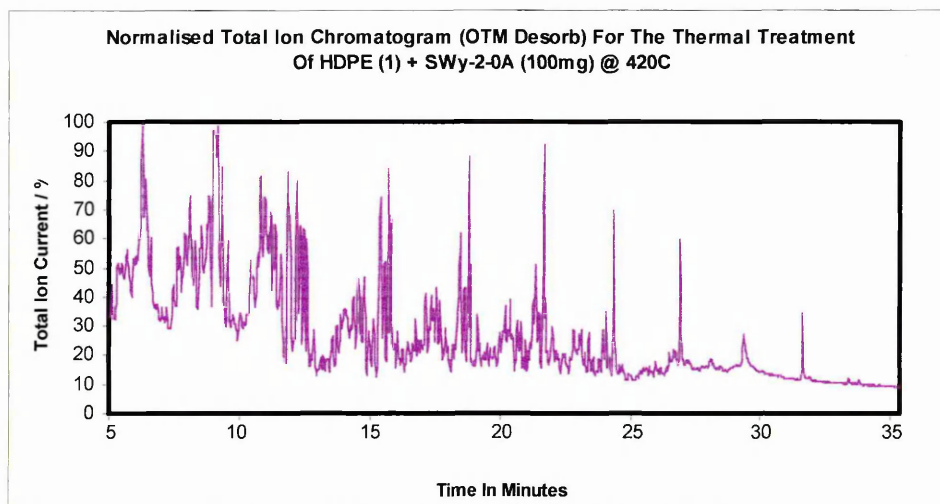
In keeping with previous studies, these activated materials were used as transformation agents to promote catalytic transformation of the thermally generated off gases from HDPE pyrolysis.

9.2.1 HDPE CATALYTIC TRANSFORMATION ACTIVITY

It was found that the acid activated SWy-2 derivatives were able to convert the HDPE pyrolysate gases into commercially important hydrocarbons including aromatics and branched aliphatics.

These materials showed that changing the severity of the activation treatment has the effect of altering the aromatic product selectivity. It should be noted that in none of the ensuing cases was the DHC activity of these materials greater than seen previously for the acid activated Stebno and Jelsovy Potok samples.

A sample of the non activated parent clay was run for comparative purposes. In contrast to the ST material presented previously, SWy-2-0A (non activated product) did present some DHC activity which ran at approximately 60% of the cyclisation activity of the most active SWy-2 derivative. Figure 75 illustrates an nTIC recorded for a TG-OTM-GC-MS run carried out in the presence of SWy-2-0A as the post pyrolysis transformation agent.



Clearly, this trace contains evidence for the presence of unsaturated hydrocarbons in the product gas stream, and this was confirmed during analysis of the data set. This indicates that the base clay has insufficient acidity to effect hydrocarbon reforming reactions of the type observed over ST00 and JP00, namely skeletal isomerisation of alkene species. However, as outlined above, this material was effective in promoting respectable levels of DHC activity when compared (in relative terms) to its acid activated counterparts.

It should be noted that Na is the predominant resident interlayer and surface and exchange site cation present in SWy-2, although lesser quantities of both Ca^{2+} and Mg^{2+} are also present. In a recent study, Baba and Ono²⁵⁸ reported that for zeolites, the introduction, through ion exchange, of small alkali cations such as Na^+ results in a severe reduction in the acid based catalytic properties of these materials. In the case of cyclopropane isomerisation, a 1% exchange of Na^+ for H^+ gave rise to an 80% reduction in activity, as a direct consequence of poisoning of the active sites. The authors concluded that the effect of the poisoning was species dependant, and that

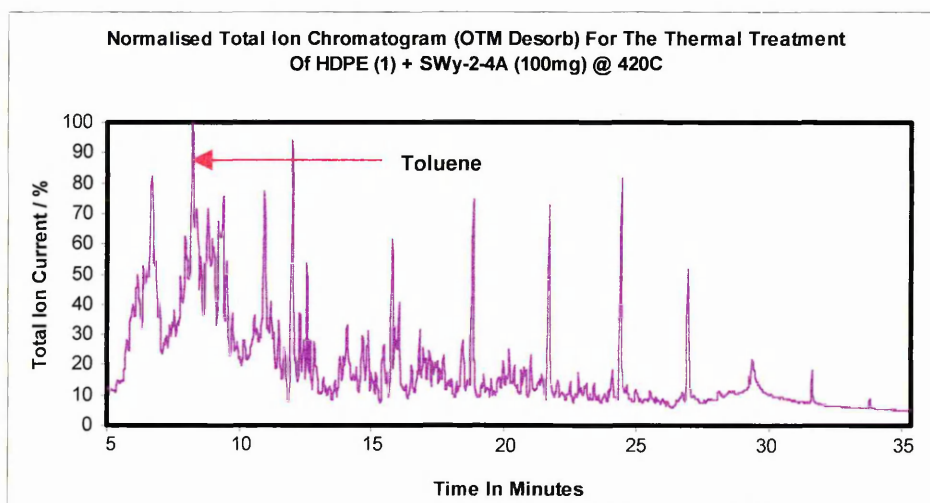
²⁵⁸ T. Baba & Y. Ono, *Applied Catalysis A: General*, **181** (1999) 227 – 238.

the properties of individual acid sites in materials such as zeolites are not independent.

The three signals attributable to the unsaturated aliphatics found in the product stream from HDPE pyrolysis were not present after contact with any of the acid activated SWy-2 samples. The TIC's obtained in the presence of all of the activated materials shared many similarities, although there was a very evident increase in the amount of branched aliphatic species as acid activation increased. In the presence of SWy-2-8A both the number and relative quantities of branched aliphatic products generated (identified from their fragmentation patterns) increased relative to the products over the lessor treated products. Figure 76 illustrates the nTIC recorded using Swy-2-4A as the catalytic material.

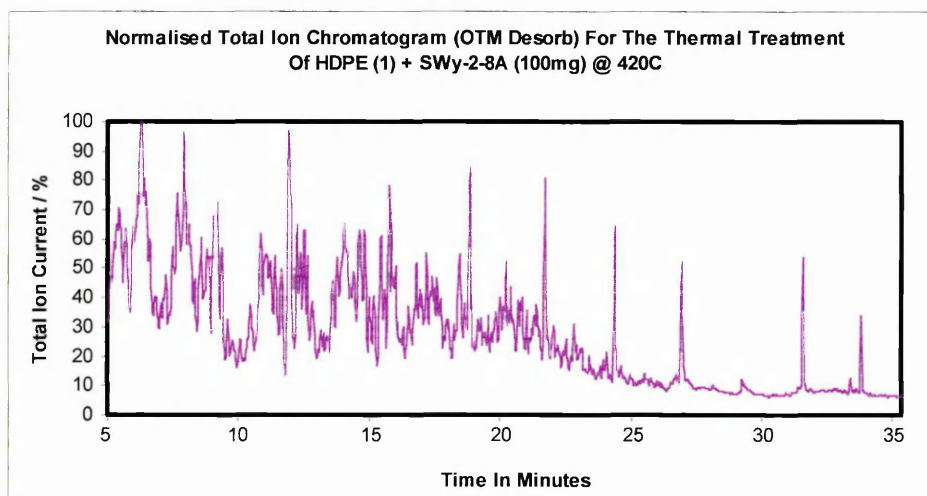
It transpires that this material is the most active in terms of DHC capability, and displays a high selectivity towards the production of toluene, being some 63% more active in this respect than any of the other materials studied in this class.

Figure 76 – nTIC for the Thermal Treatment of HDPE + SWy-2-4A (Isothermal)



Comparison of the trace in figure 76 to that for SWy-2-8A (Figure 77) provides visual confirmation of the increase in both the number and quantity of branched aliphatic products present in the product stream. It will be shown later that this enhancement in skeletal isomerisation is at the expense of cyclisation activity.

Figure 77 – nTIC for the Thermal Treatment of HDPE + SWy-2-8A (Isothermal)

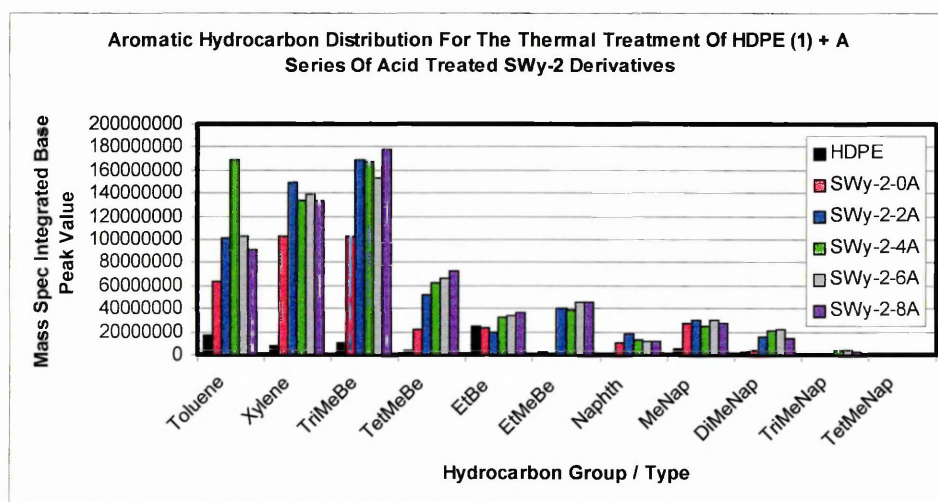


This may once more provide evidence for physical passivation of the clay, or erosion of the DHC active sites to the degree that they are no longer accessible to the feedstock gas molecules. This forces the unsaturated species present in the pyrolysate gases to react on surface active sites which may present lower acidity compared to those formed during the activation process at edge sites through structural depletion. There was no evidence to support the occurrence of cracking reaction of the n-alkane components of the HDPE decomposition products.

Figure 78 shows that relative to uncatalysed pyrolytic process, all of the materials in this series gave an enhanced aromatic composition in the product gas stream, as did the untreated parent mineral. The sites required to promote dehydrocyclisation reactions were present even after the mildest acid treatment used. This is illustrated

by the fact that SWy-2-2A was as active as the other transformation agents for the generation of single ring aromatic hydrocarbons, particularly in the case of the di and tri methyl substituted ring systems. In contrast to the metakaolin samples, the activity and or availability of these sites to the feedstock gas molecules was not affected as the severity of the acid activation process was increased, with little change in total aromatic production or selectivity as a consequence of increasing the severity of the activation. As with the AAMK's, none of the samples produced significant quantities of polyaromatics.

Figure 78 – Aromatic Hydrocarbon Distribution Achieved Over Activated SWy-2



The apparent activity of the untreated mineral is somewhat misleading. While the material appears to present appreciable activity in terms of the formation of single ring aromatics, in relative terms (c.f. HDPE alone), the levels are very low when compared to the commercially available acid activated clays used later in these investigations.

Assuming toluene to be the primary DHC product, the prevalence of this material in the SWy-2-4A transformed product stream may indicate that those sites required to promote post cyclisation catalytic alkylation (in addition to the transalkylation and

disproportionation reactions required to yield polymethyl substituted aromatics), are not available. This may relate to total surface acidity, in addition to site availability. The AAMK's exhibited similar behaviour, in that total aromatic production was not high compared to the uncatalysed process, and that individual product selectivity was low. Comparison of the Si/Al ratios for these two distinct classes of materials reveals that for SWy-2-4A which is most similar to that of AAMK3.6. In the case of the latter, this material demonstrated lower overall DHC activity than its lessor treated counterparts.

It is notable that while toluene production peaks over SWy-2-4A and then declines, the levels of the xylenes and trimethylbenzenes remained constant across the entire series. This may provide evidence for a degree of shape selectivity over these materials. As pore dimensions change due to enhanced activation, those pores optimised for toluene formation may no longer be available. Alternatively, if final product formation is effected through the catalytic alkylation of toluene formed from elementary DHC reactions of C₇₊ alkenes, the change in toluene levels may represent an alteration in the kinetics of the reaction processes, and therefore site availability, due to the formation of sites of elevated activity in the more extensively treated materials.

Again, there is a complete absence of benzene while levels of xylene and trimethylbenzenes are comparable to the toluene production. This suggests that as seen previously, post cyclisation catalytic alkylation is a distinct possibility. In contrast to the AAMK's, branched products are much more prevalent over the activated smectites, thereby presenting the possibility that some of the poly substituted aromatics observed here are the consequence of prearomatisation skeletal isomerisation. The enhanced reactivity of alkyl substituted aromatics towards

electrophilic aromatic substitution reactions due to the positive inductive effect of the alkyl group does provide evidence for the former process.

Examination of the acidity values for the AAMK's and SWy-2 samples, shows once again that the acidity of SWy-2-4A (0.44mmol H⁺ / g⁻¹ clay) is comparable to that of AAMK3.6 (0.49mmol H⁺ / g⁻¹ clay). On the basis of isomerisation activity, it could be postulated that a greater proportion of the acidity determined for the smectite sample is associated with weakly acidic surface sites which promote skeletal isomerisation, when compared directly to the kaolin derived sample. This would favour, or at least enhance the potential occurrence of the latter mechanism of xylene and trimethylbenzene formation.

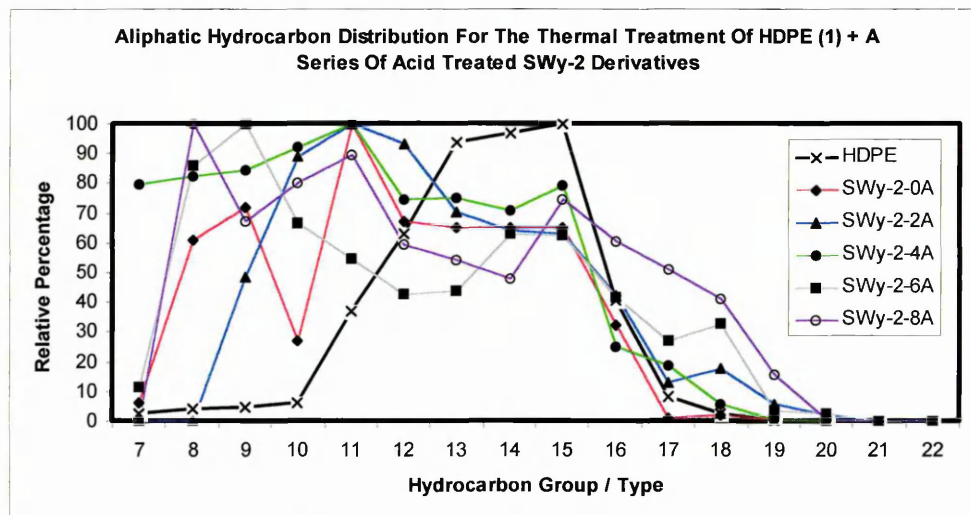
With respect to the formation of polyaromatics, none of the materials screened exhibited appreciable activity in this respect. Selectivity towards polyaromatics was low in all cases, with the di and tri methyl substituted derivatives being the most abundant polyaromatic products seen in all cases.

Commercially available acid activated and pillared smectites generally produce more of the trimethylbenzenes than either the xylenes or toluene.^{8,198} Thus, these materials mirror the activity of AAMK's in that toluene was one of the preferred products, but they were less active than the commercially available acid activated clays for which direct comparisons were meaningful.

As inferred above, none of the transformation agents in this study were effective in promoting the cracking of the n-alkanes present in the feedstock gas, this information being determined through numerical analysis of the mass spectral data for each individual run. However, figure 79 presents data suggesting that in all cases, including

the untreated material, there is a significant shift towards shorter chain alkanes in the transformed product stream relative to the uncatalysed process.

Figure 79 – Aliphatic Hydrocarbon Distribution Achieved Over Activated SWy-2



In the absence of cracking, the most likely explanation for the data given here is that the hydrogen evolved as a consequence of DHC reactions is being used to hydrogenate the shorter chain length alkenes. The apparent broadening of these traces illustrating the effect of elevated levels of shorter chain materials formed in the process. DHC can occur using C₇+ alkenes to yield toluene. This may in part be why the distribution is not broadened significantly. Longer chain alkenes may be involved in cyclisation reactions, and those of intermediate and shorter chain length in hydrogenation / isomerisation reactions.

9.2.2. DETERMINATION OF COKE

Table 33 shows the coke values determined for each of the acid activated SWy-2 derivatives employed as transformation agents in this investigation. The data is presented together with the acidity data for these materials.

Table 33 - Determination of Coke Content for SWy-2 Spent Transformation Agents

Sample	Acidity (mmol H ⁺ / g clay ⁻¹)	Weight %
SWy-2-0A	0.22	0.77
SWy-2-2A	0.38	0.83
SWy-2-4A	0.44	0.96
SWy-2-6A	0.57	1.17
SWy-2-8A	0.69	1.32

These samples share commonality with those clay based transformation agents screened previously in that they present low levels of coke deposition in contrast to other materials used in hydrocarbon reforming processes.¹⁹⁸ It should be noted that levels of coke in these materials is high in relation to the determined acidities, which are relatively low in all cases. In light of the data in the table above, in respect of the difference in the levels of coke deposition seen between SWy-2-4A and SWy-2-6A, it may be accurate to suggest that physical barriers presented as a consequence of coke deposition alter the selectivity of these materials in respect of DHC products and their relative quantities.

Differences in coke levels may also represent differences in the isomerisation activity of the different activated materials. As activation severity is increased, isomerisation versus DHC efficiency also increase, as does coke, thereby signalling that those sites of lower acidic strength may be involved in enhancing coke deposition.

As a repercussion of the impoverished aromatic yields seen in previous sections when employing dynamic conditions, a decision was taken to run these materials under only isothermal conditions.

9.3. SUMMARY OF CATALYTIC BEHAVIOUR

These results suggest that acid activation has had only a minimal effect on the overall activity of these materials in relation to their transformation activity. Figure 74 clearly illustrates that at the process temperature, there is little or no residual Lewis acidity associated with these activated products. This may strongly influence the ability of the system to catalytically recombine free hydrogen, resulting from DHC, to form dihydrogen, thus allowing for the accumulation of free hydrogen and as such a barrier to further DHC reactions taking place.

It is notable that across the entire range of materials investigated there was little alteration in the total DHC capability of these activated products with respect to changes in the severity of the activation conditions used. Likewise selectivity was low, with almost equal quantities of those single ring aromatics identified, being produced. Indeed, aromatic formation was only 40 – 60% higher than seen with the untreated parent mineral. This may indicate that the activation parameters applied were insufficient to induce the degree of structural alteration required to introduce the necessary pore network and acidity needed to efficiently promote DHC reactions.

Despite this, these materials were active isomerisation catalysts. In view of the potential application of the transformed product streams as commercial fuel mixtures, the ability to promote the formation of branched aliphatics is important, as these species represent high octane material, which would enhance fuel quality.

Despite these results, the XRD data for these materials (table 32) shows that 50% of the original Al content of these materials has been removed under the most severe of the treatments applied (SWy-2-8A). In previous cases where minerals have been subjected to such levels of octahedral sheet depletion¹⁴¹ these materials have been shown to be effective solid acid catalysts. Indeed, ST240 has a similar level of

octahedral sheet depletion¹⁹⁸ and similar levels of acidity to those seen for SWy-2-8A. It can also be seen that both are active isomerisation catalysts. The activity of the lesser treated montmorillonite derivatives do not mirror the activity of the lesser treated ST clays. This may indicate that in the case of the former, a form of mild passivation during the early stages of activation may allow octahedral sheet depletion to continue, as evidenced by XRF, while limiting the accessibility of the edge sites, thereby inhibiting transformation behavior. During the process of passivation, exposed silanol groups at edge sites become involved in cross polymerisation reactions, the result of which is the formation of a three dimensional silica framework as detailed in section 2.8.2.4.

As with previous samples the absence of benzene is indicative of the requirement of the linear to cyclic transition state to hold a formal positive charge. The instability of this species limits its potential formation. Dealkylation of alkylaromatics is also unlikely as this reaction only becomes predominant under thermal cracking conditions at temperatures above 500°C.²⁹

CHAPTER TEN

-Characterisation Results-
Commercial Acid Activated Clays

10. INTRODUCTION

As delineated in the introductory chapters, acid activated clays find widespread employment in the industrial world. They are mass produced materials which are typically manufactured to satisfy particular applications. Through links with industry, the department was able to obtain samples of these materials for investigation in this work. The following acid activated minerals were employed;

1. Fulacolor™
2. Fulcat 22B™
3. Fulcat 40™
4. K10™

It should be noted that all of the above products are registered trademarks (™) of the company which produces them. From this point forward, the '™' notation will not be used.

The materials were investigated to determine their ability to act as transformation agents for the conversion of HDPE pyrolysate gases into potentially useful hydrocarbons, and in particular aromatic species. Comparisons will be drawn to the materials screened previously.

10.1 MATERIALS CHARACTERISATION

Inkeeping with previous work, Synergic Chemical Analysis was used in the TG-OTM-GC-MS configuration to obtain the data presented. Again, one HDPE pellet (15mg, Aldrich) was used and covered with silanised glass wool (70mg, Phase Separations). A 100mg portion of the selected transformation agent was spread evenly over the glass wool prior to the analysis. Samples were heated at 10°C min⁻¹ from room temperature to 420°C and held isothermally for 1 hour.

10.1.1. THERMOGRAVIMETRIC ANALYSIS

Thermogravimetric analysis was performed to determine the effect of the various acid activation treatments on the thermal behaviour of these commercially available acid activated smectite derivatives (Table 35).

Table 35 – Weight Loss Data for Commercial Acid Activated Clays

Sample	Weight Loss to 800°C / wt%
Fulacolor	19
P.L.T.	14
Fulcat 22B	15
Fulcat 40	18
K10	21

P.L.T = Purified Los Trancos is the base beidellite used in the manufacture of Fulacolor. A sample of this material was kindly supplied by Dr. Richard M^cCabe from the University of Central Lancashire. No transformation data is available for this material.

Inkeeping with other acid activated smectites evaluated in this work, the total weight loss increases as a consequence of the surface area enhancements following activation, which facilitate water sorption (Table 35).

Values up to 20% total weight loss are indicative of materials which have been subjected to severe activation and have had their structures severely disrupted during the activation process. Weight losses due to the loss of hydration water <200°C are also seen, as are thermal events relating to the loss of more tightly bound water and structural degradation at temperatures >200°C. In the case of Fulacolor, dehydroxylation can be seen to begin at 380°C which is unusually low. It could be anticipated that the water produced would interfere with the activity of this material and the chemistry taking place on the surface of this material when used as a transformation agent. As indicated, the feedstock gases provided to the catalysts through HDPE pyrolysis are rich in unsaturated hydrocarbons. The addition of water

across the double bond of an alkene is a well documented proton catalysed reaction. The addition follows Markovnikov's rule for the ionic addition of an unsymmetrical reagent to a double bond, in which the positive portion (proton) attaches the carbon atom of the double bond which yields the more stable carbocation intermediate. As such, these additions typically give rise to secondary and tertiary alcohols and dialkylethers. The possibility of alcohol formation was monitored in all cases.

10.1.2. ELEMENTAL ANALYSIS

As with the thermogravimetric data, meaningful comparisons are difficult due to the fact that samples of the parent minerals are not available for contrast. However, samples of P.L.T. are available, and so the appropriate elemental data has been included. (Table 36)

Table 36 – XRF Data for the Acid Activated Commercially Available Samples

%	P.L.T.	Fulacolor	Fulcat 22B	Fulcat 40	K10
Al ₂ O ₃	22.32	14.75	15.07	9.03	15.17
SiO ₂	65.73	77.39	69.34	78.47	76.24
Fe ₂ O ₃	2.49	1.55	6.65	4.21	3.46
MgO	5.25	3.56	3.31	1.67	1.66
Na ₂ O	3.42	0.45	0.41	0.40	0.33
CaO	0.27	0.68	2.21	2.68	0.26
K ₂ O	0.11	0.10	0.81	0.94	2.13
Others	0.41	1.62	2.20	2.60	0.75
TOTAL	100	100	100	100	100

Comparison of the data for the P.L.T. and Fulacolor samples clearly indicates that the resident exchange cation in the P.L.T. beidellite is Na. This may prove important, as the commercial samples were used as received. Examination of figure 80 suggests the presence of NaCl on the surface of Fulacolor. This deposit may alter the chemical and physical properties of the activated material. Corroboration of this inference can be made by reference to the XRD data available for these materials.

It should be noted that on transition from PLT to Fulacolor, the reduction in Na content is 3.42% to 0.45%, whereas 3.42% to 1.6% is seen with SWy-2-8A. This may infer that the activation associated C.E.C. reduction in Fulacolor is significantly greater than seen with the activated montmorillonite, thereby lowering the compensating cation requirement of the former. However, it should be noted that some of the Na in SWy-2 is present in illite.

In addition, table 36 shows that PLT undergoes a 33% reduction in its Al content during the activation procedures employed to generate Fulacolor. Likewise similar relative percentages of Fe₂O₃ and MgO are also lost. Such depletions are not high in contrast to other smectites activated through acid treatment,¹⁴¹ indicating that this material is not subjected to extensive depopulation when acid treated. Maintenance of structural integrity may prove important. Structural degradation may limit the availability of potentially catalytically active centres available in transformation processes. Likewise, pore structures may be significantly affected if the structure breaks down to a significant degree.

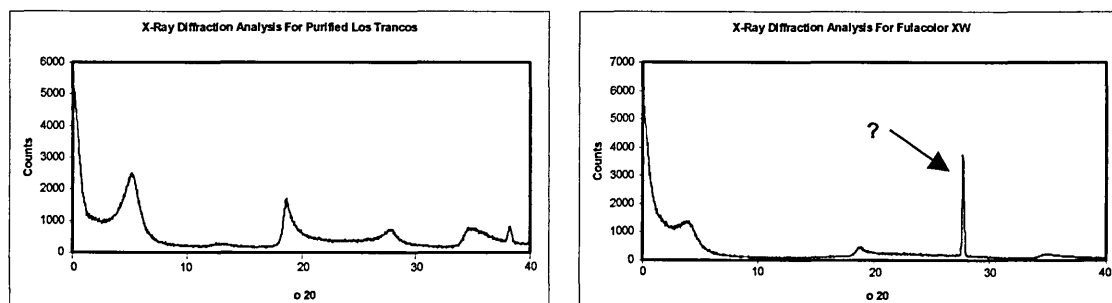
The apparent increase in Ca can be accounted for on the basis that it is present within an acid insoluble inclusion within the mineral matrix, and upon structural depopulation assumes a more prominent appearance in the XRF data. An alternative explanation may be the presence of residual CaSO₄ if sulphuric acid had been used as the activating medium. However, there is no evidence for the presence of CaSO₄ in the XRD traces of Fulacolor, although evidence for the presence of NaCl is available, thereby suggesting that the PLT is activated in HCl.

10.1.3. X-RAY DIFFRACTION ANALYSIS

Figure 80 presents the XRD traces obtained for both Purified Los Trancos and Fulacolor clays used in this investigation. The traces clearly illustrate the characteristic d_{001} reflection indicative of all smectites at 2θ values of around 12.29° . This feature is present in all of the samples, but is of lower intensity in the case of K10, Fulcat 22B and Fulcat 40 (not illustrated), thereby indicating that these products have been subject to severe activation treatments which have led to substantial breakdown of the lamellar structure of the parent mineral. This observation may indicate that these materials are not well ordered. Further analytical data, such as relative cation exchange capacities would be required to verify the latter point.

The most prominent signal in the Fulacolor trace is the signal at a 2θ value of 27.37° . The signal at a 2θ value of 27.37° (3.86\AA) was difficult to produce a definitive assignment for. This signal is absent from the P.L.T. trace, thus highlighting that this signal arises as a consequence of changes taking place during the activation step of PLT to yield Fulacolor, or that the apparent increase in intensity is a consequence of the loss of intensity associated with other structural components of the clay. Traces recorded for Fulcat 22B, Fulcat 40 and K10 have not been included in the absence of a reference material. However, all three were shown to give rise to low intensity d_{001} signals, and are therefore likely to be highly disordered. Also, these results suggest that Fulacolor is significantly more ordered, although disruption of the lamellar structure cannot be discounted.

Figure 80 – X-Ray Diffraction Traces For Commercially Available Acid Treated Clays



Examination of the traces for P.L.T. and Fulacolor confirm that the feature at a 2θ value of 27.37 (3.26\AA) is significantly lower in intensity in the former, thereby providing supplementary evidence that reduction in other signals in the trace account for the apparent increase in intensity. Moreover, the traces for these two materials can be compared to elucidate the degree of structural delamination induced by the treatment process. The intensity of the d_{001} signal in the Fulacolor trace is over 50% lower than the corresponding signal in the P.L.T. trace. This suggests that the structure of the parent mineral has been severely affected by the activation techniques employed. Delamination is extensive, although there is little evidence in the respective traces to support the formation of amorphous silica by-products which can lead to the passivation of the mineral structure.^{129,182} The lack of such a material also suggests that although the tactoid units break down, localised layer structures may remain intact, thereby reducing the amount of free silica breaking away from the main body of the mineral tactoids. Retention of the integrity of the 2-dimensional silica framework of the tetrahedral sheets ensures that the formation of free amorphous silica is much reduced. Similarly, the maintenance of the silica layer structure is potentially aided by conservation of the octahedral sheet. Fulacolor was seen to show only a 33% reduction in its octahedral sheet components. This infers that the silica fronds which form at mineral edge sites during acid activation¹²⁹ and which lead to interlayer and intralayer silanol crosslinking (passivation)^{129,138,143} following protonation, are not extensively formed, as octahedral sheet depletion is not excessive. Other analytical data, including ^{27}Si NMR would be required to confirm, or otherwise, the presence of such groups. In summary, although the PLT tactoids may be extensively delaminated, the structural integrity of the individual layers comprising those tactoids remains high. Combination of the XRD and XRF data for PLT and Fulacolor shows that as a consequence of activation, there is a relatively low level of depletion in the aluminium content of the activated product (30%). It should be noted that as a beidellite, P.L.T. contains both tetrahedral and octahedral aluminium,

and as the dissolution rates of the two species are comparable¹²¹, it could be assumed that half of the aluminium removed came from the octahedral sheet (Al_{OCT}), and half from the tetrahedral sheet (Al_{TET}). If correct, the amount of Al_{OCT} removed is low, and this may explain the fact that layer integrity remains in Fulacolor, and that the primary consequence of activation is tactoid delamination.

The surface area of Fulacolor has recently been measured by colleagues in Portugal, and found to be in the region of $400\text{m}^2\text{g}^{-1}$, which is significant in terms of acid activated smectites.

In the case of the Fulcat products, no starting material was available for examination, and therefore comparisons can only be made between the two activated products used. Derived from the same starting material, the major difference between the materials is believed to be the duration of activation, and the relative intensities of the d_{001} reflections corroborate this observation, in that the signal for Fulcat 40 (300 counts) is low in comparison to that for the 22B (700 counts) derivative which itself, is of relatively low intensity. As in the previous cases, K10 appears to be an extensively treated mineral. Few other features of relevance were seen.

10.1.4. FTIR ANALYSIS (DRIFTS)

Infra red spectroscopic investigation of pyridine treated acidic solids remains an invaluable technique for distinguishing between Brønsted and Lewis acid sites on the surface and provide semi quantitative estimates of the number of each type. As will be seen later, of the commercially treated samples studied in this work, Fulacolor is by far the most active of these materials in terms of its DHC activity. Indeed, this material is more active than any of the modified minerals used in this work. As such, Fulacolor has been chosen for this investigation.

The room temperature DRIFTS spectrum for pyridine saturated Fulacolor (Figure 81) exhibits bands due to Brønsted bound pyridine at 1636 and 1531 cm^{-1} and for Lewis bound pyridine at 1611 cm^{-1} (not marked) together with a shoulder on the higher wavenumber side of the 1442 cm^{-1} band. The 1442 cm^{-1} band in combination with the 1599 cm^{-1} band can be assigned to hydrogen bonded pyridine, HPYR.²⁴⁸ The 1486 cm^{-1} band is attributable to pyridine bonded to both Brønsted and Lewis acid sites, although the Brønsted bound species is known to contribute a greater intensity.

Increasing the sample temperature to 125°C results in a notable reduction in the intensity of the bands at 1442 and 1599 cm^{-1} attributed to hydrogen bonded pyridine. The reduction in the 1442 cm^{-1} reveals a 1452 cm^{-1} band which has been assigned to Lewis bound pyridine. The intensity of the 1537 cm^{-1} band increased and the width decreased as the hydrogen bonded pyridine bands became less intense. This behaviour resembles SWy-2-4A, and suggests that some of the hydrogen bonded pyridine forms hydrogen bonds with the proton on the Brønsted bound pyridine as observed in Al³⁺ exchanged²⁴⁹ and acid treated smectites.²¹⁰ As seen with the metakaolin samples, the strong 1547 cm^{-1} band at room temperature indicates that there is residual Brønsted bound pyridine which cannot form hydrogen bonds with

excess pyridine due to steric constraints, insufficient excess pyridine or inefficient pyridine adsorption arising from pore size constraints.

At temperature above 125°C the bands for hydrogen bonded pyridine had completely gone. At 200°C, the intensity of the bands for Brønsted bound pyridine had significantly reduced whereas the intensity of the bands for Lewis bound pyridine diminished less. The extinction coefficient for the 1450cm⁻¹ band is lower than that for those bands attributable to Brønsted bound material. This would indicate that although the bands at 1540 and 1490cm⁻¹ share similar intensities at 200°C, there is probably a greater quantity of Brønsted bound pyridine at this temperature. At 375°C, the spectrum indicates that no pyridine remains on the sample at this temperature. The weak contributions from Brønsted bound pyridine at 1531cm⁻¹ and 1636cm⁻¹ seen at 200°C have been lost, as has any residual Lewis bound material. It should be noted that in contrast to previous samples, this apparent loss of Brønsted acidity has occurred at a much lower temperature (<250°C). This again raises questions over the apparent activity of these materials when it is considered that the formation of aromatics from alkenes is a proton catalysed reaction. More in depth studies involving in situ doping of the sample with pyridine may aid in attaining a fuller understanding of the acidity / activity relationships. As with the other samples in this study, this apparent loss of Brønsted acidity can be explained on the basis of dehydration effects.

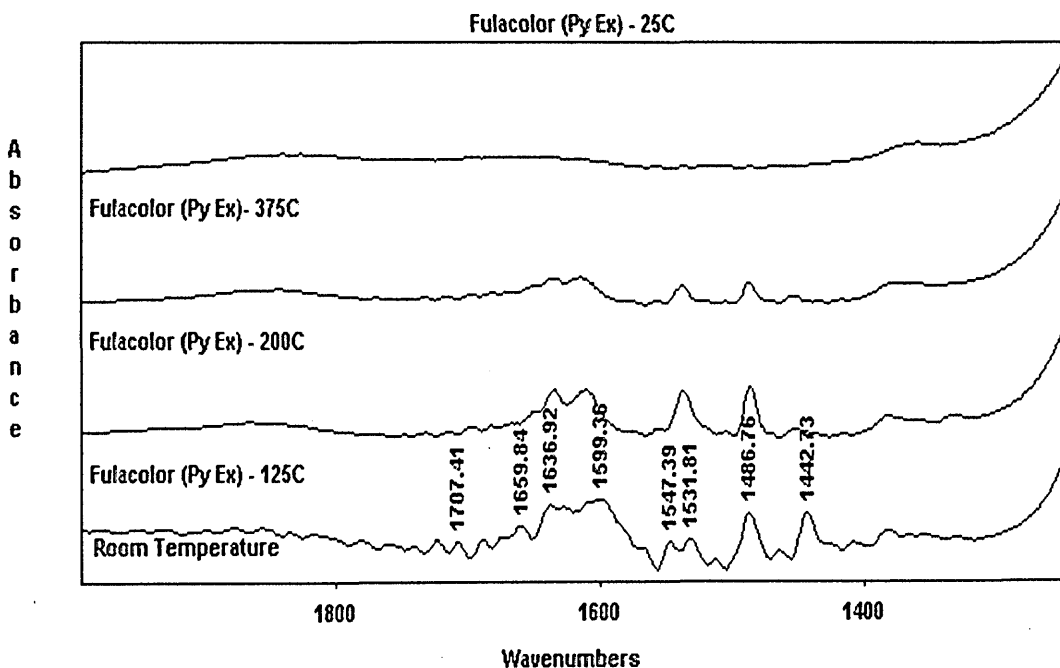
Above 400°C (not shown), no traces of Brønsted or Lewis acidity are apparent. Once again, such observations are not inkeeping with the apparent catalytic activity of these materials, and their ability to carry out dehydrocyclisation reactions using alkene feedstocks. This again raises questions over the sampling methods used here to determine the acidity of these samples. Exposure of the sample to pyridine followed by heating to 420°C would provide a more realistic explanation of the

acidity of these materials at the transformation temperatures employed. However, the pyridine may swell the clay and thereby access sites that are not available in the collapsed clay when it is used in the transformation reactions at 420°C.

As will be seen in the next chapter, Fulacolor exhibits unusual thermal behaviour characteristics, in that it begins to dehydroxylate at temperatures as low as 360°C. This means that the structural hydroxyl groups which impart acidity to the materials are actively broken down above this temperature and infers that this material will be thermally unstable at the transformation temperatures used in this work.

However, it does provide a possible explanation for the catalytic activity of Fulacolor. While infra red studies indicate that Fulacolor has no discernable acidity above 300°C, the material is highly active in the promotion of DHC activity, and as such must have acidity at 420°C. Kloprogge *et al*⁸² have shown that Beidellites dehydroxylate by a two stage process which involves loss of octahedral hydroxyl groups as water, followed by loss of hydroxyl groups from the tetrahedral sheet. These groups diffuse through the structure and reform, in particular, silanol groups on the octahedral sheet. It is potentially these groups that are catalytically active. These groups would not be seen using the infra red analysis techniques used here.

Figure 81 – VT – DRIFTS Spectra for Pyridine Treated Acid Activated Fulacolor



10.2. CATALYTIC ACTIVITY

Inkeeping with previous studies, attempts were made to employ these activated materials to promote catalytic transformation of the thermally generated off gases produced as a consequence of HDPE pyrolysis.

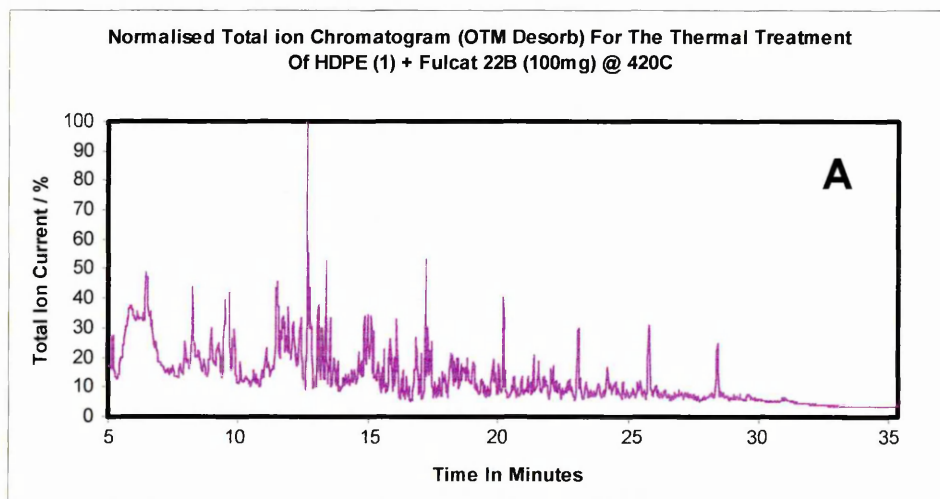
10.2.1 HDPE CATALYTIC TRANSFORMATION ACTIVITY

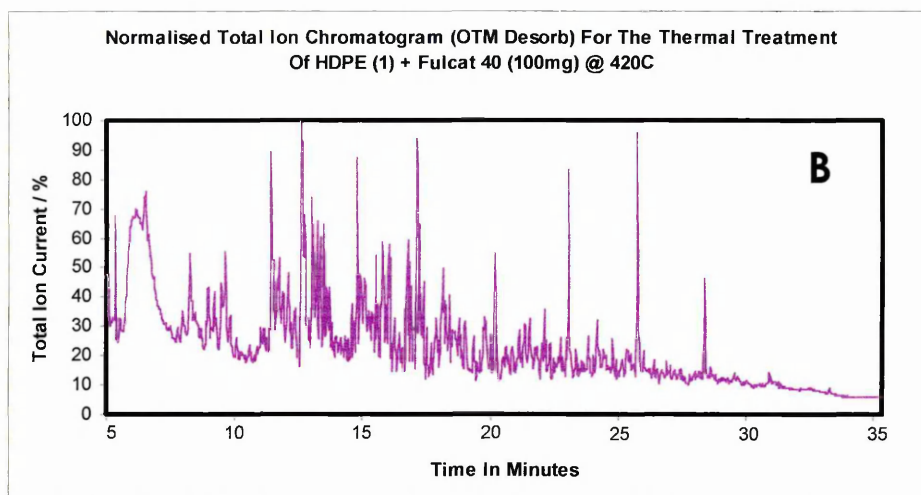
It was found that the inclusion of these commercially available acid activated clays as post pyrolysis transformation agents provided a means of converting HDPE pyrolysate gases into commercially important hydrocarbons including aromatics and branched aliphatics. All materials studied were active in this respect, but Fulacolor was by far the most active in terms of DHC activity.

Each material will now be taken in turn, its nTIC presented, and brief comments made regarding the overall form of the trace in view of those seen for other acid activated clays. Conclusions regarding activity will then be drawn by presenting data relating to the aliphatic and aromatic hydrocarbon distributions arising from these samples.

Figure 82 a and b show the nTIC traces obtained for isothermal runs performed in the presence of both Fulcat 22B (A) and Fulcat 40 (B).

Figure 82 – nTIC for the Thermal Treatment of HDPE + Fulcats 22B (a) & 40 (b) at 420°C



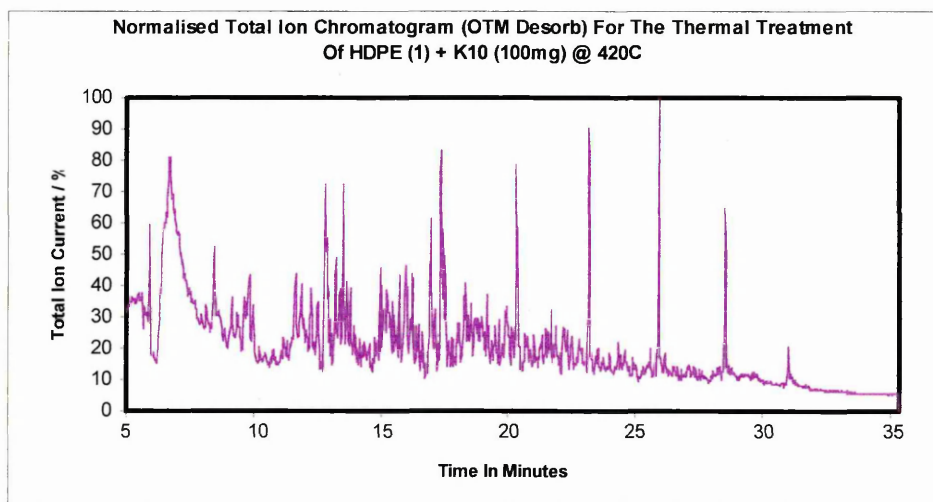


In line with the observations made through the SWy-2 series of modified minerals, the more severe activation process yielded a product stream richer in branched aliphatic species. This observation holds true here, where Fulcat 40 can be seen to be more active in promoting skeletal isomerisation reactions than Fulcat 22B. While the two traces present obvious differences, numerical analysis of the data shows that the two materials had similar DHC capability. The prominent signal (100%) on the Fulcat 22B trace (Figure 82a) can be assigned to the formation of 1,2,4-trimethylbenzene. Figure 83 shows that both Fulcat 22B and Fulcat 40 produce almost identical levels of aromatic formation across all of the species monitored in this work. This infers that Fulcat 40 is much less selective in terms of the isomeric variants of the species produced. This material was found to generate all three trimethylbenzene isomers in similar quantities in contrast to Fulcat 22B, in which the 1,2,3 and 1,3,5 isomers were formed in much lower quantities relative to the aforementioned predominant isomer.

A further observation relates to the n-alkane distribution observed following passage of the HDPE pyrolysate gases over each of these materials. Analysis confirms that cracking is not an important process, thus suggesting that the aliphatic isomerisation products arise as a consequence of the action by the transformation agent on the alkene content of the feedstock gas.

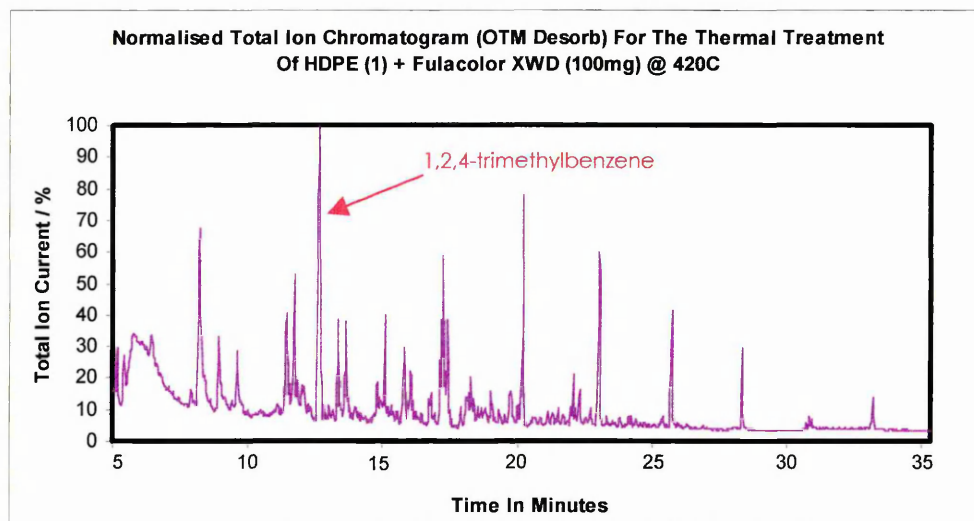
Figure 83 shows the nTIC trace arising from an isothermal process employing K10 as the transformation agent. Of all of the commercial products used here, this material gave the lowest activity in terms of DHC. As with both of the Fulcat species, skeletal isomerisation was a prevalent reaction over this material, giving rise to a large number of branched aliphatic products in respectable yields. Respectability assessments are based upon the amount of product observed relative to the uncatalysed process. Relative yields achieved over different modified minerals can also be monitored in this way.

Figure 83 – nTIC for the Thermal Treatment of HDPE + K10 at 420°C



Visual examination of the trace confirms the low levels of aromatics in the product gas stream through the low intensity signals attributable to these products. Another common feature shared between this material and the Fulcat products is that of minimal or no cracking of the saturated molecules present in the feedstock gas occurred.

Finally, Fulacolor emerged as the most interesting of all the commercially available clays, and indeed of all of the acid activated clays examined as part of this work. Figure 84 displays the nTIC in the presence of Fulacolor.



The most noticeable feature of this trace, in contrast to all others presented herein, is the small number of product peaks. In most cases, there is evidence for >200 major products, whereas with Fulacolor, only 67 major products were identified.

Two key issues in catalysis are activity and selectivity. Fulacolor appears to fulfil both of these requirements in that it is very active towards the formation of a select number of products, which numerically are very few in relation to those formed over similar catalysts. Table 37 lists the names of 57 of the 67 products generated over Fulacolor and groups them according to general type. Of the remaining 10, no definitive identification was possible, and therefore no assignment has been made.

Clearly the catalytic activity of this material is heavily biased towards the formation of substituted aromatic molecules. Whereas the other three commercial clays have produced high levels of branched aliphatic species, Fulacolor produces very few of these species. Figure 85 shows that this DHC activity favours the formation of trimethylbenzene, and in particular 1,2,4 trimethylbenzene. Such a finding is inkeeping with similar observations made using Fulcat 22B in the transformation role.

Table 37 – Major Transformation Products Isolated In Fulacolor Products at 420°C

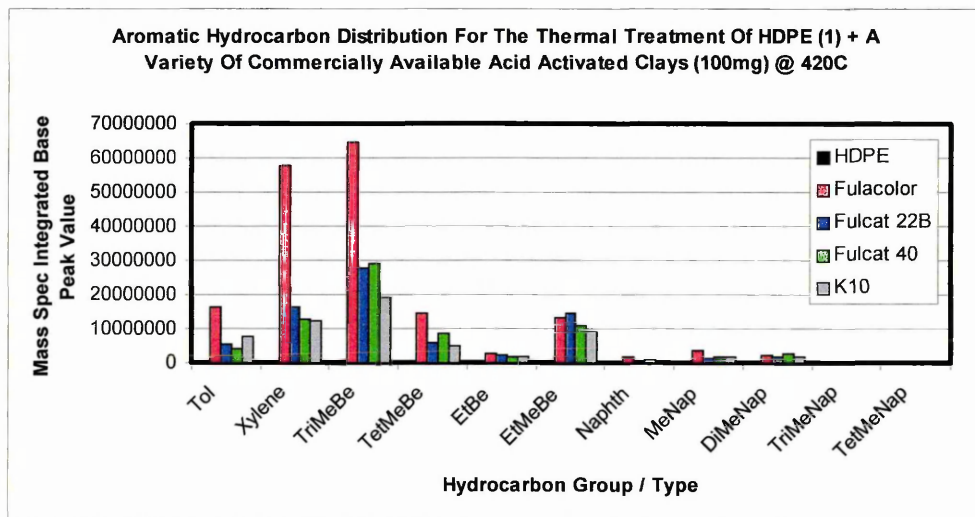
<i>n</i>-alkanes	<i>Branched Aliphatics</i>
Decane	2,4-Dimethylhexane
Undecane	3,7-Dimethylundecane
Dodecane	4-Ethyldecane
Tridecane	4,4-Dimethylundecane
Tetradecane	2,6,10-Trimethyldodecane
Pentadecane	2,6,11-Trimethyldodecane
Hexadecane	
Heptadecane	
	<i>Alkenes</i>
	Trans 2,2-dimethyl 3-heptene
	8-Methyl-1-Decene
	(Z) 4-C ₉ H ₁₈
	E-Tetradecene
<i>Aromatics</i>	
Toluene	
Ethylbenzene	
o-Xylene	
m-Xylene	
p-Xylene	
Propylbenzene	
Ethylmethylbenzene	
1,3,5-trimethylbenzene	
1,2,4-trimethylbenzene	
1,2,3-trimethylbenzene	
1-propenylbenzene	
1 methyl, 3-propylbenzene	
1,2,3,5-tetramethylbenzene	
1,2,4,5-tetramethylbenzene	
3 ethenyl-1,2-dimethyl-1,4-cyclohexadiene	
1,1,2-trimethylpropylbenzene	
Ethyl dimethylbenzene	
1,1-dimethylbutylbenzene	
Octadecylbenzene	
4-ethyl, 1,2-dimethylbenzene	
(3 methyl-4-pentyl) Benzene	
1,3 diethyl-5 methyl Benzene	
1,1-dimethylpropylbenzene	
(1,1,2-trimethylpropyl) Benzene	
1 ethyl, 2,4,5-trimethylbenzene	
1,4-dipropylbenzene	
1,3-dimethylbutylbenzene	
2-methylpentylbenzene	
(2,3,4,5,6-pentamethylheptyl) Benzene	
1,4-dimethyl-2-(2-methylpropyl) Benzene	
1-Methyl-2-n-Hexylbenzene	
Pentamethylbenzene	
	<i>Naphthalenes</i>
	Naphthalene
	1,2,3,4,5,6-hexahydro-1,1,6-trimethylnaphthalene
	2-methylnaphthalene
	1-methylnaphthalene
	<i>Others</i>
	1-(1,5-dimethylhexyl)-4-methyl-cyclohexane
	Bis-1,1-(1,1,3,3-tetramethyl-1,3-propanediyl)
	<i>Misc.</i>
	There were 10 products to which no definitive identification was made.

A second prominent product in the gas stream generated over Fulacolor is m-xylene. The selectivity over Fulacolor will be discussed in chapter 12.

The three signals attributable to the unsaturated aliphatics found in the HDPE decomposition product stream were not present after contact with any of the transformation agents subjected to acid activation.

An important aim of this work was to employ these modified clays as transformation agents to enhance the aromatic content of the hydrocarbonaceous product mixture produced during the pyrolysis of post consumer HDPE plastic waste. Figure 85 shows that relative to HDPE, all of the materials in this series used gave an enhanced aromatic composition in the product gas stream.

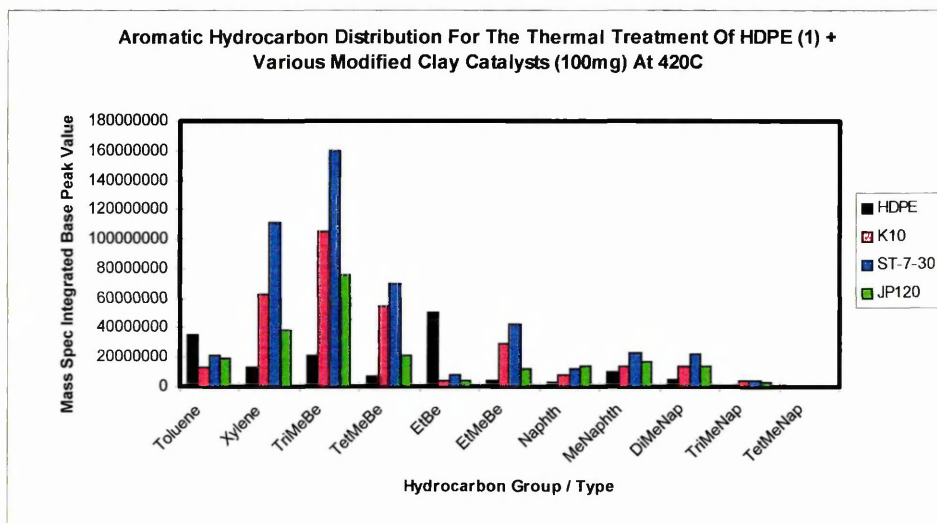
Figure 85 – Aromatic Hydrocarbon Distribution Achieved Over Commercial Clays



The data in figure 85 confirms the excellent DHC capability of Fulacolor when presented with the complex hydrocarbon mixture arising from HDPE decomposition. The material is over 50% more active than its commercial counterparts in respect of the methyl substituted benzenes. In an annex study (figure 86) K10 was found to be more active in performing DHC reactions than SWy2-4A or JP120. All of these

materials gave excellent activity in their own individual classes. The only material more active than K10 was the beidellitic clay ST30. In this case, Fulacolor outperforms K10 by a factor greater than 50%, thus confirming the selectivity of Fulacolor towards the generation of species of this molecular type.

Figure 86 – Aromatic Hydrocarbon Distribution Over Active Clays



As identified in all previous cases to date in this work, there is a complete absence of Benzene in the product stream. Polyaromatic formation was poor in all cases. This is inkeeping with the other modified minerals used in this work.

In the case of Fulacolor, the high levels of xylene and trimethylbenzenes in addition to the low levels of branched aliphatics suggests that catalytic methylation occurred after cyclisation / aromatisation, as opposed to pre cyclisation isomerisation.

Commercially available acid activated and pillared smectites generally produce more of the trimethylbenzenes than either the xylenes or toluene.^{8,198} Thus, these materials closely resemble the activity of Fulacolor.

As illustrated in figure 85, the two major products isolated from the Fulacolor product stream were trimethylbenzene and xylene, with the 1,2,4 and meta isomers respectively being the most abundant species. It has been reported that these two molecules have exactly the same minimum Van der Waals diameters, with both registering at 7.4Å.²⁵⁹ This introduces the possibility that pore size constraints may affect product selectivity or that surface templating effects lead to the formation of products of preferential size.

Comparison of figures 82 A and B for the Fulcat clays with that of figure 84 shows a clear difference in the activity of these two different material types. While the Fulacolor trace contains relatively few signals, those traces for the Fulcat clays contain a much greater number of signals. Analysis of these traces confirms that the signals present, in addition to the aromatics and alkanes are attributable to a variety of iso-alkanes. This infers that these materials are active skeletal isomerisation catalysts, an observation which provides similarity to the data recorded for the both the AAMK's and SWy-2 samples. In contrast to Fulacolor, the Fulcat clays have a significantly reduced DHC activity (figure 85), and as has been demonstrated, the reduction in aromatisation activity can be accounted for on the basis of increased isomerisation activity.

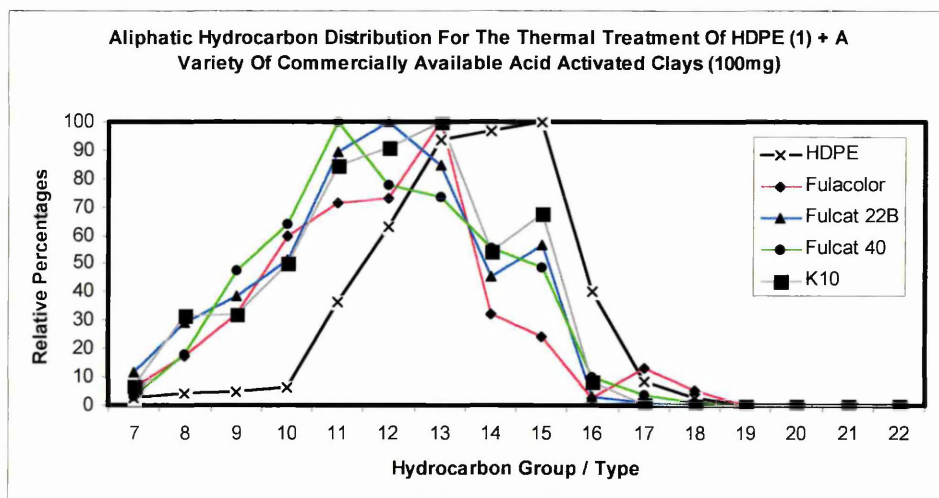
Comparison of figure 82a (Fulcat 22B) to 84 (Fulacolor) clearly shows that the major signal on both is that for 1,2,4-trimethylbenzene. Despite this, Fulacolor is twice as active in generating trimethylbenzene than the Fulcat clay. This may infer that the additional production over Fulacolor is composed of other isomers of this species. However, figures 82 a and b in combined with figure 87 confirm that the Fulcat clays are active in altering the n-alkane distribution. In the absence of any quantitative data, the conclusion that this alteration is due to alkane removal by cracking cannot

²⁵⁹ H. P. Roger, K. P. Moller & C. T. O'Connor, *Microporous Materials*, **8** (1997) 151 – 157.

be supported. However, this leaves the possibility that the trimethylbenzene signal on the fulcat trace appears more significant due to an alteration of the n-alkane components, and not because the trimethylbenzene content is high.

As outlined above, none of the transformation agents in this study were active in promoting the cracking of the n-alkanes present in the feedstock gas, this information being attained through numerical analysis of the mass spectral data for each individual run. Figure 87 presents data suggesting that in all cases, there is a slight shift towards shorter chain alkanes in the transformed product stream relative to the uncatalysed process.

Figure 87 – Aliphatic Hydrocarbon Distribution Achieved Over Commercial Clays



As with the SWy-2- samples, in the absence of cracking, the most likely explanation for the data given here is that the hydrogen evolved as a consequence of DHC reactions is being used to hydrogenate the shorter chain length alkenes. There is no real broadening of any of the traces, simply a downward shift in carbon number.

10.2.2. DETERMINATION OF COKE

Table 38 shows the coke values and acidity data determined for each of the commercial acid activated clays employed as transformation agents in this investigation.

Table 38 - Determination of Coke Content for Commercial Transformation Agents

Sample	Acidity (mmol H⁺ / g clay⁻¹)	Weight %
Fulacolor	1.29	0.78
Fulcat 22B	0.98	1.01
Fulcat 40	0.90	0.82
K10	0.74	0.94

These samples share commonality with those clay based transformation agents screened previously in that they present low levels of coke deposition in contrast to other materials used in hydrocarbon reforming processes.¹⁹⁸ The Fulcat samples also follow previously seen trends in that enhancement of the activation severity leads to less heavy coking as a consequence of lower surface acidity. The level of coke determined on Fulacolor is very low in contrast to the SWy-2 samples, bearing in mind its determined acidity which is much higher.

As a repercussion of the impoverished aromatic yields seen in previous sections when employing dynamic conditions, a decision was taken to run these materials under only isothermal conditions.

10.3. SUMMARY OF CATALYTIC BEHAVIOUR

Of the materials studied thus far, this series has proven to be the most interesting. In particular the additional activity of Fulacolor over any other material surveyed has opened a debate relating to the cause of product selectivity over modified minerals. Fulacolor has been shown to exhibit only low levels of residual protonic acidity at the

transformation temperatures used in this work. Despite this, the material has proven to be both active and selective towards the formation of single ring aromatics and in particular those of minimal Van der Waals radius of 7.4Å, namely 1,2,4-trimethylbenzene and m-Xylene. While both Fulcat clays also presented good DHC activity, these materials were also active in the formation of branched aliphatic species, with subsequent detrimental effect on their cyclisation activity. The activity of the Fulcat clays is similar to that of the SWy samples, although the aromatic selectivity of the former is much more apparent. However, both are good hydrocarbon isomerisation agents, and thus their potential use in the conversion of waste HDPE to potentially useful fuel mixtures is of interest⁶. However, the aromatic selectivity means that there is potential application of these materials for the conversion of waste polymers into organic chemical feedstocks for application in the bulk or fine chemical manufacturing industries. The absence of any branched aliphatics in the transformed product stream over Fulacolor must indicate that the pore structure and acidity and free cation content of this material is optimised for the execution of DHC reactions to yield aromatics.

In view of this data, the following chapter presents data on a series of modifications applied to Fulacolor in order to ascertain a fuller understanding of the transformation activity of this material.

CHAPTER
ELEVEN

-Further Investigations-
Fulacolor™ Derivatives

11. MODIFIED FULACOLOR

In light of the extraordinary DHC behavior exhibited by Fulacolor in contrast to the other acid activated clays it was decided to study the material in more detail. In particular, the effect of a series of modification treatments on the catalytic activity of the material were investigated.

It has been shown that certain species, particularly small alkali cations²⁵⁸ can poison active sites in protonic solids, even when they are present in low concentrations. Following activation, Fulacolor will be a predominantly proton exchanged clay, with protons residing in the interlayer and surface exchange sites. The instability of H⁺ saturated clays is well documented¹³² and these materials are susceptible to spontaneous autotransformation, a process in which structural ions are leached from the structural matrix as a consequence of proton migration through the available ditrigonal cavities into the octahedral sheet region of the mineral sheets. There is a subsequent back exchange of these structural ions into the interlayer and surface exchange sites of the mineral, with the resident protons.

The sample of Fulacolor used in this investigation was not freshly prepared. It can therefore be assumed that the material will have undergone some autotransformation, and that it is no longer a fully proton exchanged clay. In order to determine the nature of the cations on exchange sites, samples of the clay were subjected to cation exchange (as detailed in the experimental section) using solutions of cobalt sulphate equivalent to 25, 50 75 and 100% of the known cation exchange capacity of the clay (68meq/100g⁻¹). This value had previously been determined using a cobalt sulphate based technique.²⁶⁰

²⁶⁰ C. N. Rhodes and D. R. Brown, *Clay Minerals*, **29** (1994) 799 – 801.

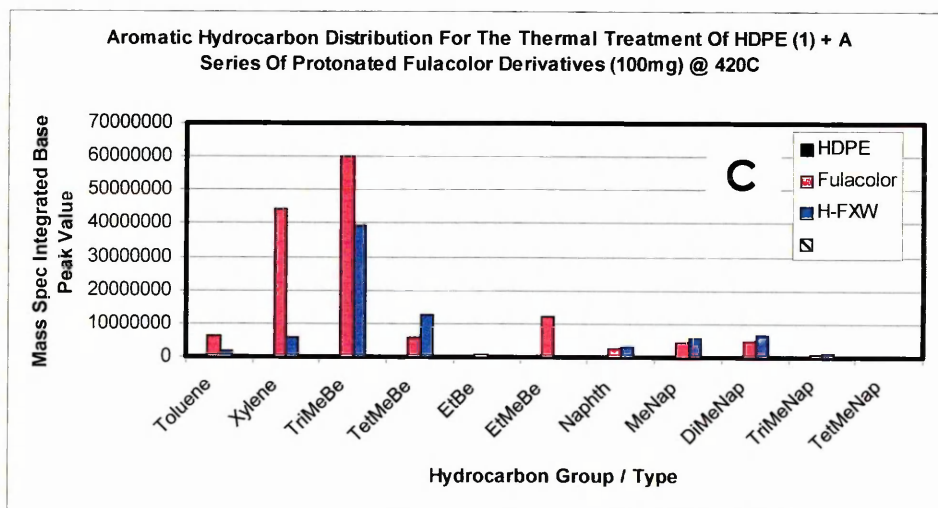
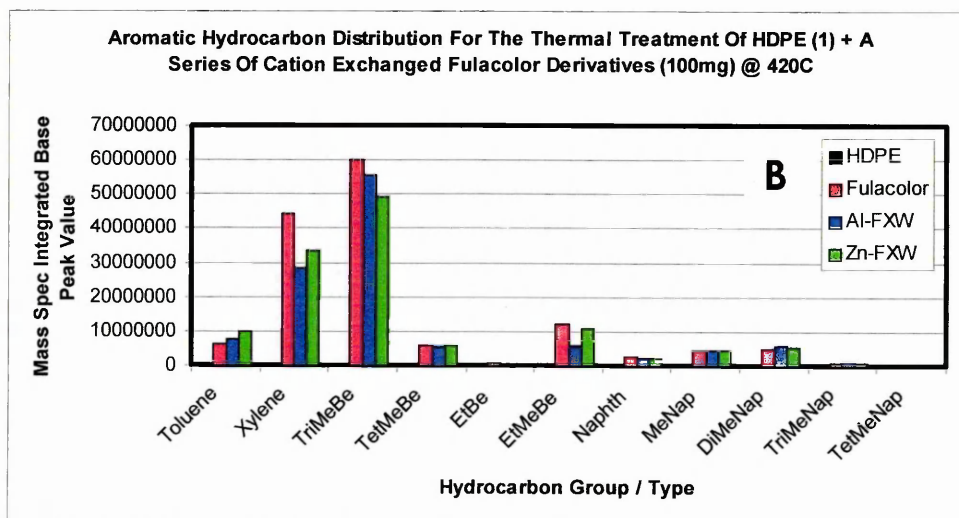
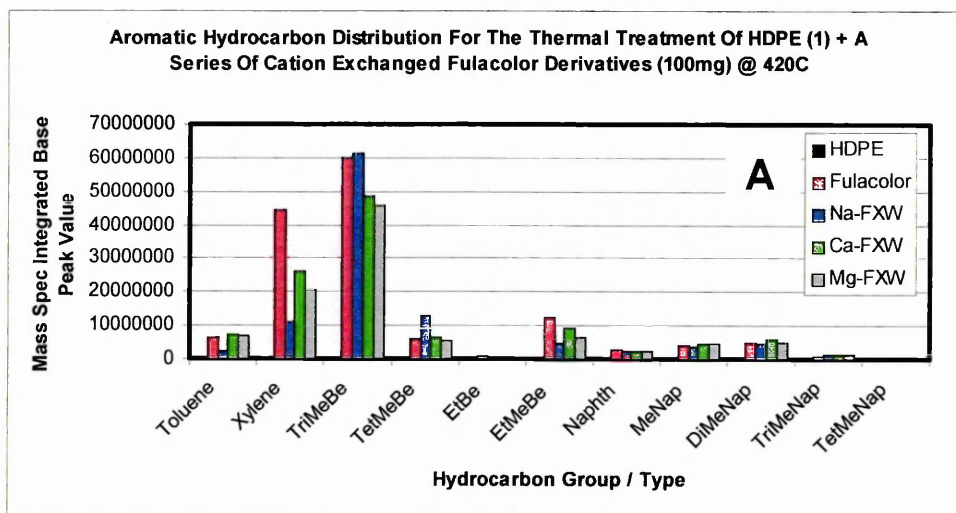
The treatment solutions were analysed by ICP-MS to determine their elemental content. It was found that the predominant cations displaced from the clay, were $\text{Ca} > \text{Na} > \text{Mg} > \text{Al}$. Subsequent XRD analysis of these samples confirmed that the intense NaCl reflections were no longer present. In addition, confirmation was also gathered regarding the potential for the deposition inorganic salts (including cobalt sulphate) on the surface of these exchanged products. No evidence was obtained to support this possibility. XRF data confirmed the increase in the cobalt content of these materials in addition to the drop in the levels of Ca and Na. Ca is not a structural ion in mineral bodies.

In view of this information, attempts were made to completely exchange the resident interlayer and surface exchange site cations of Fulacolor for a variety of other ions;

1. Al^{3+}
2. Zn^{2+}
3. Na^{+}
4. Ca^{2+}
5. Mg^{2+}
6. H^{+}

Figure 88 below illustrates the aromatic hydrocarbon distributions recorded over each of these modified Fulacolor derivatives.

Figure 88 – Effect of Cation Exchange of Fulacolor DHC Activity

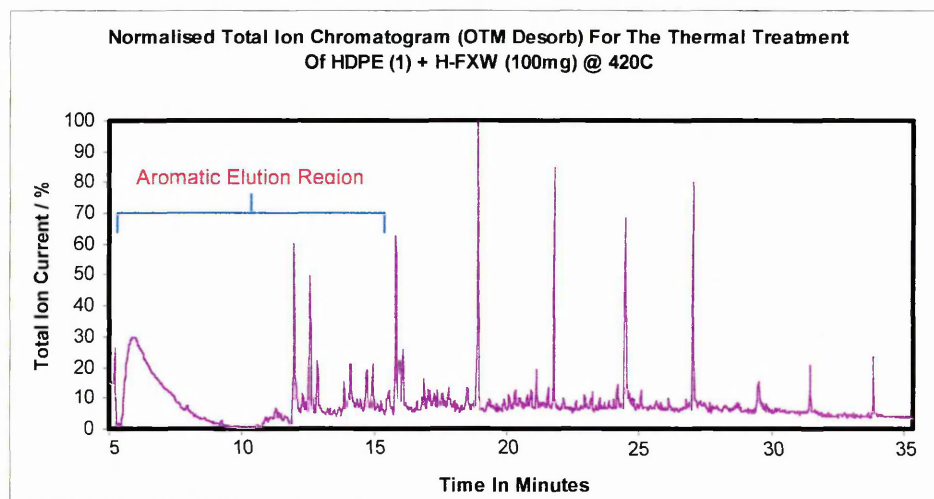


Clearly, replacement of the resident interlayer cation with either Na^+ or H^+ has a detrimental effect on the ability of Fulacolor to catalyse the formation of the xylenes. It may be the case that these cations are better able to selectively poison those surface active sites required for DHC, whereas Ca, Mg and Zn are not able to do so, perhaps as a consequence of their cationic character. Another important note is that those cations responsible for promoting loss of xylene yield are both monovalent. This may reflect the ability of these cations to efficiently catalyse the recombination of free hydrogen to form dihydrogen. This in turn will have the effect of lowering aromatisation activity. However, it is notable that only xylene appears to have been affected significantly, while levels of trimethylbenzene production have been maintained. A second explanation may be that Na^+ and H^+ selectively displace a given cation, that remains less affected than when Fulacolor is treated with the other cations used. ICP analysis of the wash solutions confirmed that those cations removed during cation exchange were not dependant on the exchanging species and that those cations displaced were always $\text{Ca}^{2+} > \text{Mg}^{2+} > \text{Na}^+$. Al^{3+} was also removed when the cation loadings were increased, but in much lower (25% Na^+ value) when measured in parts per million in the treatment solutions. In view of previous work¹⁴¹, this order of displacement is unusual and may indicate a concentration effect.

Restoration of Fulacolor to its activated state through a process of proton exchange yields a product, which was shown by XRF to have lower levels of both Na and Ca than those found in the product used to collate the original data presented in this work. Proton exchange has a detrimental effect on both the activity and selectivity of Fulacolor towards the execution of DHC reactions to yield aromatics. In particular, xylene production has fallen by 88%, with trimethylbenzene production being subject to a 33% reduction. This loss can be seen in the nTIC trace (figure 89) which shows

that the portion of the trace in which methyl substituted aromatics are evolved (5-15 minutes) contains very few features when compared to that for Fulacolor (fig 84).

Figure 89 – nTIC for the Thermal Treatment of HDPE + H⁺-Fulacolor (Isothermal)



These factors provide two important pieces of evidence, firstly, the important role assumed by the resident exchange cations in the Fulacolor product. Secondly, this information strongly suggests that the parent Fulacolor had undergone some autotransformation and that the material is no longer fully proton exchanged.

The reduction in DHC capability following proton exchange of Fulacolor suggests that the exchange cations assume a role in the overall process of aromatic formation. It has been shown that when impregnated with certain cationic species, aromatisation over zeolites can be enhanced via the ability of these cationic centres to act as atomic hydrogen acceptors. This reduces the concentration of free atomic hydrogen in the gaseous reaction mixture, and thus reduces potential barriers associated with the elimination of dihydrogen during the DHC process.^{260,261} The cationic centres act as recombination sites which facilitate the formation of dihydrogen. This latter suggestion, if operative may account for the lack of branched

²⁶⁰ K. M. Dooly, G. L. Price, V. I. Kanazirev & V. I. Hart, *Catalysis Today*, **31** (1996) 305 – 315.

²⁶¹ O. V. Chetina, T. V. Vasina & V. V. Lunin, *Applied Catalysis A: General*, **131** (1995) 7 – 14.

aliphatics found in the product stream over Fulacolor. Removal of the free hydrogen (via its conversion to dihydrogen), prevents protonation of feedstock alkenes, and thus the accompanying skeletal isomerisation reactions to promote stability prior to involvement of the species in hydride abstraction reactions to yield branched alkanes.

The anticipated reduction in DHC activity allied to acid site poisoning by small alkali earth metal cations in Na exchanged Fulacolor is not seen. Figure 88a does indicate a reduction in selectivity towards the formation of xylenes over this modified Fulacolor derivative, trimethylbenzene production reduces only slightly. In the case of Ca and Mg exchanged derivatives, the results are similar, and in all cases, yields are lower than in the presence of the unmodified product.

Literature reports have suggested that ZnO inclusions in ZSM-5 can be active in the direct aromatisation of linear alkanes, with the dehydrocyclisation activity of the metallic species being exploited to promote a concerted reaction.²⁶² Figure 93b shows that following exchange with Zn aromatic production over Fulacolor was lower than seen with the standard sample. In addition, no change in the n-alkane distribution was found.

Note that in the case of the work in the literature pertaining to the use Zn, this material was subject to metallic oxide formation through a process of calcination in air. This process was not repeated here, as the aim of this work was to determine the effect of a variety of exchange site cations on DHC activity relative to Fulacolor, and not to study the effect of oxide inclusions. It is of interest to note that in none of the cases presented in figure 88a-c was the total DHC activity of the modified Fulacolor derivatives lower than other acid activated clays studied in this work.

²⁶² N. Viswanadham, A. R. Pradhan, N. Ray, S. C. Vishnoi, U. Shanker & T. S. R. Prasada Rao, *Applied Catalysis A: General*, **137** (1996) 225 - 233.

As with the other acid activated clays, Fulacolor was found to be effective in acting catalytically upon the unsaturated components of the feedstock gases arising from HDPE pyrolysis. Nevertheless, as with these materials, Fulacolor was found to be relatively ineffective in handling the linear alkane component to the degree that no discernable activity is evident.

However, in view of the extensive literature on the use of Platinum impregnated zeolites as catalysts for hydrocarbon reforming, experiments were performed to determine the effect of this species on the cyclisation behavior of Fulacolor. In particular, the effect of these modifications on the alkane conversion activity of Fulacolor was a primary concern. Firstly, a wet impregnation (ion exchange) method was employed, with the resultant material being air dried prior to use. The product of this process was labeled as FXW/Pt. In the second case, the above process was repeated, but following air drying, the material was calcined in air (to promote oxide formation) at 873K for 20 hours.²⁶³⁻²⁶⁵ The product in this case was identified as FXW/Pt*

Platinum is extensively used in commercial reformers in the petroleum refining industry and improving the behavior of Pt loaded catalysts remains an active field of research. Recently, Sinfelt²⁶³ was able to confirm the importance of Pt clusters on commercial reforming catalysts in the dehydrogenation of cycloalkanes (naphthenes) to yield aromatics. Moreover, attempts to improve the ability of Pt impregnated catalysts to yield aromatics from short chain alkanes (C₄-C₉) is also of current interest.^{264,265} With this in mind, Pt impregnated Fulacolor derivatives were employed in the transformation role outlined in this work. The materials were used

²⁶³ J. H. Sinfelt, *Journal of Molecular Catalysis A: Chemical*, **163** (2000) 123 – 128.

²⁶⁴ W. J. H. Dehertog & G. F. Fromen, *Applied Catalysis A: General*, **189** (1999) 63 – 75.

²⁶⁵ K. Matusek, A. Wootsch, H. Zimmer & Z. Paal, *Applied Catalysis A: General*, **191** (2000) 141 – 151.

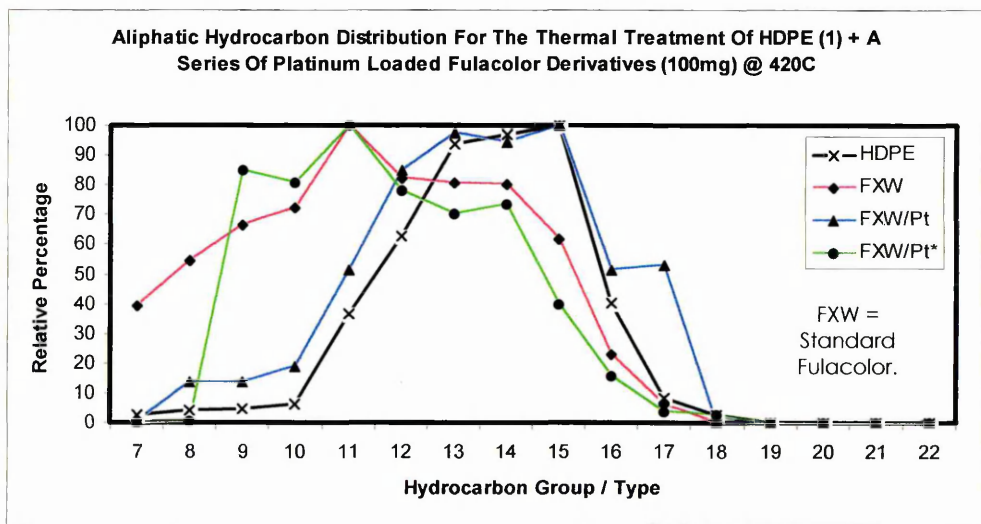
under isothermal conditions only. In the case of the referenced work,²⁶³⁻²⁶⁵ there was no direct evidence for the reduction of loaded Pt in the presence of molecular H₂.

Figure 90 shows the results of the n-alkane distribution analysis performed to determine the potential cracking activity of these Fulacolor derivatives. The known de / hydrogenation activity Pt on such acidic solids is well documented.

Pt exchange had little effect on the distribution of n-alkanes found in the product gas stream over FXW/Pt. In contrast, passing the HDPE pyrolysate gases over FXW/Pt* broadened the linear alkane distribution, by enhancing the relative quantities of shorter chain species. In this respect, FXW/Pt* is similar to Fulacolor its self, which gives rise to an alkane distribution broadening.

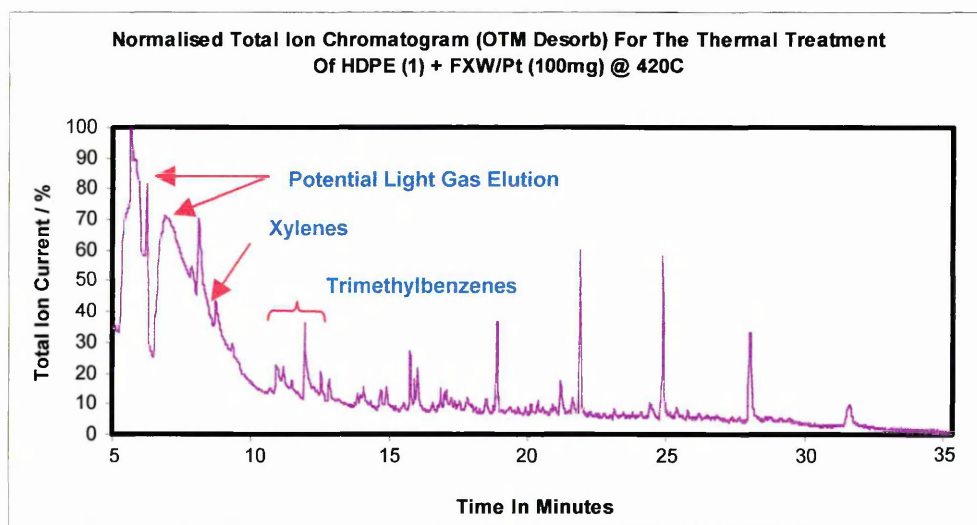
Numerical analysis of the actual data sets presents a different perspective to the results. It can be seen that in the case of FXW/Pt, although the relative distribution remains similar to that for the uncatalysed process, the actual amounts are significantly less across the entire carbon chain length surveyed. Such observations were not made in the case of Fulacolor or FXW/Pt*. This data suggests that a straightforward exchange of the resident interlayer and surface exchange site cations of Fulacolor with Pt installs a cracking function to the material.

Figure 90 – Aliphatic Hydrocarbon Distribution Achieved Over FXW, FXW/Pt & FXW/Pt*



Although the adsorbent traps used in this work were inefficient in trapping species of carbon chain lengths less than C₅, the nTIC recorded in the presence of FXW/Pt does contain features which are highly indicative of light gas formation. Figure 91 illustrates this trace, and emphasises the feature, the components of which were not readily identifiable due to co-elution. Attempts to re-run these samples with different GC ramp rates to aid in separation of these early eluting species were inconclusive. However, it should be noted that FXW/Pt was not active in forming significantly greater quantities of shorter chain alkanes than seen with non modified Fulacolor, thereby indicating that cracking is excessive, and the products of such an event are light gases.

Figure 91 – nTIC for the Thermal Treatment of HDPE + FXW/Pt (Isothermal Conditions)

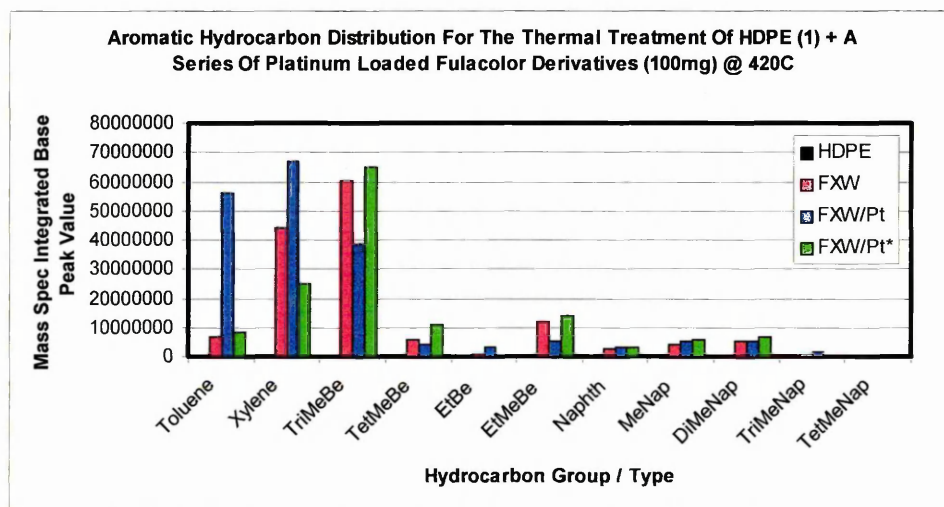


In view of this apparent cracking activity of FXW/Pt it may be assumed that the Pt is acting very efficiently as a Lewis acid centre. Hydride abstraction from paraffins is a primary step in the formation of carbocations which subsequently undergo cracking. This apparent high level of Lewis acidity may also infer that the material will present good DHC capabilities in respect of its ability to efficiently catalyse the recombination of free hydrogen to form dihydrogen. This in turn promotes the

dehydrogenation required to form aromatic species from cycloalkanes following ring closure reactions.

Examination of the aromatic hydrocarbon distribution over this series of materials (figure 92) supports the above assumption. However, the replacement of the exchange site cations resident on the autotransformed Fulacolor surface with Pt has a very profound effect on the selectivity of this product as a transformation catalyst. Whereas Fulacolor was most active in the formation of m-xylene and 1,2,4-trimethylbenzene, FXW/Pt, while maintaining high levels of DHC activity was more selective towards the formation of toluene and p-xylene. While both of these materials are important industrial chemicals, the cost of impregnating a cheap disposable catalyst such as a modified clay mineral with a precious metal such as Pt may not be a viable possibility.

Figure 92 – Aromatic Hydrocarbon Distribution Achieved Over FXW, FXW/Pt & FXW/Pt*



These results infer that total aromatic production and product selectivity is determined by the relative strengths of the Lewis acid sites available for utilisation and involvement in the various reforming reactions executed over the surface of these transformation agents. As illustrated by figure 88A-C, in the presence of

compensating cations of lower Lewis acidity than Pt, such as the monovalent cation Na^+ , total aromatic production was lower than seen with Fulacolor, and selectivity was also lower, particularly with regard to the xylenes. Similar behaviour was also observed with FXW/Pt* in addition to a corresponding increase in trimethylbenzene production.

As outlined in previous sections, the formation of methyl substituted aromatics can potentially occur via one of two routes, namely pre cyclisation isomerisation, or post cyclisation catalytic alkylation. Over Fulacolor and all of its derivatives, the production of branched aliphatics is virtually non-existent. In contrast all of these materials share a common feature in that they are highly effective in forming rings. This would suggest that over these materials, the latter mechanism is favoured. Analysis has shown that the HDPE decomposition products consist mainly of linear species. Bearing this in mind, the most likely aromatic products are toluene, ethylbenzene, propylbenzene, butylbenzene and so on, formed through direct ring closure and subsequent dehydrogenation of the appropriate alkenes. It can therefore be assumed that the other methyl substituents on the ring arise as a consequence of catalytic alkylation. Such electrophilic aromatic substitution (EAS) reactions utilise monoalkyl benzenes as feedstock molecules, which are activated towards EAS reactions due to the positive inductive effect provided by the alkyl substituent. This means that following their formation, molecules such as toluene are then involved in alkylation reactions to yield xylenes, tri, tetra, penta and hexamethylbenzenes. These species subsequently form an equilibrium mixture in which levels are maintained on the basis of the occurrence of a concurrent set of disproportionation and transalkylation reactions. The elevated levels of toluene and xylenes seen in figure 92 for FXW/Pt may be the consequence of a stockpiling of the molecule due to its efficient formation in the presence of the active

dehydrogenating function provided by the Pt prior to toluene's direct involvement in the post cyclisation reactions detailed above.

In previous studies, the combination of zeolites with montmorillonites has proven to be an effective method for altering the inherent acidity of the former.²⁶⁶ Similarly, the physical mixing of zeolites and clays has been used as a method of introducing secondary hydrocarbon reforming behavior to these hybrid materials.²⁶⁷ The use of clays as a physical diluent has the effect of altering the catalytic behavior of the primary catalyst.

In light of the inability of Fulacolor to alter the nature of the n-alkane distribution achieved as a consequence of post pyrolysis catalytic transformation of HDPE, a series of experiments were performed to determine the effect of the presence of a secondary component in the bulk catalyst. The following three materials were selected for investigation;

1. H⁺-ZSM-5

The material was selected as a co-catalyst because of its known ability to induce n-alkane cracking under the catalytic cracking / reforming conditions employed in this work. The use of ZSM-5 as a cracking agent could subsequently provide suitable carbocations for incorporation into DHC reactions taking place over the surface of the acid activated clay. A 5% w/w addition was made to standard Fulacolor, with the hybrid catalyst being noted as F5ZCC. To prevent excessive overcracking, 5% was selected as it represented a small enough quantity without being too little.

²⁶⁶ M. D. Romero, J. A. Calles, A. Rodriguez & A. de Lucas, *Microporous Materials*, **9** (1997) 221 – 228.

²⁶⁷ P. Cañizares, A. Durán, F. Dorado & M. Carmona, *Applied Clay Science*, **16** (2000) 273 – 287.

2. Sand

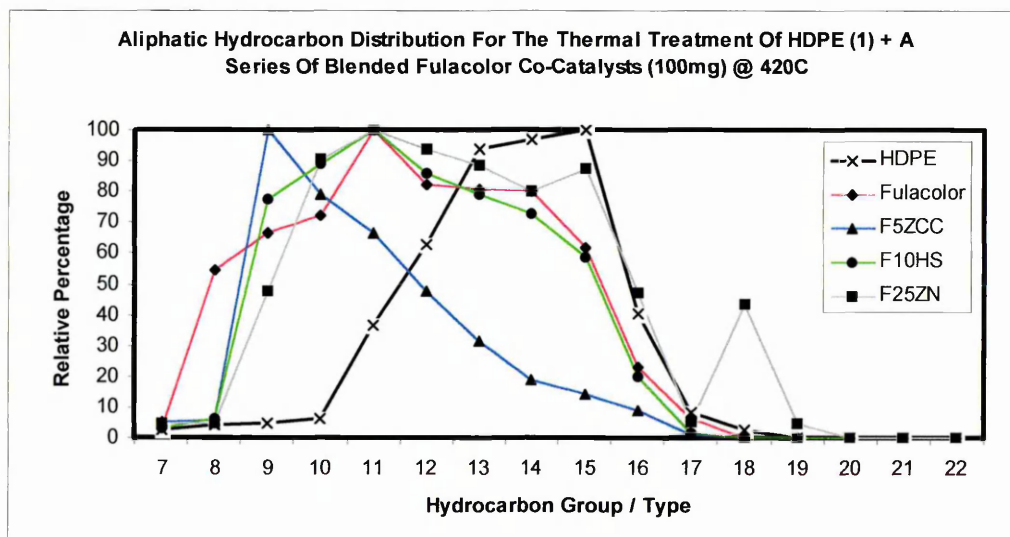
Sand was used to determine the effects of an inert diluent material on the activity of the base Fulacolor. A 10% w/w addition of sand was made to Fulacolor, with the product identified as F10HS. 10% was selected arbitrarily as a dilution factor, so as to assess the effect of such a diluent.

3. Zenith-N

Zenith-N is an unmodified montmorillonite of Greek origin, which had been shown previously (results not shown) to exhibit skeletal isomerisation activity similar to that seen for unmodified SWy-2 (Figure 75). The potential combination of the isomerisation activity of Zenith-N with the DHC activity of Fulacolor, may yield an admixture with the appropriate reforming behavior to give product streams with compositions like those found in commercial fuel mixtures. Zenith-N was added to Fulacolor as a 25% w/w dilution (F25ZN). 25% was chosen to ensure that any enhancement seen in the isomerisation activity of the hybrid mixture was evident.

Figure 93 illustrates the effect that these hybrid mixtures had on the relative n-alkane distributions attained. Standard Fulacolor is also presented for comparative purposes.

Figure 93 – Aliphatic Hydrocarbon Distribution Achieved Over Fulacolor Admixtures

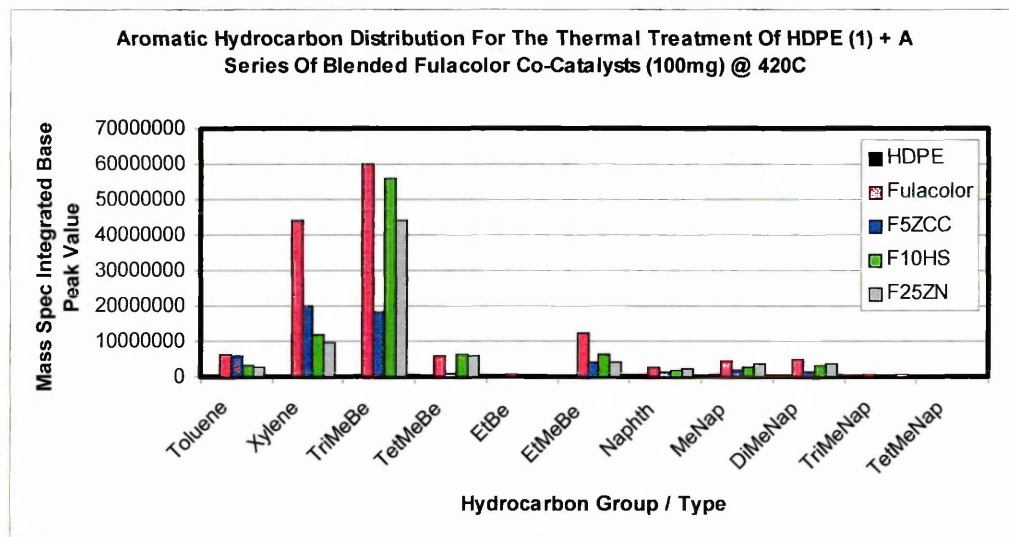


The data above clearly illustrates the effect of incorporating strongly acidic H⁺ZSM-5 into the catalyst bed. The n-alkane distribution has shifted significantly towards shorter chain alkanes in accord with the anticipated behavior of H⁺ZSM-5 which as a consequence of its inherent acidity is active in alkane cracking.²⁶⁸ In addition, the trace for the zeolite containing admixture trails off towards higher order analogues, indicating the increased susceptibility of such species to cracking.

In the case of the admixtures containing sand and Zenith-N, no real deviation is observed when compared directly to the Fulacolor trace. This indicates that the sand is too inert to crack long chain n-alkanes.

The effect of the incorporation of these various admixtures on DHC activity was also determined (Figure 94).

Figure 94 – Aromatic Hydrocarbon Distribution Achieved Over Fulacolor Admixtures



Again, the most significant alteration of the Fulacolor data set occurs with the addition of H⁺-ZSM-5 as co-catalyst. In this case, overall DHC activity is significantly

²⁶⁸ G. L. Woolery, G. H. Kuehl, H. C. Timkin, A. W. Chester & J. C. Vartuli, *Zeolites*, **19** (1997) 288 – 296.

lower than seen with Fulacolor, with selectivity towards the xylenes and trimethylbenzenes being particularly affected. This is in all probability the result of high levels of feedstock alkene cracking over the surface of the H⁺ZSM-5 inclusion. These observations are analogous to the results presented in figure 88c for H⁺ exchanged Fulacolor, although trimethylbenzene production was affected to a much lesser degree in the case of the latter. One possible explanation to account for this observation may be the cross exchange of protons from the zeolite to the clay, with the corresponding back exchange of the Fulacolor exchange site cations to the zeolite matrix.^{266,267} This would yield a partially proton exchanged Fulacolor, the activity of which, in respect of HDPE pyrolysis gas transformation, has been determined previously and is mirrored here.

Note that the addition of both sand and Zenith-N to the catalyst bed, alters both the activity and selectivity of Fulacolor in that xylene production is markedly reduced. Changes relating to the formation of differential equilibria between the various poly methylated single ring aromatics is one plausible explanation. Effects relating to the possible physical blockage of the pore structure of Fulacolor by these co-catalytic materials can be discounted on the basis that in the case of both F10HS and F25ZN, levels of the trimethylbenzenes remain high, thereby suggesting that the surface pore structure remains available for transformation. In the case of F25ZN, while aromatic production remains high, it can be seen to fall by 33% relative to the Fulacolor only run. This assessment can be clarified by examination of the nTIC trace for the run performed using Zenith-N as co-catalyst (not shown). As anticipated, the incorporation of Zenith-N has the effect of providing low levels of skeletal isomerisation reactions to render the formation of branched aliphatics. Levels of these species remain low in contrast to other acid activated clays surveyed herein, although their formation emphasises the potential competition between the execution of skeletal isomerisation and aromatisation reactions over the surfaces of

these modified minerals. Likewise, it also highlights the possibility of using hybrid mixtures to tailor catalytic activities to particular applications.

It has been proposed that hybrid catalysts containing zeolites combined with irreducible oxide co-catalysts such as silica and alumina can be up to twice as active in promoting the aromatisation of short chain alkanes than the zeolite itself.²⁶⁹ In addition, intentional contamination of the co-catalyst with certain oxides further enhances this ability. In view of this information, attempts were made to contaminate sand (irreducible silica) with Pt, followed by calcination in air to yield the appropriate oxide. Combination of this co-catalyst with Fulacolor was found to support these findings in respect of an increase in total aromatic production. However, selectivity was affected, with xylene diminishing and toluene increasing. In keeping with previous observations, the effect on trimethylbenzene production was minimal, thereby confirming the preferential formation of this product, over the pore structure and associated acidity of Fulacolor. There was evidence to support a reduction in the levels of short chain alkanes in the product streams. This suggests that the increase in DHC behaviour is a direct result of the catalytic matrix acting on these feedstock components. This material was prepared by washing the sand with an acidic solution of Pt metal, and calcining in air. The dilution effect noted previously with sand (F1OHS) in which the total number of acid sites was reduced was not seen here. This may arise due to the enhanced efficiency of the post cyclisation dehydrogenation function which is required to promote DHC reactions. In addition, reaction of the alkane components of the feedstock gas is not facilitated over the Fulacolor/Sand mixture, although in the case of the Pt treated material, this is the case.

²⁶⁹ R. Le van Mao, J. Yao, L. A. Dufresne & R. Carli, *Catalysis Today*, **31** (1996) 247 – 255.

Again, trimethylbenzene has proven to be the preferred product over these materials. However, it is entirely possible that this material is not the species formed at the active sites. It may be that as a consequence of diffusional barriers, aromatics formed at the sites responsible for DHC are forced to rearrange to leave the pore structure. While in zeolites, the pore network is closed to some degree, it could be expected that the external pore structure is more open, thereby limiting diffusional pore constraints. This improves the selectivity of Fulacolor arising through size selectivity of the pores themselves.

No data is available regarding the effects of individual isomers of the products surveyed as a result of the modification processes described here.

In order to understand the unusual behaviour of Fulacolor in contrast to other acid activated smectites used in this work, a further series of analyses were performed. The material was subjected to a detailed thermogravimetric analysis to determine its actual thermal behaviour. Two runs were performed, under the following conditions;

1. 35 – 800°C at a ramp rate of 10°C / min⁻¹ under an atmosphere of nitrogen.
2. 35 – 420°C at a ramp rate of 10°C / min⁻¹ under an atmosphere of nitrogen.

This initial heating stage was followed by a 1 hour isothermal segment during which the material was held at 420°C for 1 hour, as in the transformation process.

The Los Trancos beidellite used in the manufacture of Fulacolor was also subjected to the above regimes to provide a means of comparison. Data relating to total, dehydration and dehydroxylation weight losses are given in table 39.

Table 39 – TGA Data for Fulacolor and Los Trancos Under Dynamic Conditions

	Fulacolor	Los Trancos
Dehydration Weight Loss (%)	14	9
Dehydroxylation Weight Loss (%)	4.5	5
Total Weight Loss (%)	18.5	14

Clearly, the major differences in the thermal behaviour of these materials relates to their percentage weight loss attributed to dehydration. As anticipated, surface area enhancements achieved via the acid activation process promote the physisorption of water and thus present enhanced water sorption levels in the activated product relative to the base clay.

As evidenced by the data in table 39, Fulacolor gives rise to a 4.5% dehydroxylation weight loss under dynamic conditions. This weight loss, attributable to structural degradation, occurs over the temperature range 380°C to 800°C, under isothermal

conditions, Fulacolor behaves similarly. The material can be seen to give rise to a 4.1% dehydroxylation weight loss over the temperature range 380°C to 420°C and while isothermal at the upper temperature for 1 hour. This means that under the thermal profile used in the catalytic process, Fulacolor loses 91% of its structural hydroxyl groups. This means that water is evolved from the surface of the modified mineral throughout the transformation process and opens up the possibility of hydrating the alkenes in the feedstock gas to yield alcohols. However, none of the products isolated from the Fulacolor transformed product stream contained oxygen atoms in any functional grouping (table 37 – chapter 10). It should be noted that in the practical interpretation of mass spectral data, alkenes and alcohols often share molecular ions, and sometimes fragment ions, thus making definitive identification of these species difficult. In the case of alcohols, the formation of the molecular ion is often accompanied by rapid decomposition of this metastable species, through the elimination of water, to give a misleading representation of the relative molecular mass of the molecule from which it was formed. The mass to charge ratio of these ions is identical to that yielded by alkenes in the formation of their molecular ions, and as such, care must be exercised in assigning functionality to ions identified in mass spectra. Reference to table 37 shows that only 4 aliphatic alkenes were identified. The spectra for these species were examined to ensure that they were not of alcohol origin. Confirmatory evidence was provided on the basis of the low number of unsaturated aliphatic species present. The potential formation of aromatic alcohols can be discounted, as none of the spectra associated with the aromatic species produced over Fulacolor showed any evidence of oxygen containing fragment ions. In addition, water (m/z 17 and 18) was not a feature of the spectra for these products, which would indicate that the decomposition mechanism for alcoholic molecular ions outlined above was not operating.

Two key points arise from this discussion, these being the very low onset temperature of dehydroxylation seen with Fulacolor, and associated with this, the potential for the material to exhibit proton delocalisation (2.5.2.1).^{83,84,85}

One of the major advantages of the synergic chemical analysis system, is the identification of molecular species in either real time or in post run analysis. The former was employed to establish the potential evolution of water from the Fulacolor surface under temperature regimes identical to those for the isothermal runs performed. Real time TG-MS was able to show that water was evolved from the surface of Fulacolor under these conditions and that evolution was continuous across the entire duration of the isothermal segment of the run. Despite these findings, no oxygen containing species were apparent in the Fulacolor transformed product stream. Recently, de Lucas *et al*²⁷⁰ have presented data showing that the incorporation of water into hydrocarbon feedstocks has the effect of reducing the deactivation of H⁺ZSM-5 arising from coke deposition. The authors attributed this to the transformation of strong Brønsted acid sites into weak Lewis acid sites which has been demonstrated to occur when zeolites are treated with water at high temperature, with coking being promoted by the former. Aromatisation activity was not affected by either the inclusion of water, or indeed the amount. Attempts to reproduce the data under nitrogen were unsuccessful, thereby confirming water as the active species.

Fulacolor produced the least coke of the all the materials studied, despite its high levels of surface acidity. This coincides with the observations of de Lucas *et al*²⁷⁰, and may also explain why Fulacolor is so active in executing DHC reactions. In the absence of physical pore blockage by coke deposition, all active sites, including those responsible for DHC, remain available for longer and thus their DHC efficiency is

²⁷⁰ A. de Lucas, P. Cañizares & A. Durán, *Applied Catalysis A: General*, **206** (2001) 87 – 93.

extended. Assuming coke deposition to be a Brønsted aided process, and bearing in mind the role of protonic catalysis in inducing cyclisation of linear alkenes, the low dehydroxylation temperature of Fulacolor may be advantageous. As the surface continuously degrades as a consequence of water evolution, coking is inhibited. Concurrently, as detailed in chapter two, the continuous renewal of the surface hydroxyl groups by mobile protons and hydroxyl groups from within the mineral matrix, during the dehydroxylation process, provides fresh surface hydroxyl groups for active participation in aromatisation reactions.

CHAPTER
TWELVE

-Discussion Forum-
Acid Activated Smectites

12. AA-CLAY CATALYTIC ACTIVITY DISCUSSION

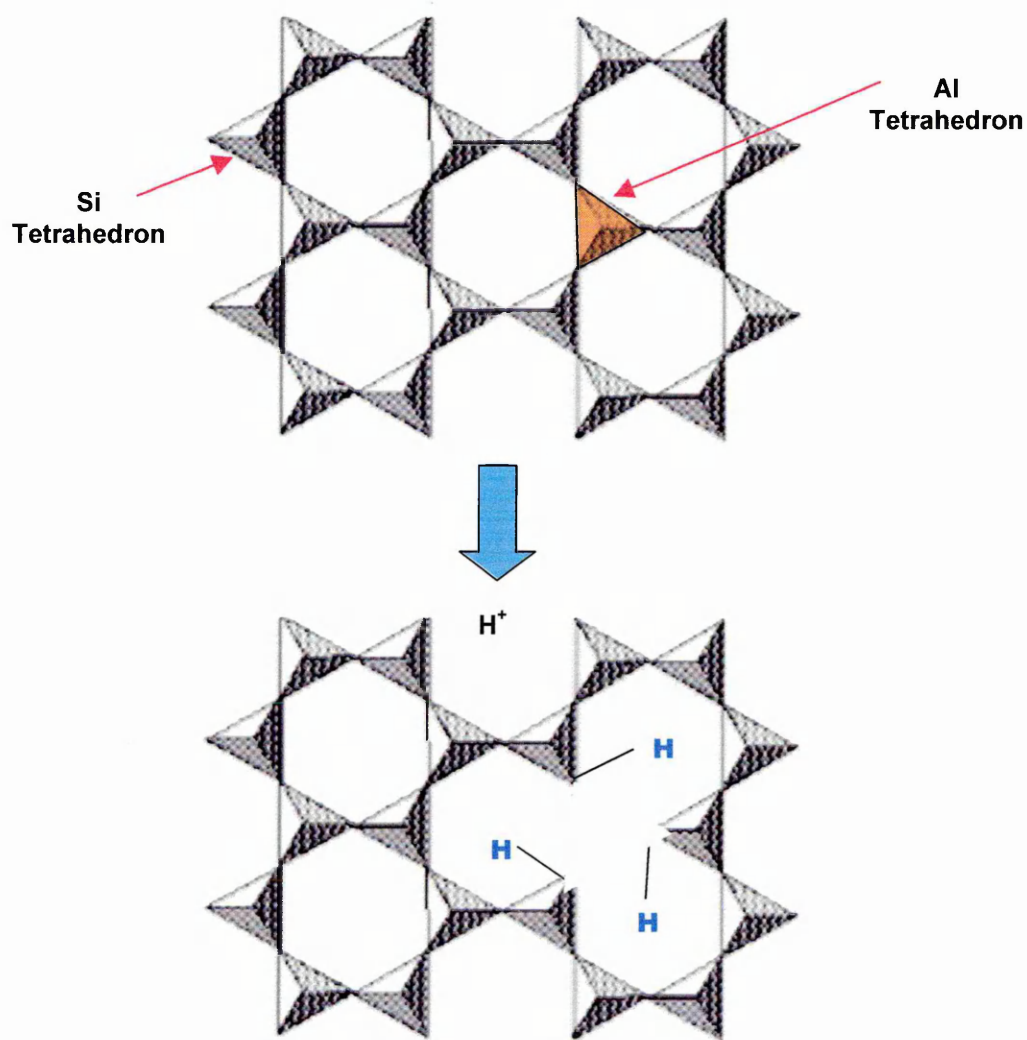
The fact that Fulacolor is so active in promoting DHC reactions relative to other acid activated smectites may relate to the types of hydroxyl groups on the surface. While the inhibition of coking is clearly important in maintaining cyclisation behavior, the types of active sites available for interaction with the feedstock gas molecules is equally as important. This work shows that unmodified minerals are poor transformation agents, which indicates that the catalytically active groups are either installed or exposed as a consequence of the acid activation procedure. As unmodified clays naturally possess aluminol, magnesol and silanol groups on exposed surfaces at loci of sheet termination,⁹⁷ a degree of activity for HDPE transformation may be anticipated. However these groups are probably removed by the activation process which leaches octahedral cations from the layer, consequently modified minerals could be expected to be less active than untreated clays. This is clearly not the case.

12.1 SURFACE LOCALISED ACID POOLS

Most smectites contain some Al^{3+} for Si^{4+} isomorphous substitution in their tetrahedral sheets (<10%). Beidellites are so classified because they contain >10% of Al^{3+} for Si^{4+} substitutions in their tetrahedral sheets. It has been demonstrated that during the activation of smectites with hot mineral acids, dissolution rates of both octahedral and tetrahedral Al^{3+} is comparable.^{123,124} Moreover, when clusters of Al are removed from adjacent sheets within tactoid units, there exists a possibility for interlayer and intralayer silanol crosslinking.¹²³ However, where individual Al^{3+} ions are leached from the tetrahedral sheets, such crosslinking reactions cannot occur. Likewise, localised structural rigidity of the mineral matrix prevents cross polymerisation of silanol groups,¹²⁴ and results in a situation where three neighboring silica tetrahedra are left with unsatisfied valencies. In the proton rich environment provided by the treatment acid, the most likely event is the direct protonation of these $Si-O^-$ groups to yield

structural silanol groups. As a consequence of the rigidity installed to the arrangement by the mineral sheets, the result of this protonation is a localised region on the sheet surface which contains a relatively high concentration of strongly Brønsted acidic silanol groups. Essentially, this process results in the formation of what could be termed a Surface Localised Acid Pool (SLAP) which is illustrated in figure 95.

Figure 95 – Nature of the Surface Localised Acid Pool (SLAP)



Of all the potential structural hydroxyl groups which can be formed on smectite surfaces, aluminol, magnesol and silanol, the latter has by far the strongest Brønsted acidity, a consequence of electronegativity considerations. However, it is of interest to note that pure silica is not acidic despite being rich in silanol groups. This

observation has been explained using ^1H MAS NMR studies of the surface hydroxyl groups of a range of acidic solids.²⁷¹ It has been proposed that when silanol groups are formed in particular environments, such as pores, there exists the potential for these groups to become actively involved in hydrogen bonding. The silanol protons hydrogen bond to framework aluminium (present in the octahedral sheet), thereby altering their acidity characteristics. In addition, interaction with non framework Al cations (present in these activated mineral systems as a consequence of autotransformation) has also been shown to influence the ^1H MAS NMR spectra of these materials, and likewise their acidity. It may be the case that the pore structure of Fulacolor facilitates the formation of hydrogen bonding, and interaction with the Lewis acidic interlayer and more probably the surface exchange site cations, a situation which has the effect of optimising the acidity of the surface silanol groups formed during the activation process. Indeed, room temperature acid washing of Fulacolor gave wash liquors with elevated aluminium contents as determined by ICP spectrometry. These ions are most probably present as a consequence of autotransformation of the activated mineral, to yield an aluminium exchanged material. The resultant, proton exchanged clay, subsequently gave poor performance when employed in transformation reactions.

In the initial stages of activation, the formation of these surface localised acid pools will occur internally to individual tactoid units, although the upper and lower exposed surfaces will be affected. However, as the activation severity increases, as detailed by Pasquera *et al*¹²⁹ and as confirmed by XRD measurements, these tactoids are susceptible to delamination. The effect of this is to expose the upper and lower surfaces of each of the individual smectite layers composing the ordered tactoid. Of the materials used in this work, the acid activated SWy-2 derivatives showed minimal delamination while the commercially available materials, and in particular Fulacolor, were extensively delaminated. The primary consequence of delamination is an

increase in accessible surface area, as individual layers separate. The result of this increased exposure of the mineral to the treatment acid, is that SLAPs formed inside tactoids are now available as surface active sites, when the material is employed in catalytic applications. Effectively, these groupings represent active sites with sufficient Brønsted acidity to protonate double bonds. This contrasts with other possible surface hydroxyl groups, such as aluminol and magnesol groups, which are of weak acidity and can only catalyse double bond shift reactions.²⁹ It has been noted that identical silanol groups are found in catalytically active zeolites including H⁺ZSM-5. In such materials, these 'true' silanol groups (SiOH), in contrast to bridging hydroxyls (SiOHAl), are found in locations of framework defects. Such defects are typically located in regions where Al has been leached from the structural framework as a consequence of hydrothermal treatment.^{271,272} Their occurrence, associated acidity strength, and potential involvement in hydrocarbon conversion reactions have been noted elsewhere.^{273,274} While it remains true that such groups will be formed at edge sites of acid activated smectites, the enhanced freedom of movement associated with the resultant silica fronds aids in the occurrence of inter and intralayer crosslinking to yield passivated products. This in turn limits the accessibility of these edge sites, thereby increasing the role of other surface active sites in the promotion of transformation reactions.

12.2 EFFECT OF ACIDITY ON AROMATIC PRODUCTION

In this work, total aromatic production has been found to diminish as the severity of the acid treatments increases, a finding which contradicts the view that the number of potential active DHC sites increases as a consequence of intensifying the

²⁷¹ M. Hunger, S. Ernst, S. Steuernagel & J. Weitkamp, *Microporous Materials*, **6** (1996) 349 – 353.

²⁷² E.F. Rakiewicz, K. T. Muller, T. P. Jarvie, K. J. Sutovich, T. G. Roberie & A. W. Peters, *Microporous Materials*, **7** (1996) 81 – 88.

²⁷³ J. W. Ward, *Journal of Catalysis*, **9** (1967) 225 – 236.

²⁷⁴ F. Ramôa Ribeiro, F. Alvarez, C. Henriques, F. Lemos, J. M. Lopes & M. F. Ribeiro, *Journal of Molecular Catalysis A: Chemical*, **96** (1995) 245 – 270.

activation process. One viable explanation is that relating to total acidity. This work has shown that the more extensively treated minerals generally have lower levels of total acidity than the lesser treated species. While there are errors in the sampling method, this apparent decrease in acidity may reflect edge site erosion taking place as a result of the operation of edge attack mechanisms during activation (figure 16). These sites may recede to the degree that they are no longer accessible to the probe species. This diminished acidity will prove less active in generating coke and deactivating the catalyst as detailed previously,²⁷⁰ and as evidenced by the lower coking levels associated with the materials surveyed in this work. In the case of Fulacolor, in which water evolution may actively inhibit coking, acidity is high but coke levels are very low, thereby suggesting the operation of supplementary mechanisms.

12.3 INFLUENCE OF TETRAHEDRAL AL ON PRODUCTS

The acid activated smectites surveyed in this work have proven effective in promoting the catalytic transformation of the thermally generated off gases produced during HDPE pyrolysis.

Modified SWy-2 derivatives have been shown to be effective in converting unsaturated hydrocarbons present in the feedstock gases into respectable quantities of a range of methyl substituted single ring aromatics, although selectivity in this regard was low, with similar quantities of mono, bi and tri methyl substituted benzenes being produced. In addition, increasing activation severity had the effect of elevating both the number and quantity of branched aliphatics isolated in the product stream, with little detrimental effect on the aromatic yield. This may suggest that some of the acidic sites on the more severely treated materials are less active in promoting light gas formation, or are perhaps active in catalysing the oligomerisation of short chain hydrocarbons to yield larger molecules capable of forming either aromatics²⁵³ and / or branched alkanes²²⁵.

Similar activities were observed when using both Stebno and Fulacolor as transformation agents in this role. However, one important factor differentiated the activity of these materials, which exhibit isomorphous substitution in their tetrahedral sheets, to that of SWy-2 which, being a montmorillonite does not possess appreciable substitution in its tetrahedral sheets. The beidellitic clays proved themselves to be much more effective in terms of total DHC activity than did SWy-2, although skeletal isomerisation activity is much lower than seen with the latter. In addition, and perhaps more importantly, these acid activated beidellites have exhibited remarkable selectivity towards two particular products, these being m-xylene (1,3-dimethylbenzene) and 1,2,4-trimethylbenzene (12.4). In the case of the Stebno clays, skeletal isomerisation activity was low in all cases, and as shown in chapter eleven, in the case of Fulacolor, there were no branched aliphatic products in the transformed product stream. These observations suggest that skeletal isomerisation activity over acid leached tetrahedrally substituted smectites is minimal at best in contrast to the pillared clays, AAMK's and acid activated montmorillonites used here. A combination of this DHC efficiency and low level skeletal isomerisation activity would provide supplementary evidence for the post cyclisation catalytic alkylation mechanism being the primary route for the formation of substituted aromatics in these transformation reactions.¹⁵¹

12.4 PRODUCT SELECTIVITY - MECHANISTIC FACTORS

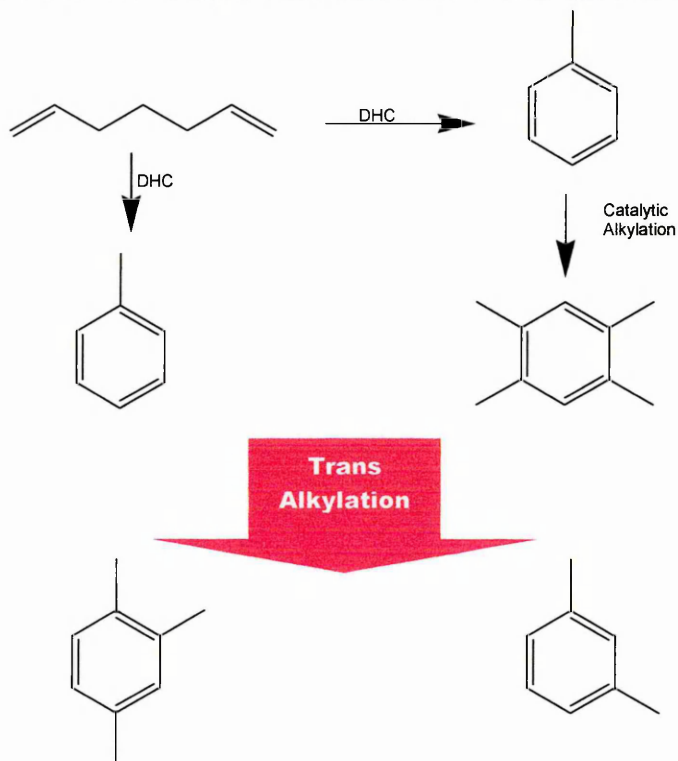
As detailed previously, unsaturated hydrocarbons of chain lengths greater than C₇ will be subject to potential DHC reactions in the presence of solid acid catalysts. Under catalytic reforming conditions, the resultant aromatics undergo side chain cracking to yield toluene²⁹. The methyl substituent of toluene has the effect of activating the aromatic ring with respect to electrophilic aromatic substitution (EAS). As a consequence of the positive inductive effect of the methyl group, incoming electrophiles (R⁺) are directed into positions ortho and para to the original methyl

group. The result is the formation of 1,2,4,6-tetramethylbenzene. In cases where the incoming electrophile has more than 1 carbon atom, following its attachment to the ring system, it too will undergo side chain cracking to yield a methyl group.

In addition, following the ring closure reaction and subsequent dehydrogenation to yield the aromatic, alkylation can be promoted via a second mechanism in which short chain alkenes present in the feedstock gas can become adsorbed onto the surface of the transformation agent surface via an interaction with siloxane bridge protons.¹⁵¹ The resultant charged species has electrophilic properties and can participate in ring alkylation reactions.

The low levels of tetramethylbenzene found in any of the product streams examined in this work would appear to dismiss the feasibility of this mechanism. However, this reaction sequence is in keeping with the results seen over the activated beidellites. While levels of toluene and tetramethylbenzene are low, those of xylene and trimethylbenzene are high. These observations can be accounted for on the basis of transalkylation reactions. As indicated, low level isomerisation activity over these materials confirms that substituted aromatics result from post cyclisation catalytic alkylation, rather than pre cyclisation isomerisation. This dictates that toluene is the primary aromatic. Its relatively low abundance infers that it undergoes secondary reactions following formation. As described tetramethylbenzene, and particularly the 1,2,4,6 derivative is a potential secondary product. The transalkylation reaction between these primary and secondary products yields both xylene and trimethylbenzene, as illustrated in figure 96.

Figure 96 – Transalkylation of Primary and Secondary DHC Products.



It has been noted previously that Benzene, Toluene and Xylene (BTX Hydrocarbons) comprise the majority of the amounts of aromatics found in transformed product streams generated from polyethylene pyrolysis employing a range of catalytically active materials.^{27,203,230,238} Such findings contradict those recorded here, where benzene has never been seen in the product streams generated over the materials selected for study. This could infer that formation of benzene is inhibited due to the instability of the primary carbocation intermediates generated during its formation, or that any benzene generated is consumed in subsequent reactions. A further point to note is that if, as predicted, toluene is a major primary product of DHC reactions catalysed on the surface of the modified minerals employed in this work, the disproportionation of this species would yield benzene. This suggests that transalkylation reactions are executed preferentially under the acid conditions offered by the modified clays.

12.5 PRODUCT SELECTIVITY – PORE SIZE EFFECTS

It has been suggested elsewhere^{241,272} that the removal of tetrahedrally coordinated aluminium from zeolite type structures has the effect of introducing structural defects to the material surface. The result of structural dealumination of zeolite type structures, including clay minerals, through the removal of tetrahedral aluminium is the installation of a defined mesoporosity to the material surface. Here, the SLAPs represent the structural defect forming on the mineral surface. While no porosity data is available for the transformation agents used here, assumptions could be drawn regarding the size and geometry of these surface features. The selectivity of the modified beidellites to the formation of m-xylene and 1,2,4-trimethylbenzene, both of which have identical minimal Van der Waals radii (7.4\AA^{259}), suggests that the structural defects formed during dealumination of the tetrahedral sheet are influential in the determination of the aromatic product distribution. Such defined geometry in combination with the acidity associated with the features may provide a suitable environment for the formation of products of a given molecular size.

The acidity of the SLAPs is primarily associated with bridged silanols of which these features are composed. While the pore itself would be considered to be catalytically inactive on the grounds that pure silica is non acidic and non catalytically active, it should be remembered that in the case of these clays, the silicon atoms forming these groupings are bridged to residual aluminium atoms comprising the octahedral sheet, thereby forming acidic bridged silanols, AlSiOH .

12.6 PRODUCT SELECTIVITY-PROXIMITY OF ACID SITES

As outlined previously, acid activated clay minerals possess a greater number of milder acid sites compared to most zeolites, the acid sites of which are typically stronger. Materials of lower surface acidity than zeolites have been shown to be effective in the promotion of both the disproportionation and transalkylation

reactions of alkyl benzenes.^{153,240} Both reactions occur via a bimolecular reaction pathway involving a diphenylmethyl intermediate. In the presence of a single reacting species, such as toluene, disproportionation is favoured. While initially this may be the case, the subsequent formation of other BTX hydrocarbons will alter the equilibrium of these species within the reaction atmosphere. Furthermore, in the presence of a second reacting species such as trimethylbenzene, transalkylation becomes the dominant reaction. As the latter mechanisms avoid the formation of benzene, these results would seem to favour transalkylation over the former. In either case, the reacting species must assume positions on adjacent sites. In the case of the AAMK's in which aromatic selectivity was low, it could be concluded that product selectivity is impoverished through a combination of variable pore size, thereby not restricting products to a given molecular size under steric considerations, and secondly, there are insufficient numbers of surface acid sites in close enough proximity to catalyse the transalkylation of aromatics towards a thermodynamically favoured product. In the case of dealuminated beidellites, the prevalence of SLAPs arising from tetrahedral dealumination and subsequent delamination of mineral tactoids to expose these surface defects, may heighten the probability of surface sites being close enough to allow transalkylation reactions to occur efficiently. The limited Al^{3+} for Si^{4+} substitution in montmorillonites would also explain the observations made over these materials, in which both selectivity and total DHC activity were lower than over Stebno and Fulacolor. The activity of the unmodified saponite used in the pillared clay study would also fit in with this mechanism of operation, with the protonated surface siloxane bridges serving as the active sites. In the absence of delamination, fewer sites are available, and as such, DHC activity is inhibited, thereby lowering yield. Reductions in selectivity can be accounted for on the basis of limited pore availability.

Note should be made that transalkylation reactions are proton catalysed. Infra red data for both Stebno and Fulacolor, both of which exhibit, in relative terms, excellent activity and selectivity towards the formation of m-xylene and 1,2,4-trimethylbenzene, suggests that the acidity of these clays is predominantly Lewis in nature at temperatures above 300°C. In the case of the modified beidellites, both of which exhibit limited thermal stability, low temperature dehydroxylation of the clay may aid in its activity. Dehydroxylation of the external surfaces of the clay will initially yield Lewis acid sites. However, proton mobility considerations²⁵⁸, and the potential of the reformation of surface silanol groups as interior hydroxyl groups are lost and diffuse through the matrix, both have the potential to restore Brønsted acidity at high temperature.⁸² This may account for the absence of oxygen containing products in the transformed product streams, with the water of dehydroxylation being used to regenerate protonic sites rather than being used as a reagent for the addition of water across the double bond of feedstock alkenes.

A predominance of Lewis acid sites at the operating temperature would therefore limit transalkylation and disproportionation reactions. In cases where Fulacolor was exchanged with a variety of cations, only certain species, among them Na⁺ and H⁺, had a detrimental effect on xylene yield. This may indicate the importance of the surface exchange site cations in catalytically recombining free hydrogen in order to promote DHC reactions. The inability of small alkali cations to fulfil this role could account for these observations. Likewise, the smaller size of these cations may allow them to reside in the surface pores, thereby removing the acid functionalities associated with these defects on the active surface. Such an effect has been noted previously.²⁵⁸

In cases where xylene production is impoverished, there does not appear to be any parallel increase in any of the other aromatics. This indicates that total DHC activity is

reduced in these cases. Again, in the case of the Na⁺ and H⁺ Fulacolor derivatives, the inability of these ions to catalyse the recombination of free hydrogen is a distinct possibility. In these cases, there are no indications that light gas formation is higher, although the content of branched aliphatics does increase slightly. Such products are formed through the interaction of both alkenes and alkanes with surface protons of low inherent acidity.²²² As small alkaline earth metal cations are known to 'poison' protonic acidity, these observations could be expected. The diluent effect of mixing Fulacolor with other materials has the same effect, and the conclusion must be that this arises as a consequence of a reduction in the total number of acid sites available for transformation. Retention of trimethylbenzene production clearly highlights the stability of this product, and its preferential formation under the conditions employed.

In reality, the number of potential reactions taking place over the surface of acid activated smectites could run to their thousands, and as such, a definitive explanation of the results obtained in this work could never be given within the relative constraints of this discussion forum.

The predominance of DHC over skeletal isomerisation reactions over both Stebno and Fulacolor is indicative of the operation of a primary series of reactions which yield aromatics which subsequently undergo further secondary reactions to yield the products observed.

The distinct contrast in activity observed in those smectites having tetrahedral substitution, and those without is quite staggering. SWy-2 was much less active than the modified beidellites in promoting DHC reactions, but presented considerable activity as an isomerisation catalyst. Such activity may arise due to the lack of a defined pore structure which forces molecules in the feedstock gas to react on the outermost surfaces of these materials. While montmorillonites do exhibit isomorphous

substitution in their tetrahedral sheets, it occurs at levels much lower than seen in beidellietes. However, during acid activation, assuming the conditions to be of sufficient severity, tetrahedral Al will be leached to yield SLAPs. In the case of these materials, initial aromatic formation most probably takes place via similar pathways to those outlined above. Unsaturated molecules in the feedstock gas interact with highly acidic surface silanols to yield toluene, with surface exchange sites recombining hydrogen to enhance aromatisation. In the absence of a sufficient number of surface defects (SLAPs) to promote efficient transalkylation of toluene and secondary aromatic products such as tetramethylbenzene, to yield aromatic products of controlled molecular size, transalkylation reactions are much more random, and as such aromatic production is much less selective. Such reactions may also occur more slowly as a consequence of insufficient controlled acidity and porosity to execute these reactions. This allows other reaction mechanisms, such as skeletal isomerisation to compete more effectively.

The mechanisms of acid catalysed hydrocarbon transformations over solid acids have been known for some time.²⁹ Typically, alkene transformations take place through the formation of adsorbed carbenium ions which form following the addition of a proton to a double bond. Likewise, alkanes are believed to undergo skeletal isomerisation by an identical mechanism, involving direct protonation of the alkane followed by protolytic cracking and protolytic dehydrogenation, to give adsorbed carbenium ions. Of all of the materials studied in this work, none were effective in promoting catalytic cracking of feedstock alkanes, with changes in the aliphatic hydrocarbon distribution being attributable to recombination reactions of fragments produced during side chain cracking reactions of alkyl substituted aromatics.

More recently, quantum mechanical calculations have been used to attain a better understanding of the interactions taking place between acidic surfaces and

adsorbed carbocations.²²² While these studies have provided supplementary evidence for the formation of cyclopropyl intermediates, as detailed in chapter six (figure 42), as the key intermediates in skeletal isomerisation reactions.

The preferential formation of aliphatic isomerisation products over aromatic products over the modified montmorillonites and kaolinites used in this work, must represent differences in the surface chemistry of these materials relative to that of acid activated beidellites. In the case of the former, it could be anticipated that there are a lower number of acid sites of sufficient strength to formally protonate alkenes, and thereby promote DHC. Assuming the silanol groups associated with the formation of surface defects (SLAPs) to be the primary source of these groups, the lower number of such defects generated in minerals exhibiting low levels of isomorphous substitution in their tetrahedral sheets, may force alkenes to react on edge sites as opposed to exposed surfaces. Edge sites present sources of aluminol and magnesol groups, which on the basis of electronegativity considerations, are of lower acidic strength than silanol species. This inhibits their ability to formally donate protons and enhances the execution of reactions involving surface / feedstock interactions, of which skeletal isomerisation is one.

The potential involvement of dynamic protons (section 2.5.2.1) in the mechanisms of hydrocarbon reforming outlined above can be deemed unlikely on the basis that such a phenomenon, while observed in both smectites²⁶⁰ and kaolinites⁶³ does not seem to generate uniform product streams over the materials used here. While the AAMK's and the acid activated SWy-2 derivatives shared similar DHC and skeletal isomerisation activity, the significant differences observed over the beidellites reduce the chances that mobile protons are involved in product selectivity.

In all cases, the apparent broadening of the n-alkane distribution associated with these transformation processes is probably attributable to the hydrogenation of, in particular, short chain alkenes in the feedstock gas which are of insufficient carbon number to undergo cyclisation reactions, using free hydrogen generated in preceding DHC reactions.¹⁷ In the case of this work, the VOCARB™ trap used is not capable of efficiently trapping molecular species with carbon numbers greater than 5 or 6, and this definitive identification of these species has not been possible.

The fact remains that while the chemistry involved in the reforming of hydrocarbons over solid acid catalysts is increasingly understood to more complex levels, the precise mechanisms operating, and their relative effectiveness over competing processes are still not fully understood. Therefore it becomes difficult to directly compare the results seen over some materials, including zeolites, with those seen in this work. While similarities are apparent, the sheer complexity of the effects of acid activation, coupled with the complexity of the feedstock gases in terms of the number and types of species present, limit any definitive conclusions being drawn in regard of the data obtained. While informed assumptions can be made, no complete understanding of the processes operating in these modified mineral / polymer pyrolysis gas systems can be made with 100% certainty.

12.7 CATALYST REQUIREMENTS

Overall optimisation of activity in respect of the execution of DHC reactions may require adhesion to the following requirements;

1. The correct cation residency in the surface exchange sites to promote catalytic recombination of free hydrogen released during aromatisation. Freshly prepared acid activated clays (proton exchanged) have been found to be inactive in this role. Figure 88c illustrates the effect of proton

exchanging Fulacolor, and the subsequent detrimental effect on its DHC activity.

2. A relatively thermally unstable mineral which will actively dehydroxylate at the transformation temperature, thereby inhibiting the deposition of deactivating coke species. A similar effect could be simulated by bleeding water into the feedstock gas stream. Such an addition may facilitate alcohol formation, and further investigations would be required to determine the potential consequences of such an addition. As detailed in chapter two (section 2.5), at their dehydroxylation temperature, many minerals exhibit conductivity, an observation explained on the basis of proton mobility^{83,84}. This important mechanistic aspect of smectite dehydroxylation may provide an alternative explanation of activity. Two distinct mobile proton types have been identified, fully delocalised and free protons, either of which may be active participants in the catalysis taking place. However, in light of the apparent size selectivity of beidellitic clays, and the 'respectable' quantities of methyl substituted aromatics over montmorillonite derived catalysts (which have higher dehydroxylation temperatures than beidellites) would suggest that this is not the primary mechanism of hydrocarbon reforming over these transformation agents.
3. A mineral with high levels of Al³⁺ for Si⁴⁺ isomorphous substitution in their tetrahedral sheets. This will promote SLAP formation and thus provide a suitable environment, in terms of acidity and size, for DHC reactions to occur.
4. Finally, the activation parameters should be chosen to induce delamination without inducing total structural degradation. This would be particularly important when activating minerals which are tetrahedrally charged but have

high octahedral magnesium contents which are highly susceptible to acid leaching, such as saponites. As dioctahedral minerals, beidellites are more resistant to structural attack than saponites, thereby facilitating the use of severe activation parameters to promote delamination.

It can be seen that beidellites clearly represent the best candidates to fulfil the above criteria. It would therefore be useful in future to study synthetic beidellites²⁷⁵ in which tetrahedral sheet composition can be controlled to a degree, in order that a more homogeneous activated product may be obtained. By controlling the position of the tetrahedral isomorphous substitution, it may be possible to generate transformation agents in which those sites required for cyclisation / post cyclisation catalytic alkylation can be optimised.

As highlighted previously, the evolution of volatile species from HDPE begins at around 350°C, a temperature at which the gallery region of smectites will not be available as a result of layer collapse due to dehydration. As such, those surfaces available to the feedstock gas molecules correspond to external pores produced by acid leaching.

At the catalyst surface, the sheer volume of material and number of species present as a consequence of HDPE pyrolysis make a definitive realisation of the actual reaction pathways extremely difficult.

12.8 COMPARISON OF AAC ACTIVITY WITH ZEOLITES

Typically, mildly acid activated clays produce most aromatics, although in the case of the materials used here, molecules larger than ethyltoluene were not present in the transformed product streams. This may be related to the relative stability of

²⁷⁵ J. T. Kloprogge, J. B. H. Jansen & J. W. Geus, *Clays and Clay Minerals*, **38** (4) (1990) 409 – 414.

methylaromatics.^{20,198} Although these findings agree with the work of Uemichi et al, using silica alumina,¹⁶ they contrast with results using the zeolite ZSM-5^{17,27} where in addition to the toluenes and xylenes, benzene was clearly identified. There is no evidence in this work to support the formation of benzene over any of the acid activated clays examined.

One advantage of AAC's over zeolites is the reduction in light gas formation. While there is no quantitative evidence to support this statement, the relative strength of the acid sites of modified minerals are lower than those found in zeolites, and the latter have been shown to be active in light gas formation through alkane cracking.^{29,273,274} Indeed, catalytic degradation over ZSM-5 produces large quantities of low molecular weight gases (C₃-C₄), because this zeolite prevents more than four carbon atoms from entering the channel network – this being a feature which is exploited in the dewaxing process.²⁷⁶ Nevertheless, ZSM-5 does produce aromatics when molecules, pre-cracked on the external surfaces, enter the channel network.²¹ In a detailed study by Ohkita et al,¹⁷ a correlation was made between surface acidity of a series of SA's with differing compositions, and the nature of the products obtained from HDPE pyrolysis. They found that at 400°C, gas production increased with increasing surface acidity. Of the acid activated clays used here, all gave initial increases in surface acidity as the activation parameters became more severe, before declining, but there was never evidence to support elevated levels of light gas production. Indeed, evidence pertaining to alteration of the n-alkane distribution was not obvious. Although relative n-alkane distributions have broadened in some of the cases presented here, this is likely to be the result of cracking, but of a series of reactions involving short chain adsorbed carbocations becoming involved in hydride abstraction reactions to yield short chain alkanes, or through hydrogenation of feedstock alkenes which are too short to undergo direct cyclisation.

²⁷⁶ D. C. Longstaff & F. V. Hanson, *Journal of Catalysis*, **164** (1996) 54 – 61.

It has been demonstrated¹⁹⁸ that H⁺ZSM-5 is not suitable for the reforming of heavy oils derived from polyethylene pyrolysis, despite not coking up readily. The fuel mixture produced had a good octane rating, but potential fuel yield was particularly low at only 20%, with the gas yield at 68%. This is in contrast to proton exchanged (HY) and rare-earth exchanged (REY) zeolite-Y which gave up to 30% less gas. As evidenced by the work carried out on proton exchanged Fulacolor here, proton exchange is detrimental to DHC activity while not significantly altering selectivity (trimethylbenzene), and the effect may be as a consequence of light gas formation, through a process of proton induced cracking. In this respect, proton exchanged clays would mimic the activity of the stronger zeolites. HY contains a larger number of more acidic sites than REY, which in turn leads to a lower potential liquid fuel yield (27% against 49%), and larger amounts of both gas (44% against 35%) and coke (6% against 3%). In relation to coke deposition, these values are significantly higher than ascertained for the AAC's indicating the lower total acidity associated with the modified minerals relative to their zeolitic counterparts. It should be noted that the polymer:catalyst ratios employed in this work are significantly lower than used elsewhere. However, the lack of any quantitative data for these modified materials makes the exact ratio's less of an issue. Future work would rely heavily on the correlation of such a ratio to observed activities in respect of quantitative analysis.

In view of the information above, REY would represent the most suitable choice of zeolite because its bigger pore size allowed heavy oil in and it has fewer acid sites which resulted in a slower deactivation rate and lower levels of coke deposition.

AAC's have a larger number of milder acid sites than most zeolites¹⁶² and they have predominantly Lewis acidity after activation at high temperature.¹³⁰ Consequently, their behavior mirrors that of REY and the large, unsaturated molecules produced during the thermal degradation of HDPE are broken down into smaller molecules. Following this event a variety of reactions occur of which DHC and skeletal

isomerisation predominate, the relative amount of each being determined by the precise make up and acidic strength of the surface active sites on the AAC's.

In the case of the Slovak clays (ST), the greatest relative yield of aromatics was obtained for materials which were found to have high relative acidities thereby confirming the role of surface acidity in promoting DHC reactions. In the case of the SWy-2 derived materials, aromatic yields were relatively low, as were acidities. The most notable correlation between high acidity and efficient DHC behavior was given with Fulacolor. This material demonstrated very high levels of surface acidity which coincided with excellent aromatic yields. Direct comparison between these clays can be made on the basis of their respective aromatic yields relative to the uncatalysed process. Despite the high levels of surface acidity seen with Fulacolor, coking was 25% lower than other AAC's of similar acidity and type (ST30). In addition, coking over Fulacolor was a staggering 125% lower than over JP120 which exhibited lower levels of acidity than the Laporte product, the reverse of the expected. ST30 is derived from a beidellitic clay which was shown by TGA to begin dehydroxylation at temperatures as low as 450°C under dynamic conditions.

As highlighted in the introductory chapters, the proposed mechanism for the dehydroxylation of smectites consists of two independent events⁸². The delocalisation and subsequent interaction of mobile protons with structural hydroxyl groups within the octahedral sheet results in the formation of water molecules, a process which induces the formation of a new metal-oxygen bonds in the tetrahedral sheet. Concurrently, vibrational spectroscopy of heat treated beidellites has shown the appearance of a new band at 3715cm⁻¹ attributed to the formation of structural silanol groups on the exposed surfaces of the tetrahedral sheet, arising from the hydroxylation of coordinatively unsaturated silicon ions on the surface of the mineral matrix. It should be noted that Fulacolor gave rise to a band at 3722cm⁻¹ at

temperatures above 350°C (dehydroxylation begins at 380°C). This provides supplementary evidence to the fact that the DHC activity associated with acid activated beidellites in this role is associated with the types of sites available, and not simply total surface acidity.

While the pyrolysis of HDPE in this work gave very reproducible data, it can be seen from the literature that the composition of polymer pyrolysis gas streams is dependant upon a wide range of factors including the chemical composition of the plastic²¹¹⁻²¹⁴ and the temperature of pyrolysis^{218,219} in addition to other factors including duration and method of treatment. Such factors make it extremely difficult to derive a systematic methodology for the direct comparison of the results presented here, with those in the literature for processes of a similar nature. This, combined with the wide range of materials employed in these transformation roles (zeolites, activated carbon, modified clays, sulphated zirconia) reduces the possibility of drawing meaningful comparisons between data sets without further practical work.

12.9 CONCLUDING REMARKS

This work has highlighted the degree of control which can be exerted over the acid activation of clay minerals, and in particular trimorphic species such as smectites. By selecting suitable starting materials and appropriate activation parameters, it is possible to produce catalytically active materials which are economically viable alternative to more expensive commercially manufactured acid solids such as zeolites. Those aromatic hydrocarbons resulting from the transformation process can be used in a variety of roles, including fuel blending and the production of commodity chemicals including pharmaceuticals.

CHAPTER THIRTEEN

-Conclusions & Further Work-

13. CONCLUSIONS & FURTHER WORK

This work provides impetus to the potential application of modified clay minerals as transformation agents for use in the field of spent polymer recycling. Polymers, and in particular plastics, represent a versatile, durable and variable range of materials which find widespread employment in a vast array of fields. Primarily as a consequence of their relative economy, barrier attributes and aesthetic properties, plastics are routinely selected as the material of choice for a variety of single use disposable items such as food and beverage packaging. Consequently, the volume of spent polymeric materials entering post consumer waste streams is at an all time high, with levels showing scant signs of diminishing in the near future.

In these times of environmental awareness, the waste disposal and treatment strategies of the past have come under increasing scrutiny. Two of the most commonly applied, landfilling and direct incineration have received considerable attention. In the case of the former, the committal of waste plastics to landfill sites means that the valuable chemical and potential energy content of these materials are lost. Likewise, uncontrolled combustion of spent polymeric materials in industrial incinerators generates considerable air pollution, with the emission of carcinogens being of particular concern in respect of human health.⁶

Thermal depolymerisation (feedstock recycling) is viewed as a potential candidate for the future of polymer recycling. While effective in yielding the monomer for many commercial plastics, in the case of the mass manufactured polyolefins, the process yields a complex hydrocarbon mixture, which is unsuitable for blending into virgin polymer resins.

The incorporation of catalytically active materials into existing feedstock recycling programs has proven effective in altering the chemical make up of intermediate

mixtures obtained through established feedstock recycling technologies. By far the most widely employed of the synthetic acidic solids used to effect these preferential hydrocarbon reforming reactions have been the zeolites, and in particular H⁺ZSM-5. It has been found that in addition to enhancing aromatic yields, zeolites offer the economic benefits of lower pyrolysis temperatures,¹⁰ (when the polymer and catalyst are in physical contact) an increase in the rate of polymer decomposition¹⁸ in addition to an increase in product selectivity, and therefore individual component yield.¹⁶

In contrast to zeolites, which represent a commercially manufactured product of high relative cost, clay minerals are a cheap, abundant resource, which following modification through pillaring, acid activation or ion exchange, show appreciable activity towards the catalytic transformation of polymer pyrolysate gases into potentially useful, fuel applicable hydrocarbons.

In particular, this work has highlighted the benefit of combining acid activated clays with HDPE pyrolysis to yield processes, which give transformed product streams rich in aromatic and / or branched aliphatic species.

13.1 MODIFIED MINERAL SUMMARIES

The following sections will emphasise the primary conclusions drawn from the results obtained over each of the modified mineral types investigated. Moreover, any future work which may enhance understanding of the structure / activity relationships of each of the mineral types will be elucidated. Finally, overall conclusions will be presented and collated according to importance in terms of fulfillment of the original aims of this work.

13.1.1 SPANISH PILLARED SAPONITES (R)

While these materials presented good DHC activity, the results obtained indicate that they are too active in the generation of polyaromatic species, which are of little use in commercial fuel mixtures because of their low volatility. (B.Pt of Naphthalene = 218°C) This has the result of lowering the smooth ignition characteristics of fuel mixtures containing hydrocarbons of higher octane rating. The detrimental effect of polyaromatic molecules in fuels can be evidenced by the time and money expended by fuel refiners in eliminating such molecules from their crude oil stocks through catalytic reforming processes.

These pillared saponites are particularly active (relative to single ring aromatic yields) in producing naphthalene and a variety of its methyl substituted derivatives. While the latter are of little industrial importance, the former are widely employed, most notably in the production of phthalic anhydride for incorporation into plasticisers, alkyd resins and polyesters. Similarly, derivatised naphthalenes are important precursors in the synthetic dyestuff industry.

Methyl naphthalenes can be converted to the naphthalene through treatment with hydrogen under conditions of elevated temperature (750°C) and pressure (10-70atm.). Such procedures are costly, and when considered in combination with the cost of separating these materials from the gross product streams generated over these pillared clays, these modified minerals do not present themselves as the most suitable candidates for use as HDPE transformation catalysts. Previous work by Breen et al⁸ has shown that both Al and Fe pillared clays are active in the formation of polyaromatic species when presented with the thermally generated off gases arising from HDPE pyrolysis.

In view of this information pertaining to the lack of selectivity towards the generation of particular aromatics or polyaromatics, and in light of the relatively low total DHC activity (in contrast to AAC's), PILC's do not fulfil any of the original criteria comprising the original aims of this work. In addition, the significant intra batch activity variability of these materials, attributed to difficulties arising from control over the acidity and porosity of PILC's,¹⁵⁵ effectively eliminates pillared clays as potential transformation agent candidates for this type of work under the conditions used here.

Excessive polyaromatic formation could be attributed to the formation of siloxane bridges on the surfaces of mineral tactoids as a consequence of the Al³⁺ for Si⁴⁺ which occurs in saponitic mineral structures. Such groups are strongly protonic and install significant levels of acidity to these materials. The availability of transition metals may also play a role in this activity.

13.1.2 ACID ACTIVATED METAKAOLINS (AAMK)

These materials showed much better reproducibility than demonstrated by the Spanish pillared saponites.

While the activity of these kaolin derivatives towards the generation of single ring aromatics was higher than seen with the pillared clays, they produced few polyaromatic species. However, in respect of the potential formation of commercially viable fuel mixtures, this is not an important feature.

Of all of the materials investigated, this series gave the lowest total aromatic yield in respect of the species surveyed. Moreover, although skeletal isomerisation activity increased slightly as a function of the severity of the activation parameters applied, it never reached significant levels. Combination of the latter two points limits the potential application of these materials in the role envisaged. Similarly, aromatic

yields and selectivities are insufficient to promote consideration of single species isolation from the transformed product streams.

The preferential formation of toluene is in contrast to the selectivity towards trimethylbenzenes seen with smectite derived transformation agents. Assuming toluene to be the primary aromatic product, as detailed previously, the prevalence of toluene in the product stream may indicate that there are insufficient sites to promote catalytic alkylation, or that those sites available are of insufficient acidity. This would result in toluene stockpiling awaiting site availability.

In light of their impoverished activity in the required fields, it is unlikely that investment of future time in modification of these materials to enhance their activity would be beneficial considering the apparent efficiency of modified smectites in this role. Further investigations relating to optimum metakaolin activation would be useful in this regard.

13.1.3 ACID ACTIVATED STEBNO CLAYS (ST)

These materials represent one of two modified beidellitic clays examined during the course of this work. In keeping with observation made over Fulacolor, the Stebno clays exhibit a very characteristic activity in respect of their transformation behaviors.

Over the entire range of acid activated ST derivatives, n-alkane distributions remain unaffected relative to the uncatalysed process. The slight broadening observed (figure 65) may result from the hydrogenation of feedstock alkenes or from the occurrence of hydride abstraction reactions involving adsorbed carbocations formed during alkene protonation.

A second notable aspect of their activity, which reflects that of Fulacolor, is the DHC efficiency of these materials. While it diminishes significantly with the severity of the acid treatment, it is initially high after the least severe of the treatments used (ST30). Similarly, the materials demonstrate appreciable selectivity towards the generation of xylenes and trimethylbenzenes, a trait not seen with any of the other acid activated smectites used in this work, other than Fulacolor.

A final similarity between the two relates to isomerisation activity. Branched aliphatic production enhancements across the range of ST clays used occurs at the expense of aromatics, with the latter being formed in preference over the lessor treated analogues. Likewise, the high aromatic yield over Fulacolor occurs alongside an almost zero level of branched aliphatic species.

In the light of these findings, two potential further avenues of investigation exist. In respect of commercial fuel formation from waste HDPE, more extensively treated derivatives than those employed here could be used to determine the point at which aromatic yields diminish to the point that their content in the transformed product streams is negligible, with skeletal isomerisation reactions predominating over the catalyst surfaces.

Secondly, in the absence of true quantitative analysis in this work, such investigations could be performed to determine if aromatic yields are sufficient to allow for isolation of the more abundant species.

13.1.4 ACID ACTIVATED SW_y-2 (SW_y2-XA)

In reference to the potential application of these HDPE transformed product streams directly as commercial fuels, these materials represent the most suitable candidate examined.

While aromatic selectivity is poor in contrast to all of the other modified smectites investigated, total aromatic production is high, although divided across the entire range of methyl substituted single ring aromatics selected for analysis in this work.

In addition, the more extensively treated clays present respectable quantities of branched aliphatics, without significantly affecting levels of the single ring aromatics. This combines to ensure that the product hydrocarbon mixture is rich in highly octane rated species. This would make these modified montmorillonites ideal candidates for the conversion of HDPE waste into commercially viable fuels. Similarly, the Fulcat clays, and in particular Fulcat 22B, were also active in both DHC and skeletal isomerisation, more so than SWy-2. K10 was a less active isomerisation catalyst.

Again quantitative analysis would provide critical confirmation of the suitability of these modified minerals in the role described.

13.1.5 COMMERCIAL ACID ACTIVATED CLAYS

Of all of the materials screened in this work, these products have been shown to present the most interesting data. In particular, Fulacolor has proven to be an invaluable test bed for understanding the behavior of modified smectitic clays as hydrocarbon transformation agents.

The DHC of linear alkenes on modified mineral surfaces has the potential to occur at one of two potential locations. Structural silanol, aluminol and magnesol groups are formed at edge sites as a consequence of edge attack mechanisms operating during the activation treatment. Similarly, isomorphously substituted Al^{3+} resident in the tetrahedral sheets of most smectites (>10% in beidellites and saponites) is eliminated during the acid activation process. Leaching of point loci individual Al^{3+} ions has the potential to yield SLAP's which as a consequence of the tactoid

delamination effects of activation become exposed in the modified product. Such sites represent a highly concentrated localised source of strongly Brønsted acidic silanol groups, which are readily accessible on exposed surfaces, free from potential interference from insoluble silica deposits which can lead to the passivation of edge sites.

The greater potential for the formation of SLAPs in acid activated beidellites can be accounted for on the basis of the excellent DHC activity demonstrated by these materials, thus inferring that the sites responsible for the execution of DHC reactions (strong protonating groups) are not affected by passivation, and therefore may not be resident at edge sites.

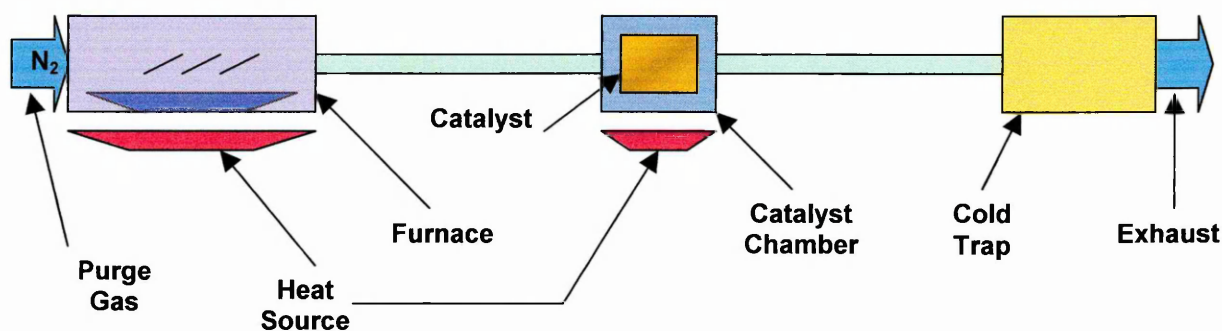
Although not used in this work, ²⁷Al MAS NMR could be used to confirm the loss of tetrahedral Al in Fulacolor relative to the unmodified Los Trancos clay. Unfortunately, due to technical problems with the instrumentation used to acquire the data presented, it was not possible to run the Los Trancos clay as a transformation agent. However, this would be a future priority for the overall progress of this work.

While Fulacolor renders a hydrocarbon product stream with no potential application as a fuel, its notable aromatic selectivity and corresponding activity do present the possibility of isolating the major aromatic product (trimethylbenzene) and using this route as a source of the chemical. While trimethylbenzenes have little industrial importance currently, it is readily convertible to benzene through a process of demethylation. Benzene remains the fundamental building block for a wide range of consumer end products including pharmaceuticals and polymers. Alternatively, such an aromatic rich effluent could be employed on refinery sites for use in the process of upgrading low quality fuels through a process of blending.²⁷⁷

²⁷⁷ R. D. White, *Drug and Chemical Toxicology*, **22(1)**, (1999) 143 – 153.

Attempts to alleviate the lack of quantitative analysis in this work was considered through construction of a flow reactor, a diagrammatic representation of which is given in figure 97.

Figure 97 – Diagrammatic Representation of Flow Reactor



The flow reactor was manufactured entirely from 316 stainless steel components supplied by Swagelock®. The transfer lines were made from stainless steel tubing (1/8 inch i.d. x 15cm length), and were insulated with fire retardant materials. The furnace was made from stainless steel tubing (1/2 inch i.d. x 5cm length). HDPE pellets were positioned in a specially crafted stainless steel vessel and inserted into the furnace prior to purging and heating. The catalyst chamber was a Tee Type in-line removable filter into which the powdered catalyst was packed. The cold trap was a glass cold finger cooled by means of an ice bath. The appropriate fittings were used to connect the various components of the system. The purge gas was pre heated by passing the nitrogen through a stainless steel coil housed in a low temperature tube furnace. The catalyst chamber was heated by means of a cartridge heater positioned in an aluminium heating block secured against the metallic catalyst chamber. The primary heating source for the furnace was a highly rated heating tape. Under the test conditions employed, the heating tape failed, thus maintenance of the required temperatures was not possible. No suitable alternative heating sources were available within the proposed budget, and as such, the flow

reactor was not able to provide the required quantitative data for which it was commissioned.

This piece of equipment is invaluable to future work, and investment in adequate heating apparatus will yield a facility capable of high throughput analysis of sample. In particular the effect of catalyst temperature could be determined in respect of the activity of these materials. It may be the case that the catalysts will function efficiently at temperature significantly below the polymer pyrolysis temperature. These variable can not currently be operated independently using the synergy system in its current configuration.

13.2 ACTIVITY SUMMARY

One of the most important conclusions relating to the work presented herein, must relate to the variability of the activity of the materials screened. In particular, the nature of the starting materials has proven itself to be of prime importance in the determination of the physiochemical properties of the modified minerals used in this work. Kaolinite has been seen to exhibit activity different from that of some smectites, while being similar to others. Within the latter group, differentiation has been made between montmorillonites and beidellites. The ultimate conclusion must therefore be one which is representative of these findings.

When this project was proposed, the initial aim was to identify modified minerals (ion exchanged, acid activated or pillared) which were potential candidates for use in the role of a cheap disposable catalyst for application in the recycling of spent polymeric materials. The benefits of employing post pyrolysis transformation agents to enhance liquid hydrocarbon yields is well established, with a variety of materials being used in the role, including synthetic silica alumina's^{12,24,27,201}, solid super acids²²⁷ and most notably zeolites.^{202,228,230,231}

A key study in the field, which compared the relative effectiveness of silica alumina's and zeolites was made by Songip *et al.*²²⁹ This work concluded that, in terms of fuel formation, with its octane requirements, zeolites are unsuitable as a consequence of their, limited pore geometry, high acidity, leading to impoverished shape selectivity and excessive overcracking of feedstock molecules to light gases. While zeolites are suitable for the treatment of crude oil feedstocks to yield fuels, their activity in respect of handling the smaller molecules arising through polymer pyrolysis is detrimental to the octane rating of the product mixture.

Of all of the materials used, Fulacolor has given the most unusual results. However, there are certain observations which could account for its activity. Of all of the materials screened, Fulacolor gave one of the lowest coke levels. Coking precursors are generated through the hydrogenation of surface adsorbed species.¹⁶ The efficient catalytic recombination of the free hydrogen generated during the DHC of unsaturated hydrocarbons to yield aromatics has the effect of lowering the level of coke deposition. This subsequently ensures that those acid sites required for reforming are available for longer, and are not obstructed through physical coke deposition.

As outlined previously, fuel quality can be enhanced by elevating the quantity of aromatics and or iso-alkanes in the fuel mixture. In particular, fuels that require high specifications and burning characteristics such as those used in commercial jet engines, have very high levels of aromatics and branched aliphatics.^{21,277}

While Fulacolor outperformed all of the competing materials in terms of total DHC activity and selectivity, iso-alkane production was non-existent, and as such the product mixture obtained over this transformation agent would be unsuitable for application as a fuel. Isolation of the m-xylene and 1,2,4-trimethylbenzene which predominate over this material would yield a bulk chemical supply of these desirable

products. M-xylene in particular is used in the manufacture of terephthalic acid which is used as a monomer for the production of the plastic polymer polyethylene terephthalate (PET) which is used extensively in the manufacture of disposable bottles for use in the soft drinks industry. While none of the isomers of trimethylbenzene are of industrial importance in isolation, current stocks are used as blending agents to increase the octane rating of fuels which are below specification for their intended application. Small amounts are also used in the preparation of trimellitic anhydride.

Despite its high surface acidity, Fulacolor was not heavily coked, thereby providing supplementary evidence to support the inhibition of coke formation through the evolution of water, arising from the low thermal stability of this material, even at low temperature.

In the case of Stebno, aromatic production was about 50% of that seen with Fulacolor, but the production of iso-alkanes was also a feature. Although these species were not in abundance, when compared to the modified montmorillonites used, the combination of aromatic production, even with low level isomerisation activity yields the potential to use the product mixture in fuel applications. Despite the fact that aromatisation activity is lost in favour of isomerisation activity as this material is subject to increasing amounts of activation, even with ST240, it is questionable as to whether skeletal isomerisation activity would be sufficient enough to produce fuels of adequate quality.

In the case of SWy-2, aromatic selectivity is low, and total DHC activity is lower than seen with either of the beidellitic clays employed. However, branched aliphatic activity is respectable and is seen to increase with increasing levels of activation without any apparent loss of aromatic product formation. This particular combination would, of the materials surveyed, perhaps present the most realistic possibility of

generating a fuel of sufficient quality to be used commercially. Although selectivity is low in regard of aromatic formation, this point is of no importance, because methyl substituted aromatics are all ranked similarly in terms of their RON's.

The AAMk's were not active DHC catalysts, and isomerisation activity was also somewhat retarded. These materials were subject to heavy coke formation, and this may account for their stunted activity. These materials appear to have been active in broadening the n-alkane distribution, a process involving the hydrogenation of feedstock alkenes. This would suggest that these materials were ineffective in promoting the catalytic recombination of free hydrogen resulting from DHC, and as such the resultant hydrogen being available for feedstock hydrogenation.

The mixed metal pillared clays have shown themselves to be the least suitable materials to yield commercially viable fuel mixtures. The apparent high level of polyaromatic formation is the result of significantly lower aromatisation activity, thereby giving a disproportionate representation of the actual activity

13.3 CONCLUDING REMARKS

This work has highlighted the relationship between the surface acidity of modified minerals and their associated transformation behavior in respect of the conversion of HDPE pyrolysate gases into potentially useful hydrocarbons. In particular, those species of high octane rating which would constitute advantageous components in a commercial fuel mixture have been of particular interest.

There are typically two such types of species, namely aromatics and branched aliphatic hydrocarbons. Higher relative percentages of the former constitute a prerequisite for enhancing the quality of any hydrocarbon mixture intended for commercial fuel applications.

This work has emphasised that in the case of acid activated smectites, appropriate activation parameters can be selected to exert control over the resultant chemical and physical properties of the activated products. These properties can be tailored to fulfil requirements in terms of the hydrocarbon reforming activity of the modified mineral.

This most basic of summaries does not explicate the entire situation. As shown by the work using modified derivatives of Fulacolor, the resident exchange site cation is important in aiding aromatisation reactions, having particular effect on product selectivity.

This work has also given credence to the relationship between residence time and product selectivity. Isothermal runs have been shown to favour the formation of cyclic species when compared to runs using the same transformation agent in higher temperature applications (dynamic).

Of the AAC's employed as transformation agents in this work, those exhibiting the highest levels of acidity have both been derived from beidellitic clays. In addition, both have shown minimal (ST) or no (Fulacolor) activity in respect of the formation of branched aliphatics through a mechanism of skeletal isomerisation. These findings are indicative of the fact that the hydrocarbon reforming activity of these materials is related not only to total accessible activity, but also to the strength of the acid sites available for interaction with the feedstock gas molecules. It has been shown previously²⁹ that sites offering weakly Brønsted acidic protons are active in promoting double bond shift reactions. Those of intermediate strength effect skeletal isomerisation reactions, while those Brønsted acid sites of highest strength (SiOH) allow for the direct protonation of unsaturated hydrocarbons to yield carbocations, this being the first stage of the DHC sequence leading to the formation of aromatics.

All smectites hold the potential for the formation of SLAP's when activated in hot concentrated mineral acids. Such features are likely to be more prevalent on the exposed surfaces of beidellites as a consequence of their substitution patterns. Thus beidellites would be expected to have a greater number of more strongly Brønsted acidic protons than minerals whose active sites predominate at their edge of each individual tactoid unit. Such sites, although containing silanol groups readily become depleted as the activation proceeds via the afore mentioned edge attack mechanism.

Overall, the type and associated strength of the acidic sites installed (mineral dependant) and the degree to which these sites are available through delamination effects (activation dependant) combine to provide a means of manufacturing these materials to promote certain reaction, such that the composition of the product stream can be engineered to benefit the world of polymer recycling.

CHAPTER FOURTEEN

- Conferences Attended-
- Postgraduate Studies-
- Publications-

14.1. CONFERENCES ATTENDED

◇ = Denotes the presentation of a poster at this event.

* = Denotes the presentation of an oral contribution at this event.

'Industrial Catalytic Processes'
University of Bath, UK
21st – 26th November 1998
(Institute of Applied Catalysis)

'Infra Red & Raman Discussion Group'
Sheffield Hallam University, UK
1st – 2nd July 1999
(I.R.D.G.)

'Industrial Clays'
University of Exeter, UK
16th – 19th April 2000
(The Mineralogical Society – Clay Minerals Group)

◇
'The Use of Acid Treated Swy-2 Derivatives in the Catalytic Transformation of High Density Polyethylene'

'Engineering Catalytic Chemistry'
University of Durham – Stockton Campus, UK
18th – 22nd July 2000
(Royal Society of Chemistry / Institute of Applied Catalysis)

'The Mineralogy of Waste & Waste Disposal'
British Geological Survey – Keyworth, UK
15th September 2000
(The Mineralogical Society – Applied Mineralogy Group)

*
'The Catalytic Transformation of Polymer Waste Using Modified Clay Catalysts'

'Materials Research Institute – Research Open Day'
Sheffield Hallam University, UK
16th January 2001
(Materials Research Institute – Sheffield Hallam University)

◇*
'Synergic Chemical Analysis'

'Mid European Clay Conference'
Slovak Academy of Science - Bratislava, Slovakia
8th – 15th September 2001
(European Clay Groups)

◇
'Preparation and Characterisation of Dealuminated Metakaolin and its Use in the Transformation of Waste Plastics to Aromatic Hydrocarbons.'

14.2. POSTGRADUATE STUDY

The following taught units were attended as an integral component of the research studies aspect of the degree;

Date	Location	Course	Duration
1998	Sheffield Hallam University	Vibrational Spectroscopy	8 hours
1998	Sheffield Hallam University	Polymers and Liquid Crystals	8 hours
1999	Sheffield Hallam University	Crystallography	8 hours
1999	Sheffield Hallam University	Electron Microscopy	8 hours
2000	Sheffield Hallam University	x-ray Fluorescence Spectrometry	8 hours

14.3. PUBLISHED MATERIALS

The following articles have been prepared using data presented in this thesis. All have been published in the scientific press, and are referenced as such;

Title: Synergic Chemical Analysis – The Coupling of TG with FTIR, MS and GC-MS. 2.Catalytic Transformation of the Gases Evolved During the Thermal Decomposition of HDPE Using Acid Activated Clays.

Author: Christopher Breen, Phillip. M. Last, Scott Taylor & Peter Komadel.

Journal: Thermochemica Acta.

Volume: 363.

Year: 2000.

Page: 93 – 104.

Title: Preparation and Characterisation of Dealuminated Metakaolin and its Use in the Transformation of Waste Plastics to Aromatic Hydrocarbons.

Author: C. Breen, S. Taylor, E. Burguin & M. Centeno.

Journal: Journal of Colloid and Interface Science

Volume: 247.

Year: 2002.

Page: 246 - 250.

Title: Adsorption of Olefins on Al – and Al/TMA – Exchanged Bentonites.
Author: A. Moronta, S. Taylor & C. Breen.
Journal: Clays and Clay Minerals.
Volume: April.
Year: 2002.
Page: In Press.

CHAPTER
FIFTEEN

-Appendix-

Synergic chemical analysis — the coupling of TG with FTIR, MS and GC-MS

2. Catalytic transformation of the gases evolved during the thermal decomposition of HDPE using acid-activated clays

Christopher Breen^{*}, Philip M. Last, Scott Taylor, Peter Komadel¹

Materials Research Institute, Sheffield Hallam University, Sheffield, S1 1WB, UK

Received 19 May 2000; accepted 5 July 2000

Abstract

High-density polyethylene, HDPE, has been thermally decomposed in a thermobalance and the evolved gases passed through a bed of catalyst. The resulting transformation products were trapped and subsequently identified using GC-MS. Two smectites of different octahedral compositions were acid-activated under conditions known to produce catalysts of differing activity. Three different treatments were used for each smectite, thus providing six samples for evaluation. The thermal and catalytic decomposition of HDPE was studied under isothermal (60 min at 420°C) and dynamic (35–650°C at 10°C min⁻¹) conditions. The thermal decomposition of HDPE yielded characteristic quartets of peaks in the chromatogram which were assigned to *n*-alkanes, *l*-alkenes, *x*-alkenes and α,ω -dienes in the range C₄–C₂₂. Species of higher molecular weight than C₂₂ were not detected. All six catalysts converted the alkenes present in the thermally generated off gases into light gases and aromatic species. Mono-, di- and trimethylbenzenes were the most abundant aromatic species although small quantities of ethylbenzenes and naphthalenes were produced. More aromatics were produced at 420°C than at temperatures up to 650°C, whereas the reverse was true for branched alkanes. The total conversion of HDPE increased with both the extent of acid treatment and the process temperature, whereas the proportion of aromatics produced was greatest for catalysts prepared using short acid-treatment times. © 2000 Elsevier Science B.V. All rights reserved.

Keywords: Synergic chemical analysis; High-density polyethylene (HDPE); Thermal decomposition

1. Introduction

The low weight-to-volume ratio and the time that waste polymers take to degrade means that land filling is not an acceptable option [1]. Nor is incineration,

because this leads to a variety of products any one of which could present an environmental hazard when released into the atmosphere. Moreover, the chemical content of the polymer is lost when either of these two options are used [2]. Consequently, as the amount of waste polymers continues to increase, investigations into the potential recycling of polymers and the successful reclamation of their chemical content are of increasing importance. Thermal pyrolysis has been studied as a means of recovering high-value products from the gases evolved during polymer degradation

^{*} Corresponding author. Tel.: +44-114-225-3008; fax: +44-114-253-3501.

E-mail address: c.breen@shu.ac.uk (C. Breen).

¹ Also, Institute of Inorganic Chemistry, Slovak Academy of Sciences, 842 36 Bratislava, Slovak Republic.

[3,4]. The products recovered from polyethylene are, in the main, alkenes and saturated hydrocarbons in the range C_2 – C_{25} of a broad distribution [3] with average chain lengths of 13.2 to 14.5 [4]. British Petroleum have established a fluidised bed reactor system but it is not considered to be a profitable process. Significant conversion to relatively high-value aromatic products is seldom achieved.

Catalytic degradation of polymers offers the potential benefits of lower operating temperatures [3] and an increase in the rate of polymer decomposition [1] together with the generation of high-value chemicals [3] in a product mixture which contains fewer components [5]. Two distinct methods have been employed when catalysts are used: (1) mixing the catalyst and polymer together thus ensuring close physical contact between the two [1–9], (2) directing the thermal decomposition products derived from the polymers over a catalyst which is physically distant from the polymer [10–13]. Most catalytic investigations have been conducted under nitrogen, but investigations involving hydrogen [2,8] and high pressures [8] have recently been reported. Both the nature and the distributions of species, evolved during pyrolysis [3,5], are changed when catalyst and polymer are present in a mixture. In the presence of a silica–alumina catalyst, Uemichi et al. [6] reported the presence of *n*-alkanes, iso-alkanes, alkenes and aromatics whilst Uddin et al. [3] observed a narrower distribution of hydrocarbons (*n*- C_2 to *n*- C_{15}). In the former case the distribution of alkanes (6% yield) focussed in a narrow range (C_3 – C_5) but isoalkanes and alkenes (35 and 44%, respectively) were more prominent than aromatics (11%).

Numerous catalysts have been evaluated for the pyrolytic decomposition of polymers, notably zeolites [2,6,7,9–12] and silica–alumina mixed oxides [3,5,6,9,10,13]. In contrast, acid-activated clays have received scant attention even though they represent a convenient, cheap and widely available alternative to expensive manufactured catalysts. A significant challenge to the use of clays as catalysts is that their potentially extensive surface area becomes unavailable at temperatures > 150 – 200°C , because the molecules occupying the clay galleries are desorbed and the layers come into direct contact forming a collapsed clay. Acid leaching of the clay was found to increase both the surface area and the available

acidity sufficiently for them to be used as cracking catalysts in the petroleum industry [14]. During acid-activation of clays the ions in the octahedral sheet are leached out, the nitrogen surface area increases, the number (and type) of acid sites changes as do the sorptive and catalytic properties. These properties generally maximise under intermediate activation conditions and, subsequently, decrease as the product takes on the properties of amorphous silica, which has been identified as the final product of acid leaching [15–18]. It is now widely accepted that clays with a high octahedral Mg content leach more readily than those which have a high octahedral Al population [18–24] and recent reports have established that clays with a high octahedral Fe content also leach rapidly [25–27]. An extensive investigation into the acid-leaching of a range of smectites (selected for their differing octahedral ion content) has shown that the elemental composition of the starting material does not make a significant contribution to the catalytic activity for the chosen test reaction, but is the critical factor when determining the severity of the activation conditions required for the optimisation of the catalyst [27]. Both the clays used herein are the fine fractions of Slovak bentonites: Jelsovy Potok, JP, and Stebno, ST. The acid-activation of these two clays [27], and their organocation exchanged counterparts, has recently been described [28].

It has recently been established that pillared and acid-activated clays have the ability to transform the thermal decomposition products of high-density polyethylene (HDPE) into useful products, although only one example of an acid-treated smectite was investigated [29]. In the present study, the distributions of the secondary cracking products obtained when the thermal degradation products from HDPE (which along with PET has been identified as a significant target for catalytic conversion into useful products [30]) are passed over the acid-activated smectites and compared with the product distribution from the thermal decomposition of HDPE alone. The primary objective of this investigation was to ascertain how the nature of the starting clays and the extent to which they were acid leached influenced their ability to transform the thermally generated off-gases into useful products. Consequently, a detailed investigation of the material balance was not a primary focus. Use of TG-OTM-GC-MS (*vide infra*) permits the identification of the

products of either thermal decomposition or secondary cracking from each catalyst and comparison of the relative abundances of the products.

2. Experimental

2.1. Materials

The polymer used throughout this study was high-density polyethylene, HDPE, (Aldrich). JP is a hydrothermal, aluminium rich, dioctahedral montmorillonite from the Kremnica Mountains in central Slovakia [31,32]. In contrast, the main mineral in Stebno, ST, from the Czech Republic is Fe-beidellite which has an octahedral sheet rich in iron and 57% of the charge on the layer arises from substitution in the tetrahedral sheet. ST contains about 21% of total iron bound in goethite [33] which is present as an admixture in the $< 2 \mu\text{m}$ fraction and, hence, could not be removed by fractionation. However, it is readily dissolved in 6 M HCl, thus the acid-activated samples contain no goethite. Coarse samples of JP and ST were suspended in deionised water, treated five times with 1.0 M aqueous calcium chloride, washed until free of chloride, centrifuged, and the nominally $< 2 \mu\text{m}$ sample was collected, dried at 60°C and ground to $< 0.2 \text{ mm}$ prior to storage. The structural formulae of the purified smectites used are given in Table 1.

2.2. Equipment and methods

Three-gram portions of the Ca-form of each mineral were treated with 300 cm^3 of 6 M HCl for different periods of time. JP and ST were treated at 95°C and 60°C , respectively, since it has been shown that ST is

leached more readily than JP [27]. After acid treatment the samples were filtered, then washed with 1.5 dm^3 deionised water and centrifuged before being dried and ground to pass a 0.2-mm sieve. The treatment time is identified in the sample name. Thus, JP30 indicates that JP was treated in 6 M HCl for 30 min at 95°C , and ST120 means that ST was treated with 6 M HCl for 120 min at 60°C . The characterisation of these materials has been described elsewhere [27].

2.3. Apparatus

Thermal and catalytic degradations of HDPE were carried out using a synergic chemical analysis system supplied by Thermo Unicam [34]. This system consists of a thermobalance (TG131, Cahn) fitted with two outlets which are connected to heated transfer lines. One transfer line was connected to an infrared gas cell (10 cm path length) contained in an infrared (FTIR) spectrometer (Infinity Series, Mattson). The outlet from the infrared gas cell flowed into a second transfer line which was connected to an absorbent trap (VOCARB 4000 Supelco) contained in an organic trap module (OTM, Cahn). The outlet from the OTM was also connected to a gas chromatograph–mass spectrometer (GC-MS) (Automass System 2, Unicam). The third transfer line was connected directly to the mass spectrometer (Automass System 2, Unicam). Preliminary experiments established that it was impossible to obtain pertinent information from TG-FTIR and TG-MS, because of the complexity of the gas mixtures being evolved.

2.4. Procedures

HDPE (50 mg) was placed in the TGA sample crucible and glass wool (50 mg) was placed on the HDPE to cover the polymer. Two separate heating regimes were utilised; the sample was heated from 25°C to (i) 650°C at $10^\circ\text{C min}^{-1}$ or (ii) 420°C at a rate of $10^\circ\text{C min}^{-1}$, then held isothermally at 420°C for 60 min. Dry nitrogen purge gas at atmospheric pressure (40 ml min^{-1}) was used in both regimes. Identical conditions were used during catalyst evaluation, except that 200 mg of acid activated clay was spread evenly over the glass wool so that gases evolved from the sample passed through the layer of catalyst [29]. The results presented here do not contain information

Table 1
Structural formulae of smectites in the fine fractions of the samples used

Sample	M ^{1a}	Si ^b	Al ^b	Al ^c	Fe ^c	Mg ^c	Li ^c
JP ^d	0.91	7.71	0.29	3.00	0.38	0.63	0.00
ST ^e	0.95	7.22	0.78	1.96	1.60	0.58	0.00

^a Interlayer cations.

^b Tetrahedral cations.

^c Octahedral cations.

^d Ref. [19].

^e Ref. [27].

regarding the influence of the weight of catalyst used or the effect of diffusion through the catalyst bed. These operating temperatures were chosen since they represent the initial stages of and complete decomposition respectively.

On completion of the TG analysis, the species contained on the trap were thermally desorbed (4 min at 250°C) onto the GC capillary column (DB-1, 30 m × 0.25 mm I.D.) where the compounds were separated before identification by MS. The transfer lines were maintained at 250°C throughout the analyses. In a typical experiment the column was held at 35°C during the 4-min desorption period before ramping the temperature at 5°C min⁻¹ to 250°C. The final temperature was maintained for five minutes. Considerable care was exercised to ensure that no sample was left on the traps after the desorption cycle. The traps were taken through the desorption cycle again in order to confirm that all the sorbed products had entered the GC. In addition, each trap was baked at 300°C for three hours and its cleanliness was confirmed by taking it through the desorption cycle prior to collecting the evolved gases.

The relative amount of each species was determined by evaluating the area under the base peak for each aliphatic or aromatic species. This approach overcomes difficulties associated with co-eluting species. The results are reported as a percentage of the largest amount of product in a given comparative dataset.

2.5. Coke content

After a typical run, the system was cooled from its maximum temperature to 30°C so the coked catalyst

could be removed and stored. Fifty milligrams of used catalyst was later placed in the TG sample crucible and heated from 25 to 650°C at a rate of 10°C min⁻¹ under a flow of dry nitrogen (40 ml min⁻¹). At 650°C, the flow of nitrogen was replaced with a flow of dry air (40 ml min⁻¹) at atmospheric pressure and held at 650°C for 30 min to oxidise deposited coke on the catalyst. The coke content was calculated from the weight loss.

3. Results

3.1. Catalyst properties

Table 2 presents data for the depopulation of the clay layer, the acidity determined using the desorption of cyclohexylamine and the yield obtained using these catalysts in a liquid phase test reaction [27]. This data shows that ST was more readily leached under milder conditions than JP and this is attributed to the different octahedral compositions (Table 1). ST is rich in iron whereas JP contains more aluminium.

3.2. TG data

The weight loss versus temperature curve for the thermal decomposition of HDPE under a linear heating rate (Fig. 1a) shows that the decomposition was a single step process with offset and end temperatures of 380°C and 470°C, respectively, during which 98.53% of the initial weight of HDPE was lost. The temperatures chosen were also convenient for catalyst activation since they were all substantially dehydrated by the

Table 2
Relevant data for catalyst composition acidity coke content and catalytic ability

Catalyst	Octahedral sheet depletion ^a /%	Acidity ^a (mmol H ⁺ g clay ⁻¹)	Yield in ether forming reaction ^a (%)	Amount of HDPE converted at 420°C ^b (%)	Coke content for isothermal process (wt.%)	Coke content for dynamic process (wt.%)
ST30	14	1.05	83	52	1.0	0.6
ST120	29	0.97	71	76	1.0	0.4
ST240	45	0.80	68	95	0.9	0.4
JP120	11	1.00	97	70	2.0	0.9
JP240	22	0.96	92	80	1.7	0.8
JP360	39	0.70	68	98	1.5	0.6

^a Ref. [27].

^b The conversion of HDPE at 650°C was virtually 100%.

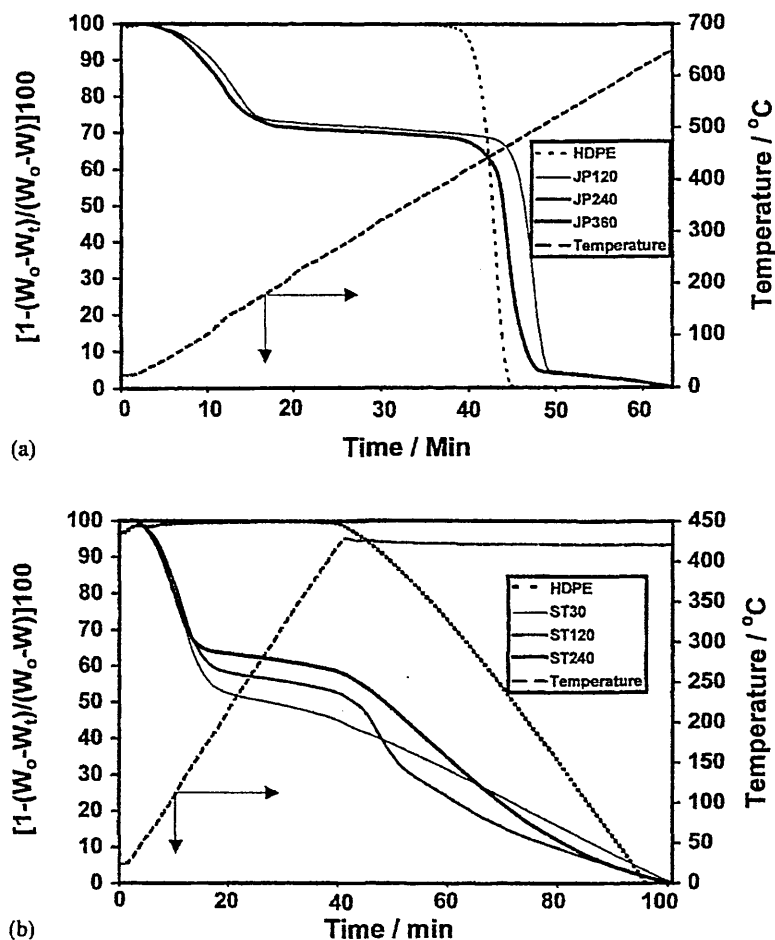


Fig. 1. Weight loss curves for the uncatalysed and catalysed processes under (a) dynamic, and (b) isothermal conditions. The curves for JP240 and JP360 overlap in 1(a) and are not distinguishable.

onset temperature of polyethylene volatilisation. FTIR analysis (not shown) of the off gases produced in the temperature region 35–300°C (Fig. 1) confirmed that only water was evolved. It is well known that clays are effectively dehydrated by 300°C and the layers would have collapsed leaving only the pores created by acid-activation available for the catalytic process. Incidentally, no hydroxylated compounds could be found in the product stream confirming that there was little or no interlayer water remaining on the catalyst surface to react with the alkenes. Fig. 1, in which the weight losses are normalised, shows that there were noticeable differences in the rate of weight loss during the isothermal process (Fig. 1b) and that the weight losses occurred more gradually at 420°C than at 650°C. This means that the rate at which HDPE was delivered to the catalyst at 420°C was much slower than at 650°C.

In addition, whilst all the HDPE was thermally degraded at 650°C, up to 50% remained at 420°C depending on the extent of acid treatment of the catalyst (Table 2). The catalysts with the more extensive octahedral depopulation caused the most extensive reduction in the amount of HDPE remaining.

3.3. Thermal degradation

Fig. 2a shows the total ion chromatogram (TIC) versus time curve obtained when HDPE was heated at 420°C. A similar distribution was obtained under dynamic conditions. The general character of the distributions is very similar to published data for the thermal degradation of HDPE [2–5,10] and shows that the major products eluted as quartets of peaks. Mass spectrometric analysis of each individual peak

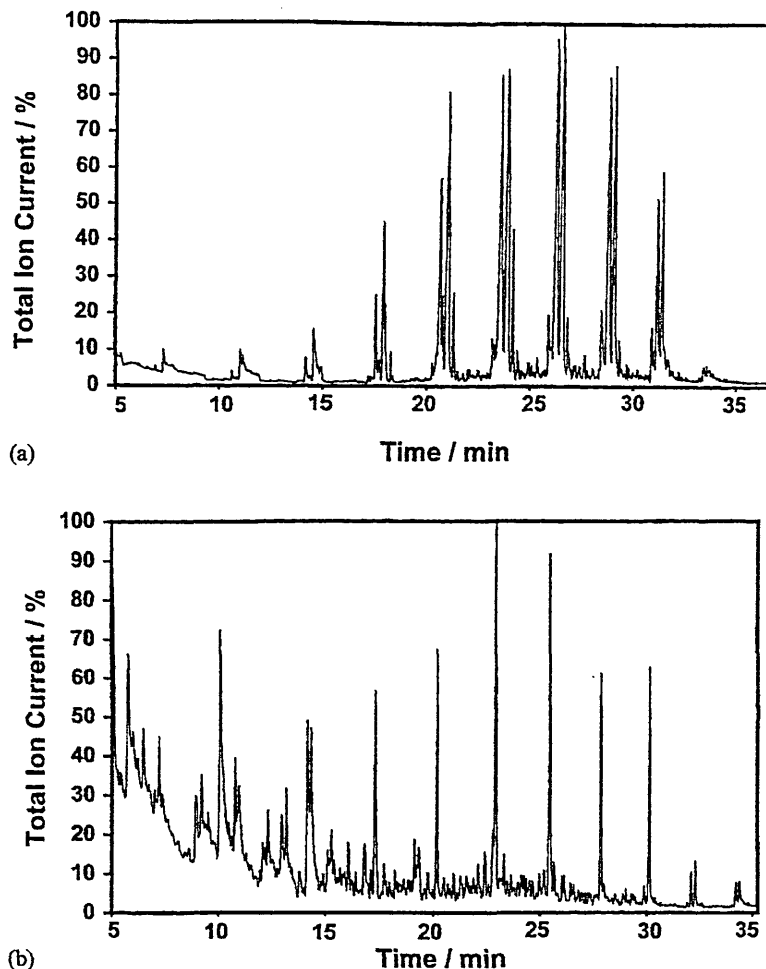


Fig. 2. GC-MS chromatogram of the products evolved during (a) the thermal decomposition of HDPE and (b) the ST-30 catalysed transformation of the product distribution shown in Fig. 2a under isothermal conditions.

showed that the product gases were a mixture of *n*-alkanes, *I*-alkenes, *x*-alkenes (alkene with internal double bond), α,ω -dienes and a range of branched aromatic and polyaromatic species. In order of increasing retention time, the four major components in the 'quartet' of peaks were α,ω -diene, *I*-alkene, *n*-alkane and *x*-alkene. All these organic compounds were present in all the product mixtures, but the reaction temperature and the catalyst used significantly influenced the amount of each product. Each named compound was identified from its fragmentation pattern and parent ion. Alkanes exhibit a parent ion of mass $C_nH_{2n+2}^+$, alkenes exhibit parent ions of mass $C_nH_{2n}^+$ and dienes exhibit parent ions of mass $C_nH_{2n+2}^+$. *I*-Alkenes and *x*-alkenes were identified (and discriminated between) by the fragmentation

patterns obtained for each compound. Fig. 2b shows that only one of the quartet of peaks remained after passing the vapours evolved during dynamic thermal decomposition through ST30. These peaks were those of the *n*-alkanes and there was little evidence of the *I*-alkenes, *x*-alkenes and *x*-dienes. This dramatic transformation in the chromatogram occurred with all of the catalysts studied.

The thermal decomposition of HDPE up to 650°C also yielded *n*-alkanes, *I*-alkenes, *x*-alkenes and α,ω -dienes in the range C_4 – C_{22} . Molecules longer than C_{22} were not detected, and there was no evidence for branched alkanes. There was evidence for branched alkenes at low molecular weights ($\leq C_7$) but no branched, unsaturated species of higher molecular weight were identified. These observations are in

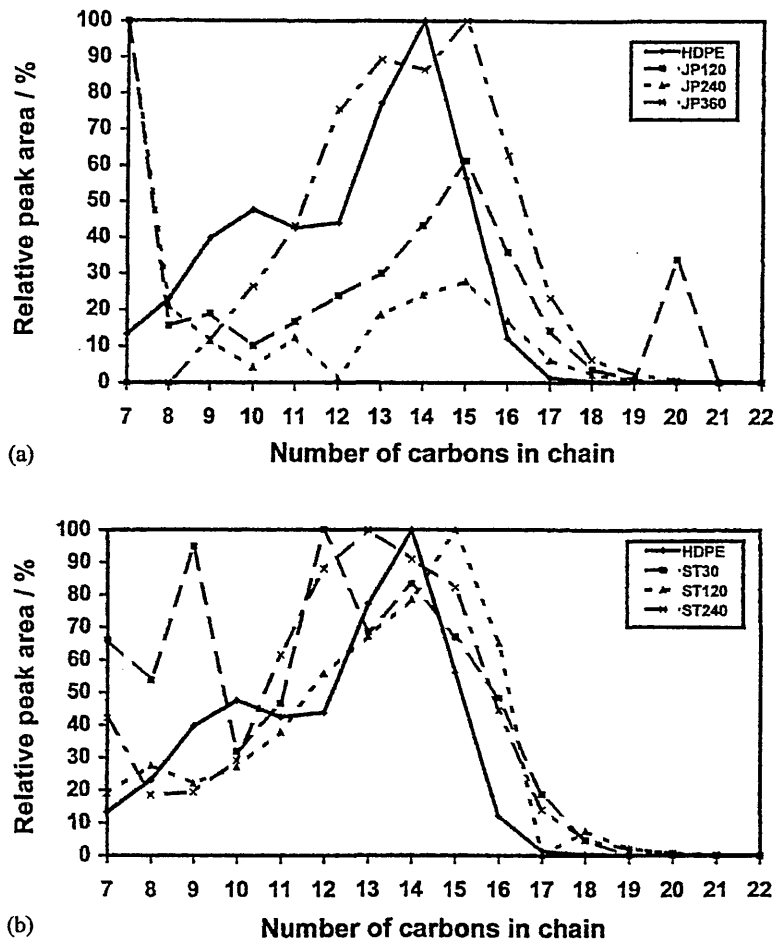


Fig. 3. Comparison of the distribution of carbon chain lengths (derived from GC-MS chromatograms) obtained under isothermal conditions for (a) JP and (b) ST. The distribution of the thermally derived products is shown in both (a) and (b) for direct comparison.

accord with those of others [5,10]. The extremely low yield of aromatic species was anticipated [5].

The approach of Uddin et al. [3] has been used to present changes in the distribution of linear products, i.e. the relative base peak area of the alkane was plotted against the number of carbon atoms in the chain. Comparison of the TICs in Fig. 2 with the distributions in Fig. 3 shows that the distribution refers to both the alkanes and alkenes (for the thermally decomposed products), whereas for the products obtained after contact with the catalysts (Fig. 2b) only the alkane distribution is reflected. The distribution of saturated aliphatic hydrocarbons evolved during thermal decomposition of HDPE at 420°C is similar to that found by others [3,29].

Small quantities of several aromatics were identified at both process temperatures (Figs. 4 and 5) using

GC-MS. The most abundant of these was toluene with lesser amounts of the xylenes along with traces of ethylbenzene, ethylmethylbenzenes naphthalene and substituted naphthalenes.

3.4. Catalytic transformation of evolved gases

The action of the catalysts on the thermally generated decomposition gases of HDPE generally produced a distribution of n-alkanes in the range C_4 – C_{22} (which maximised at C_{11} – C_{18}), with branched alkanes up to C_{20} . Indeed many more branched alkanes were produced at 650°C than at 420°C with ST30 producing the most. There was a complete absence of polyunsaturated species, and the mono-unsaturated species (both branched and linear) were confined to $< C_7$ as observed for the decomposition of

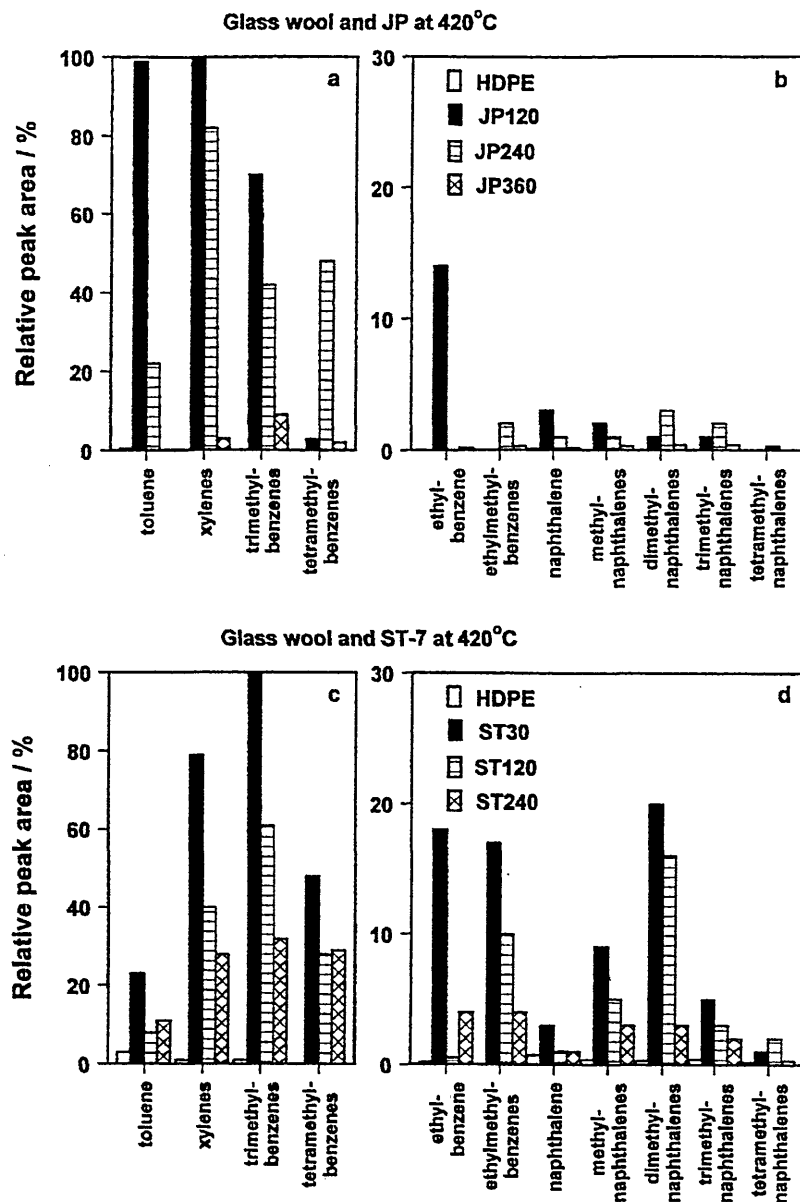


Fig. 4. Distribution of unsaturated products from the catalysed transformation of thermally evolved products over ST and JP under isothermal conditions. (a) and (b) HDPE and JP; and (c) and (d) HDPE ST.

HDPE over silica–alumina [4] and a selection of acid-treated and pillared clays [29]. The distribution of alkanes obtained over both sets of catalysts was broader at 420°C than at 650°C.

All the catalysts produced more aromatics than thermal decomposition at the same temperature (Figs. 4 and 5). The yield of polyaromatic products, which never exceeded 30% of the most abundant single ring compounds, was higher at 650°C. In gen-

eral, the aromatic production was lower at 650°C than at 420°C and decreased with the extent of acid treatment of the catalyst with JP120 at 420°C producing the most aromatic species. In contrast, the production of branched species was much higher at 650°C, but was also dependent on the level of acid treatment. The production of aromatics over JP360 at 420°C was lower than anticipated, given that it converted the most HDPE and was also an effective catalyst for

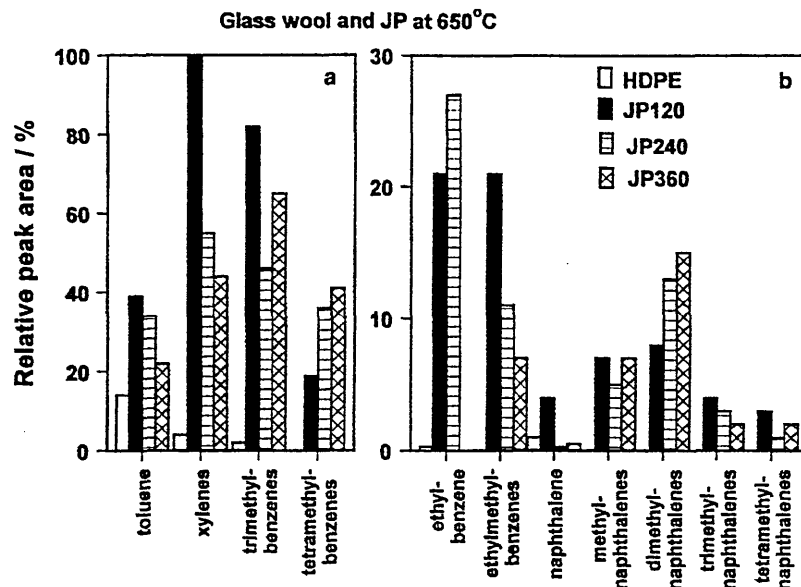


Fig. 5. Distribution of unsaturated products from the catalysed transformation of thermally evolved products over JP under dynamic conditions.

the formation of tetrahydropyran ether from dihydropyran and methanol [27]. However, it is important to realise that the formation of tetrahydropyran ether occurs under very mild conditions in the presence of liquid reactant, whereas the transformation of HDPE occurs at high temperatures when the clay is substantially dehydrated and not expanded.

Earlier work on the transformation of HDPE to useful products showed that aluminium pillared clays were selective to trimethylbenzenes at 420°C and xylenes at 650°C. The acid-treated clays used herein produce a wider range of single ring products similar to that reported for the transformation over K10, a commercial acid-treated material, of unspecified extent of leaching [29]. The extent of dealkylation on solid acid catalysts generally depends on the relative ease of formation of alkyl carbonium ions [35]. Since methylcarbonium ions are very difficult to form, most of the aromatics produced would be unlikely to undergo decomposition. These considerations are supported herein insofar as the composition of the aromatics changed relatively little with process temperature.

The coke values collected in Table 2 show that, despite the relatively high iron content in the catalysts derived from ST, they generally produced less coke than those derived from JP. Nonetheless, these values

are considerably lower than the 7% reported for the zeolite US-Y [36], 6% over silica–alumina [37] and up to 19% on Ca-exchanged zeolite-X [6] when the catalyst was ground together with the polymer. Given that aromatics are adsorbed more strongly on acid catalysts than saturated hydrocarbons it is assumed that aromatics, particularly the naphthalenes, most closely relate to coke deposition [6]. A 95% reduction in surface area occurred when the pores in CaX were severely congested with a 19% coke deposition during the catalytic degradation of polypropylene [6]. This severely restricted the inward diffusion of the polypropylene decomposition products and hence their catalytic reformation.

4. Discussion

The thermal degradation of polyethylene begins with a reduction in molecular weight near 290°C and the rate of degradation to volatile products becomes more rapid as the temperature increases. Chain cleavage, which occurs via β -scission, produces one double bond per cleavage event giving rise to the 1-alkenes, x -alkenes and α,ω -dienes mentioned above. The small quantities of aromatic products are probably caused by thermally induced dehydrocyclisation.

The evolution of volatile species from HDPE begins near 350°C (Fig. 1), a temperature at which all the interlayer galleries in each of the catalysts will be completely collapsed and only the external pores produced by acid leaching of the clay layer will be available to the thermal degradation products of HDPE. Moreover, only those acid sites on the external surface and within the pores will be accessible, since it is unrealistic to assume that the non-polar alkenes will penetrate into the clay galleries at these elevated temperatures and re-expand the collapsed layers.

The situation at the catalyst surface is very complex involving protonation, isomerisation, alkylation, dehydrogenation/rehydrogenation coupled with the separate influences of temperature and residence time. All of these combine to make a clear interpretation of data presented in Fig. 3 difficult. The systems involving ST at 420°C serve to broaden the alkane distribution with respect to that in the absence of catalyst, whereas the distribution for systems involving JP at 420°C did not behave in a systematic manner. The increase in alkane chain length over K10 has recently been attributed to catalytic alkylation on the open, porous surface [29]. At 650°C, the tendency was towards the production of shorter alkanes which is probably related to an increase in the amount of cracking compared to isomerisation which takes place at elevated temperatures [38].

Figs. 4 and 5 also show that other low molecular weight species, particularly methylaromatics, were obtained yet the relative amount of aromatics produced decreased as the extent of acid leaching increased. This shift towards lower molecular weight and/or aromatic species was attributed to β -scission plus cracking and dehydrocyclisation, respectively [13,29]. In general, the catalysts decreased in their ability to produce aromatics as JP120 > JP240 > JP360; ST30 > ST120 > ST240. Moreover, at 420°C the selectivity over the ST and JP catalysts were significantly different whilst both the quantity produced and the selectivity were reduced in the dynamic process.

Clearly, the mildly activated clays produced the most aromatics but no molecules larger than ethyltoluene were identified in the catalytically transformed products which may be a consequence of the relative stability of the methylaromatics [6]. Although this agrees with Uemichi's work using silica-alumina

[5], it contrasts with results using the zeolite ZSM-5 ([13,39] where, in addition to toluene and the xylenes, benzene was clearly identified. Benzene was produced by the acid clays, but it co-eluted with several low boiling point species making quantitation difficult. Indeed, catalytic degradation over ZSM-5 produces large quantities of low molecular weight gases (C_3 – C_4), because this zeolite prevents more than four carbon atoms from entering the channel network — a feature which is effectively exploited in the dewaxing process [40]. Nonetheless, ZSM-5 does produce aromatics when molecules, pre-cracked on the external surfaces, enter the channel network [7]. In a more detailed study than that of Uddin et al. [3], Ohkita et al. [39] correlated surface acidity with the products formed when thermally degraded polyethylene was passed over silica-alumina, of selected compositions. They found that at 400°C gas production increased with increased surface acidity while oil production decreased.

Songip et al. [41,42] showed that H-ZSM-5 was not suitable for the reforming of heavy oil derived from polyethylene even though it did not readily coke up. The gasoline produced had a good octane number, but the yield was low (20%) compared to the gas production (68%), whereas proton-exchanged (HY) and rare earth-exchanged (REY) zeolite-Y produced gasoline of similar quality with up to 30% less gas. HY contains a larger number of more acidic sites than REY leading to a lower gasoline yield (27 vs. 49%) and larger amounts of both gas (44 vs. 35%) and coke (6 vs. 3%). Thus, REY was the optimum choice because its bigger pore size allowed heavy oil in and it had fewer acid sites which resulted in a slower deactivation rate and less coke deposition when compared to HY [41,42].

Acid-activated clays have a larger number of milder acid sites than most zeolites [43] and they are predominantly Lewis acid sites after activation at high temperatures [44]. Consequently, their behaviour mimics that of REY and the large, unsaturated molecules produced during the thermal degradation of HDPE are cracked into smaller molecules. Dehydrocyclisation also occurs and aromatics are formed. Moreover, whilst cracking to small gaseous molecules does occur, particularly at 650°C it is low in comparison to that which occurs over the large number of strong acid sites in the microporous ZSM-5. Figs. 4 and 5 show that there was a shift in the products

formed over JP from toluene and xylenes, in the isothermal process, to xylenes and trimethylbenzene, in the dynamic process. These products are the same as found over silica–alumina [6].

The greatest proportional yield of aromatics and branched alkanes was obtained for clays with the least acid treatment which suggests that both processes relied in some way on small pores and high relative acidities (Table 2). The formation of branched alkenes from linear alkenes is essential to the provision of secondary carbenium ions which can then undergo the required ring closure and dehydrogenation reactions to produce aromatics. However, it is apparent that more aromatics were produced when the feed rate of the reactants was low and/or the residence time at the catalyst surface was long. In the current experimental configuration it is not possible to separate these two variables. However, it is clear that when rapid transport to and through the catalyst bed occurs then the proportion of aromatics was reduced in favour of branched alkanes. Uemichi et al. [6] also noted an increase in the aromatic/aliphatic ratio as the residence time increased.

Moreover, isomerisation is favoured over cracking at low temperatures [38]. These parameters combine to maximise the production of aromatics at low operating temperatures whereas branched alkanes are favoured at higher temperatures. When the extent of acid treatment is increased the surface area reaches a maximum and then begins to decline whilst the acidity decreases.

5. Conclusions

The thermal decomposition of HDPE up to 650°C yielded characteristic quartets of peaks assigned to *n*-alkanes, 1-alkenes, *x*-alkenes and α,ω -dienes in the range C₄–C₂₂. Species of higher molecular weight than C₂₂ were not detected. All six catalysts converted the alkenes present in the thermally generated off gases into light gases, branched alkanes and aromatic species including good quantities of toluene, xylenes, tri- and tetramethylbenzenes. Ethylbenzenes and naphthalenes were produced to a lesser extent. More aromatics were produced at 420°C than at 650°C whereas the reverse was true for branched alkanes. The total conversion of HDPE increased with both the

extent of acid treatment and the process temperature, whereas the proportion of aromatics produced was greatest for catalysts prepared using short acid-treatment times at low process temperatures. Thus, there is considerable potential to control the product distribution by choosing appropriate combinations of acid-treatment of the catalyst and the process temperature.

Acknowledgements

We are grateful to the European Regional Development Fund and Sheffield Hallam University for financial assistance towards the purchase of the Synergy system and support for P.M. Last. S. Taylor is grateful for a Joint Bursary from Sheffield Hallam University and the University of Sheffield. The financial support of the Slovak Grant Agency (Grant 2/4042/99) is acknowledged.

References

- [1] W. Ding, J. Liang, L. Anderson, *Fuel Proc. Techn.* 51 (1997) 47.
- [2] K. Liu, H. Meuzelaar, *Fuel Proc. Techn.* 49 (1996) 1.
- [3] M. Uddin, K. Koizumi, K. Murata, Y. Sakata, *Polym. Deg. Stab.* 56 (1997) 37.
- [4] W. McCaffrey, M. Kamal, D. Cooper, *Polym. Deg. Stab.* 47 (1995) 133.
- [5] Y. Uemichi, A. Ayame, Y. Kashiwaya, H. Kanoh, *J. Chrom.* 259 (1983) 69.
- [6] Y. Uemichi, Y. Kashiwaya, M. Tsukidate, A. Ayame, H. Kanoh, *Bull. Chem. Soc. Jpn.* 56 (1983) 2768.
- [7] R. Mordt, R. Fields, J. Dwyer, *J. Anal. Appl. Pyrolysis* 29 (1994) 45.
- [8] X. Xiao, W. Zmierczak, J. Shabtai, *Div. Fuel Chem.* 40 (1995) 4.
- [9] G. Audisio, A. Silvani, P. Beltrame, P. Carniti, *J. Anal. Appl. Pyrolysis* 7 (1984) 83.
- [10] P.L. Beltrame, P. Carniti, G. Audisio, F. Bertini, *Polym. Deg. Stab.* 26 (1989) 209.
- [11] T. Yoshida, A. Ayame, H. Kanoh, *Bull. Jpn. Petrol. Inst.* 17 (1975) 218.
- [12] C. Vasile, P. Onu, V. Barboiu, M. Sabliovschi, G. Moroi, D. Ganju, M. Florea, *Acta Polymerica* 39 (1988) 306.
- [13] C. Vasile, P. Onu, V. Barboiu, M. Sabliovschi, G. Moroi, *Acta Polymerica* 36 (1985) 543.
- [14] C.L. Thomas, J. Hickey, G. Stecker, *Ind. Chem. Eng.* 42 (1950) 866.
- [15] R. Fahn, *Fette Seifen Anstrichm.* 75 (1973) 77–82.
- [16] P. Komadel, D. Schmidt, J. Madejová, B. Čičel, *Appl. Clay Sci.* 5 (1990) 113–122.

- [17] I. Tkač, P. Komadel, D. Muller, *Clay Miner.* 29 (1994) 11–19.
- [18] C. Breen, J. Madejová, P. Komadel, *J. Mater. Chem.* 5 (1995) 469–474.
- [19] C. Breen, J. Madejová, P. Komadel, *App. Clay Sci.* 10 (1995) 219–230.
- [20] B.B. Osthaus, *Clays Clay Miner.* 4 (1956) 301–321.
- [21] I. Novak, M. Gregor, *Proceedings International Clay Conference, Tokyo, 1969*, pp. 851–857.
- [22] B. Čičel, I. Novak, in: J. Konta, *Proc. 7th Conf. Clay Miner. Petrol.*, Karlovy Vary, 1976, Charles University, Prague, pp. 163–171.
- [23] I. Novak, B. Čičel, *Clays Clay Miner.* 26 (1978) 341–344.
- [24] P. Komadel, J. Madejová, M. Janek, W.P. Gates, R.J. Kirkpatrick, J.W. Stucki, *Clays Clay Miner.* 44 (1996) 228.
- [25] M.A. Vincente, M. Suaréz, J.D. López-González, M.A. Bañares-Muñoz, *Clays Clay Miner.* 44 (1994) 724.
- [26] M. Janek, P. Komadel, *Geol. Carpath. Ser. Clays* 44 (1993) 59.
- [27] C. Breen, D. Zahoor, P. Komadel, J. Madejová, *J. Phys. Chem. B.* 101 (1997) 5324.
- [28] C. Breen, R. Watson, P. Komadel, J. Madejová, *Z. Klapya, Langmuir* 13 (1998) 6473.
- [29] C. Breen, P.M. Last, *J. Mater. Chem.* 9 (1999) 813.
- [30] T. Curlee, S. Das, *Resources Conser. Recyc.* 5 (1991) 343.
- [31] V. Šucha, I. Kraus, C. Mosser, Z. Hroncová, K.A. Soboleva, V. Širánová, *Geol. Carpath. Ser. Clays* 43 (1992) 13.
- [32] E. Šamajová, I. Kraus, A. Lajčáková, *Geol. Carpath. Ser. Clays* 43 (1992) 21.
- [33] B. Čičel, P. Komadel, S. Lego, J. Madejová, L. Vicková, *Geol. Carpath. Ser. Clays* 44 (1993) 121.
- [34] C. Breen, P.M. Last, M. Webb, *Thermochim. Acta* 326 (1999) 151.
- [35] V. Haensel, *Adv. Catal.* 3 (1951) 194.
- [36] Y-H. Lin, P.N. Sharrat, A.A. Garforth, J. Dwyer, *Thermochim. Acta* 294 (1997) 45.
- [37] Y. Ishihara, H. Nanbu, T. Ikemura, T. Takesue, *Fuel* 69 (1990) 978.
- [38] S. Moreno, R. Sun Kou, G. Poncelet, *J. Phys. Chem. B* 101 (1997) 1569.
- [39] H. Ohkita, R. Nishiyama, Y. Tochiyama, T. Mizushima, N. Kakuta, Y. Morioka, A. Ueno, Y. Namiki, S. Tanifuji, H. Katoh, H. Sunazuka, R. Nakayama, T. Kuroyanagi, *Ind. Eng. Chem. Res.* 32 (1993) 3112.
- [40] W.O. Haag, R.M. Largo, P.B. Weisz, *Faraday Discuss. Chem. Soc.* 72 (1981) 317.
- [41] A.R. Songip, T. Masuda, H. Kuwahara, K. Hashimoto, *Appl. Catal. B: Environ.* 2 (1993) 165.
- [42] A.R. Songip, T. Masuda, H. Kuwahara, K. Hashimoto, *Energy&Fuels* 8 (1994) 136.
- [43] S. Chevalier, R. Franck, J.F. Lambert, D. Barthelemy, H. Suquet, *Appl. Catal. A: Gen.* 110 (1994) 153.
- [44] F. Kooli, W. Jones, *Clay Miner.* 32 (1997) 633.

NOTE

Preparation and Characterization of Dealuminated Metakaolin and Its Use in the Transformation of Waste Plastics to Aromatic Hydrocarbons

Acid activated metakaolins (AAMKs) have been prepared by calcination of the natural clay at 600°C to provide a metakaolin which was then leached at 80°C for 3 h using 1M, 2M, 3M, and 6M HCl. These materials were characterized and their ability to transform the off gases from HDPE decomposition into useful aromatic species was evaluated. The amount of adsorbed water and the number of acid sites increased with the severity of acid treatment. Infrared and DRIFTS spectroscopy of pyridine treated samples revealed that both Brønsted and Lewis acid centers were present until 425°C. Pyridine bonded to the Lewis acid centers was more thermally stable. The AAMKs were all selective to the production of toluene with respectable, but lesser, amounts of xylenes and trimethylbenzenes. This selectivity contrasts with that of acid leached and pillared smectites which are selective toward trimethylbenzene.

© 2002 Elsevier Science (USA)

1. INTRODUCTION

Seventeen million tons of waste plastic was produced in 1997 alone and only 6% of it was recovered via recycling or chemical recovery with 76% of the remainder being committed to landfill or direct incineration (1–3). Incineration is considered to have a negative environmental impact (4) and the number of landfills is limited so alternative strategies including the recovery of high value hydrocarbons via thermal or catalytic processes are receiving much attention. Under pyrolytic conditions high density polyethylene (HDPE) yields an homologous series of saturated (*n*-alkanes) and unsaturated (α , ω -dienes, alk-1-enes, alk-*x*-enes) hydrocarbons with carbon numbers in the C₄–C₂₀ range (5–8). Catalytic degradation produces insignificant amounts of aromatic species. Catalytic transformation increases the rate of polymer decomposition (9) forming shorter chain (liquid) hydrocarbons (5, 10) including high octane hydrocarbons such as iso-alkanes and aromatics (11). Currently, two distinct methods are used to study the effect of transformation agents on the product distribution from pyrolysis: (1) physical mixing of the polymer and catalyst (6, 8, 10, 12–16); (2) the exposure of post pyrolysis gas streams to catalyst beds which are physically distant from the site of pyrolysis (3, 5, 7, 9, 11, 19–21). Acidic solids, including commercial silica-aluminas and zeolites, have proven to offer greater selectivity toward a small range of desirable products. Park *et al.* (12) have shown that silica-alumina (SA) produces a significantly narrower range of aromatic hydrocarbons (C₅–C₁₃) than the thermal process (C₃–C₂₆). Zeolite ZSM-5 produced more aromatic hydrocarbons than SA (9–11) due to the significant number of Brønsted acid sites in H⁺-ZSM-5 which promote efficient hydrocyclisation/aromatization reactions (11). Longip *et al.* (22, 23) showed that H⁺-ZSM-5 produced low gasoline (20%) and high gas (68%) yields during the reforming of polyethylene-derived heavy hydrocarbons whereas proton-exchanged (HY) and rare earth-exchanged (REY) zeolite-Y produced higher yields of gasoline (of comparable quality) with up to 30% less

gas. Thus, REY was the optimum choice since its larger pore size permitted ingress of the heavy oil and it had fewer acid sites which resulted in a reduced deactivation rate and less coke deposition (22, 23).

Recent preliminary investigations into the use of pillared clays, acid-activated bentonites, and smectites have shown that these materials are capable of producing respectable quantities of toluene, xylenes, and trimethylbenzenes from the gases produced during the thermal pyrolysis of HDPE (5, 24). Given the recent return of interest in acid-activated kaolins as solid acids it was considered timely to compare the activity of these clay-based materials with those derived from bentonites and smectites.

Kaolin is a 1:1 type clay mineral in which an octahedral alumina sheet is fused to a silica tetrahedral sheet. The layers are held together by hydrogen bonding between hydroxyl groups on the gibbsite surface and the oxygens of the adjacent siloxane surface. Despite having a low surface area (10–30 m² g⁻¹), acid-leached kaolin was among the first solid acids to be used in the Houdry process for catalytic cracking in the petroleum reforming industry (25–27). The high octahedral aluminum content makes kaolin resistant to acid leaching (28, 29), but metakaolin (produced by heating kaolin in air at temperatures > 450°C (29)) is much more susceptible to acid activation, producing a catalyst with the same activity as acid activated montmorillonite at about half the fresh surface area (29). Thus, acid-activated metakaolin (AAMK) is a material which offers both enhanced surface area and acidity compared with either kaolin or metakaolin (29–31). As with acid treated bentonites, the activity of AAMKs reaches a maximum and then declines as the severity of the activation process increases although Lussier has reported that AAMKs with high surface areas and activities can be prepared using very low acid concentrations if the metakaolin was produced in a narrow calcination window (29).

This study focuses on a series of metakaolins which have been dealuminated by treatment with aqueous HCl of differing concentration at 80°C for 3 h. It will identify how the extent of acid activation affects the structure and resultant properties of the materials, including their acidity and how effective and selective these materials are in transforming the pyrolysis products of HDPE into high value, industrially useful aromatic hydrocarbons.

2. EXPERIMENTAL

2.1. Materials

The polymer employed throughout the following investigations was high density polyethylene, HDPE (Aldrich). Transformation agents were prepared by acid activation of a metakaolin derived from a well-crystallized Cornish kaolin from English China Clays, according to the method of Perissinoto *et al.* (31).

2.2. Preparation of Transformation Agents

Metakaolin was prepared by calcining the kaolin at 600°C under air for 15 h. The resultant metakaolin was cooled, ground, and acid leached with constant stirring at 80°C for 3 h using aqueous HCl concentrations of 1, 2, 3, and 6M. The leached samples were rapidly filtered under vacuum to remove the excess acid and prevent further structural attack. The filtered samples were air dried

TABLE 1

Sample Designation, Treatment Parameters, Weight Loss, Elemental Composition, and Acidity Data for the Samples Studied

Sample designation	Treatment time/h	[HCl]/mol dm ⁻³	Weight loss to 800°C/wt%	Acidity mmol/g ⁻¹ clay	Al ₂ O ₃ /wt%	SiO ₂ /wt%
kaolin	n/a	n/a	16	n/a	43.73	54.06
metakaolin	n/a	n/a	4	0.01	43.69	54.06
AAMK3.1	3	1M	7	0.22	36.54	61.41
AAMK3.2	3	2M	10	0.32	26.94	71.14
AAMK3.3	3	3M	12	0.34	23.60	74.57
AAMK3.6	3	6M	13	0.49	12.34	86.05

d ground prior to use. The resulting AAMKs were named according to the duration of their immersion in the treatment acid (Table 1).

3. Characterization of AAMKs

The equipment and sample preparation procedures used to obtain X-ray fluorescence data, X-ray diffraction profiles, and thermogravimetric traces are identical to those reported elsewhere by the authors (5, 24, 32–36).

2.3.1. Infrared analysis (VT-DRIFTS). The infrared spectrum of adsorbed pyridine is the most commonly used method for differentiating between Brønsted and Lewis acid sites on solid acid materials (32). In this investigation, samples were dried at 120°C for 24 h prior to exposure to vapor phase pyridine for 8 h. Spectra were recorded using a DRIFTS accessory (Graseby Specac) on a Mattson Polaris FTIR spectrometer. Spectra were recorded over the 2500–500 cm⁻¹ temperature range with individual spectra recorded at 25°C intervals (33, 34). A 4-cm⁻¹ resolution was employed throughout. Desorption products were removed from the sample chamber using dry nitrogen gas.

2.3.2. Investigation of transformation behavior. *Apparatus:* Thermal and catalytic degradation of HDPE was carried out using a Synergic chemical analysis system supplied by Thermo Unicam (5, 24, 35). This system consists of a microbalance (TG131, Cahn) which is connected to an infrared gas cell (10 cm length) contained in an infrared (FTIR) spectrometer (Infinity Series, Mattson) via a transfer line maintained at 250°C. The outlet from the infrared gas cell flowed into a second transfer line which was connected to an absorbent trap (OCARB 4000, Supelco) contained in an organic trap module (OTM, Cahn). The outlet from the OTM was also connected to a gas chromatograph-mass spectrometer (GC-MS) (Automass System 2, Unicam).

Procedures: HDPE (15 mg) was placed in the TG crucible and covered with mg of silanized glass wool before the furnace temperature was raised to 420°C at 10°C min⁻¹ and then held at 420°C for 60 min under a flow of dry nitrogen (40 ml min⁻¹). Identical conditions were used during catalyst evaluation except that 100 mg catalyst was spread evenly over the glass wool so that gases evolved from the sample passed through the layer of catalyst.

On completion of a TG run, the species contained on the trap were thermally desorbed (4 min at 250°C) onto the GC capillary column (DB-1, 30 m × 0.25 mm i.d.), where the compounds were separated before identification by MS. In a typical experiment the column was held at 35°C during the four-minute desorption period before ramping the temperature at 5°C min⁻¹ to 250°C. The final temperature was maintained for 5 min.

3. RESULTS & DISCUSSION

1. X-Ray Fluorescence Spectrometry (XRF)

As anticipated, the acid activation of metakaolin resulted in structural dealumination (Table 1). Clearly, an appropriate choice of activation parameters (acid concentration, temperature, time) can control the degree of structural degradation

and hence the characteristics of the activated products. The relative amounts of dealumination agree with the results of Perissonoto *et al.* (31) in that the Si/Al ratio after treatment with 6M HCl are the same at 12.6 ± 0.1.

3.2. X-Ray Diffraction (XRD)

The XRD profiles obtained (not illustrated) displayed intense, characteristic d₀₀₁ and d₀₀₂ reflections diagnostic of kaolin at 2θ values of 12.29° and 25.03°. These reflections were no longer present in the metakaolin or its acid-leached counterparts. This, together with a broad hump in the 16–32° 2θ range (which increased in intensity with the severity of acid treatment (36)) confirmed the loss of structural integrity and the presence of an amorphous product. The parent kaolin contained a small amount of biotite impurity with peaks arising from d-spacings of 9.91, 6.46, 4.97, 3.32, and 3.24 Å. The position and intensity of these peaks were not substantially affected by calcination and subsequent acid treatment as reported by others (38).

3.3. Thermo Gravimetric Analysis (TGA)

Kaolin lost 16 wt% by 800°C, whereas the metakaolin lost only 4 wt% by 800°C and there was no evidence of any layer dehydroxylation (Table 1). As the concentration of the acid used was increased, the weight loss attributed to the desorption of sorbed water (<200°C) also increased from 0.1% for metakaolin to 3.1% for AAMK3.1 and then to 7.5% for AAMK3.3 and AAMK3.6. The weight loss above 200°C varied in a systematic manner, but was not as marked. The increase in the loss of sorbed water at temperatures <200°C was attributed to an increase in available surface for water adsorption following acid activation.

The total acidity of each of the AAMKs, determined from the desorption of cyclohexylamine (Table 1), increased as the molarity of the acid used to prepare each AAMK was increased. However, the results for the individual AAMKs were low compared to those obtained for a series of acid activated smectites (27).

3.4. Infrared Analysis (VT-DRIFTS)

Infrared spectroscopic investigation of pyridine treated acidic solids can readily distinguish between Brønsted and Lewis acid sites on the surface and provide semiquantitative estimates of the number of each type (32, 39). The room temperature DRIFTS spectrum for pyridine saturated AAMK3.2 (Fig. 1a) exhibited bands due to Brønsted bound pyridine (BPYR) at 1634 and 1541 cm⁻¹ and for Lewis bound pyridine (LPYR) at 1616 cm⁻¹ together with a shoulder on the higher wavenumber side of the 1445 cm⁻¹ band. The 1445 cm⁻¹ band, in combination with that at 1596 cm⁻¹, was assigned to hydrogen bonded pyridine, HPYR (40). The 1490 cm⁻¹ band was assigned to pyridine bonded to both Brønsted and Lewis acid sites, although the Brønsted bound base is known to contribute a greater intensity at this frequency.

Raising the sample temperature to 150°C (Fig. 1b) significantly reduced the bands at 1445 and 1596 cm⁻¹ (HPYR) revealing the 1452 cm⁻¹ (LPYR) band. The intensity of the 1540 cm⁻¹ band increased and the width decreased as the HPYR bands became less intense (40). This suggests that some of the HPYR was actually forming a hydrogen bond with the proton on the BPYR as observed in Al³⁺ exchanged (41) and acid treated smectites (32).

At 200°C the HPYR bands had been removed and the intensity of the Lewis and Brønsted bands in relation to the AAMK combination bands at 1856 and 1923 cm⁻¹ had reduced a little (Fig. 1c). At 275°C (Fig. 1d), the BPYR band intensity had significantly reduced, whereas the LPYR bands remained relatively constant. At 425°C, the LPYR band dominated the spectrum, although there were weak contributions from BPYR at 1539 and 1636 cm⁻¹ (Fig. 1e). This loss of Brønsted acidity was probably due to the removal of acidic aluminol or silanol groups, although the possibility of conversion to Lewis acid sites via dehydration cannot be overlooked.

The first step in the formation of aromatics from alkenes involves the protonation of the alkene to yield a carbocation. Evidently, this small quantity of Brønsted acid sites facilitated the dehydrocyclisation reactions involving the alkenes produced during the thermal pyrolysis of HDPE (Section 3.5), although carbocations can be formed through Lewis acid site promoted hydride ion abstraction from alkanes.

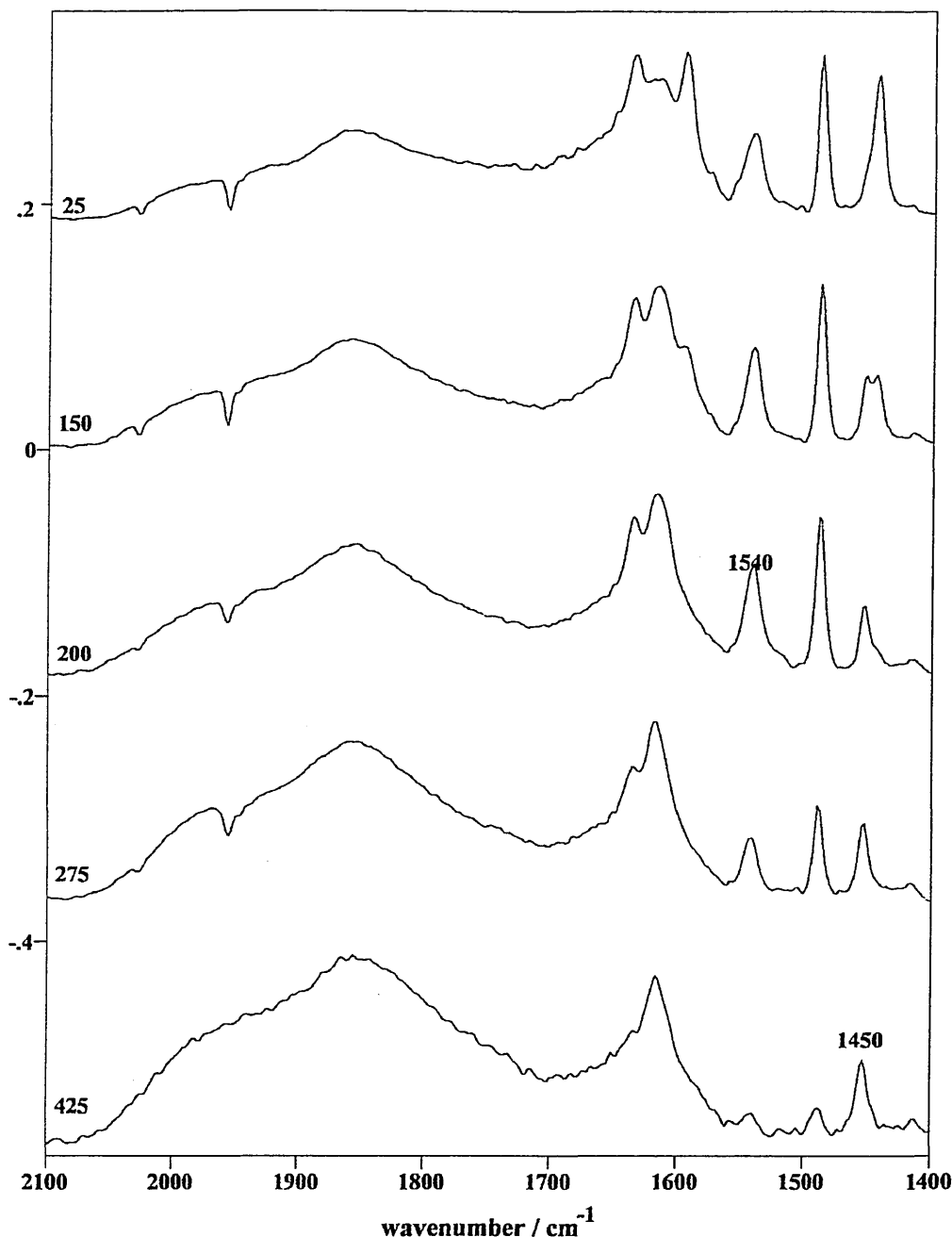


FIG. 1. VT-DRIFTS spectra for pyridine treated AAMK3.2 recorded at (a) 25°C, (b) 150°C, (c) 200°C, (d) 275°C, and (e) 425°C.

5. Investigation of Transformation Behavior

The pyrolysis of HDPE yielded an homologous series of saturated and unsaturated hydrocarbons, as seen in previous studies (5–8, 24). The total ion chromatogram, TIC (not illustrated), exhibited a characteristic quartet of peaks, which in order of increasing retention time, consisted of: α , ω -dienes, alk-1-enes, n -alkanes, and alk- x -enes. As in other studies no evidence of branched aliphatic species or even low levels of aromatic products was found (5–8, 24). Passing the gases derived from HDPE over the AAMKs significantly altered product distribution, both in terms of the species present and their relative quantities. The TIC associated with the gases transformed over the AAMKs was significantly altered and did not contain any evidence of the alkenes listed above but did exhibit peaks for an homologous series of n -alkanes (C_7 – C_{21}) with the most intense being C_{10} – C_{15} . The overall distribution of alkanes was broadened over the AAMKs, indicating a combination of cracking and recombination re-

actions. Both the number and relative quantities of branched aliphatic products increased over AAMK3.6 compared to those produced over AAMK3.1, 3.2, and 3.3. Direct protonation of an alkene by a Brønsted acid site or hydride ion abstraction by a strong Lewis site are both realistic routes to the formation of branched aliphatic molecules from linear alkenes. The resultant carbocation is unstable and rearranges through a series of methyl group shift reactions in order to stabilize the formal positive charge on the ion.

An important aim of this work was to use AAMKs to transform the hydrocarbons produced from HDPE into useful aromatic products. Figure 2 shows that all the AAMKs used gave an enhanced aromatic yield relative to the thermal pyrolysis of HDPE. The levels of toluene were relatively high over all the AAMKs compared to the thermal process and the production of xylenes and trimethylbenzenes was also respectable. The sites required to promote dehydrocyclisation were present even after the mildest acid treatment in that AAMK3.1 was as active as the other AAMKs in generating single ring aromatic

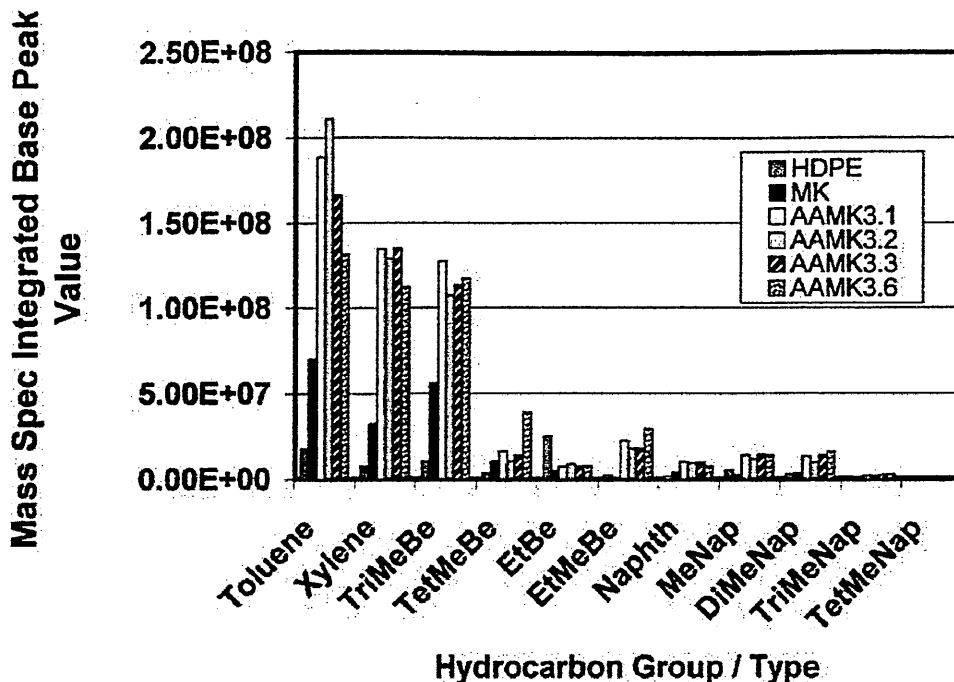


FIG. 2. (a) Aliphatic hydrocarbon and (b) aromatic hydrocarbon distribution produced over each of the AAMKs.

drocarbons. Moreover, the activity and/or availability of these sites to the PE pyrolysis products was not significantly altered by the severity of the acid activation process. None of the AAMK's produced significant quantities of aromatic hydrocarbons.

The complete absence of benzene in the product stream probably reflects the relative instability of linear, primary carbocations derived from a C_6 alkene compared with the much easier formation of toluene from the more stable secondary carbocation formed from a C_7 alkene. Alkylbenzenes of higher carbon number would also be produced through a stable, secondary carbocation. The amount of ethylbenzenes produced was significantly lower than that under thermal conditions alone (Fig. 2) which could indicate that AAMKs are able to promote side chain cracking of alkyl substituted aromatics to yield toluene.

The respectable levels of xylene and trimethylbenzenes suggest that either catalytic methylation occurred after cyclization/aromatization or that structural isomerization of the protonated alkene occurred prior to cyclization. The former is more likely because under cracking conditions, alkylaromatics undergo partial or total dealkylation to yield benzene or short chain alkyl aromatics such as methyl- or ethylbenzenes. The absence of benzene in the product stream suggests that the latter two products are preferentially formed during dehydrocyclization reactions involving carbocations originating from linear alkenes of length $>C_7$. Moreover, the methyl substituent on toluene enhances its reactivity toward electrophilic aromatic substitution reactions compared to benzene. Hence, the first step in the probable mechanism is the protonation of a linear alkene by strong Brønsted acid sites on the surface of the AAMK, possibly a hydroxyl group or a bridging hydroxyl. The resultant carbocation then undergoes hydrocyclization to stabilize the positive charge. The resulting alkylaromatic undergoes side chain cracking to yield toluene which may then undergo an electrophilic aromatic substitution reaction. The adsorbed carbocation attacks the toluene ring system and in doing so eliminates a proton which is taken up at the site vacated by the previously sorbed carbocation, thus reforming the original Brønsted acid group.

Commercially available acid-activated and pillared smectites generally produce more of the trimethylbenzenes than either the xylenes or toluene (5, 24). Thus, the AAMKs were unusual in that toluene was the preferred product, but they were less active than the commercially available acid-activated clays for which direct comparisons are meaningful. For example, freshly prepared acid-activated smectites produced similar quantities of xylene, 60% more trimethyl-

benzene and 50% less toluene. The relative activity of MK in the production of aromatics was higher than anticipated although Perissonotto *et al.* (31) reported that MK was able to promote double bond isomerisation in 1-butene (55% conversion based on 1-butene).

4. CONCLUSIONS

Acid leaching of metakaolin removed aluminum from the structure and produced an acidic solid in which the amount of adsorbed water and surface acidity increased with the severity of acid treatment. The AAMKs produced exhibited both Lewis and Brønsted acidity. Pyridine bound to the latter was held to temperatures lower than that coordinated to Lewis acid sites. The increase in the amount of sorbed water together with the increase in physisorbed and hydrogen-bonded pyridine suggested that the available surface area increased as the severity of acid treatment increased. All the AAMKs were active in the conversion of the off-gases produced during HDPE pyrolysis into aromatic species. Toluene was the major product over most of the AAMKs, followed by xylenes and trimethylbenzene. This selectivity pattern contrasts with that found over acid treated and pillared smectites where trimethylbenzene is generally preferred. Non-acid-leached metakaolin produced much smaller quantities of these aromatics.

REFERENCES

1. "Plastics—Meeting Today's Building and Construction Needs." ADME Technical Publication 1997.
2. Liu, K., and Meuzelaar, H., *Fuel Process. Technol.* **49**, 1 (1996).
3. Halliwell, S. M., "Plastics Recycling in the Construction Industry." BRE Information Paper PD 66/97.
4. Buekens, A. G., and Huang, H., *Res. Conserv. Recycling* **23**, 164 (1998).
5. Breen, C., and Last, P. M., *J. Mater. Chem.* **9**, 185 (1999).
6. Uddin, M., Koizumi, K., Murata, K., and Sakata, Y., *Polym. Degr. Stab.* **56**, 37 (1997).
7. Horvat, N., and Ng, F. T. T., *Fuel* **78**, 462 (1999).
8. McCaffrey, W., Kamal, M., and Cooper, D., *Polym. Degr. Stab.* **47**, 133 (1995).

9. Sakata, Y., Uddin, M. A., and Muto, A., *J. Anal. Appl. Pyrolysis* **51**, 135 (1999).
0. Uemichi, Y., Ayame, A., Kashiwayu, Y., and Kamoh, H., *J. Chromatog.* **259**, 69 (1983).
1. Park, D. W., Hwang, E. Y., Kim, J. R., Choi, J. K., Kim, Y. A., and Woo, H. C., *Polym. Degr. Stab.* **65**, 195 (1999).
2. Ding, W., Liang, J., and Anderson, L., *Fuel Process. Technol.* **51**, 47 (1997).
3. Mordi, R., Fields, R., and Dwyer, J., *J. Anal. Appl. Pyrolysis* **29**, 45 (1994).
4. Xiao, X., Zmierczak, W., and Shabtai, J., *Div. Fuel Chem.* **40**, 4 (1995).
5. Audisio, G., Silvani, A., Beltrame, P., and Carniti, P., *J. Anal. Appl. Pyrolysis* **7**, 83 (1984).
6. Kaminsky, W., and Kim, J. S., *J. Anal. Appl. Pyrolysis* **51**, 127 (1999).
7. Beltrame, P. L., Carniti, P., Audisio, G., and Bertini, F., *Polym. Degr. Stab.* **26**, 209 (1989).
8. Yoshida, T., Ayame, A., and Kanoh, H., *Bull. Jpn. Petrol. Inst.* **17**, 218 (1975).
9. Vasile, C., Onu, P., Barbiou, V., Sabliovski, M., Moroi, G., Ganju, D., and Florea, M., *Acta Polymerica* **39**, 306 (1988).
0. Vasile, C., Onu, P., Barbiou, V., Sabliovski, M., and Moroi, G., *Acta Polymerica* **36**, 543 (1985).
1. Pinto, F., Costa, P., Gulyurtla, I., and Cabrita, I., *J. Anal. Appl. Pyrolysis* **51**, 57 (1999).
- . Songip, A. R., Masuda, T., Kuwahara, H., and Hashimoto, K., *Appl. Catal. B: Environ.* **2**, 165 (1993).
3. Songip, A. R., Masuda, T., Kuwahara, H., and Hashimoto, K., *Energy Fuels* **8**, 136 (1994).
4. Breen, C., Last, P. M., Taylor, S., and Komadel, P., *Thermochim. Acta* **363**, 93 (2000).
5. Smith, K. (Ed.), "Solid Supports and Catalysts in Organic Synthesis." Ellis Horwood, Chichester, 1992.
6. Adams, J. M., *Appl. Clay Sci.* **2**, 309 (1987).
7. Rupert, J. P., Granquist, W. T., and Pinnavaia, T. J., in "Chemistry of Clays and Clay Minerals" (A. C. D. Newman, Ed.). The Mineralogical Society, 1997.
8. Aglietti, E. F., Lopes J. M. P., and Pereira, E., *Appl. Clay Sci.* **3**, 155 (1988).
29. Lussier, J., *J. Catal.* **129**, 225 (1991).
30. Macedo, J. C., Mota, C. J. A., de Menezes, S. C. M., and Camorim, V., *Appl. Clay Sci.* **8**, 321 (1994).
31. Perissinotto, M., Lenarda, M., Storaro, L., and Ganzerla, R., *J. Mol. Catal. A: Chem.* **121**, 103 (1997).
32. Breen, C., *Clay Miner.* **26**, 487 (1991).
33. Breen, C., Clegg, F. C., Yarwood, J., and Hughes, T., *Langmuir* **16**, 6648 (2000).
34. Breen, C., Clegg, F. C., Yarwood, J., and Hughes, T., *J. Phys. Chem. B* **105**, 4872 (2001).
35. Webb, M., Last P. M., and Breen, C., *Thermochim. Acta* **326**, 151 (1999).
36. Breen, C., Madejova, J., and Komadel, P., *Appl. Clay Sci.* **10**, 219 (1995).
37. Breen, C., Zahoor, F. D., Madejova, J., and Komadel, P., *J. Phys. Chem.: B* **101**, 5324 (1997).
38. Kaviratna, H., and Pinnavaia, T. J., *Clays Clay Miner.* **42**, 717 (1994).
39. Ward, J., *J. Colloid Interface Sci.* **28**, 269 (1968).
40. Buzzoni, R., Bordiga, S., Ricciardi, G., Lamberti, C., Zecchina, A., and Bellussi, G., *Langmuir* **12**, 930 (1996).
41. Breen, C., Deane, A. T., and Flynn, J. J., *Clay Miner.* **22**, 169 (1987).

C. Breen¹
 S. Taylor
 E. Burguin
 M. Centeno

Materials Research Institute
 Sheffield Hallam University
 Pond Street Sheffield S1 1WB
 United Kingdom

Received May 16, 2001; accepted November 8, 2001

¹ To whom correspondence should be addressed. E-mail: c.breen@shu.ac.uk.